Justus-Liebig-Universität Gießen

Fachbereich Medizin

Aus dem Zentrum für Innere Medizin

Abteilung für Kardiologie

des Universitätsklinikums Gießen und Marburg GmbH, Standort Gießen

Direktor: Univ. Prof. Dr. med. Samuel Tobias Sossalla

Moderne Verfahren zur Charakterisierung und effektiven interventionellen Behandlung von Vorhofflimmern und komplexen atrialen Tachykardien

Habilitationsschrift

zur Erlangung der Lehrbefähigung für das Fach Kardiologie

im Fachbereich Medizin der Justus-Liebig-Universität Gießen

vorgelegt von

Dr. med. Melanie Anuscha Gunawardene

Gießen (2024)

Inhaltsverzeichnis

Abkürzungsverzeichnis

AT – Atriale Tachykardie

BMI – Body-Mass-Index

CB - Cryoballon

CCE – kombinierter Komplikationsendpunkt (*Combined Complication Endpoint*)

CF – Anpresskraft (*Contact-Force*)

GI – Generator-Impedanz

HFS – Hochfrequenzstrom

KI – Konfidenzintervall

LAPWI- Isolation der linksatrialen Hinterwand (*left atrial posterior wall isolation*)

LAT – Linksatriale Tachykardie

LI – lokale Impedanz

NOAK – Neues orales Antikoagulanz

OAK – Orale Antikoagulation

OR – Odds Ratio

PFA – Pulsed Field Ablation

PV – Pulmonalvenen

PVI – Pulmonalvenenisolation

TIA – transitorisch ischämische Attacke

UHDx – ultra-hochauflösendes Mapping

VHF – Vorhofflimmern

VKA – Vitamin-K-Antagonisten

Die vorliegende kumulative Habilitationsschrift basiert auf folgenden Publikationen:

1. **Gunawardene M**, Willems S, Schäffer B, Moser J, Akbulak RÖ, Jularic M, Eickholt C, Nührich J, Meyer C, Kuklik P, Sehner S, Czerner V, Hoffmann BA. Influence of periprocedural anticoagulation strategies on complication rate and hospital stay in patients undergoing catheter ablation for persistent atrial fibrillation. Clin Res Cardiol. 2017 Jan;106(1):38-48. doi: 10.1007/s00392-016-1021-x. Epub 2016 Jul 19.

2. **Gunawardene M,** Münkler P, Eickholt C, Akbulak RÖ, Jularic M, Klatt N, Hartmann J, Dinshaw L, Jungen C, Moser JM, Merbold L, Willems S, Meyer C. A novel assessment of local impedance during catheter ablation: initial experience in humans comparing local and generator measurements. Europace. 2019 Jan 1;21(Supplement_1):i34-i42. doi: 10.1093/europace/euy273.

3. **Gunawardene MA,** Eickholt C, Akbulak RÖ, Jularic M, Klatt N, Hartmann J, Schlüter M, Meyer C, Willems S, Schaeffer B. Ultra-high-density mapping of conduction gaps and atrial tachycardias: Distinctive patterns following pulmonary vein isolation with cryoballoon or contact-force-guided radiofrequency current. J Cardiovasc Electrophysiol. 2020 May;31(5):1051-1061. doi: 10.1111/jce.14413. Epub 2020 Mar 9.

4. **Gunawardene MA,** Schaeffer BN, Jularic M, Eickholt C, Maurer T, Akbulak RÖ, Flindt M, Anwar O, Pape UF, Maasberg S, Gessler N, Hartmann J, Willems S. Pulsed-field ablation combined with ultrahigh-density mapping in patients undergoing catheter ablation for atrial fibrillation: Practical and electrophysiological considerations. J Cardiovasc Electrophysiol. 2022 Mar;33(3):345-356. doi: 10.1111/jce.15349. Epub 2022 Jan 9.

5. **Gunawardene MA,** Schaeffer BN, Jularic M, Eickholt C, Akbulak RÖ, Hedenus K, Wahedi R, Anwar O, Gessler N, Hartmann J, Willems S. Pulsed field ablation in patients with complex consecutive atrial tachycardia in conjunction with ultra- high density mapping: Proof of concept. J Cardiovasc Electrophysiol. 2022 Dec;33(12):2431-2443. doi: 10.1111/jce.15713. Epub 2022 Nov 9.

1. Einleitung

1.1 Vorhofflimmern

Vorhofflimmern (VHF) ist die häufigste anhaltende Herzrhythmusstörung mit einer aktuellen Prävalenz von 2-4% (1). Ab einem Index-Alter von 55 Jahren beträgt das Lebenszeit-Risiko in Europa VHF zu entwickeln 37% (1). Da VHF weltweit Millionen von Menschen betrifft, führt die Erkrankung zu einer zunehmenden Belastung für das Gesundheitssystem (1). Dies liegt zu einem an der immer älter werdenden Gesellschaft, zum anderen an intensiverer Diagnostik zur Früherkennung von VHF, z.B. durch sogenannte „Wearables“ (Smartwatches, Eventrekorder) (1,2).

VHF ist ein komplexes Krankheitsbild, welches neben der kardialen Symptomatik, neurologische Auswirkungen haben kann und mit einer erhöhten Morbidität und Mortalität assoziiert ist (1). Zudem beeinflussen modifizierbare (z.B. arterielle Hypertonie, Adipositas) und nicht-modifizierbare Risikofaktoren (z.B. Alter, Geschlecht) den Krankheitsverlauf des VHF (3).

Die Symptomatik des VHF variiert stark zwischen den Individuen. Es findet sich eine große Bandbreite möglicher Symptome - von asymptomatischen Patient:innen bis hin zum Vollbild der Tachykardiomyopathie. Typische Symptome sind Palpitationen, Schwindel, Dyspnoe, eingeschränkte Belastbarkeit, Angina pectoris und gelegentlich auch Synkopen. Die Einteilung der Symptomatik erfolgt ähnlich der NYHA-Klassifikation für Herzinsuffizienz anhand des EHRA Scores („European Heart Rhythm Association“: EHRA I: asymptomatisch bis EHRA IV: hochsymptomatisch, sodass alltägliche Tätigkeiten nicht mehr ausgeübt werden können), (1).

Aufgrund der durch VHF verursachten Hyperkoagulabilität sind bis zu 30% der ischämischen Schlaganfälle und 10% der initial kryptogenen Schlaganfälle auf VHF zurückzuführen. Insbesondere bei Patient:innen mit asymptomatischem VHF kann die Komplikation (also z.B. das Auftreten eines Schlaganfalls) der Diagnose des VHF und einer möglichen präventiven Therapie durch eine orale Antikoagulation vorausgehen (1,4).

Die 2020 veröffentlichten europäischen Leitlinien empfehlen aufgrund der Komplexität des VHF integrierte Behandlungspfade zur strukturierten Charakterisierung und Therapie des VHF (1). Dies soll zu einem optimierten und „ganzheitlichen“ Management beitragen.

Der Behandlungspfad „**CC**“ („**C**onfirm-**C**haracterize“) bezieht sich neben der Bestätigung der Diagnose auf 4 wichtige Schwerpunkte (**4S**-Schema) in der Charakterisierung des VHF und beinhaltet die Bewertung des **S**chlaganfallrisikos, der **S**chwere der Symptome, der **S**chwere der Vorhofflimmer-Last und des vorliegenden rhythmogenen **S**ubstrates und soll eine umfangreichere „ganzheitliche“ Einschätzung der individuellen Patienten:innen ermöglichen (5).

Das anschließende Management und die Therapie des VHF beruht auf dem **ABC**-Schema: (**A**ntikoagulation, **B**essere Symptomkontrolle, **C**ardiovaskuläre Risikofaktoren / **C**omorbiditäten) (1,5).

Zur besseren Symptomkontrolle, wird zwischen einer frequenzkontrollierenden und einer rhythmuserhaltenden Therapie des VHF unterschieden (1).

Schwerpunkt dieser Habilitationsschrift ist die Rhythmuskontrolle des VHF, sodass auf diese im Folgenden näher eingegangen wird.

1.2 Rhythmuskontrolle bei Vorhofflimmern

Rhythmuskontrolle kann durch eine antiarrhythmische Medikation, eine elektrische Kardioversion und/ oder mit einer Katheterablation, die im Sinne eines kurativ intendierten Behandlungsansatzes erfolgt, erreicht werden.

Nachgewiesen ist, dass die Katheterablation der medikamentösen antiarrhythmischen Therapie zur Etablierung des Sinusrhythmus überlegen ist (6–8). Das Vorhandensein von Sinusrhythmus wiederum ist mit einem Überlebensvorteil assoziiert (9), welcher möglicherweise aufgrund des ungünstigen Nebenwirkungsprofils von antiarrhythmischen Medikamenten verschleiert wird (9).

Die aktuelle Leitlinie empfiehlt eine rhythmuserhaltende Therapie des VHFs bislang vorwiegend für symptomatische VHF-Patient:innen trotz adäquater Frequenzkontrolle (1). Die Begründung liegt darin, dass randomisierte Studien bislang nicht nachweisen konnten, dass sich durch eine rhythmuserhaltende Therapie in Form einer Katheterablation ein Mortalitätsbenefit für die generelle VHF-Population erbringen ließ (10).

Ein erstes Signal bezüglich des Einflusses auf klinische Endpunkte durch eine frühe Rhythmuskontrolle lieferte die randomisierte EAST-AFNET-4 Studie (11). In dieser Studie war eine frühe rhythmuskontrollierende Therapie (beinhaltete sowohl die medikamentöse Therapie als auch die Katheterablation) bei neu aufgetretenem VHF und Vorhandensein von

kardiovaskulären Risikofaktoren mit einer Reduktion kardiovaskulärer Ereignisse bei VHF-Patient:innen assoziiert (11).

1.2.1 Katheterablation von Vorhofflimmern

1.2.1.1 Pulmonalvenenisolation

Der Grundpfeiler der heutigen Katheterablation bildet die Durchführung der Pulmonalvenenisolation (PVI). Im Jahr 1998 wurden von Haissaguerre et al. die Pulmonalvenen als wesentlicher Trigger von VHF beschrieben und seither sind Ablationsverfahren entwickelt und kontinuierlich verbessert worden, um die Pulmonalvenen effektiv, sicher und anhaltend elektrisch zu isolieren (12). Somit ist die PVI die Therapie der Wahl während der Erstablation und geht insbesondere bei paroxysmalem VHF mit hohen Erfolgschancen einher (1). Neben der Verwendung von möglichen dreidimensionalen Mappingverfahren, zeigte sich in den letzten Jahren eine rasante Entwicklung hinsichtlich der verwendeten Katheter und Verfügbarkeit neuer Energieformen.

1.2.1.2 Energiequellen

Bislang galt die sogenannte „Punkt-für-Punkt“-Ablation mittels Hochfrequenzstrom als Goldstandard für die Durchführung einer PVI. Unter Verwendung eines dreidimensionalen Mappingssystems (und so möglicher Kartierung des linken Vorhofes) wird hier „Punkt-für-Punkt“ mit der Katheterspitze das jeweilige ipsilaterale Pulmonalvenenpaar bis zur elektrischen Isolation behandelt. Ziel ist es hier kontinuierliche und transmurale Ablationslinien im Vorhof zu hinterlassen. Wesentliche Entwicklungen der Hochfrequenzablation beinhalten diesbezüglich u.a. die Möglichkeit zur Messung der Anpresskraft auf das Gewebe, aber auch die Option zur Messung lokaler Impedanzen, von Temperaturverläufen und Abständen zwischen den Ablationspunkten (13,14). Diese Methoden liefern so einen indirekten Surrogatparameter zur Abschätzung der Läsionstiefe während der Ablation.

Neben der Hochfrequenzstromablation, hat sich neben der „Punkt-für-Punkt“-Katheter auch der Cryoballon in der klinischen Routine durchgesetzt, welcher aufgrund des Ballondesigns einen anatomischen Ansatz für die PVI liefert und der Hochfrequenzstromablation bei paroxysmalem VHF nicht unterlegen ist (15). Bei der rein fluoroskopisch-geführten Cryo-

Ablation erfolgt zunächst eine Okklusion der jeweiligen Pulmonalvene mit dem Ballon. Anschließend wird die Pulmonalvene durch Kälteablation mit verdampfendem Kühlmittel innerhalb des Ballons, isoliert (16,17).
Auch weitere Energieformen wie Laser oder die Verwendung von Hochfrequenzstrom-Ballons im Sinne der „Single-Shot"-Katheter sind verfügbar, spielen aber bisher eine untergeordnete klinische Rolle (18,19).

Die jüngste zum Einsatz kommende, erstmals nicht-thermale Energieform, bietet die Pulsed Field Ablation (PFA). Durch Aufbau eines sehr schnellen elektrischen Feldes kommt es durch die Energieabgabe zu einer Destabilisierung der Myozyten-Zellmembran (20,21). Es entstehen mikroskopisch kleine Poren, die konsekutiv zum Zelltod führen. Bei diesem Prozess handelt es sich um die sogenannte irreversible Elektroporation (20,21). Das Besondere hierbei ist, dass für verschiedene Gewebetypen unterschiedliche Nekrose-Schwellenwerte existieren. Das elektrische Feld, welches bei der PFA im Herzen eingesetzt wird, hat einen niedrigeren Nekrose-Schwellenwert für Kardiomyozyten, als für andere Gewebearten – es entsteht somit eine Selektivität für Herzmuskelgewebe (20,21). Der Vorteil ist eine effektive Ablation unter Schonung angrenzender Gewebsstrukturen während der Ablation im Vorhof, wie z.B. des Ösophagus oder des Nervus phrenicus (20,22). Selten kommt es bei der Katheterablation zu gefährlichen Komplikationen wie der sehr seltenen atrio-ösophagealen Fistel (Auftreten <0,5%, häufig letal, (1)). Theoretisch können diese also durch Verwendung von PFA vermieden werden (23). Die bislang veröffentlichten Daten zur PFA-gestützten Vorhofflimmerablation sind noch limitiert. Der berichtete Erfolg mit initialen klinischen Daten scheint jedoch vielversprechend: neben einer hohen Effektivität mit Nachweis hoher Isolationsraten der Pulmonalvenen (in der Literatur mit 84,4-100%) zeigt sich auch eine niedrige Komplikationsrate, bislang ohne Auftreten ösophagealer Läsionen nach Ablation (20,24–26).

1.2.1.3 Katheterablation von persistierendem Vorhofflimmern

Der Erfolg der Katheterablation ist bei paroxysmalem VHF höher als bei persistierendem VHF nach Erstprozedur (27). Mutmaßlich aufgrund eines postulierten ausgedehnteren arrhythmogenen Substrats, reicht die reine PVI insbesondere bei Patient:innen mit persistierendem und somit fortgeschrittener Stadien von VHF häufig nicht aus. Die meisten Ablationskonzepte, die über die reine PVI hinausgehen, wie die Ablation von fibrotisch

veränderter atrialer Areale beispielsweise in Form von linearen Läsionen, haben bisher bei der Erstablation keine reproduzierbar besseren klinischen Ergebnisse aufweisen können (28–31). Zudem gibt es Hinweise, dass diese komplexeren Ablationsstrategien bei persistierendem VHF möglicherweise mit einer erhöhten Komplikationsrate einhergehen könnten (28,31).
Lediglich eine randomisierte Studie, die ERASE-AF Studie konnte eine höhere Rate an Vorhofflimmerfreiheit nach substratbasierter Ablation im linken Vorhof nachweisen (32).
Auch wenn die randomisierte CAPLA Studie (30) zur Untersuchung der Hochfrequenzstrom-basierten Isolation der linksatrialen Hinterwand, welche eine Rolle in der Pathogenese des VHF spielen könnte, gescheitert ist, könnte PFA - insbesondere aufgrund der höheren Effektivität und des guten Sicherheitsprofils aufgrund der Nähe der linksatrialen Hinterwand zur Speiseröhre, hier eine alternative Möglichkeit bieten (22). Randomisierte Daten hierzu fehlen jedoch bislang.

1.2.1.4 Sicherheit der Katheterablation

Die Katheterablation von VHF hat sich in den letzten Jahren als sicheres Verfahren in der interventionellen Elektrophysiologie etablieren können. Komplikationsraten liegen laut prospektiver, register-basierter Daten bei 4-14%, wobei lebensbedrohliche Komplikationen deutlich seltener auftreten (1). Das Risiko für eine Perikardtamponade liegt laut Leitlinie bei 1%, das Auftreten eines thrombembolischen Ereignisses <1%, einer atrioösophagealen Fistel oder Ösophagusperforation <0,5% und die periprozedurale Mortlität bei <0,01% (1).
Insbesondere in erfahrenen Zentren liegen diese Komplikationsraten deutlich niedriger (1,10).
Da es während der Katheterablation sowohl zu einer Blutungs- als auch einem thrombembolischen Ereignis kommen kann, spielt das Management der periprozeduralen oralen Antikoagulation (OAK) eine große Rolle. Hierbei kam es in den letzten Jahren zu einer Weiterentwicklung der Antikoagulationsstrategien, von initialer Therapie mit Vitamin-K-Antagonisten (VKA) und Heparin-Bridging zu kontinuierlicher VKA-Gabe während der Ablation (33,34). Bei den heutzutage eingesetzten neuen oralen Antikoagulanzien (NOAK) kann eine durchgehende bzw. minimal pausierte (in der Regel am Morgen des Eingriffs) OAK erfolgen, ohne das Risiko für Blutungen zu erhöhen (35).

1.2.1.5 Arrhythmierezidive nach Katheterablation

Nach Katheterablation kann es zu Arrhythmie-Rezidiven kommen. Hierbei kann VHF oder eine konsekutive, meist komplexe atriale Tachykardien (AT) auftreten, sodass eine erneute Katheterablation notwendig werden kann.

Nach initialer PVI ist eine elektrische Rekonnektion der Pulmonalvenen die häufigste Ursache für ein VHF-Rezidiv (36), sodass wie bereits erwähnt, an der Verbesserung der initialen Läsionsbildung durch o.g. Weiterentwicklung der Technologien geforscht wird.

Entweder primär oder konsekutiv nach Katheterablation kann sich ein Arrhythmierezidiv auch in Form einer AT präsentieren. Aufgrund von atrialem Remodelling mit Ausbildung atrialer Fibrose (primär durch atriale Myopathie oder sekundär nach Substratmodifikation einer vorherigen Katheterablation) mit Narbenarealen, nach herzchirurgischen Eingriffen oder bei kongenitalen Herzvitien können sich hierbei geordnete Reentries (als Makro- oder lokalisiertem Reentry) in den Vorhöfen finden (37–40). Die Identifikation des zugrundeliegenden AT-Mechanismus durch Zuhilfenahme von Mappingsystemen sowie die Ablationsbehandlung als solche, kann aufgrund des komplexen Substrates dieser AT eine Herausforderung in der invasiven elektrophysiologischen Untersuchung darstellen (40,41).

Bessere Detektion der elektrischen Signale durch ultra-hochauflösendes Mapping, Betrachtung der Aktivierungs- und Voltagemaps sowie Verwendung sog. Post-Processing-Algorithmen können zur Identifikation des AT-Mechanismus herangezogen werden (40,42).

2. Fragestellung und Zielsetzung der Arbeit

Ziel der vorliegenden Habilitationsschrift ist es, den Stellenwert hochauflösender dreidimensionaler Mappingverfahren, innovativer Katheterdesigns und neuer Energieformen zur interventionellen Behandlung von VHF und komplexen AT im Kontext der Effizienz und Sicherheit zu evaluieren. Die Katheterablation hat sich in der Behandlung symptomatischen VHF und konsekutiver AT etabliert. Um die Effektivität und Sicherheit zu steigern, wurden die Ablationsmethoden der invasiven Elektrophysiologie in den letzten Jahren kontinuierlich verbessert. Ebenso wurde das Management rund um die Prozedur, insbesondere in Bezug auf die periprozedurale Gabe der oralen Antikoagulation weiter optimiert. Es ist Gegenstand aktueller wissenschaftlicher Bemühungen diese optimierten Methoden im klinischen Einsatz zu evaluieren.

Vor diesem Hintergrund wurden folgende Themenbereiche in der vorliegenden Habilitationsschrift behandelt:

1. Der Einfluss verschiedener periprozeduraler Antikoagulationsstrategien auf Komplikationsraten und Krankenhausaufenthaltsdauer bei der Katheterablation von persistierendem Vorhofflimmern
2. Die initiale Anwendung eines Ablationskatheters mit lokaler Impedanzmessung während der Katheterablation von Vorhofflimmern – Vergleich zwischen lokaler und Generator-Impedanz
3. Auftreten komplexer atrialer Tachykardien und die Charakterisierung von Leitungslücken in den initialen Ablationslinien um die Pulmonalvenen nach initialer Hochfrequenzstrom- und Cryoablation unter Verwendung eines ultra-hochauflösenden Mappingssystems
4. Pulsed Field Ablation unter Verwendung eines ultra-hochauflösenden Mappingssystems – Elektrophysiologische Charakteristika und praktische Herangehensweise
5. Pulsed Field Ablation in Kombination mit einem ultra-hochauflösenden Mappingssystem zur interventionellen Behandlung komplexer konsekutiver linksatrialer Tachykardien

3. Ergebnisse

3.1 Einfluss der Antikoagulationsstrategie auf Komplikationsraten und Krankenhausaufenthaltsdauer bei der Katheterablation von persistierendem Vorhofflimmern

In den letzten Jahren wurde die OAK-Behandlung zur Schlaganfallprophylaxe bei VHF durch die Einführung sogenannter NOAK, als Alternative zu Vitamin-K-Antagonisten (VKA), reformiert (35). Da die Katheterablation von VHF heutzutage einen häufigen Einsatz bei der Rhythmuskontrolle findet, spielt die Etablierung einer sicheren periprozeduralen OAK-Strategie eine wichtige Rolle (35). Idealerweise sollte die periprozedurale OAK-Strategie unter Abwägung sowohl der Blutungs- als auch der thrombembolischen Komplikationen gewählt werden. Die erste Form der periprozeduralen OAK war ein Pausieren von VKA mit Überbrückung durch Heparingaben; gefolgt von einer kontinuierlichen Gabe der VKA und anschließendem Einzug der NOAK (33,34,43–46). Trotz des im klinischen Alltags routinemäßigen Einsatzes der NOAK, variierten die periprozeduralen OAK-Strategien bezüglich der Weitergabe und des Pausierens vor, während und nach der Katheterablation, stark (43).

Im Allgemeinen konnte gezeigt werden, dass der periprozedurale Einsatz von Heparin zur Überbrückung der VKA mit einem erhöhten schwerwiegenden Blutungsrisiko assoziiert ist (47).

Trotz zahlreicher Studien auf diesem Gebiet, sind Daten bezüglich der periprozeduralen Antikoagulationsstrategie bei rein persistierendem VHF spärlich. Ablationsprozeduren bei Patient:innen mit persistierendem VHF sind häufig länger und komplex, u.a. aufgrund der Ablation konsekutiver atrialer Tachykardien, sodass sich hieraus eine höhere Wahrscheinlichkeit für das Auftreten von Komplikationen ergibt.

Ziel der im Folgenden genannten Publikation war es, die periprozedurale Komplikationsrate der verschiedenen OAK-Strategien (1. NOAK, 2. kontinuierliche VKA Gabe und 3. unterbrochene VKA mit Heparin-Überbrückung) bei Patient:innen, die sich einer Katheterablation von persistierendem VHF und/oder konsekutiven atrialen Tachykardien unterzogen, zu untersuchen. Zudem wurde der Einfluss der Komplikationsraten im Kontext der Krankenhausaufenthaltsdauer betrachtet.

Publikation Nr. 1:

***Gunawardene M**, Willems S, Schäffer B, Moser J, Akbulak RÖ, Jularic M, Eickholt C, Nührich J, Meyer C, Kuklik P, Sehner S, Czerner V, Hoffmann BA. Influence of periprocedural anticoagulation strategies on complication rate and hospital stay in patients undergoing catheter ablation for persistent atrial fibrillation. Clin Res Cardiol. 2017 Jan;106(1):38-48. doi: 10.1007/s00392-016-1021-x. Epub 2016 Jul 19. PMID: 27435077.*

Bei den Untersuchungen dieser Arbeit handelt es sich um eine retrospektive Analyse mit konsekutivem Einschluss aller Patient:innen, die sich einer Katheterablation von persistierendem VHF und/oder konsekutiven Arrhythmien unterzogen und eine präprozedurale OAK mit VKA oder NOAK erhielten. Patient:innen ohne OAK wurden von der Analyse ausgeschlossen. Abhängig von der vorbestehenden OAK wurden drei periprozedurale OAK-Strategien und somit Gruppen definiert: 1. NOAK, 2. kontinuierliche VKA Gabe im INR-Bereich von 2 bis 3 und 3. unterbrochene VKA mit Heparin-Überbrückung (in der Regel niedermolekulares Heparin, gewichtsadaptiert).

In Gruppe 1 wurde das Pausieren der NOAK-Therapie 48 Stunden präprozedural, entsprechend der damaligen klinischen Routine und Leitlinie (48), empfohlen. Zum Einsatz kamen zu dieser Zeit die folgenden NOAK: Dabigatran, Rivaroxaban und Apixaban. In dieser Gruppe erfolgte keine Überbrückung mit Heparin und die OAK wurde am selben Abend der Prozedur wiederbegonnen.

Alle Patient:innen der Studie erhielten eine Katheterablation von persistierendem VHF (Erst- oder Folgeprozedur aufgrund von VHF oder konsekutiven atrialen Tachykardien eingeschlossen) unter Analgosedierung mit Verwendung von dreidimensionalen Mappingsystemen und Hochfrequenzstrom-Ablationskathetern.

Alle aufgetretenen Komplikationen, mit Fokus auf schwerwiegende und nicht-schwerwiegende Blutungen sowie thrombembolische Ereignisse, wurden erfasst (49,50).

Ein kombinierter Endpunkt aus Blutungs- und thrombembolischen Ereignissen wurde in der Studie definiert (CCE = combined complication endpoint), (33,34,47,51,52).

Im Rahmen dieser Arbeit wurden 1440 Katheterablationsbehandlungen von 1092 Patient:innen mit persistierendem VHF (entsprechend 1,3 Prozeduren pro Patient:in) in einem Zeitraum von Januar 2011 bis Dezember 2014 untersucht (**Abbildung 1**).

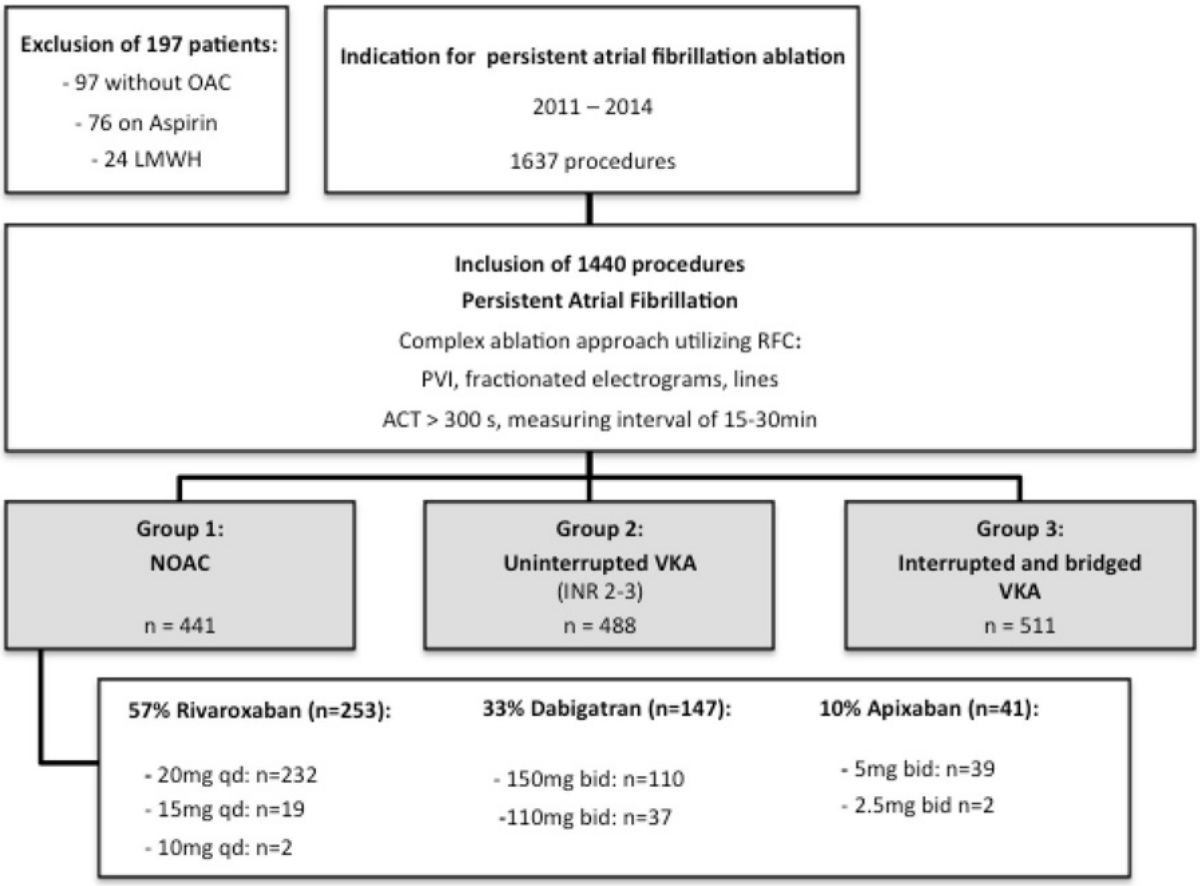

Abbildung 1: Studienablauf. Darstellung der verschiedenen Gruppen sowie die Dosierung der einzelnen NOAK. ACT, activated clotting time (aktivierte Gerinnungszeit); bid, ‘‘bis in die’’ = zweimal tägliche Einnahme; LMWH, nierdermolekulares Heparin; mins, Minuten; NOAC, neues orales Antikoagulanz; OAC, orale Antikoagulation; PVI, Pulmonalvenenisolation; qd, ‘‘quaque die’’ = einmal täglich; RFC, radiofrequency current energy = Hochfrequenzstrom; s, Sekunden; VKA, Vitamin-K- Antagonist

Das mittlere Alter der Patient:innen betrug 64,1 ± 9,93 Jahre. Die meisten Patient:innen waren männlich (67,4%), **Tabelle 1**. Die Verteilung der Gruppen zeigte sich wie folgt: n=441 (31%) Gruppe 1 (57% Rivaroxaban, 33% Dabigatran und 10% Apixaban), n=488 (34%) Gruppe 2 und n=511 (35%) Gruppe 3.

Die häufigste Indikation der Ablationsprozeduren war persistierendes VHF (n=882, 61,3 %), gefolgt von konsekutiven atrialen Tachykardien nach vorheriger Katheterablation (n=445, 30.9 %).

Die PVI, ob de novo oder als erneute „Re-Isolation“, war die am häufigsten verwendete Ablationsstrategie (78%), gefolgt von der Ablation komplex fraktionierter Elektrogramme/Defragmentierung (52%), Anlage von Ablationslinien (26%), fokaler Ablation (21%) und rechtsatrialer Isthmusablation (22%), **Tabelle 2**.

Tabelle 1. Basischarakeristika

Patienten	Alle n=1092	NOAK n=329	Kontinuierliche VKA n=333	Unterbrochene VKA n=430
Geschlecht:				
- männlich	**736 (67.4%)**	233 (70.8%)	214 (64.3%)	289 (67.2%)
- weiblich	**356 (32.6%)**	96 (29.2%)	119 (35.7%)	141 (32.8%)
Alter [Jahre]	**64.1±9.93**	64.1±10.4	65.2±9.06	63.1±10.3
Initialer VHF Typ [n,%]				
- Persistierend	**1008 (92.3%)**	312 (94.8%)	296 (88.9%)	400 (93.0%)
- Langanhaltend persistierend	**84 (7.69%)**	17 (5.2%)	37 (11.1%)	30 (7.0%)
Arterielle Hypertonie [n,%]	**845 (77.4%)**	233 (70.8%)	265 (79.6%)	347 (80.7%)
Hyperlipoproteinämie [n,%]	**455 (41.7%)**	113 (34.4%)	136 (40.8%)	206 (47.9%)
Koronare Herzerkrankung [n,%]	**223 (20.4%)**	71 (21.6%)	67 (20.1%)	85 (19.8%)
Valvuläre Herzerkrankung [n,%]	**106 (9.71%)**	20 (6.07%)	48 (14.4%)	38 (8.84%)
Tachykardiomyopathie durch VHF [n,%]	**70 (6.41%)**	24 (7.29%)	24 (7.21%)	22 (5.12%)
Kardiomyopathie [n,%]	**135 (12.4%)**	44 (13.4%)	40 (12.0%)	51 (11.9%)
Diabetes mellitus [n,%]	**103 (9.43%)**	26 (7.90%)	31 (9.31%)	46 (10.7%)
Vorheriger Schlaganfall/ TIA [n,%]	**120 (11.0%)**	28 (8.51%)	44 (13.2%)	48 (11.2%)
pAVK [n,%]	**44 (4.03%)**	10 (3.04%)	15 (4.50%)	19 (4.42%)
BMI [kg/m²]	**27.3±4.05**	26.9±3.96	27.2±3.86	27.7±4.26
Längste VHF Episode [Tage]	**148.3±246.6**	102.4±134.4	168.1±271.6	170.3±289.3
Anti-arrhythmische Medikation (median, n)	**2 (2;3)**	2 (1;3)	2 (2;3)	2 (2;3)
Linksventrikuläre Funktion [%]	**57.4±8.4**	56.8±8.5	57.2±8.6	58.1±8.3
Labor:				
TSH [µU/l]	**1.76±2.19**	1.79±2.08	1.74±2.74	1.75±1.76
GFR [ml/min]	**74.2±20.8**	78±22.9	72±20	73±19.5
Kreatinin [g/dl]	**1.06±0.41**	1.02±0.33	1.10±0.56	1.07±0.32
INR	**1.67±0.6**	1.06±0.12	2.37±0.36	1.52±0.29
Scores: Median (Q1;Q3)				
CHA_2DS_2-VASc	**2 (1;3)**	2 (1;3)	2 (2;3)	2 (1;3)
$CHADS_2$	**1 (1;2)**	1 (1;2)	1 (1;2)	1 (1;2)
HAS-BLED	**2 (1;2)**	1 (1;2)	2 (1;2)	2 (1;2)
EHRA	**2 (2;3)**	2 (2;3)	2 (2;3	2 (2;3)

Tabelle 2. Prozedurale Parameter

Prozeduren	Alle n=1440	NOAK n=441	Kontinuierliche VKA n=488	Unterbrochene VKA n=511
Indikation aktuelle Prozedur:				
PAF bei initial persistierendem VHF [n,%]	**33 (2.29%)**	11 (2.49%)	15 (3.07%)	7 (1.37%)
Persistierendes VHF [n,%]	**882 (61.3%)**	277 (62.8%)	256 (52.5%)	349 (68.3%)
Langanhaltend persistierendes VHF [n,%]	**80 (5.51%)**	16 (3.63%)	31 (6.35%)	33 (6.46%)
Atriale Tachykardie [n,%]	**445 (30.9%)**	137 (31.0%)	186 (38.1%)	122 (23.9%)
Elektrophysiologischer Ansatz (mehrere möglich):				
PVI [n,%]	**666 (46.3%)**	215 (48.8%)	199 (40.8%)	252 (49.3%)
Re-PVI [n,%]	**461 (32.0%)**	128 (29.0%)	169 (34.6%)	164 (32.1%)
Defragmentierung [n,%]	**742 (51.5%)**	215 (48.8%)	254 (52.1%)	273 (53.4%)
Ablationslinien [n,%]	**381 (26.5%)**	109 (24.7%)	153 (31.4%)	119 (23.3%)
Cavotrikuspidaler Isthmus [n,%]	**317 (22.0%)**	100 (22.7%)	107 (21.9%)	110 (21.5%)
Fokale Ablation [n,%]	**303 (21.0%)**	82 (18.6%)	116 (23.8%)	105 (20.6%)
Ablationsprozedur:				
Dauer [min]	**174.2±63.5**	171.6±62.6	176.4±62.9	174.3±64.8
Durchleuchtungszeit [min]	**37.9±19.6**	34.9±18.9	37.8±19.3	40.5±20.0
Flächendosisprodukt [cGycm²]	**5567.4± 20071.7**	4715.6± 6148.4	4629.4± 5292.1	7203.9± 32794.9
Kumulative Energie [J]	**102874.9± 70801**	98799.8± 60418.9	104307.3± 80168.3	105035.6± 69600.4
Dauer Hochfrequenzstrom [s]	**3927.5± 3033.7**	3771.3± 2318.7	3924.1± 2511.8	4065.6± 3905.2
Hochfrequenzstrom Abgaben [n]	**40.1±26.2**	39.5±26.4	39.3±25.7	41.3±26.5
Mittlere Energie [W]	**26.9±10.9**	26.9±9.6	26.8±11.0	27.2±11.9
Intra-prozedurale ACT-Werte:				
ACT > 300 s [%]	**48.7±31.3**	40.6±28.2	64.4±27.9	39.9±31.3
Mittlere ACT [s]	**303.5±38.7**	293.0±34.9	324.3±38.9	291.5±32.5
Standardabweichung ACT [s]	**40.0±30.8**	42.2±30.7	43±36.5	34.7±22.4
Heparin [IU]	**9909± 3789.5**	11975.6± 4166.1	8142.0± 2702.4	9753.6± 3381.5

Tabelle 1 und 2: Basischarakteristika und Prozedurale Parameter des Studienkollektivs. ACT, aktivierte Gerinnungszeit; BMI, Body-Mass-Index; GFR, glomeruläre Filtrationsrate; INR, International normalized ratio; min, Minuten; paVK, periphere arterielle Verschlusskrankheit; PVI, Pulmonalvenenisolation; s, Sekunden; TIA, transitorisch ischämische Attacke; TSH, Thyreoidea-stimulierendes Hormon; VHF, Vorhofflimmern. *Scores:* CHA2DS2-VASc Score (Score zur Evaluation des Schlaganfallrisikos), CHADS2-Score (Score zur Evaluation des Schlaganfallrisikos), EHRA Score (Score zur Evaluation der Symptome unter Vorhofflimmern), HAS-BLED Score (Score zur Evaluation des Blutungsrisikos). Werte sind als Mittelwert ± Standardabweichung angegeben, [n] oder n (%).

Die Gesamtkomplikationsrate lag bei 14,6% (n=210/1440) mit einer Rate schwerwiegender Komplikationen von 0,9% (n=13/1440). Die schwerwiegenden Komplikationen bestanden aus einem Schlaganfall, 4 Perikardtamponaden, 7 schwerwiegenden Leistenkomplikationen mit Notwendigkeit der Transfusion und/oder chirurgischen Intervention, eine Lungenblutung mit bronchoskopischer Intervention und Bluttransfusion. Bei einem der Patient:innen kam es im Verlauf zur kardialen Intervention (Mitralklappen-Clipping) bei akuter kardialer Dekompensation. Kein Patient verstarb. Die höchste Blutungsrate fand sich in Gruppe 3 mit 10,8% (**Tabelle 3**).

Tabelle 3. Periprozedurale Komplikationsraten

Alle n (%)	**Alle n=1440**	**NOAK n=441**	**Kontinuierliche VKA n=488**	**Unterbrochene VKA n=511**
Combined complication endpoint (CCE),	**113 (7.85%)**	**23 (5.22%)**	**35 (7.17%)**	**55 (10.8%)**
• **Blutungen:**	112 (7.78%)	23 (5.22%)	34 (6.97%)	55 (10.8%)
○ **Schwerwiegend:**	12 (0.83%)	2 (0.45%)	3 (0.61%)	7 (1.37%)
- Perikardtamponaden	4 (0.28%)	1 (0.23%)	2 (0.41%)	1 (0.2%)
- Leistenblutung	7 (0.49%)	1 (0.23%)	1 (0.20%)	5 (0.98%)
- Hämoptysen(inkl. Transfusion)	1 (0.07%)	0	0	1 (0.2%)
○ **Nicht-schwerwiegend:**	101 (7.01%)	21 (4.76%)	31 (6.35%)	48 (9.39%)
- Leistenblutung	96 (6.67%)	20 (4.54%)	29 (5.94%)	46 (9.00%)
- Andere*	5 (0.35%)	1 (0.23%)	2 (0.41%)	2 (0.39%)
• **Schlaganfall / TIA [MACCE]**	1 (0.07%)	0	1 [stroke] (0.20%)	0
Andere Komplikationen	**97 (6.73%)**	**32 (7.25%)**	**31 (6.35%)**	**34 (6.65%)**
Hämodynamisch nicht-relevanter Perikarderguss	67 (4.65%)	24 (5.44%)	19 (3.89%)	24 (4.7%)
MACE	0	0	0	0
Herz-OP/Intervention	1 (0.07%)	0	0	1 [Mitraklappen-Clip] (0.2%)
Weitere Komplikationen**	29 (2.01%)	8 (1.81%)	12 (2.46%)	9 (1.76%)
Gesamt Komplikationsrate	**210 (14.6%)**	**55 (12.5%)**	**66 (13.5%)**	**89 (17.4%)**
Gesamt Komplikationsrate pro Prozedur (mindestens 1 Komplikation)	**200 (13.9%)**	**53 (12.0%)**	**66 (13.5%)**	**81 (15.9%)**

*** Hämaturie, Epistaxis, Hämoptysen ohne Interventionsbedarf**
**** Herzschrittmacher-Implantation, kardiale oder respiratorische Insuffizienz, Fehlpunktion der Aortenwurzel**

Tabelle 3: Periprozedurale Komplikationsrate. MACE= “major adverse cardiac event”; MACCE= “major adverse cardiac and cardiovascular event”; NOAK =neues orales Antikoagulanz; TIA = transitorisch ischämische Attacke; VKA = Vitamin K Antagonist.

Die adjustierte CCE-Rate war 5,5 % [95 %-Konfidenzintervall (KI) (3,1–7,8)] in Gruppe 1, 7,5 % [95 % KI (5,0–10,1)] in Gruppe 2, und 9,9 % [95 % CI (6,6–13,2)] in Gruppe 3. Hierbei wurden 8 Confounder (Alter, Hypertonie, koronare Herzerkrankung, Body-Mass-Index, Geschlecht, Prozedurdauer, Anzahl der Prozedur und Jahr der Prozedur) im Regressionsmodell berücksichtigt.

Es zeigte sich ein signifikanter Unterschied bezüglich der CCE-Raten zwischen den Gruppen: Im Vergleich zur Gruppe 1, fand sich ein fast doppelt erhöhtes CCE-Risiko für Gruppe 3 [Odds Ratio (OR) 1.9, 95 % KI (1,0–3,7). Ein erhöhtes Alter war mit erhöhten CCE-Raten assoziiert (**Abbildung 2**).

Das Auftreten von Komplikationen war mit einer erhöhten Krankenhausaufenthaltsdauer assoziiert (Median von 4 Tagen (q1-3: 3–7) mit vs. 3 Tage (q1-3: 3–4) ohne Auftreten von Komplikationen, p = 0.0002).

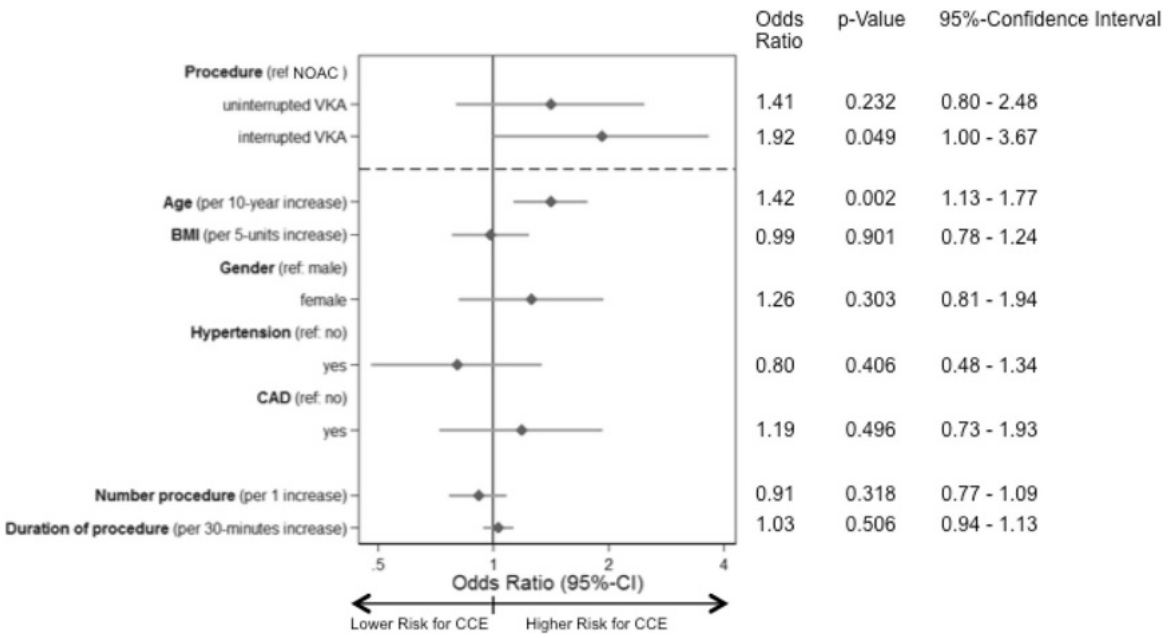

Abbildung 2: Kombinierter Komplikationsraten-Endpunkt (CCE) in den verschiedenen Gruppen und Einfluss möglicher Confounder - dargestellt im Forest Plot des linearen Regressionmodels. BMI, Body-Mass-Index; CAD, coronary artery disease = koronare Herzerkrankung; CCE, kombinierter Komplikationsendpunkt; NOAC, neues orales Antikoagulanz; VKA, Vitamin-K-Antagonist.

Patient:innen, die sich aufgrund von persistierendem VHF und/oder konsekutiven atrialen Tachykardien einer Katheterablation unterziehen, sind somit einem erhöhten Komplikationsrisiko ausgesetzt, wenn eine periprozedurale Überbrückung der VKA-Therapie mit Heparin im Vergleich zu NOAK durchgeführt wird. Diese periprozedurale OAK-Strategie kann heutzutage als obsolet betrachtet werden und ist nicht mehr zu empfehlen. Dass eine NOAK-Gabe im Vergleich zu VKA zu niedrigeren Raten an schwerwiegenden Blutungen im Rahmen der Katheterablation führt, konnte zudem durch eine Metaanalyse gezeigt werden (53).

Schwerwiegende Komplikationen sowie das Auftreten thrombembolischer Ereignisse waren in dieser Studie auch bei Patient:innen mit persistierendem VHF trotz komplexer Prozeduren gering, auch unter Pausieren der NOAK-Therapie 48 Stunden vor der Prozedur. Seit Durchführung dieser Arbeit wurden zahlreiche Studien publiziert, die auch eine kontinuierliche Gabe der NOAK im Rahmen der Ablationsbehandlung als sicher evaluiert haben (46,54). Im heutigen klinischen Alltag gilt eine kontinuierliche oder nur minimale Unterbrechung der NOAK Therapie am Morgen der Ablationsbehandlung als Standard (35).

3.2 Die initiale Anwendung eines Ablationskatheters mit lokaler Impedanzmessung während der Katheterablation von Vorhofflimmern – Vergleich zwischen lokaler und Generator-Impedanz

Aufgrund der kontinuierlichen Weiterentwicklung der Ablationstechnologien spielt neben der stetigen Re-Evaluation der Sicherheit der Katheterablation, die Steigerung der Effektivität und deren klinische Untersuchung eine entscheiden Rolle. Ziel aller Verfahren ist das Erreichen einer optimierten intrakardialen Läsionsbildung.

Der Einsatz von Hochfrequenzstrom (HFS) als Energiequelle zur Durchführung der Katheterablation galt bislang als Goldstandard. Die intrakardiale Läsion ist abhängig von der manuellen Kontaktaufnahme der distalen Katheterelektrode an das Gewebe. Die Läsion entsteht hierbei durch zwei Komponenten: erstens durch die Widerstandserwärmung direkt an der Gewebeoberfläche, zweitens über konduktive Wärmefortleitung vom Ort der Widerstandserwärmung (v.a. zeitliche Komponente), (27). Ein Abfall der Impedanz während der HFS-Ablation ist prädiktiv für die Läsionsbildung, da es einen Schaden des zugrundeliegenden Gewebes impliziert (55,56). Die über den Generator abgeleitete Impedanz (beinhaltet ebenfalls die intrathorakalen Impedanzen von Muskeln, Lunge, Knochen) scheint jedoch als Messinstrument zur genauen Bestimmung der Katheter-Gewebe-Kopplung limitiert und unpräzise (55).

Im Rahmen der im Folgenden genannten Publikation wurde daher erstmals ein Ablationskatheter im Menschen untersucht, welcher die Möglichkeit bietet eine lokale Impedanz (LI), durch Einsatz von Mini-Elektroden, zu messen. Ziel der Arbeit war die Untersuchung des Nutzens eines solchen neuen Katheters zur Messung der LI sowie der Vergleich zwischen LI mit der etablierten Generator-Impedanz (GI).

Publikation Nr. 2:

Gunawardene M, *Münkler P, Eickholt C, Akbulak RÖ, Jularic M, Klatt N, Hartmann J, Dinshaw L, Jungen C, Moser JM, Merbold L, Willems S, Meyer C. A novel assessment of local impedance during catheter ablation: initial experience in humans comparing local and generator measurements. Europace. 2019 Jan 1;21(Supplement_1):i34-i42. doi: 10.1093/europace/euy273. PMID: 30801126.*

In diese Studie wurden 25 konsekutive Patient:innen eingeschlossen, die sich mit der Indikation zur Re-Ablation von rezidivierendem VHF und/oder atrialen Tachykardien vorstellten (**Tabelle 4:** Basischarakteristika und prozedurale Daten). Bei allen Patient:innen wurde eine Katheterablation mit Verwendung eines ultra-hochauflösenden Mappingsystems und dem gespülten, LI-messenden Ablationskatheter durchgeführt. Die LI wurde hierbei über ein 4-Elektrodenprinzip gemessen mit separaten Kreisläufen für die Etablierung und Messung des elektrischen Feldes. Zwischen proximaler und distaler Elektrode wurde ein nicht-stimulierender Wechselstrom appliziert, während passiv zwischen den Minielektroden und dem distalen Ring des Katheters die LI gemessen wurde (55).

Im Rahmen der Arbeit wurde die LI im Blut (als kontaktlose Referenz), sowie die Ausgangs-LI und Ausgangs-GI vor Ablationsbeginn am Gewebe, sowie der Abfall der LI (△LI) und GI (△GI) während der HFS-Ablation untersucht.

Basischarakteristika	**Patienten (n=25)**
Männliches Geschlecht [n, %]:	15 (60%)
Alter [Jahre]	66,3 ± 12,8
Arterielle Hypertonie [n, %]	15 (60%)
Kardiomyopathie [n, %]	3 (12%)
Koronare Herzerkrankung [n, %]	3 (12%)
Diabetes mellitus [n, %]	1 (4%)
Schlaganfall/ TIA [n, %]	5 (20%)
BMI [kg/m^2]	27,0 ± 4,1
CHA_2DS_2-VASc score [n, %]	2,6 ± 1,6
Indikation zur Re-ablation [n, %]	4 (16%)
- Rezidiv paroxysmales VHF	11 (44%)
- Rezidiv persistierendes VHF	10 (40%)
- Links-/Rechts- atriale Tachykardie	
Anzahl an Vorablationen [n]	2,4 ±1,6
Prozedurale Parameter	
Prozedurdauer [min]	156,6 ± 53,1

Durchleuchtungszeit [min]	18,1 ± 10,3
HFS Abgaben [n]	24,6 ± 16,5
HFS Dauer [s]	1637,8 ± 1190,0
Kumulative Energie [J]	44.605 ± 34.869
LA Volumen [ml]	96,6 ± 51,4
LA Mappingzeit [min]	13,2 ± 10,3
LA Mapping Punkte [n]	9958,1 ± 8064,1
Komplikationen:	
- Leistenkomplikation [n, %]	1 (4) minor groin hematoma
- Perikardtamponade [n, %]	1 (4)
- TIA/Schlaganfall	-

Tabelle 4: Basischarakteristika und prozedurale Daten. BMI, Body-Mass-Index; CHA2DS2-VASc Score (Score zur Evaluation des Schlaganfallrisikos); J, Joule; min, Minuten; ml, Milliliter; s, Sekunden; TIA, transitorisch ischämische Attacke; VHF, Vorhofflimmern. Werte sind als Mittelwert ± Standardabweichung angegeben, [n] oder n (%).

Bei 381 analysierten HFS-Abgaben mit dem Ablationskatheter konnte dargestellt werden, dass die Ausgangs-LI niedriger war als die durch den Generator gemessene Ausgangsimpedanz (GI) [LI: 99,9 ± 14,9 Ω (n = 447) vs. GI: 115,1± 11,7 Ω GI, P< 0,001]. Das gemessene △LI war mehr als doppelt so groß wie das △GI [LI: 13,1± 9,1 Ω (n=389) vs. GI: 6,1± 4,2 Ω (n=362), P< 0,001]. Zudem sagte eine höhere Ausgangs-LI ein größeres △LI vorher (adjustiertes R^2=0,41, P<0,001, 95%-KI [0,34 - 0,44]), während die Ausgangs-GI kein guter Prädiktor für △GI war (adjustiertes R^2=0,06; P<0,001, 95%-KI [0,05- 0,14]), (**Abbildung 3**).

Zudem waren die Werte der Ausgangs-LI mit der Voltage des zugrundeliegenden Myokards assoziiert. Eine höhere Ausgangs-LI fand sich in Arealen mit hoher Voltage > 0,5mV (also im gesunden Gewebe; (LI: 110,5 ± 13,7Ω)) im Vergleich zu narbigen Myokard mit entsprechend intermediären 0,1-0,5mV (LI: 90,9±10,1Ω, P<0,001), oder niedrigen <0,1mV (LI 91,9±16,4Ω, P<0,001) Voltagewerten, sowie im Vergleich zur Impedanz des Blutes (LI: 91,9±9,9Ω, P<0,001) (**Abbildung 4**).

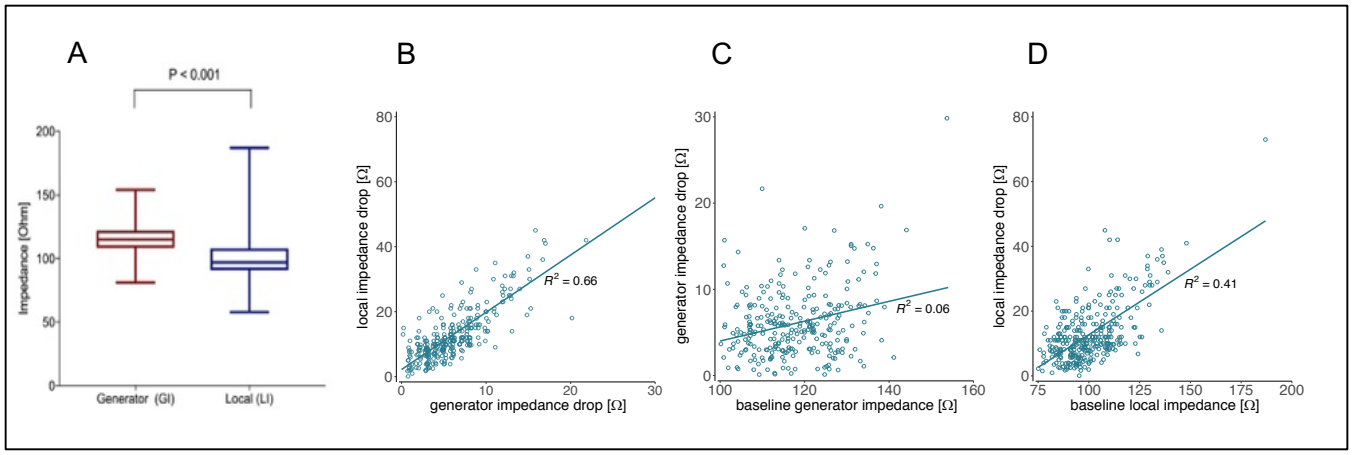

Abbildung 3: Lokale Impedanz im Vergleich zur Generatorimpedanz während der Katheterablation.

3A: Diskriminierung zwischen Ausgangs-GI und –LI. 3B: Vergleich △LI und △GI. 3C: Korrelation zwischen Ausgangs-GI und △GI. 3D: Korrelation zwischen Ausgangs-LI und △LI.

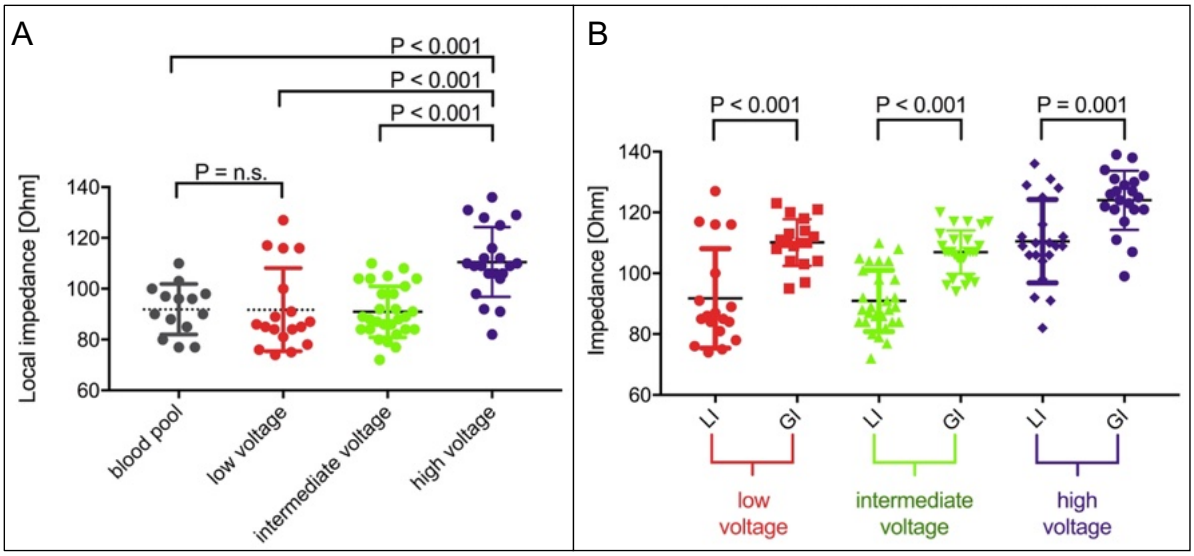

Abbildung 4: Zusammenhang zwischen Impedanz und Voltage des Myokards. 4A: Ausgangs-LI in verschiedenen Voltagearealen. 4B: Vergleich Ausgangs-LI und –GI in verschiedenen Voltagearealen.

HFS-Applikationen zeigten zum Zeitpunkt der Terminierung atrialer Tachykardien ein △LI von 8,5 ± 4,6 Ω mit einem Maximum nach 25 Sekunden von △LI 14,8 ± 8,3 Ω.

Des Weiteren kam es in der Studie bei einem Patienten während der HFS-Ablation zu einem rasanten △LI von 45 Ω und zum Auftreten einer behandlungsbedürftigen Perikardtamponade.

Zusammenfassend kann festgehalten werden, dass durch die LI der Kontakt zwischen Katheter und Gewebe bestätigt werden kann. Die LI scheint, wie in einer präklinischen Studie bereits analysiert (55), auch im Menschen aufgrund der besseren Sensitivität ein geeigneterer Indikator zur Bestimmung der Katheterstabilität, Evaluation der Gewebeeigenschaften (gesunde vs. Narbenareale) und Läsionsbildung im Vergleich zur GI. Eine Limitation der Arbeit ist allerdings die fehlende Messung der Anpresskraft ans Gewebe um den vermuteten Grad des Kontaktes genauer zu verifizieren, besonders in Narbenarealen mit niedriger Voltage. Der in der Arbeit verwendete Katheter besitzt keine technische Möglichkeit zur Messung der genauen Anpresskraft.

Ein gewisser Abfall der LI ist notwendig, um eine Läsion während der Ablation zu bilden. In dieser Studie zeigte sich, dass es bei im Mittel 8,5 Ω zu einer Terminierung der atrialen Tachykardien und somit klinischen Effektivität kam (Beispiel der Katheterablation mit dem LI-messenden Ablationskatheter in **Abbildung 5**). Dieser Wert kann somit als Surrogatparameter für akute Effektivität herangezogen werden. Bei einem zu rasanten Abfall der LI sollte die Ablation jedoch vorzeitig beendet werden, da dies mit einem erhöhten Komplikationsrisiko assoziiert ist. Bei einem Cut-off von $\triangle$LI 40 Ω kam es in den darauffolgenden 97 Prozeduren mit diesem Ablationskatheter zu keiner weiteren Perikardtamponade.

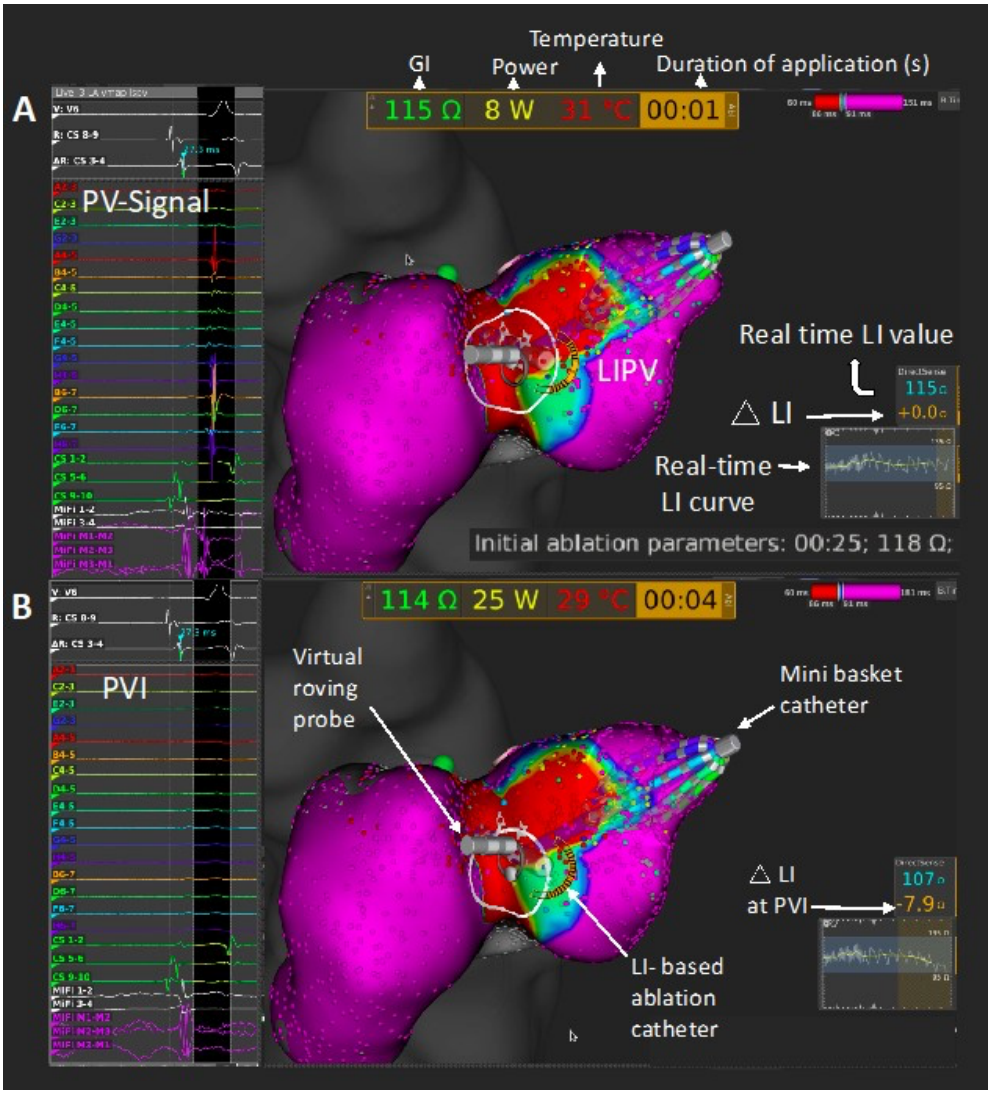

Abbildung 5: Re-Pulmonalvenenisolation mit einem LI-messenden Ablationskatheter. Gezeigt wird ein ultra-hochauflösendes Aktivierungsmap einer linken unteren Pulmonalvene (PV) im linken Vorhof, welche eine Leitungserholung mit verbliebendem PV-Signal am anterioren PV-Ostium und eine Ausgangs-LI von 115 Ω und einer Ausgangs-GI von 118 Ω kurz vor Ablationsbeginn aufwies (**5A**). Während der HFS-Ablation kam es innerhalb von 4 Sekunden unter Echtzeitdarstellung bei einem △LI von 7,9 Ω zu einer Blockierung der PV mit Nachweis einer nun isolierten PV (PVI) (**5B**). Das PV Signal zeigte sich nun verschwunden.

3.3. Auftreten komplexer atrialer Tachykardien und die Charakterisierung von Leitungslücken in den initialen Ablationslinien um die Pulmonalvenen nach initialer Hochfrequenzstrom- und Cryoablation unter Verwendung eines ultra-hochauflösenden Mappingssystems

Die Erfolgsraten der Katheterablation haben sich mit den aktuellen Technologien verbessert: die Cryoballon-geführte PVI ist der HFS-PVI nicht unterlegen (15). Dennoch kann es zu Arrhythmierezidiven nach initialer PVI kommen. Die häufigste Ursache hierfür ist eine Rekonnektion der Pulmonalvene im Bereich der initialen Ablationslinie (36). Seltener kommt es auch ohne vorheriger Substratmodifikation zum Auftreten komplexer atrialer Tachykardien (AT) nach reiner PVI (57,58).
Die Verwendung von Mappingkathetern mit multiplen Elektroden ermöglicht in Verbindung mit einem 3D-Mappingsystem eine ultra-hochauflösende Kartierung der Vorhöfe (bzw. Kammern) unter Einbeziehung einer hohen Anzahl von Elektrogrammen. Die hierdurch gegebene, hohe räumliche Auflösung ermöglicht einen genaueren Einblick in die elektrophysiologischen Abläufe während der Katheterablation.

Ziel der im Folgenden genannten Publikation war die Untersuchung elektrophysiologischer Charakteristika bei Patient:innen mit Arrhythmie-Rezidiv nach initialer PVI mit entweder Anpresskraft-kontrollierter HFS-Ablation (CF-HFS Gruppe) oder initialer PVI mit dem Zweitgenerations-Cryoballon (2CB-Gruppe) unter Verwendung eines ultra-hochauflösenden Mappingsystems. Der Schwerpunkt bestand hier vor allem in der Charakterisierung und dem Vergleich der Pulmonalvenen-Rekonnektion in den beiden Gruppen sowie der Analyse konsekutiver AT.

Publikation Nr. 3:

Gunawardene MA, *Eickholt C, Akbulak RÖ, Jularic M, Klatt N, Hartmann J, Schlüter M, Meyer C, Willems S, Schaeffer B. Ultra-high-density mapping of conduction gaps and atrial tachycardias: Distinctive patterns following pulmonary vein isolation with cryoballoon or contact-force-guided radiofrequency current. J Cardiovasc Electrophysiol. 2020 May;31(5):1051-1061. doi: 10.1111/jce.14413. Epub 2020 Mar 9. PMID: 32107811.*

Insgesamt wurden 50 Patient:innen mit Arrhythmierezidiv 335 Tage (Median; q1-q3:232-622 Tage) nach Index-Ablation eingeschlossen und mittels ultra-hochauflösenden Mappings und HFS-Ablation mit Verwendung eines LI-messenden Ablationskatheters erneut abladiert.

Es gab keinen Unterschied zwischen den beiden Gruppen in Bezug auf den Typ der indikationsrechtfertigenden Arrhythmieform beim Zweiteingriff (VHF in 38 %, AT 40 %, beide Arrhythmieformen in 22 %, p=0,094 im Gruppenvergleich; **Abbildung 6**).

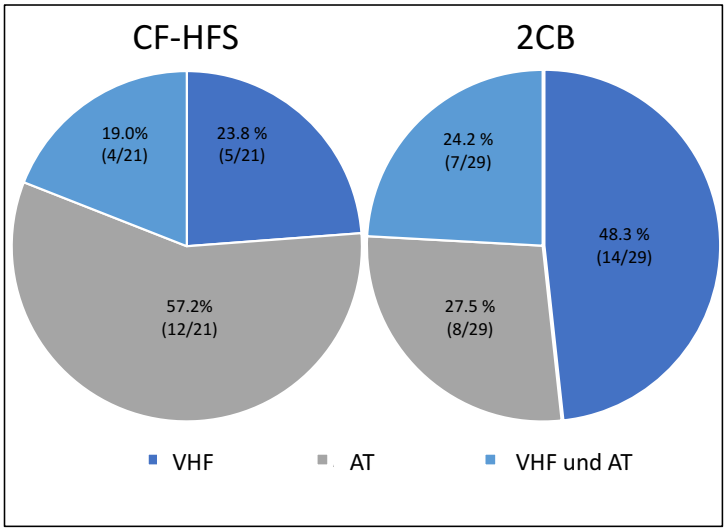

Abbildung 6: Verteilung der Arrhythmierezidiv-Typen auf die beiden Gruppen. AT, atriale Tachykardie; VHF, Vorhofflimmern

Die prozeduralen Parameter und Komplikationen werden in **Tabelle 5** zusammengefasst.

Prozedurale Parameter	**Alle n=50**	**CF-HFS n =21**	**2CB n = 29**	**P-Wert**
Initialer Rhythmus bei Re-Prozedur				0,127
• Sinusrhythmus	28 (56,0)	9 (42,9)	19 (65,5)	
• Vorhofflimmern	10 (20,0)	4 (19,0)	6 (20,7)	
• Atriale Tachykardie	12 (24,0)	8 (38,1)	4 (13,8)	
Prozedurdauer (min)	153,2 ± 54,9	161,5 ±57,8	147,6 ± 53,0	0,387
Durchleuchtungszeit (min)	18,3 ± 9,2	19,0 ± 10,8	17,8 ± 8,2	0,649
UHDx- LA Mapping Punkte	10.438 ± 6.639	11.951 ± 6.181	9.390 ± 6.859	0,212
Gemapptes LA Volume (ml)	126,2 ± 57,2	112,9 ± 39,1	135,2 ± 66,0	0,219
Ablationsstrategien				
• Re-Pulmonalvenenisolation	45 (90,0)	20 (95,2)	25 (86,2)	0,383
• Substratmodifikation	11 (22,0)	2 (9,5)	9 (31,0)	0,098
• Ablation von AT	31 (62,0)	16 (76,2)	15 (51,7)	0,139
• Ablation fraktionierter Signale entlang der initialen Ablationslinie	11 (22,0)	2 (9,5)	9 (31,0)	0,098
Gesamtkomplikationsrate	4 (8)	1 (4,8)	3 (10,3)	0,630

• Perikardtamponade	1 (2)	1 (4,8)	0 (0)
• Intermittierende Dysarthrie*	1 (2)	0 (0)	1 (3,4)
• Nichtschwerwiegende Leistenkomplikation	2 (4)	0 (0)	2 (6,9)

Tabelle 5: Prozedurale Parameter und Komplikationen. Werte sind als Mittelwert ± Standardabweichung angegeben, [n] oder n (%). AT, Atriale Tachykardie; CB, Cryoballon; CF, Anpresskraft; HFS, Hochfrequenzstrom-Ablation; LA, linkes Atrium; PV, Pulmonalvenen;

*Dysarthrie unmittelbar nach Prozedurende, ohne weitere Fokalneurologie und mit normalem kranialen CT (a. e. sedierungsbedingt).

Die durch ultra-hochauflösendes Mapping identifizierte Rate an rekonnektierten Pulmonalvenen (PV) war nach initialer CF-HFS PVI (2,5 ± 1,3 PV pro Patient:in) höher als nach 2CB PVI (1,4 ± 0,9 PV, p=0,003). Hierbei kam es häufiger zu einer Rekonnektion der linken Pulmonalvenen nach CF-HFS (27/42 [64,3%]) als nach 2CB (20/56 [35,7%], p=0,0077). Die Rekonnektionsrate der rechten Pulmonalvenen unterschied sich in den beiden Gruppen nicht (25/43 [58,1%] vs. 24/58 [41,4%], P=0.110).

Insgesamt wurden 58 (CF-HFS: 58/52PVs, 1.12 Leitungslücken pro rekonnektierter PV) und 49 Leitungslücken (2CB: 49/41 PVs, 1.20 Leitungslücken pro rekonnektierter PV) erfasst.

Dabei fanden sich die Leitungslücken an den linken Pulmonalvenen vor allem anterior und im Bereich der Carina nach CF-HFS PVI und im inferioren Bereich der rechten unteren Pulmonalvene nach initialer 2CB PVI, **Abbildung 7**. Alle Pulmonalvenen konnten erfolgreich re-isoliert werden, 63,6% (68/107) hierbei unter Echtzeit-Beobachtung. Bezüglich der Ablationsparameter, unterschieden sich die Ausgangs-LI (CF-HFS 100,7±14,6 Ω vs. 2CB 100,5±12,36 Ω; p=0,942) sowie das △LI (CF-HFS: Median 9,9 [8-18] Ω vs. 2CB: Median 12 [7-18] Ω; p=0,981) während der Re-Pulmonalvenenisolation nicht zwischen den beiden Gruppen.

Durch ultra-hochauflösendes Mapping detektierte fraktionierte Signale im Bereich der initialen antralen Ablationslinie entlang der Pulmonalvenen fand sich bei zwei Patient:innen (9,5%) nach CF-HFS und bei neun Patient:innen (31,0%) nach 2CB PVI (p=0,092) **(Abbildung 8)**. Interessanterweise konnten diese fraktionierten Signale bei insgesamt 5 Patient:innen (5/11; 45,5% bei 1 CF-HFS (1/2, 50%) und 4 2CB (4/9, 44,4%)) als kritischer Isthmus der zugrundeliegenden Makroreentry-AT identifiziert werden. Alle 5 AT konnten in diesem

Bereich durch Ablation terminiert werden und alle Pulmonalvenen erfolgreich re-isoliert werden.

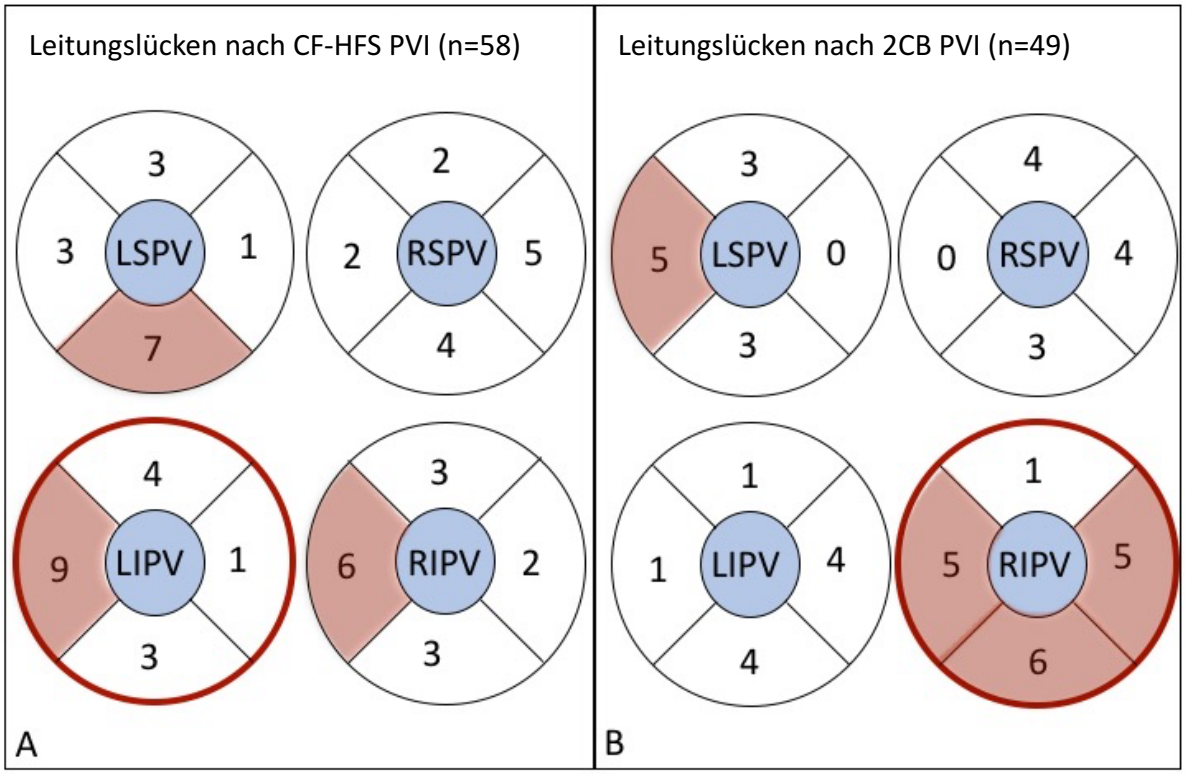

Abbildung 7: Verteilung der Leitungslücken entlang der Pulmonalvenenostien beider Gruppen.

Unterteilt sind die Pulmonalvenenostien in Quadranten. Die Zahl gibt die Anzahl der identifizierten Leitungserholungen pro Lokalisation an. Bereiche mit mindestens fünfmaligem Auftreten einer Leitungserholung sind in rot markiert. A: Anpresskraft-kontrollierte Hochfrequenzstrom-Gruppe (CF-HFS); B: Zweitgenerations Cryoballon-Gruppe (2CB). RSPV, rechte superiore Pulmonalvene; RIPV, rechte inferiore Pulmonalvene, LSPV, linke superiore Pulmonalvene; LIPV, linke untere Pulmonalvene.

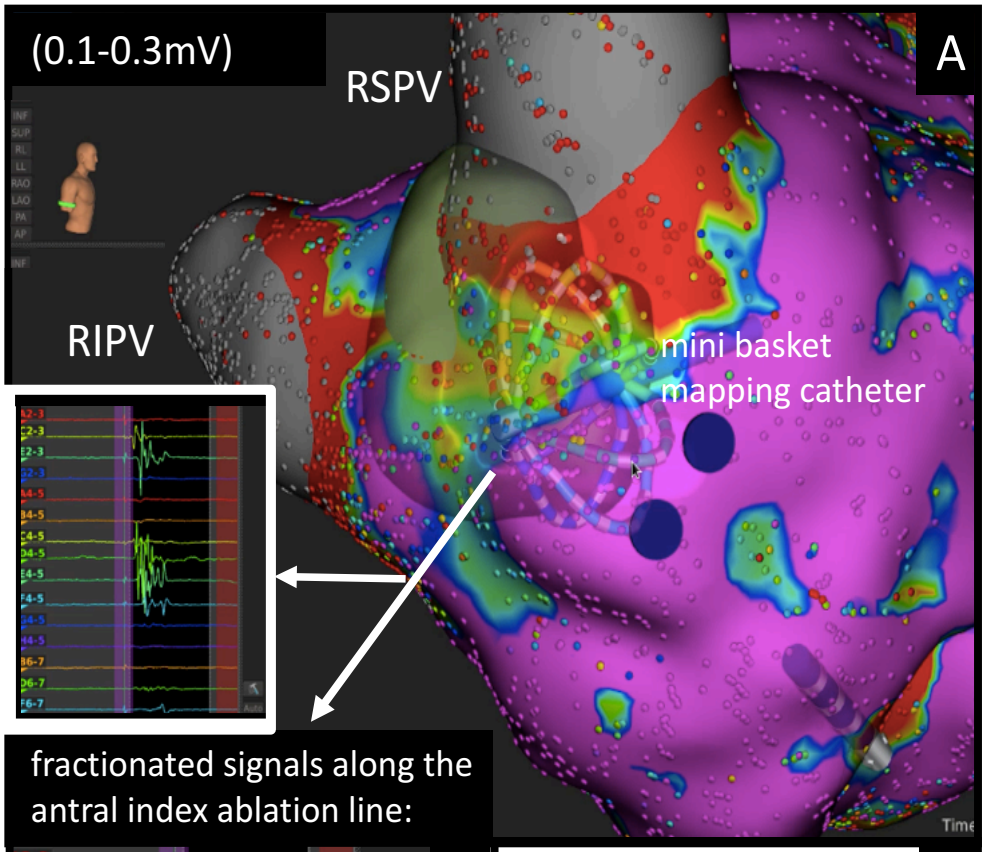

Abbildung 8: Fraktioniertes Signal entlang der initialen antralen Ablationslinie vor den rechten Pulmonalvenen im ultra-hochauflösenden Voltage-Map – detektiert durch den am Pulmonalvenenostium positionierten multipolaren korbförmigen Mappingkatheter. RSPV, rechte superiore Pulmonalvene; RIPV, rechte inferiore Pulmonalvene.

Insgesamt 45 atriale Tachykardien fanden sich bei 31 Patient:innen (31/ 50; 62%) des Studienkollektivs ohne Gruppenunterschied (CF-HFS 16/21 [76,2%] und 2CB 15/29 [51,7%], p=0,139). Der häufigste zugrundeliegende Mechanismus der AT waren Makro-Reentry-Tachykardien (n=36; CF-HFS: 15/19 [78,9%] vs. 2CB: 21/26 [80,8%]; P=1.0), gefolgt von Mikroreentry-Tachykardien (n=8; CF-HFS: 3/19 [15,7%] vs. 2CB: 5/26 [19,2%], P=1.0) und fokaler AT (n=1; CF-HFS: 1/19 [5,4%] vs. 2CB: 0%, p=0,422), **Abbildung 9**.

Es gab keinen Unterschied zwischen den Gruppen im Auftreten der AT, welche mit der initialen PVI assoziiert waren (inkl. AT entlang der initialen antralen Ablationslinie, AT aus dem Bereich des Übergangs zwischen linken Pulmonalvenen und Vorhofohr, sowie PV-abhängige AT; CF-HFS: 7/19 [36,8%] vs. 2CB: 5/26 [19,2%], p=0,306).

Während der Zweitprozedur konnten alle AT erfolgreich behandelt werden. Die Terminierung der AT durch Ablation wurde bei △ LI von 6,7 ± 4,3 Ω bei CF-HFS Patient:innen und bei einem △ LI von 12,8 ± 9,4 Ω in 2CB Patient:innen (P=0.087) erreicht.

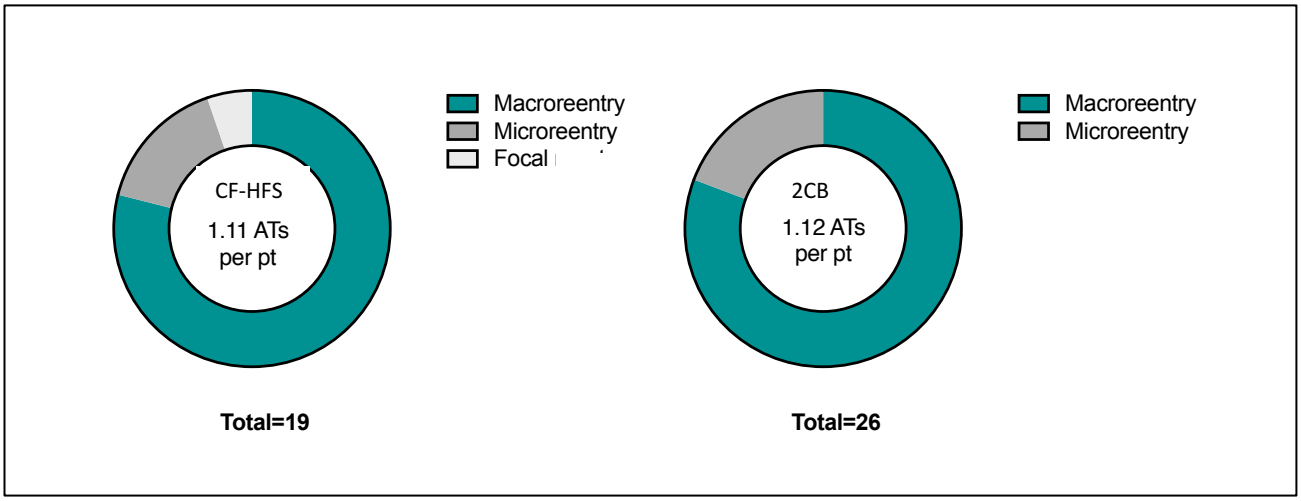

Abbildung 9: Verteilung der atrialen Tachykardie-Mechanismen in beiden Gruppen. CF-HFS, anpresskraftkontrollierte Hochfrequenzstrom-Ablation; 2CB, Zweitgenerations-Cryoballon Ablation; per pt, pro Patient.

Die Ergebnisse dieser Arbeit zeigen, dass das ultra-hochauflösendes Mapping geeignet ist Leitungserholungen entlang der initialen Ablationslinie nach vorheriger PVI genau zu lokalisieren und diese erfolgreich durch erneute Ablation zu isolieren.

Ein typisches, sich zwischen den Energieformen unterscheidbares Verteilungsmuster dieser Leitungslücken konnte identifiziert werden: vor allem die linken Pulmonalvenen zeigten sich häufiger nach CF-HFS Ablation leitungserholt, im Vergleich zu einer vorherigen 2CB PVI.

Konsekutive atriale Tachykardien nach initialer PVI waren am häufigsten durch Makro-Reentry-Mechanismen verursacht. Diese atrialen Tachykardien können mit fraktionierten Potenzialen entlang der initialen antralen Ablationslinie assoziiert sein und sind häufiger nach Index-PVI mit 2CB.

Die in dieser Arbeit gewonnenen elektrophysiologischen Erkenntnisse der Zweitprozedur können die Durchführung der Indexprozedur mit anpresskontrollierter HFS oder Cryoballongeführten Ablation somit optimieren und bieten hierdurch das Potenzial Arrhythmierezidive nach initialer PVI zu vermeiden.

3.4 Pulsed Field Ablation unter Verwendung eines ultra-hochauflösenden Mappingssystems – Elektrophysiologische Charakteristika und praktische Herangehensweise

Pulsed Field Ablation (PFA) bietet eine nicht-thermale Energiequelle zur Katheterablation von VHF. Klinische Daten, unter anderem zur Charakterisierung der PFA-Läsionen im linken Vorhof sind limitiert. Eine Analyse aus Daten der initialen Zulassungsstudien konnte zeigen, dass sich die durch PFA erzeugten Ablationslinien entlang der Pulmonalvenenostien über die Zeit beständig zeigten mit Nachweis hoher Isolationsraten (59). Zudem war eine routinemäßige Visualisierung des multipolaren PFA-Katheters im Mappingsystem zum Zeitpunkt unserer Arbeit noch nicht untersucht. Wie bereits erwähnt, ermöglicht die Verwendung von Multielektroden-Mappingkathetern die Möglichkeit einer hohen räumlichen Auflösung und so einen detaillierten Einblick in die elektrophysiologischen Gegebenheiten.

Ziel der hier genannten Publikation war die Evaluation der Visualisierung des PFA-Ablationskatheters im ultra-hochauflösenden Mappingsystem mit Charakterisierung der akuten PFA Läsionen bei symptomatischen Patient:innen mit paroxysmalem und persistierendem VHF, die sich einer PFA-geführten Katheterablation unterzogen. Diese Arbeit lieferte weltweit die ersten Untersuchungen zu einem multipolaren PFA-System außerhalb der Zulassungsstudien.

Publikation Nr. 4:

Gunawardene MA, *Schaeffer BN, Jularic M, Eickholt C, Maurer T, Akbulak RÖ, Flindt M, Anwar O, Pape UF, Maasberg S, Gessler N, Hartmann J, Willems S. Pulsed-field ablation combined with ultrahigh-density mapping in patients undergoing catheter ablation for atrial fibrillation: Practical and electrophysiological considerations. J Cardiovasc Electrophysiol. 2022 Mar;33(3):345-356. doi: 10.1111/jce.15349. Epub 2022 Jan 9. PMID: 34978360.*

Im Rahmen der Katheterablation erfolgte bei allen Patient:innen nach linksatrialem Zugang zunächst das Erstellen einer ultra-hochauflösenden 3D-Anatomie des linken Vorhofs (ein sogenanntes „Map“) vor Ablation. Anschließend erfolgte die PFA (PVI alleine oder PVI inklusive Substratmodifikation) mit Impedanz-gesteuerter Visualisierung des PFA-Katheters.

Nach Ablation erfolgte ein erneutes ultra-hochauflösendes Mapping des linken Vorhofs. Dargestellt wurden die äquatorialen Elektroden als zirkuläre Form, größenadaptiert an die möglichen zwei Konfigurationen des mulitpolaren PFA-Katheters in „Korb"-und „Blumen"-Konfiguration. Für die PVI wurden je Pulmonalvene 8 PFA-Impulse (je 2x2 in „Korb"- und 2x2 in „Blumen"-Konfiguration) appliziert. Für die Isolation der linksatrialen Hinterwand (LAPWI, englisch *left atrial posterior wall isolation*) und Mitralisthmuslinie wurde nur die „Blumen"-Konfiguration des Katheters verwendet.

Für die Analyse der Ebene, Kontinuität und Homogenität der PFA-Läsionen wurden in den prä- und post-Ablationsmaps des linken Vorhofs Oberflächen und - Abstandsmessungen erhoben, sowie die Elektrogrammaplitude vor und nach Ablation bestimmt (**Abbildung 10**). Zudem erfolgte eine nachbearbeitete Untersuchung komplexer fraktionierter Signale durch die Software des Systems.

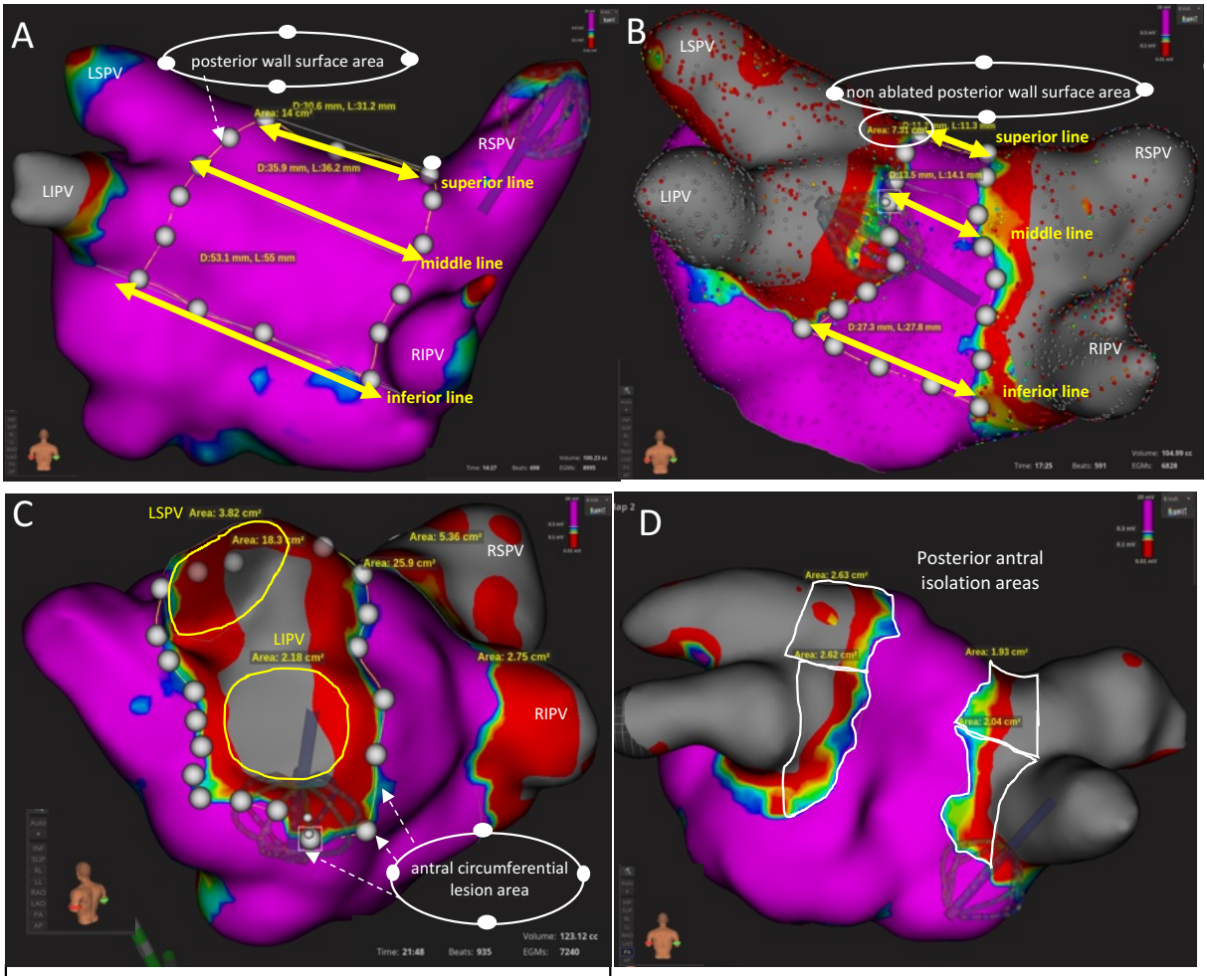

Abbildung 10: Methodik zur Vermessung der Oberflächen und Abstände in den prä und post Ablations-Voltage-Maps (ultrahochauflösende 3D Rekonstruktionen des linken Vorhofs). Bestimmung von Fläche der antralen Isolation entlang der posterioren rechten und linken PV (D, *posterior antral isolation areas*), Fläche der

linksatrialen Hinterwand vor und nach Ablation (A, B *posterior wall surface area*), Abstand der PV-Ostien bzw. antralen Isolationslinien posterior vor und nach Ablation (A, B superiore, mittlere und inferiore Linie), Fläche des PV-Ostiums (C, gelb) und zirkumferentielle antrale Läsionsfläche, (C, *circumferential lesion area*).

Zwanzig konsekutive VHF-Patient:innen (n=7 (35%) paroxysmal; n= 13 (65%) persistierend) erhielten entweder eine reine PFA-geführte PVI (n=11, 55%) oder eine PFA-geführte PVI und zusätzliche Substratmodifikation (n= 9; 45%) mit LAPWI (n=9) und/oder Anlage einer Mitralisthmuslinie (n=2), (**Tabelle 6**: Patientencharakteristika und prozedurale Parameter).

Die Visualisierung des PFA-Katheters war bei 17/19 (89.5%) Patient:innen möglich. Initial konnte der PFA-Katheter bei zwei Patient:innen nicht visualisiert werden. Nach Adaptation der Methodik (Belassen des Mappingkatheters in der Vena cava inferior zur Stabilisierung der Felddetektion) war dies in allen weiteren Fällen möglich. Die Visualisierung korrelierte gut mit der Ebene der Ablationslinie im post-Ablations-Map (17/17, 100% linke PV und 15/17 (88.2%) rechte PV der Patient:innen; 7/8 (87.5%) LAPWI) mit nur einem „Shift“ der Anatomie in einem der Patient:innen (**Abbildung 11**).

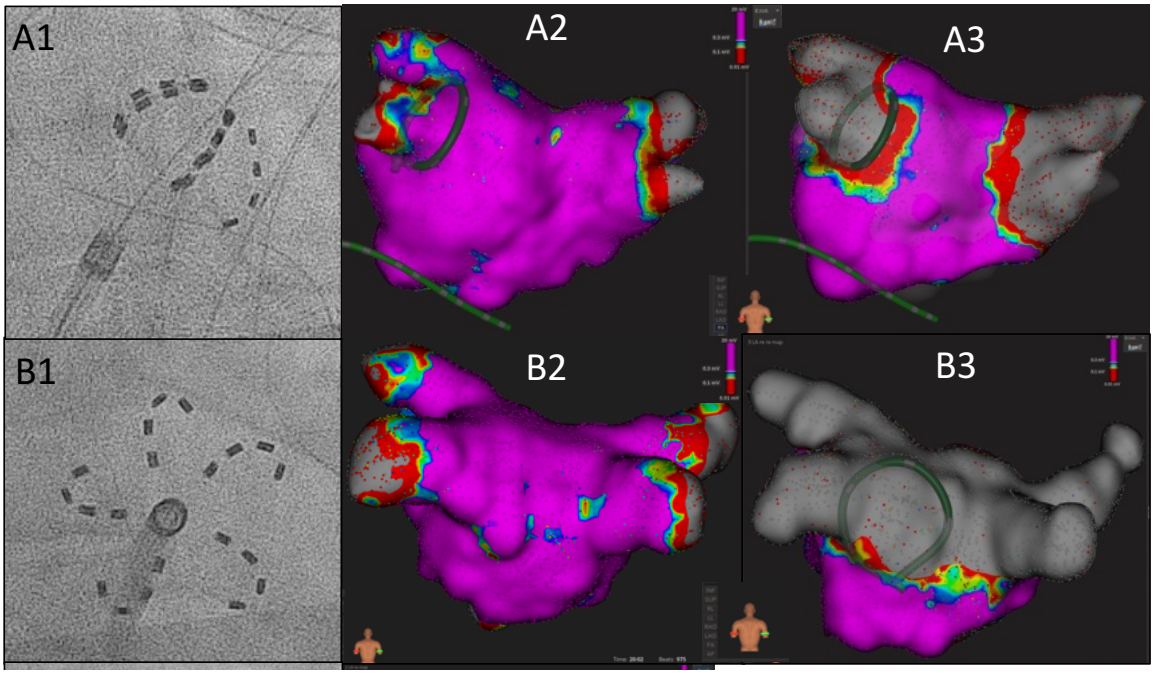

Abbildung 11: Prä- und post-Ablations-Map des linken Vorhofes mit Visualisierung des PFA-Katheters. A1+B1: Fluoroskopische Darstellung des multipolaren PFA-Katheters (A1:“Korb“-Konfiguration; B1 „Blumen“-Konfiguration). A2+A3: Prä (A2)- und post (A3)- ultrahochauflösendes Voltagemap des linken Vorhofs mit Darstellung der Pulmonalvenenisolation und Ebene der Ablationslinie mit Visualisierung des PFA-Katheters in

„Korb"-Konfiguration im Bereich der linken unteren Pulmonalvene (Aufsicht von hinten auf den linken Vorhof). B2+B3: Prä (B2)- und post (B3)- ultrahochauflösendes Voltagemap des linken Vorhofs mit Darstellung der linksatrialen Hinterwand mit Visualisierung des PFA-Katheters im Bereich der isolierten Hinterwand in der „Blumen"-Konfiguration (Aufsicht von hinten auf den linken Vorhof). Farbcodierung: Rot und Grau markieren die Narbenareale bzw. durch Ablation gesetzte Narben, lila gesundes Vorhofmyokard.

	Alle **n=20**	**PVI** **n =11**	**PVI + Substratmodifikation** **n = 9**
Alter (Jahre)	70,3 ± 9,7	75,2 ± 6,2	64,4 ± 10,2
Männliches Geschlecht	12 (60,0)	6 (54,5)	6 (66,7)
Arterielle Hypertonie	16 (8,0)	9 (81,8)	7 (77,8)
BMI (kg/m^2)	26,0 ± 4,8	25,9 ± 5,3	26,1 ± 4,5
CHA_2DS_2-VASc score	2,5 [2-4]	3 [2-3,5]	2 [1-4]
Art des Vorhofflimmerns			
- paroxysmales VHF	7 (35,0)	7 (77,8)	0 (0,0)
- persistierendes VHF	13 (65,0)	4 (22,0)	9 (100,0)
Linksatrialer Diameter (mm)	43,8 ± 4,9	45,2 ± 4,1	42,1 ± 5,8
Erhaltene linksventrikuläre Funktion	15 (75,0)	10 (90,9)	5 (55,6)
Prozedurale Parameter			
Prozedurdauer (min)	123 ± 21,6	121,1 ± 20,6	125,4 ± 23,8
Durchleuchtungszeit (min)	19,2 ± 5,5	20,3 ± 5,5	17,9 ± 5,5
Pulsed Field Ablation			
PFA-Impulse			
gesamt, pro Patient	32 [32-36]	32 [32-33]	36 [32-36]
LSPV	8 [8-8]	8 [8-8]	8 [8-8]
LIPV	8 [8-8]	8 [8-8]	8 [8-8]
RSPV	8 [8-10,5]	8 [8-9]	8 [8-12]
RIPV	8 [8-8]	8 [8-8]	8 [8-8]
Linksatriale Hinterwand	10 [8-12]	N/A	10 [8-12]
Mitralisthmus Line	10 [9-11]	N/A	10 [9-11]
Ultrahochauflösendes Mapping (UHDx)			
Rhythmus während Mapping			
- Sinusrhythmus	18 (90,0)	10 (90,9)	8 (88,9)
- VHF	2*(10,0)	1 (9,1)	1 (11,1)
UHDx- LA Mapping Punkte	7261 ± 3517	7740 ± 3016	6677 ± 4162
Gemapptes LA Volumen (ml)	148 ± 24,7	134 ± 19,5	164 ± 20,4
LA Mapping Zeit, (min)	35,7 ± 10,2	36,5 ± 10,5	34,6 ± 10,3
	17,2 ± 3,0	17,9 ± 3,1	16,5 ± 2,9
Alle Komplikationen	1 (5,0)	0 (0,0)	1 (11,1)
• Koronarspasmus	1 (5,0)	0 (0,0)	1 (11,1)

Tabelle 6: Patientencharakteristika und prozedurale Daten. BMI, Body-Mass-Index; CHA2DS2-VASc Score (Score zur Evaluation des Schlaganfallrisikos); LA, linkes Atrium; min, Minuten; ml, Milliliter; PFA, Pulsed Field Ablation; UHDx ultra-hochauflösendes Mapping. Werte sind als Mittelwert ± Standardabweichung angegeben, [n] oder n (%).

Nach initialer PVI aller 80 Pulmonalvenen mit PFA, kam es bei 6,25% (n=5) der Pulmonalvenen zu einer akuten Pulmonalvenenrekonnektion (n=2 LSPV, n=3 RSPV; **Abbildung 11**). Im ultrahochauflösenden Map zeigten sich die Leitungslücken alle anterior am Pulmonalvenenostium. Durch erneute PFA konnten diese Leitungslücken erfolgreich geschlossen und alle Pulmonalvenen re-isoliert werden.
Bezüglich der Charakterisierung der Ablationsläsionen zeigte sich eine signifikante Reduktion der Voltage (Elektrogrammamplitude) im Bereich der Pulmonalvenenostien vor und nach PFA (1,67 ± 1,36 mV vs. 0,053 ± 0,038 mV, *P < 0.0001*), der posterioren Fläche (16,9 ± 3,6 cm^2 vs. 9,4 ± 2,6 cm^2, P <0.001) und der Abstände der superioren (41,2 ± 7,7 vs. 19,4 ± 10,9mm, p=0.0001), mittleren (42,5 ± 6,0 vs. 16,7 ± 6,5 mm, p < 0,0001) und inferioren Linie (47.6 ± 7.9 vs. 25.2 ± 7.7mm, p <0.001) zwischen den Pulmonalvenenostien vor PFA bzw. Ablationslinien nach PFA. Die komplette zirkumferentielle antrale Läsionsfläche betrug 20,5 ± 3,8 cm^2 für die linken und 25,5 ± 5,7 cm^2 für die rechten PV.

Bei einem Patienten kam es während der PFA am Mitralisthmus zu ST-Hebungen in den inferolateralen EKG-Ableitungen. Eine sofortige Koronarangiographie zeigte einen Koronarspasmus des Ramus circumflexus der linken Herzkranzarterie. Durch intravenöse Gabe von Nitroglycerin zeigte sich der Koronarspasmus komplett regredient. Es kam zu keiner hämodynamischen Kompromittierung oder Folgeschäden des Patienten. Dieses Vorkommnis wurde gesondert als Fallbericht publiziert (60).

Es kam zu keinen weiteren Komplikationen im Studienkollektiv. Eine im Mittel 1,4 ± 0,8 Tage nach Ablation durchgeführte Ösophagoskopie nach LAPWI zeigte keine ösophageale Läsionen.

Es kann festgehalten werden: PFA erzeugt weite antrale Ablationslinien um die Pulmonalvenen sowie eine homogene Isolation der linksatrialen Hinterwand. Durch die Ergebnisse dieser Arbeit konnten praktische Handlungsempfehlungen gegeben werden, die

zu einer Vermeidung möglicher akuter Pulmonalvenenrekonnektionen führen und somit den Erfolg der PFA-geführten Katheterablation noch weiter verbessern. Die Visualisierung des PFA-Katheters kann zudem zur Einsparung von Durchleuchtung und besserer Positionierung des PFA-Katheters am Pulmonalvenenostium führen.

Der in dieser Untersuchung aufgetretene Koronarspamus war weltweit das erste veröffentlichte Vorkommnis dieser Art während der Katheterablation mit PFA. Unsere Erkenntnisse führten zur Durchführung präklinischer und klinischer Studien mit der Untersuchung von Koronarspasmen während PFA (61,62); mit dem Ergebnis, dass eine präventive intravenöse oder auch intrakoronare Gabe von Nitroglycerin das Auftreten von Koronarspasmen verhindern kann (61).

PFA zeigte sich insgesamt als sehr sicher, es kam, wenn auch bei kleiner Fallzahl zu keinen ösophagealen Auffälligkeiten nach Isolation der linksatrialen Hinterwand.

3.5 Pulsed Field Ablation in Kombination mit einem ultra-hochauflösenden Mappingssystem zur interventionellen Behandlung komplexer konsekutiver linksatrialer Tachykardien

Neben VHF kann es auch zu atrialen Tachykardie-Rezidiven nach vorheriger Katheterablation kommen. Hier kann aufgrund des komplexen Substrates, sowohl die Identifikation des zugrundeliegenden AT-Mechanismus als auch die Ablationsbehandlung als solche eine Herausforderung in der invasiven elektrophysiologischen Untersuchung darstellen (40,41).
Bessere Auflösung der elektrischen Signale durch ultra-hochauflösendes Mapping, Betrachtung der Aktivierungs- und Voltagemaps sowie Verwendung sog. Post-Processing-Algorithmen können zur Identifikation des AT-Mechanismus herangezogen werden (40,42).
PFA basiert auf einer nicht-thermalen Energieform, die bei der PVI hohe Raten dauerhaft isolierter Pulmonalvenen erwarten lässt, sodass PFA auch eine mögliche Ablationsalternative, u.a. nach gescheiterter Ablation mit thermaler Energieform sein könnte und auch ein erweitertes Anwendungsgebiet neben der PVI ermöglicht.
Hauptgegenstand der im Folgenden berichteten *Publikation Nummer 5* war die Evaluation der neuen Ablationstechnologie PFA zur Behandlung atrialer Tachykardien nach vorheriger Katheterablation, in Verbindung mit einem ultra-hochauflösenden Mappingsystem.

Publikation Nr. 5:

Gunawardene MA, *Schaeffer BN, Jularic M, Eickholt C, Akbulak RÖ, Hedenus K, Wahedi R, Anwar O, Gessler N, Hartmann J, Willems S. Pulsed field ablation in patients with complex consecutive atrial tachycardia in conjunction with ultra- high density mapping: Proof of concept. J Cardiovasc Electrophysiol. 2022 Dec;33(12):2431-2443. doi: 10.1111/jce.15713. Epub 2022 Nov 9. PMID: 36259717.*

Es wurden insgesamt 19 linksatriale Tachykardien (LAT) bei 15 Patient:innen (Alter 70 ± 10 Jahre, 73% männlich, im Median 4. Katheterablation [q1-q3: 3-6]) mit PFA erfolgreich behandelt. Der zugrundeliegende Mechanismus war ein Makroreentry bei 18/19 LAT und ein lokalisierter Reentry im Bereich des Übergangs zwischen linkem Herzohr und linker oberer Pulmonalvene (**Tabelle 7:** Patientencharakteristika und prozedurale Daten).

Zwei atriale Tachykardien waren rechtsatrial und wurden mit Hochfrequenzstrom behandelt (insgesamt somit 21 behandelte AT (19 linksatrial, 2 rechtsatrial); Zykluslänge 312±94 ms).

Patientencharakteristika	**n=15**
Alter (Jahre)	70,2 ± 9,7
Männliches Geschlecht, n (%)	11 (73,0)
Arterielle Hypertonie, n (%)	13 (86,7)
BMI (kg/m^2)	26,9 ± 8,5
CHA_2DS_2-VASc score	2 [3-4]
Aktuell Anzahl der Katheterablation (n)	4 [3-6]
Dauer der VHF-Erkrankung (Jahre)	7,5 ± 3
Art des VHF	
- paroxysmal, n (%)	1 (7,0)
- persistierend, n (%)	14 (93,0)
Vorherige Antiarrhythmika (n)	
• keine	5 (33,3)
• Klasse- Ic	4 (26,7)
• Klasse- III	6 (40,0)
Linksatrialer Diameter (mm)	45,7 ± 15,1
Normal left ventricular function, n (%)	12 (80,0)
Prozedurale Daten	
Initialer Rhythmus	
• Atriale Tachykardie, n(%)	13 (86,6)
• Sinusrhythmus, n(%)	1 (6,7)
• Vorhofflimmern, n(%)	1 (6,7)
Prozedurdauer (min)	140,6 ± 43,4
Durchleuchtungszeit (min)	18,1 ± 10,2
LA-Zeit des PFA-Katheters (min)	40 [47,5-56]
PFA Impulse:	34 [28-44]
LAPW (n=10)	16 [11-20]
Mitralisthmus Linie (n=1)	4 [4-4]
Anteriore Linie (n=11)	20 [12-29]
Dachlinie (n=13)	7 [6-11]
Ablation Ridge (n=1)	20 [20]
Ablation am linken Vorhofohr (n=1)	4 [4-4]
Ultrahochauflösendes Mapping (UHDx)	
Rhythmus während des Mappings	
• Atriale Tachykardie, n (%)	15 (100,0)
LA Mapping Punkte (Aktivierungsmap)	10535 ± 4894
Gemapptes LA Volumen (ml)	165 ± 53
LA Mapping Zeit, (min)	15,2 ± 6,2
PFA-Katheter Visualisierung, n (%)	15 (100)
Alle Komplikationen, n (%)	**0 (0,0)**

Tabelle 7: Patientencharakteristika und prozedurale Daten. BMI, Body-Mass-Index; CHA2DS2-VASc Score (Score zur Evaluation des Schlaganfallrisikos); LA, linksatrial; min, Minuten; ml, Milliliter; PFA, Pulsed Field Ablation; UHDx ultra-hochauflösendes Mapping. Werte sind als Mittelwert ± Standardabweichung angegeben, [n] oder n (%).

Alle 15 Pat:ienntinnen zeigten eine ausgedehnte atriale Fibrose in den ultrahochauflösenden prä-Ablations-Maps. **Abbildung 12** zeigt die Verteilung der Fibrose im linken Vorhof der Patient:innen.

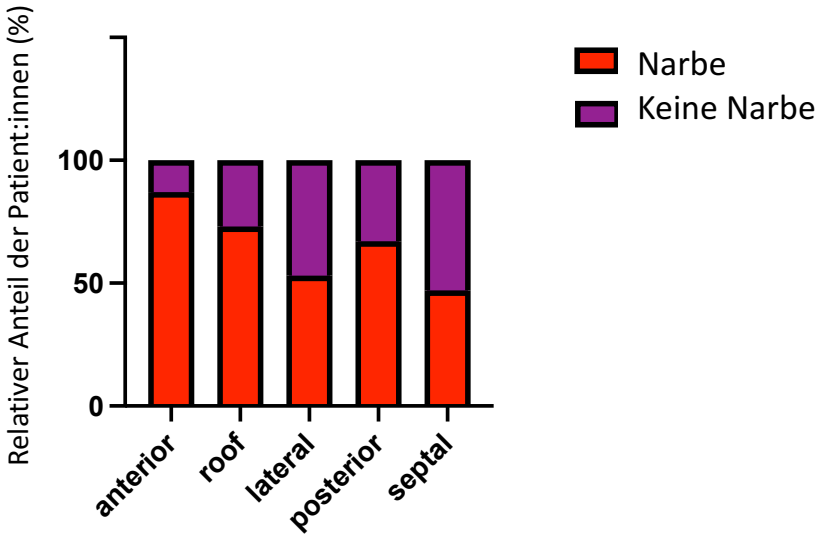

Abbildung 12: Linksatriale Verteilung der Fibrose bei den Patient:innen.

Von den 18 LAT-Makroreentries waren 7 im Bereich des anterioren linken Vorhofs, 5 perimitral, 4 am Dach, 1 am linken Vorhofohr und 1 an der linksatrialen Hinterwand lokalisiert. Der kritische Isthmus - die PFA-Zielregion - fand sich im Aktivierungsmap bei 11 LAT im anterioren LA (**Abbildung 13**), bei einer an der Ridge zwischen linkem Vorhofohr und linker oberer Pulmonalvene, bei einer an der Basis des Vorhofohrs, bei vier LAT am Dach, bei einer am Mitralisthmus und einer an der linksatrialen Hinterwand.

Alle LAT terminierten unter PFA entweder in den Sinusrhythmus (9/15) oder in eine weitere AT (6/15 und im weiteren Verlauf in den Sinusrhythmus). Insgesamt 63% (12/19) der LAT terminierten mit der 1. PFA-Applikation in den Sinusrhythmus.

Alle Ablationslinien (13 Dachlinien, 11 anteriore Linien und eine Mitralisthmuslinie) zeigten sich blockiert (**Abbildung 14**).

Bei 7 Patient:innen fanden sich im Mittel 2 ± 0,9 rekonnektierte Pulmonalvenen, die durch PFA reisoliert werden konnten. Bei 10 Patient:innen konnte die PFA-geführte Isolation der

linksatrialen Hinterwand erfolgreich durchgeführt werden ohne Nachweis ösophagealer Läsionen in der postprozeduralen Ösophagoskopie.

Es kam zu keinen intraprozeduralen Komplikationen. In einem medianen Nachbeobachtungszeitraum von 153 Tagen [q1-q3: 88-207] zeigte sich eine Arrhythmiefreiheit von 80% (12/15) bei den Patient:innen.

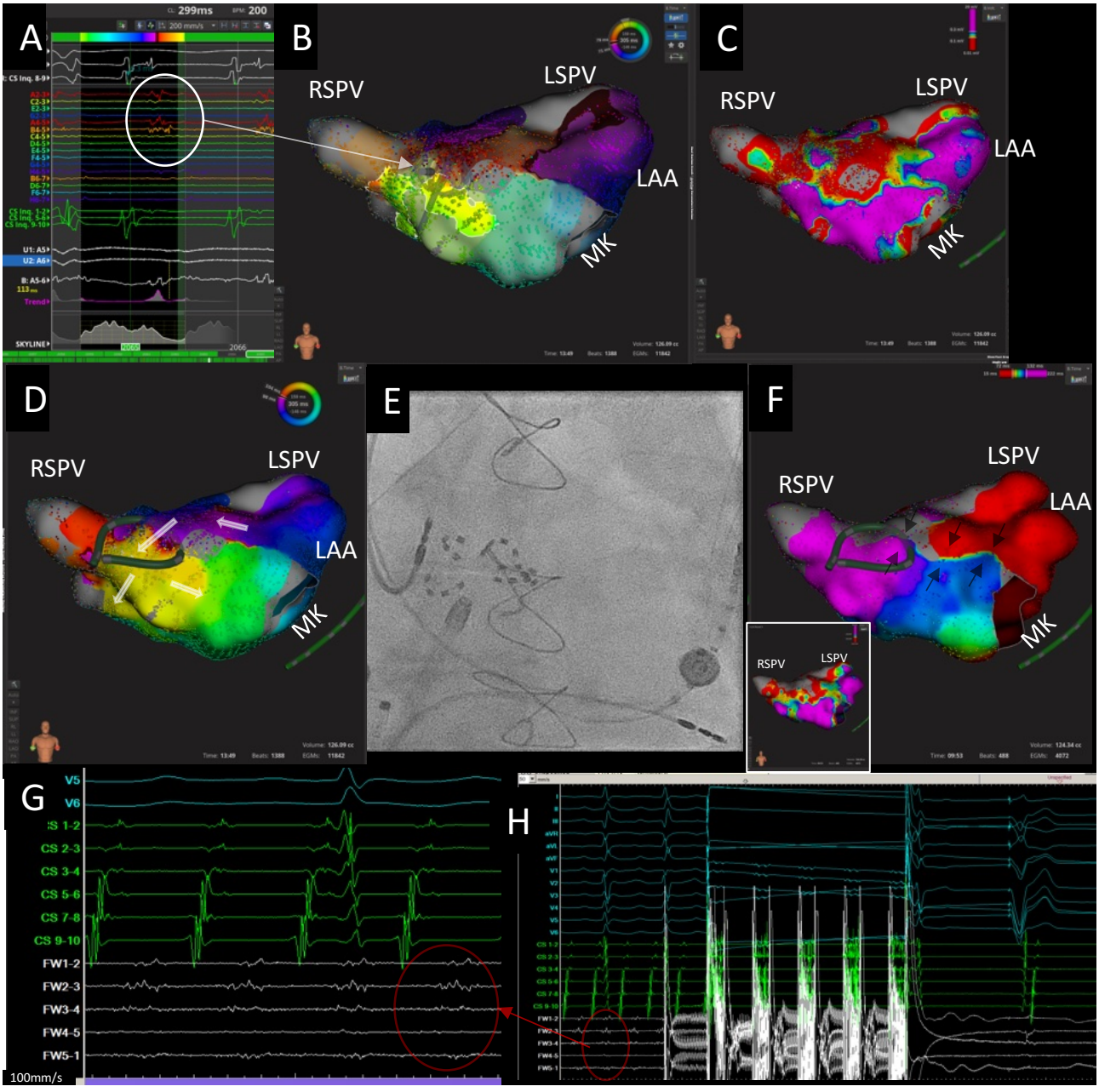

Abbildung 13: Linksatriale Tachykardie mit anteriorem Makroreentry. **A:** Fraktionierte Elektrogramme im Bereich des kritischen Isthmus des in **B** dargestellten ultrahochauflösenden Aktivierungsmaps einer linksatrialen anterioren Tachykardie (Ansicht **B** von vorne auf den linken Vorhof). **C:** Voltagemap des linken Vorhofes (Voltage ist farbkodiert: rot und grau zeigen die Narbe, lila gesundes Vorhofmyokard). **D:** Platzierung des PFA-Katheters

im Bereich des kritischen Isthmus. **E:** Fluoroskopische Darstellung der „Blumen"-Konfiguration des PFA-Katheters im Bereich des kritischen Isthmus. **G:** Fraktionierte Elektrogramme des kritischen Isthmus auf den Elektroden des PFA-Katheters während der laufenden Tachykardie. **H:** Terminierung der atrialen Tachykardie mit dem 1. PFA Impuls in den Sinusrhythmus. **F:** *Groß dargestellt*: Ultrahochauflösendes Aktivierungsmap nach PFA-Ablation und erfolgreicher Blockierung der anterioren Linie; *klein dargestellt*: linksatriales Voltagemap post Ablation.
LAA, linksatriales Vorhofohr; LSPV, links superiore Pulmonalvene, LIPV, links inferiore Pulmonalvene; MK, Mitralklappe; PFA, Pulsed Field Ablation; RSPV, rechts superior Pulmonalvene.

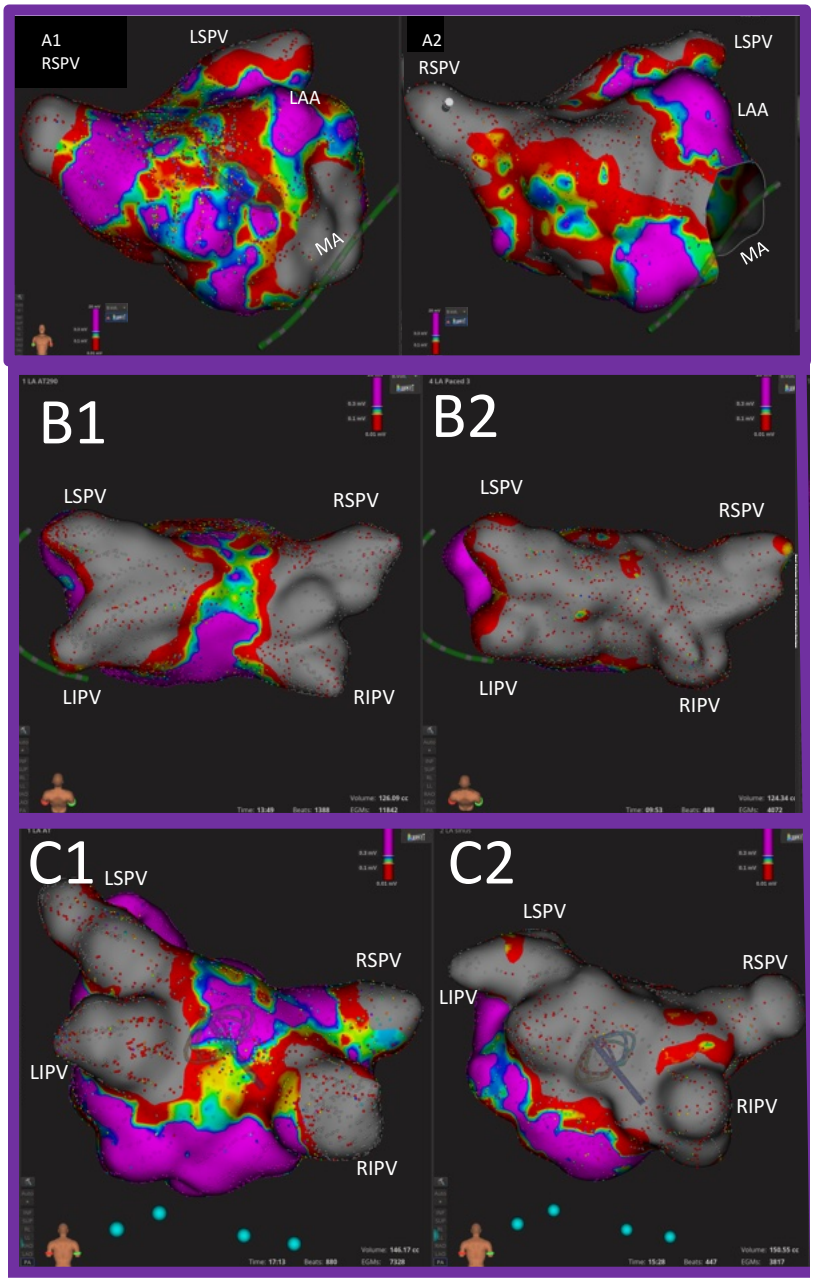

Abbildung 14: **Linksatriale ultrahochauflösende Voltagemaps prä- und post-PFA-Ablation am Beispiel blockierter Linien.** Linke Spalte prä-Ablation, rechte Spalte post-Ablation. Jede Zeile zeigt eine(n) Patient:in. Die Voltage ist farbkodiert: rot und grau zeigen die Narbe, lila gesundes Vorhofmyokard

LAA, linksatriales Vorhofohr; LSPV, links superiore Pulmonalvene, LIPV, links inferiore Pulmonalvene; MA, Mitralklappe; PFA, Pulsed Field Ablation; RIPV, rechts inferiore Pulmonalvene; RSPV, rechts superior Pulmonalvene.

Die Ablation konsekutiver linksatrialer Tachykardien mit PFA nach vorheriger Ablation mit thermalen Energiequellen ist somit sicher durchführbar und bietet eine Behandlungsalternative für ein komplexes Patientenkollektiv.

PFA ermöglicht eine sichere und schnelle Anlage von Ablationslinien mit hoher Effektivität bezüglich der prozeduralen Durchführbarkeit als auch der Rhythmusstabilität. Größere Studien werden benötigt um diese ersten Erkenntnisse zu verifizieren.

4. Diskussion und Einordnung der Ergebnisse

Sicherheit der Katheterablation – Periprozedurales Management

Bisherige Daten zur Reduktion kardiovaskulärer Ereignisse und Mortalität durch Rhythmuskontrolle und womöglich Katheterablation sind aktuell noch Risikogruppen vorbehalten und nicht auf die Gesamt-VHF-Population übertragbar (11,63). Somit besteht die Indikation der Katheterablation von VHF vor allem in der Verbesserung der Lebensqualität (1). Dies wiederum bedeutet, dass ein interventionelles Verfahren wie die Katheterablation neben einer hohen Erfolgsaussicht vor allem ein hohes Maß an Sicherheit für die Patient:innen bieten sollte um die Invasivität des Eingriffs zu rechtfertigen.

Gegenstand aktueller wissenschaftlicher Arbeiten ist daher eine kontinuierliche Weiterentwicklung der Effektivität und Sicherheit. Eine wichtige Rolle spielen hier innovative Ablationstechniken und Mappingstrategien, aber auch das periprozedurale Management rund um die Prozedur zur Reduktion von Komplikationen (28,31).

Insbesondere die Katheterablation von persistierendem VHF stellt eine Herausforderung dar. Nicht nur, weil der Erfolg hier limitiert ist (27); womöglich kann es aufgrund der längeren Prozeduren zu einer höheren Rate an Komplikationen kommen.

Es konnte in einer großen dänischen Registerstudie gezeigt werden, dass insbesondere in den ersten zwei Wochen nach Durchführung der VHF-Ablation das periprozedurale Schlaganfallrisiko – unabhängig vom individuellen Schlaganfallrisiko – deutlich erhöht ist (64). Ebenso ist das Blutungsrisiko in den ersten beiden Wochen nach Katheterablation des VHF signifikant erhöht (64).

So konnte mit Hilfe dieser Arbeit gezeigt werden, dass bei Patient:innen die sich einer Erst- oder Folgeablation aufgrund von persistierendem VHF unterzogen, die Komplikationsrate durch eine periprozedurale Antikoagulation mit kurzzeitig pausiertem NOAK deutlich gesenkt werden konnte, im Vergleich zu pausierten Vitamin-K-Antagonisten und Überbrückung mit Heparin. Die Patientensicherheit kann durch diese Ergebnisse deutlich verbessert werden. Seit Durchführung unserer Untersuchung, folgten zahlreiche weitere Arbeiten zu diesem Thema (45,46). Mittlerweile hat auch eine durchgehende orale Antikoagulation mit NOAK im Rahmen der Katheterablation Einzug in den klinischen Alltag gefunden und wurde als sicher evaluiert (35,46).

Die häufigste Blutungskomplikation unserer Studie war die nicht-schwerwiegende Leistenblutung. Zum Zeitpunkt der Durchführung unserer Erhebung (in den Jahren 2011-2014) erfolgte die Punktion der Leiste konventionell durch Palpation der Leistengefäße in Seldinger-Technik (65). Mit der Einführung der ultraschallgesteuerten venösen Leistenpunktion konnte gezeigt werden, dass schwerwiegende und nichtschwerwiegende Leistenkomplikationen sowie Fehlpunktionen der Arteria femoralis und Schmerzen der Patient:innen im Vergleich zur konventionellen Leistenpunktion reduziert werden können. Neben der Schnelligkeit der Durchführung ist die ultraschall-geführte Punktion kosteneffektiv und einfach zu erlernen (66,67). Auch Strategien zum Verschluss der Leistengefäße am Ende der Prozedur sind effektive Maßnahmen zum Erreichen einer schnelleren Hämostase. Im Vergleich zu einer manuellen Kompression und Anlage eines Druckverbandes, wie es auch in unserer Studie erfolgte, bieten eine Z-Naht oder die Implantation eines Verschlusssystems hier weitere Möglichkeiten (68,69). Das periprozedurale Management zur Vermeidung von Komplikationen hat sich somit in den letzten Jahren stets weiterentwickelt.

Sicherheit der Katheterablation – Ablationsenergie

Aufgrund der bereits hohen Erfolgsraten der PVI mit etablierten Verfahren, vor allem bei paroxysmalem VHF (70), besteht ein hoher Sicherheitsanspruch an neue Ablationstechnologien. Die in unseren Arbeiten evaluierte Energieform PFA zeigte, wenn auch im kleinen Studienkollektiv, ein gutes Sicherheitsprofil. In einem von uns mit-publiziertem ersten mulitzentrischen, weltweiten Register fand sich bei 1758 PFA-Katheterablationen keine Pulmonalvenenstenose, keine Ösophagusläsion und keine anhaltende Parese des Nervus phrenicus, sodass die Kardioselektivität des Verfahrens, die Sicherheit für die Patient:innen richtungsweisend optimiert (26). In unseren Untersuchungen dieser Arbeit traten keine Ösophagusläsionen nach Isolation der linksatrialen Hinterwand auf trotz ausgedehnter Ablation und unmittelbarer Nähe dieser Gewebsstrukturen zueinander.

In unserer Folgestudie, konnte die PFA im Bereich der Hinterwand des linken Vorhofs ebenfalls bei 59 Patient:innen mit persistierendem VHF sicher eingesetzt werden. Bei 33/59 (56%) Patient:innen erfolgte am Folgetag nach der Katheterablation eine Endoskopie der Speiseröhre ohne Nachweis ablationsbedingter Läsionen. Es kam zu keinen gewebsspezifischen Komplikationen in der Studie (71). Der Erfolg einer zusätzlichen Isolation der linksatrialen Hinterwand mit PFA spiegelte sich in einer Rezidivfreiheit atrialer

Arrhythmien von 79,3% (95%-Konfidenzintervall: 62–95%) nach einem Jahr der Nachuntersuchung wieder (71).

Die bislang größte Studie zur Untersuchung der PFA-geführten Isolation der linksatrialen Hinterwand, schloss 215 Patient:innen ein. Auch hier kam es bei akut erfolgreicher Behandlung zu keinerlei Komplikationen des Ösophagus oder Schädigungen anliegender Nerven (72). Als Komplikationen wurden eine Perikardtamponade und eine Leistenkomplikation genannt, welche unabhängig von der Ablationstechnologie, bei jeglichen Katheterverfahren auftreten können und somit nicht als Energie-spezifisch gewertet werden sollten (1,26).

Auch wenn die klinische Erfahrung mit PFA noch limitiert ist, bietet PFA womöglich das seit langem größte Sicherheitspotenzial in Bezug auf den Ösophagus bei der Katheterablation von VHF.

Eine Besonderheit liefert die PFA jedoch; im Rahmen der Untersuchungen für diese Arbeit kam es bei einem Patienten zum Auftreten eines Koronarspasmus als Ausdruck der massiven transienten lokalen Effekte. Weltweit war dies der erste Fallbericht zu einem solchen Vorkommnis und führte zur Durchführung weiterer präklinischer und klinischer Untersuchungen (60–62). Die Übertragung dieser Erkenntnisse ermöglichte es, Maßnahmen zur Vorbeugung solcher Koronarspasmen zu erheben. So sollte die PFA in Nähe zu Koronararterien minimiert werden und falls diese doch unvermeidbar ist, kann eine intravenöse Prophylaxe mit Nitroglycerin appliziert werden (60,61).

Hierbei bleibt jedoch bislang unklar, ob das Auftreten von Koronarspasmen langfristige Folgen für Patient:innen haben kann, auch wenn sich der Koronarspasmus durch akute Gabe von Nitroglycerin komplett reversibel zeigt (61). In einer präklinischen Studie wurde PFA epikardial in direkter Nähe zu den Koronarien appliziert (73). Ein Auftreten signifikanter Stenosen nach PFA-Applikation konnte ausgeschlossen werden. In den histologischen Aufarbeitungen der Koronarien fanden sich jedoch Hyperplasien der Intima. Eine weitere präklinische Studie am Schweinemodell konnte dies nicht feststellen – hier kam es zu keinerlei Schädigungen der Koronarien nach epikardialer PFA Ablation (74). Es bleibt daher abzuwarten, ob das Auftreten von Hyperplasien an Koronararterien nach PFA auch in der klinischen Anwendung an Patient:innen eine relevante Bedeutung hat. Weitere präklinische Studien und Untersuchungen der verschiedenen Wellenform und –längen des PFA Generators sind

notwendig um den genauen Pathomechanismus dieser Koronarspasmen besser zu verstehen und die Sicherheit des Verfahrens weiter zu verbessern.

Insbesondere bei der Katheterablation ventrikulärer Tachykardien, stellt die Läsionsbildung in den Herzkammern eine Herausforderung dar – im Vergleich zum linken Vorhof, findet sich hier dickeres und trabekularisiertes Myokard (75,76). Das Erreichen transmuraler und effektiver Läsionen während der Katheterablation im Ventrikel ist vor allem durch Narben, aber auch anatomischen Gegebenheiten erschwert und limitiert (77,78). Aktuell findet die PFA ihren klinischen Einsatz bei der Katheterablation von VHF. Durch den Einsatz von PFA im Ventrikel könnte die Läsionsbildung jedoch verbessert und eine höhere Effektivität erreicht werden. Präklinische Studien konnten zeigen, dass die durch PFA entstandenen Läsionen insbesondere im Narbengewebe des Ventrikels im Vergleich zur Hochfrequenzstrom-Ablation homogenere und transmurale Läsionen bilden (79). Aufgrund der Nähe der Herzkammer zu den Koronarien bleibt jedoch abzuwarten, ob der Einsatz von PFA im Ventrikel routinemäßig anwendbar sein wird.

Arrhythmierezidive nach Katheterablation – Stellenwert der elektromechanischen Kopplung und Impedanzmessung

Da die häufigste Ursache für ein Arrhythmie-Rezidiv nach Katheterablation das Auftreten von Leitungslücken in den zuvor angelegten Ablationslinien ist (36), gilt das Bestreben neuer Ablationstechniken der Optimierung der Läsionsbildung sowie Verbesserung der Auflösung und Algorithmen von Mappingsystemen.

Da während der Ablation die Läsionstiefe nicht bestimmt werden kann, dienen vor allem die in präklinischen Studien evaluierten Surrogatparameter als Orientierung während der Katheterablation; so korreliert zum Beispiel ein Abfall der Impedanz unter Hochfrequenzstrom-Ablation mit der Läsionstiefe (55). In den Untersuchungen dieser Arbeit wurde der erstmalige Einsatz eines lokalen Impedanz-messenden Hochfrequenzstrom-Ablationskatheters in Kombination mit einem ultrahochauflösenden Mappingsystem evaluiert. Die Ergebnisse zeigen, dass die lokale Impedanz aufgrund der besseren Sensitivität ein geeigneterer Indikator zur Bestimmung der Katheterstabilität, Evaluation der Gewebeeigenschaften (gesunde vs. Narbenareale) und Läsionsbildung im Vergleich zur Generatorimpedanz ist. Die Ergebnisse dieser Arbeit liefern praktische Handlungshinweise für

die Katheterablation: der Abfall der lokalen Impedanz unter Hochfrequenzstromablation kann als Surrogatparameter für akute Effektivität herangezogen werden. Bei einem zu rasanten Abfall der lokalen Impedanz sollte die Ablation jedoch vorzeitig beendet werden, da dies mit einem erhöhten Komplikationsrisiko assoziiert ist.

In einer klinischen Studie von Garcia-Bolao et al. konnte bei 58 Patient:innen gezeigt, werden dass ein Abfall der lokalen Impedanz in der Index-Katheterablation mit einer chronischen und somit anhaltenden Isolation der Pulmonalvenen assoziiert war (80). Hierfür wurde bei den Patient:innen drei Monate nach der Index-PVI eine erneute Katheterablation durchgeführt und die Anzahl isolierter Pulmonalvenen sowie das Auftreten und die Lokalisation von Leitungslücken untersucht (80).

Diese Erkenntnisse auf Vorhofebene, konnten in einer weiteren Studie unseres Zentrums auch auf die lokale Impedanz-geführte Ablation ventrikulärer Tachykardien übertragen werden (81). Auch hier zeigte sich die lokale Impedanz sensibler als die Impedanzmessung des Generators und effektive Terminierungen ventrikulärer Tachykardien unter Ablation zeigten höhere Abfälle der lokalen Impedanz als nicht erfolgreiche Ablations-Applikationen (81).

Zudem konnten wir in der hier vorgestellten Arbeit zeigen, dass eine erhöhte lokale Impedanz am Anfang der Ablation mit einem größeren Abfall der lokalen Impedanz während der Ablation assoziiert war. Dies ist am ehesten dadurch zu erklären, dass eine erhöhte Start-Impedanz mit einem guten Kontakt zum Gewebe und hierdurch mit einer effektiven Läsionsbildung im Myokard assoziiert ist (55,82). Eine Limitation der hier dargelegten Arbeit ist jedoch, dass der verwendete Ablationskatheter zwar in der Lage ist die lokale Impedanz, nicht aber den direkten Kontakt zum Gewebe zu messen. Da die genaue Kraft des Kontaktes somit unklar bleibt, könnte ein zu großer und somit gefährlicher Kontakt zum Gewebe rein über die lokale Impedanzmessung hinaus, nicht bestimmt werden. Aus diesem Grunde wurde der beschriebene Ablationskatheter weiterentwickelt und beinhaltet nun die direkte Messung der Anpresskraft (83). In der klinischen Anwendung konnte gezeigt werden, dass dies dabei helfen kann, die direkte elektromechanische Kopplung des Katheters am Gewebe in Echtzeit während der Prozedur darzustellen und so womöglich die Läsionsbildung zu optimieren (84).

Arrhythmierezidive nach Katheterablation – Rekonnektion von Pulmonalvenen

Desweiteren führten wir zur Optimierung der Katheterablation und Vermeidung möglicher Arrhythmierezidive eine weitere Studie durch. Wir untersuchten Patient:innen mit

Arrhythmierezidiv nach entweder Index-PVI mit Anpresskraft-kontrollierter Hochfrequenzstrom-Ablation oder Index-PVI mit dem Cryoballon, die sich zum Zweiteingriff vorstellten. Fokus lag hier auf Patient:innen mit Rezidiv in Form einer atrialen Tachykardie, die vor allem vom Benefit der besseren Auflösung und schnelleren Erfassens einer Vielzahl von Elektrogrammen durch ein neuartiges ultra-hochauflösendes Mappingsystems profitieren könnten (40). In unserer Untersuchung fand sich eine höhere Rate an, vor allem linksseitig, rekonnektieren Pulmonalvenen in der Hochfrequenzstrom-Gruppe. Nach Cryoballon-PVI detektierten wir komplex fraktionierte Elektrogramme entlang der initialen antralen Ablationslinie, welche häufig mit dem Auftreten atrialer Tachykardien assoziiert waren. Durch diese Ergebnisse, kann die Index-Prozedur entsprechend angepasst und optimiert werden um so gegebenenfalls zukünftige Arrhythmierezidive zu vermeiden.

Auch in einer weiteren Studie konnte gezeigt werden, dass die Rekonnektionsrate der Pulmonalvenen nach Hochfrequenzstrom-geführter Ablation höher lag als nach PVI mit dem Cryoballon (85,86) – allerdings varriiert die genaue Lokalisation der Leitungslücken in der Literatur (85,86). Diese Diskrepanz der Ergebnisse könnte durch die Verwendung unterschiedlicher Katheterdesigns (Erst- versus Zweitgeneration des Cryoballons sowie Verwendung von Hochfrequenzstromkathetern mit und ohne möglicher Messung der Anpresskraft) erklärbar sein.

Eine weitere Möglichkeit mit Hochfrequenzstrom Läsionen im Myokard zu bilden, ist mittels des Ansatzes der „High Power Short Duration“ Ablationsstrategie (87). Hierbei erfolgt für eine kurze Zeit (wenige Sekunden) mit hoher Wattzahl (in der Regel 50-90 Watt) eine Hochfrequenzstromabgabe; im Vergleich zur konventionellen Ablation (in der Regel <40 Watt) wird so die Läsionsgeometrie verändert (87,88). Hierdurch konnte im Tiermodell gezeigt werden, dass die Läsionen flacher und weiter sind als bei der konventionellen Ablation (87). In der Theorie sollen so die ans Herz benachbarten Strukturen wie die Speiseröhre durch eine überschießende Wärmeabgabe ins Gewebe geschützt werden (87). Durch die „High Power Short Duration“ Strategie wird die konduktive Wärmefortleitung ins Gewebe reduziert (87). In einer Studie konnte gezeigt werden, dass sich bei Patient:innen mit Arrhythmierezidiv nach „High Power Short Duration“ –Ablation eine höhere Rekonnektionsrate der rechten Carina der Pulmonalvenen zeigte mit 46,7%, im Vergleich zu 20,6% bei konventioneller Hochfrequenzstrom-Ablation (89). Sodass auch nach Weiterentwicklung der

Hochfrequenzstrom-Technologien das Erreichen einer anhaltenden Pulmonalvenenisolation mittels thermaler Ablationsenergien eine Herausforderung darstellt.

Bezüglich der Diagnostik von Leitungslücken in der elektrophysiologischen Untersuchung spielt auch die Evaluation der effektiven PVI eine Rolle. Die hohe Rate an Rekonnektionen in der hier vorgestellten Arbeit kann unter anderem auch durch die verbesserte Detektionsmöglichkeit der Leitungslücken mittels Verwendung ultra-hochauflösenden Mappings erklärbar sein. Meissner et al konnten zeigen, dass mit Verwendung eines hochauflösenden Mappingkatheters signifikant mehr Pulmonalvenensignale in nicht isolierten Pulmonalvenen detektiert werden konnten, als mit Verwendung eines nicht-hochauflösenden Mappingkatheters (90). Diese bessere Auflösung der Elektrogramme kann somit zu einer genaueren Detektion des Ablationsziels im Myokard führen und so womöglich eine präzisere und effektivere Ablationsläsion entstehen lassen.

Arrhythmierezidive nach Katheterablation – Atriale Tachykardien

In der hier dargelegten Arbeit lag der Fokus auf Patient:innen, die sich mit einem Arrhythmierezidiv in Form einer atrialen Tachykardie vorstellten. Hierbei war der häufigste Mechanismus der zugrundeliegenden atrialen Tachykardie ein Makroreentry, sowohl in der Hochfrequenzstrom- als auch Cryoballon-Gruppe.

Das Auftreten atrialer Tachykardien nach Index-PVI ist eine bekannte, aber seltene Entität mit einer Inzidenz von 2,8 – 11,3% (57,58,91–93). Neben der Einteilung in Makro- und Nicht-Makroreentry-Tachykardien, kann man auch zwischen pulmonalvenen- und nicht-pulmonalvenenabhängigen atrialen Tachykardien unterscheiden (94,95). Die Art des häufigsten atrialen Tachykardiemechanismus variiert stark in der Literatur: hierbei gibt es Studien, die am häufigsten von pulmonalvenenabhängigen atrialen Tachykardien berichten (96) bis hin zu Studien, die vorwiegend nicht-pulmonalvenenabhängigen Makroreentry Tachykardien beschreiben (57).

Auch wenn in der hier vorliegenden Arbeit, der Hauptmechanismus ein Makroreentry war, waren 27% der atrialen Tachykardien mit der vorherigen Ablationslinie um die Pulmonalvenen aus der Index-Prozedur assoziiert – insbesondere konnte gezeigt werden, dass auch Makroreentry Tachykardien im Bereich der ehemaligen Ablationslinie zu finden waren. Diese Besonderheit kann möglicherweise auf das ultra-hochauflösende Mapping zurückzuführen

sein, welches einen detaillierteren Einblick in den zugrundeliegenden Mechanismus ermöglichte. Es bleibt abzuwarten, ob durch die Erkenntnisse dieser Arbeit und die Weiterentwicklung der Hochfrequenzstrom- und Cryoballon-PVI, die Index-Prozedur so verbessert werden kann, dass ein Auftreten von Ablationslinien-assoziierten Arrhythmien verhindert werden kann.

Neue Ablationstechnologien – Effektivität der Pulsed Field Ablation

Pulmonalvenenisolation

Die irreversible Elektroporation, auch PFA genannt, findet aktuell als nicht-thermale Energieform Einzug in die interventionelle Elektrophysiologie. Neben dem hohen Sicherheitsprofil, ist bei der PFA auch mit hohen Raten an anhaltend isolierten Pulmonalvenen zu rechnen (24). Die initialen PFA-Studien im Menschen beinhalteten eine wiederholte elektrophysiologische Untersuchung zur Evaluation der chronischen PVI drei Monate nach der Index-PVI mit PFA. Hierbei wurden verschiedene Katheter untersucht, unter anderem der in dieser Arbeit vorgestellte, mehrpolige PFA-Katheter. Nach Optimierung der PFA-Wellenlänge und Generator-Einstellungen konnte hier die Rate isolierter Pulmonalvenen von 43 auf 100% gesteigert werden (20). Eine andere PFA-Technologie konnte nach Optimierung der PFA-Wellenlänge und -form eine Rate anhaltend isolierter Pulmonalvenen von 97% nach drei Monaten, evaluiert durch invasives Mapping des linken Vorhofs, erzielen (97). Es blieb zu diesem Zeitpunkt abzuwarten, ob diese Erkenntnisse aus den ersten klinischen Studien auch auf den klinischen Alltag und größere Patientenkollektive übertragbar sein würden. Zu erwähnen ist außerdem, dass in diesen initialen Untersuchungen zusätzlich ein intrakardialer Ultraschall verwendet wurde, um den Kontakt des PFA-Katheters zum Gewebe zu evaluieren (24).

Da ultrahochauflösendes Mapping detaillierte Einblicke in elektrophysiologische Pathomechanismen bietet, wurde dieses in unseren Untersuchungen mit PFA kombiniert. Die Ergebnisse zeigten, dass PFA weite antrale Ablationslinien um die Pulmonalvenen sowie eine homogene Isolation der linksatrialen Hinterwand erzeugte. Dies ist in Übereinstimmung mit initialen klinischen Daten zu PFA, in welchen unter anderem gezeigt werden konnte, dass das Ausmaß der Läsionen über die Zeit stabil blieb und sich keine Regression dieser zeigte (59).

Durch unsere Ergebnisse konnten klinisch relevante Handlungsempfehlungen für diese noch junge Ablationstechnologie gegeben werden. Diese zielen insbesondere auf die Vermeidung möglicher akuter Pulmonalvenen-Rekonnektionen; um somit die Effektivität der PFA-geführten Katheterablation noch weiter zu verbessern und die Lernkurve für diese neue Technologie zu verkürzen.

So konnte in unserer Arbeit gezeigt werden, dass sich bei 6,25% der Patient:innen eine akute Rekonnektion im Bereich des anterioren superioren Anteils der oberen Pulmonalvenenostien zeigte. Erklärbar ist dies am ehesten durch das technische Design, welches einen über den Draht geführten Ablationskatheter beinhaltet. Hierdurch rotiert der Katheter bei Positionierung am Pulmonalvenenostium nach posterior und weg vom anterioren Aspekt des Pulmonalvenenostiums. Durch die Erkenntnisse des Auftretens anteriorer Leitungslücken, konnte die Empfehlung ausgesprochen werden, den PFA-Ablationskatheter in der Prozedur manuell weiter nach anterior zu rotieren und so koaxial den Katheter am Pulmonalvenenostium zu positionieren. Hierdurch konnten alle Pulmonalvenen in dieser Studie im Anschluss erfolgreich mit PFA isoliert werden.

Da im klinischen Alltag invasive Remapping-Prozeduren (drei Monate nach Index-PVI zur Evaluation der anhaltenden, chronischen PVI) nicht durchführbar sind, kann die chronische PVI-Rate nur anhand von Patient:innen evaluiert werden, die sich aufgrund eines Arrhythmie-Rezidivs zur erneuten Katheterablation vorstellen. Hier konnte in einer Studie von Tohoku et al. gezeigt werden, dass nach PFA 90,9% der Pulmonalvenen anhaltend isoliert waren (25). Die Lokalisation der Leitungslücken zeigte sich hierbei, vergleichbar mit der in dieser Habilitationsschrift beschriebenen akuten Rekonnektionen, vor allem im Bereich der linken, oberen Pulmonalvene (25). Insbesondere nach Verwendung des größeren PFA-Katheters (35 statt 31 Millimeter) kam es zum Auftreten von Leitungserholungen der Pulmonalvenen. Im Vergleich liegen die Raten isolierter Pulmonalvenen drei Monate nach thermaler Energieformen (Hochfrequenzstrom und Kryoenergie) bei unter 80% (20). In der bisher einzig randomisierten Studie zu PFA im Vergleich zu thermalen Energieformen, fand sich jedoch nur eine chronische PVI-Rate nach PFA von 64,8% und nach thermaler Energieform von 64,9% (98). Eine Limitation der Studie ist hier möglicherweise, die noch geringe Lernkurve für die Anwendung des Verfahrens. Zudem handelt es sich hierbei nur um die Beurteilung eines bestimmten PFA-Katheters, sodass aktuell unklar ist, ob sich die Ergebnisse dieser Studie auch auf weitere PFA-Technologien und –Katheter übertragen lassen.

Atriale Tachykardien

Patient:innen, die nach bereits mehrfachen Vorablationen erneut Rezidive einer atrialen Tachykardie präsentieren, stellen eine Herausforderung für die klinische Elektrophysiologie dar. Nicht nur die Identifikation des Pathomechanismus ist aufgrund der durch die Krankheit oder die Vorablationen entstandene atriale Fibrose erschwert und häufig komplex (40), auch die effektive Ablation als solche kann herausfordernd sein. So zeigte sich in einer Studie von Jungen et al. aus unserem Zentrum bei 250 eingeschlossenen Patient:innen eine Arrhythmiefreiheit von lediglich 53% nach einmaliger Hochfrequenzstromablation atrialer Tachykardien, trotz Verwendung ultra-hochauflösender Mappingverfahren (99). Nach im Durchschnitt 1,4 ± 0,4 Katheterablationen pro Patient:in konnte der Erfolg der Rhythmusstabilität auf 73% gesteigert werden. Neben der Erkennung des Tachykardiemechanismus, kann auch die Läsionsbildung im oftmals fibrosierten Myokard nach initialer Hochfrequenzstromablation erschwert sein (100).
In präklinischen Studien waren in vernarbtem oder vorabladiertem Myokard, PFA-Läsionen transmural und homogener als Hochfrequenzstrom-Läsionen (79,100). Sodass PFA eine effektivere Möglichkeit zur Läsionsbildung in komplexerem Substrat mit fortgeschrittener atrialer Kardiomyopathie liefern könnte.

In unserer Arbeit konnten alle linksatrialen Tachykardien mittels ultra-hochauflösendem Mapping erfolgreich nachvollzogen und mit PFA behandelt werden; die Ablationslinien zeigten sich nach Ablation mit PFA blockiert.
Bisherige Studien zeigen, dass trotz wiederholter Katheterablation mit Hochfrequenzstrom eine erfolgreiche Blockierung der anterioren Linie im linken Vorhof nur bei 58% der Patient:innen nachgewiesen werden konnte und dass eine inkomplette Linie oder Erholungen dieser zu einem Rezidiv atrialer Tachykardien führen kann (27,101). Zudem verlängerte das Anstreben erfolgreich blockierter Ablationslinien signifikant die Prozedurdauer (101). Neben einer limitierten Effektivität, ist eine ausgedehnte Hochfrequenzstrom-Ablation über eine reine PVI hinaus mit einem erhöhten Risiko für das Auftreten von schwerwiegenden Komplikationen wie der Perikardtamponade assoziiert (101,102). Nichts desto trotz hat sich neben der Entstehung neuer Ablationsenergien auch die Ablation mit konventioneller

Hochfrequenzstrom weiterentwickelt. In einer monozentrischen Beobachtung über „High Power Short Duration“ Ablation mit 50 Watt konnten 97% der anterioren Linien und 100% der Dachlinien akut erfolgreich blockiert werden (103).

In unserer Studie zeigten sich akut alle Ablationslinien mit PFA blockiert. Systematische Daten bezüglich der chronischen Rate blockierter Ablationslinien nach PFA sind noch limitiert (97). In einer Studie von Reddy et al., in welcher ein Ablationskatheter zum Einsatz kam, der in der Lage ist zwischen Hochfrequenzstrom und PFA als Energieform zu wechseln, zeigte eine 100%-ige Rate an isolierten Dachlinien im linken Vorhof nach dreimonatiger invasiver Re-Ablation (97).

Im Gegensatz zu unserer Ergebnissen, war in einer weiteren Studie zur Ablation atrialer Tachykardien mit dem multipolaren PFA-Katheter eine zusätzliche Ablation mit Hochfrequenzstrom bei 15% der mit PFA durchgeführten anterioren Ablationslinien und 50% bei den Mitralisthmuslinien notwendig, um die Linien akut zu blockieren (104). Hierbei ist zu beachten, dass das Design des multipolaren PFA-Katheters möglicherweise aufgrund seiner Größe und Form nicht ideal für ein lineares Läsionskonzept zu sein scheint.

Daten zur Evaluation chronischer PFA-Läsionen, welche über die Ablation der Pulmonalvenen hinausgeht, sind für den in unserer Studie verwendeten multipolaren PFA-Katheter auf die Isolation der linksatrialen Hinterwand limitiert. Hier konnte in einem Patientenkollektiv von 215 Patient:innen eine akute Isolation der Hinterwand bei allen Patient:innen erreicht werden (72). Insgesamt 26 Patient:innen unterzogen sich aufgrund eines atrialen Arrhythmierezidivs einer erneuten Katheterablation – die linksatriale Hinterwand zeigte sich bei 85% dieser Patient:innen mit invasivem Remapping anhaltend elektrisch isoliert (72).

Insbesondere bei der Ablation atrialer Tachykardien, kann sich der Urpsrung dieser auch im rechten Vorhof befinden. Die Ablation rechtsatrialer Tachykardien mit PFA ist aktuell noch limitiert und beschränkt sich derzeit auf einzelne Fallberichte (105,106), sodass eine Ausweitung der linksatrialen Ablation mit PFA auf den rechten Vorhof sowie die Ventrikel noch Gegenstand weiterer Untersuchungen sein wird.

Ultrahochauflösendes Mapping in Kombination mit PFA-geführter Ablation konsekutiver linksatrialer Tachykardien, nach vorheriger Ablation mit thermalen Energiequellen, ist somit sicher durchführbar und könnte eine neue Behandlungsalternative für ein komplexes Patientenkollektiv bieten. PFA ermöglicht eine sichere und schnelle Anlage von

Ablationslinien mit hoher akuter und chronischer Effektivität. Vergleichsstudien sowie Untersuchungen mit längerfristiger Nachbeobachtung der Patient:innen sind derzeit jedoch noch ausstehend.

5. Zusammenfassung

Wie in der vorliegenden Arbeit mehrfach dargestellt, ist die elektive Katheterablation aktuell der Grundpfeiler der modernen Rhythmusskontrolle bei Patient:innen mit VHF. Um Komplikationen wie Blutungen, aber auch thrombembolische Ereignisse während der Katheterablation zu reduzieren, spielen neben der Patientenselektion, das periprozedurale Management der oralen Antikoagulation, die intraprozedurale Heparingabe, die Punktionstechniken der Leiste und des transseptalen Zugangs bis hin zum Verschluss der Leiste am Ende der Prozedur eine wichtige Rolle. Durch Erkenntnisse dieser Arbeit wie der Umstellung von Vitamin-K-Antagonisten auf kurzzeitig-pausierte oder durchgehende Gabe von NOAK, sowie durch die Einführung der ultraschallgesteuerten Leistenpunktion und anschließenden Anlage eines Naht- oder Verschlusssystems der Leistengefäße konnte die Sicherheit der Katheterablation stetig verbessert werden.

Zusammenfassend wurden in der vorliegenden Arbeit Strategien und Techniken untersucht, welche die Katheterablation von VHF und atrialen Tachykardien effizienter und sicherer gestalten können. Die Ergebnisse der vorliegendenen Arbeit konnten zeigen, dass die Verwendung von hochauflösenden Mappingverfahren eine genauere Charakterisierung des Substrats und detailliertere Einblicke in den zugrundeliegenden Mechanismus der Arrhythmien liefert. Auf dem Gebiet des Mappings ist mit weiteren innovativen Entwicklungen in den kommenden Jahren zu rechnen. Neue invasive Mappingverfahren, sowie „kontaktloses“ oder auch nichtinvasives Mapping sind Gegenstand aktueller Untersuchungen (107,108).

Die Einführung der PFA birgt ein großes Potenzial in der Weiterentwicklung der klinischen Elektrophysiologie. Inwieweit sich der bislang noch limitierte aber erfolgsversprechende Einsatz der PFA im linken Vorhof auf größere Patientenkollektive oder auf die Ablation ventrikulärer Arrhythmien übertragen lässt, bleibt abzuwarten. Außerdem fehlen derzeit noch randomisierte Daten zur PFA-Ablation außerhalb der Pulmonalvenen sowie wirkliche Langzeit-Daten der Effektivität und Sicherheit.

6. Literaturverzeichnis

1. Hindricks G, Potpara T, Serbia C, Dagres N, Arbelo E, Bax JJ, Blomström-Lundqvist C, Boriani G, Castella M, Dan G, Dilaveris P, Fauchier L, Filippatos G, Kalman JM, La Meir M. 2020 ESC Guidelines for the diagnosis and management of atrial fibrillation developed in collaboration with the European Association of Cardio-Thoracic Surgery (EACTS). Eur Heart J. 2020;0:1–126.
2. Lewalter T, Jilek C, Israel C, Brachmann J. [Clinical differential indication : Wearables vs implantables]. Herzschrittmacherther Elektrophysiol. 2020 Sep;31(3):288–91.
3. Gunawardene MA, Willems S. Atrial fibrillation progression and the importance of early treatment for improving clinical outcomes. Europace. 2022 Jun;24(Suppl 2):ii22-ii28.
4. Hart RG, Pearce LA, Aguilar MI. Adjusted-dose warfarin versus aspirin for preventing stroke in patients with atrial fibrillation. Vol. 147, Annals of internal medicine. 2007. p. 590–2.
5. Willems S, Gunawardene MA, Eickholt C, Hartmann J, Schmoeckel M, Schäffer B. Medical, Interventional, and Surgical Treatment Strategies for Atrial Fibrillation. Dtsch Arztebl Int. 2022 Jan;(Jan 10; Forthcoming:arztebl.m2021.0303.).
6. Hakalahti A, Biancari F, Nielsen JC, Raatikainen MJP. Radiofrequency ablation vs. antiarrhythmic drug therapy as first line treatment of symptomatic atrial fibrillation: Systematic review and meta-analysis. Europace. 2015;17(3):370–8.
7. Andrade JG, Wells GA, Deyell MW, Bennett M, Essebag V, Champagne J, Roux J-F, Yung D, Skanes A, Khaykin Y, Morillo C, Jolly U, Novak P, Lockwood E, Amit G, Angaran P, Sapp J, Wardell S, Lauck S et al. Cryoablation or Drug Therapy for Initial Treatment of Atrial Fibrillation. N Engl J Med. 2021;384(4):305–15.
8. Wazni OM, Dandamudi G, Sood N, Hoyt R, Tyler J, Durrani S, Niebauer M, Makati K, Halperin B, Gauri A, Morales G, Shao M, Cerkvenik J, Kaplon RE, Nissen SE. Cryoballoon Ablation as Initial Therapy for Atrial Fibrillation. N Engl J Med. 2020;384(4):316–24.
9. Corley SD, Epstein AE, DiMarco JP, Domanski MJ, Geller N, Greene HL, Josephson RA, Kellen JC, Klein RC, Krahn AD, Mickel M, Mitchell LB, Nelson JD, Rosenberg Y, Schron E, Shemanski L, Waldo AL, Wyse DG. Relationships between sinus rhythm, treatment, and survival in the Atrial Fibrillation Follow-Up Investigation of Rhythm Management (AFFIRM) Study. Circulation. 2004 Mar 30;109(12):1509–13.

10. Packer DL, Mark DB, Robb RA, Monahan KH, Bahnson TD, Poole JE, Noseworthy PA, Rosenberg YD, Jeffries N, Mitchell LB, Flaker GC, Pokushalov E, Romanov A, Bunch TJ, Noelker G, Ardashev A, Revishvili A, Wilber DJ, Cappato R et al. Effect of Catheter Ablation vs Antiarrhythmic Drug Therapy on Mortality, Stroke, Bleeding, and Cardiac Arrest among Patients with Atrial Fibrillation: The CABANA Randomized Clinical Trial. JAMA - J Am Med Assoc. 2019;321(13):1261–74.
11. Kirchhof P, Camm AJ, Goette A, Brandes A, Eckardt L, Elvan A, Fetsch T, Van Gelder IC, Haase D, Haegeli F, Hammann F, Heidbuechel H, Hindricks G, Kautzner J, Kuck K-H, Mont L, Rekosz NJ, Schoen N, Schotten U et al. Early Rhythm-Control Therapy in Patients with Atrial Fibrillation. N Engl J Med. 2020;383(14):1305–16.
12. Haïssaguerre M, Jaïs P, Shah DC, Takahashi A, Hocini M, Quiniou G, Garrigue S, Le Mouroux A, Le Métayer P, Clémenty J. Spontaneous initiation of atrial fibrillation by ectopic beats originating in the pulmonary veins. N Engl J Med. 1998 Sep 3;339(10):659–66.
13. Reddy VY, Grimaldi M, De Potter T, Vijgen JM, Bulava A, Duytschaever MF, Martinek M, Natale A, Knecht S, Neuzil P, Pürerfellner H. Pulmonary Vein Isolation With Very High Power, Short Duration, Temperature-Controlled Lesions: The QDOT-FAST Trial. JACC Clin Electrophysiol. 2019;5(7):778–86.
14. Phlips T, Taghji P, El Haddad M, Wolf M, Knecht S, Vandekerckhove Y, Tavernier R, Duytschaever M. Improving procedural and one-year outcome after contact force-guided pulmonary vein isolation: the role of interlesion distance, ablation index, and contact force variability in the “CLOSE”-protocol. Europace. 2018;20(FI_3):f419–27.
15. Kuck K-H, Brugada J, Fürnkranz A, Metzner A, Ouyang F, Chun KRJ, Elvan A, Arentz T, Bestehorn K, Pocock SJ, Albenque J-P, Tondo C. Cryoballoon or Radiofrequency Ablation for Paroxysmal Atrial Fibrillation. N Engl J Med. 2016;9(374(23)):2235–45.
16. Chun KJ, Bordignon S, Gunawardene M, Urban V, Kulikoglu M, Schulte-Hahn B, Nowak B, Schmidt B. Single Transseptal Big Cryoballoon Pulmonary Vein Isolation using an Inner Lumen Mapping Catheter. Pacing Clin Electrophysiol. 2012 Aug 6;35(11):1304–11.
17. Chun KJ, Schmidt B, Metzner A, Tilz R, Zerm T, Koester I, Fuernkranz A, Koektuerk B, Konstantinidou M, Antz M, Ouyang F, Kuck KH. The “ single big cryoballoon ” technique for acute pulmonary vein isolation in patients with paroxysmal atrial fibrillation : a

prospective observational single centre study. Eur Heart J. 2008;15–8.

18. Chun JKR, Bordignon S, Last J, Mayer L, Tohoku S, Zanchi S, Bianchini L, Bologna F, Nagase T, Urbanek L, Chen S, Schmidt B. Cryoballoon Versus Laserballoon: Insights From the First Prospective Randomized Balloon Trial in Catheter Ablation of Atrial Fibrillation. Circ Arrhythm Electrophysiol. 2021 Feb;14(2):e009294.
19. Reddy VY, Al-Ahmad A, Aidietis A, Daly M, Melton I, Hu Y, Sulkin M, Rackauskas G, Ebner A, Hooks DA, Sofi A, Neužil P, Crozier IG. A Novel Visually Guided Radiofrequency Balloon Ablation Catheter for Pulmonary Vein Isolation: One-Year Outcomes of the Multicenter AF-FICIENT I Trial. Circ Arrhythm Electrophysiol. 2021 Oct;14(10):e009308.
20. Reddy VY, Neuzil P, Koruth JS, Petru J, Funosako M, Cochet H, Sediva L, Chovanec M, Dukkipati SR, Jais P. Pulsed Field Ablation for Pulmonary Vein Isolation in Atrial Fibrillation. J Am Coll Cardiol. 2019;74(3):315–26.
21. Koruth JS, Kuroki K, Iwasawa J, Enomoto Y, Viswanathan R, Brose R, Buck ED, Speltz M. Preclinical Evaluation of Pulsed Field Ablation. Circ Arrhythm Electrophysiol. 2019;12:e007781.
22. Reddy VY, Anic A, Koruth J, Petru J, Funasako M, Minami K, Breskovic T, Sikiric I, Dukkipati SR, Kawamura I, Neuzil P. Pulsed Field Ablation in Patients With Persistent Atrial Fibrillation. JACC. 2020;76(9):1068–80.
23. Koruth JS, Kuroki K, Kawamura I, Brose R, Viswanathan R, Buck ED, Donskoy E, Neuzil P, Dukkipati SR, Reddy VY. Pulsed Field Ablation Versus Radiofrequency Ablation. Circ Arrhythm Electrophysiol. 2020;(March):13(3):e008303.
24. Reddy VY, Dukkipati SR, Neuzil P, Anic A, Petru J, Funasako M, Cochet H, Minami K, Breskovic T, Sikiric I, Sediva L, Chovanec M, Koruth J, Jais P. Pulsed Field Ablation of Paroxysmal Atrial Fibrillation. JACC Clin Electrophysiol. 2021;7(5):614–27.
25. Tohoku S, Chun KRJ, Bordignon S, Chen S, Schaack D, Urbanek L, Ebrahimi R, Hirokami J, Bologna F, Schmidt B. Findings from repeat ablation using high-density mapping after pulmonary vein isolation with pulsed fi eld ablation. Europace. 2022;0:1–8.
26. Ekanem E, Reddy VY, Schmidt B, Reichlin T, Neven K, Metzner A, Hansen J, Blaauw Y, Maury P, Arentz T, Sommer P, Anic A, Anselme F, Boveda S, Deneke T, Willems S, van der Voort P, Tilz R, Funasako M et al. Multi-national survey on the methods, efficacy, and safety on the post-approval clinical use of pulsed field ablation (MANIFEST-PF). Europace. 2022 Jun;24(1256–1266).

27. Calkins H, Hindricks G, Cappato R, Kim Y, Saad EB, Aguinaga L, Akar JG, Badhwar V, Brugada J, Camm J, Chen P, Chen S, Chung MK, Day JD, Avila A, Groot NMSN De, Biase L Di, Duytschaever M, Edgerton JR et al. 2017 HRS / EHRA / ECAS / APHRS / SOLAECE expert consensus statement on catheter and surgical ablation of atrial fibrillation. Heart Rhythm. 2017;14(10):e275–444.
28. Vogler J, Willems S, Sultan A, Schreiber D, Lüker J, Servatius H, Schäffer B, Moser J, Hoffmann BA, Steven D. Pulmonary Vein Isolation Versus Defragmentation. J Am Coll Cardiol. 2015;66(24):2743–52.
29. Verma A, Jiang CY, Betts TR, Chen J, Deisenhofer I, Mantovan R, Macle L, Morillo CA, Haverkamp W, Weerasooriya R, Albenque JP, Nardi S, Menardi E, Novak P, Sanders P. Approaches to catheter ablation for persistent atrial fibrillation. N Engl J Med. 2015;372(19):1812–22.
30. Kistler PM, Chieng D, Sugumar H, Ling L-H, Segan L, Azzopardi S, Al-Kaisey A, Parameswaran R, Anderson RD, Hawson J, Prabhu S, Voskoboinik A, Wong G, Morton JB, Pathik B, McLellan AJ, Lee G, Wong M, Finch S et al. Effect of Catheter Ablation Using Pulmonary Vein Isolation With vs Without Posterior Left Atrial Wall Isolation on Atrial Arrhythmia Recurrence in Patients With Persistent Atrial Fibrillation: The CAPLA Randomized Clinical Trial. JAMA. 2023 Jan;329(2):127–35.
31. Dagher L, Kholmovski E, Mansour M, Marchlinski F, Wilber D, Hindricks G, Mahnkopf C, Wells D, Jais P, Sanders P, Brachmann J, Bax JJ, Boer LM, Deneke T, Calkins H, Sohns C, Akoum N, Ii D. Effect of MRI-Guided Fibrosis Ablation vs Conventional Catheter Ablation on Atrial Arrhythmia Recurrence in Patients With Persistent Atrial Fibrillation The DECAAF II Randomized Clinical Trial. JAMA. 2022;327(23):2296–305.
32. Huo Y, Gaspar T, Schönbauer R, Wójcik M, Fiedler L, Roithinger FX, Martinek M, Pürerfellner H, Kirstein B, Richter U, Ulbrich S, Mayer J, Krahnefeld O, Agdirlioglu T, Zedda A, Piorkowski J, Piorkowski C. Low-Voltage Myocardium-Guided Ablation Trial of Persistent Atrial Fibrillation. NEJM Evid. 2022;1(11):EVIDoa2200141.
33. Santangeli P, Di Biase L, Horton R, Burkhardt JD, Sanchez J, Al-Ahmad A, Hongo R, Beheiry S, Bai R, Mohanty P, Lewis WR, Natale A. Ablation of atrial fibrillation under therapeutic warfarin reduces periprocedural complications evidence from a meta-analysis. Circ Arrhythmia Electrophysiol. 2012;5(2):302–11.
34. Nairooz R, Sardar P, Payne J, Aronow WS, Paydak H. Meta-analysis of major bleeding

with uninterrupted warfarin compared to interrupted warfarin and heparin bridging in ablation of atrial fibrillation. Int J Cardiol. 2015;187:426–9.

35. Steffel J, Collins R, Antz M, Cornu P, Desteghe L, Haeusler KG, Oldgren J, Reinecke H, Roldan-schilling V, Rowell N, Sinnaeve P, Vanassche T, Potpara T, Camm AJ, Heidbu H. 2021 European Heart Rhythm Association Practical Guide on the Use of Non-Vitamin K Antagonist Oral Anticoagulants in Patients with Atrial Fibrillation European Society of Cardiology General practitioner Global Registry of Acute Coronary Events. Europace. 2021;23:1612–76.
36. Ouyang F, Antz M, Ernst S, Hachiya H, Mavrakis H, Deger FT, Schaumann A, Chun J, Falk P, Hennig D, Liu X. Recovered Pulmonary Vein Conduction as a Dominant Factor for Recurrent Atrial Tachyarrhythmias After Complete Circular Isolation of the Pulmonary Veins: Lessons From Double Lasso Technique. Circulation. 2005;111:127–35.
37. Rostock T, Drewitz I, Steven D, Hoffmann BA, Salukhe T V, Bock K, Servatius H, Aydin MA, Meinertz T, Willems S. Characterization, mapping, and catheter ablation of recurrent atrial tachycardias after stepwise ablation of long-lasting persistent atrial fibrillation. Circ Arrhythm Electrophysiol. 2010 Apr;3(2):160–9.
38. Saoudi N, Cosío F, Waldo A, Chen SA, Iesaka Y, Lesh M, Saksena S, Salerno J, Schoels W. A classification of atrial flutter and regular atrial tachycardia according to electrophysiological mechanisms and anatomical bases. a Statement from a Joint Expert Group from The Working Group of Arrhythmias of the European Society of Cardiology and the . Eur Heart J. 2001 Jul;22(14):1162–82.
39. Brugada J, Katritsis DG, Arbelo E, Arribas F, Bax JJ, Blomstrom-Lundqvist C, Calkins H, Corrado D, Deftereos SG, Diller GP, Gomez-Doblas JJ, Gorenek B, Grace A, Ho SY, Kaski JC, Kuck KH, Lambiase PD, Sacher F, Sarquella-Brugada G et al. 2019 ESC Guidelines for themanagement of patients with supraventricular tachycardia. Eur Heart J. 2020;41(5):655–720.
40. Schaeffer B, Hoffmann BA, Meyer C, Akbulak R, Moser J, Jularic M, Eickholt C, NÜhrich JM, Kuklik P, Willems S. Characterization, Mapping, and Ablation of Complex Atrial Tachycardia: Initial Experience With a Novel Method of Ultra High-Density 3D Mapping. J Cardiovasc Electrophysiol. 2016;27(10):1139–50.
41. Sanders P, Hocini M, Jaïs P, Hsu L, Takahashi Y, Rotter M, Scavée C, Pasquié J, Sacher F, Rostock T, Nalliah CJ, Bs C, Clémenty J, Haïssaguerre M. Characterization of Focal Atrial

Tachycardia Using High-Density Mapping. J Am Coll Cardiol. 2005;46(11):2088–99.

42. Schaeffer B, Akbulak RÖ, Jularic M, Moser J, Eickholt C, Schwarzl JM, Klatt N, Kuklik P, Meyer C, Willems S. High-Density Mapping and Ablation of Primary Nonfocal Left Atrial Tachycardia. JACC Clin Electrophysiol. 2019;5(4):417–26.
43. Weitz JI, Healey JS, Skanes AC, Verma A. Periprocedural management of new oral anticoagulants in patients undergoing atrial fibrillation ablation. Circulation. 2014;129(16):1688–94.
44. Bassiouny M, Saliba W, Rickard J, Shao M, Sey A, Diab M, Martin DO, Hussein A, Khoury M, Abi-Saleh B, Alam S, Sengupta J, Borek PP, Baranowski B, Niebauer M, Callahan T, Varma N, Chung M, Tchou PJ et al. Use of dabigatran for periprocedural anticoagulation in patients undergoing catheter ablation for atrial fibrillation. Circ Arrhythmia Electrophysiol. 2013;6(3):460–4.
45. Lakkireddy D, Reddy YM, Di Biase L, Vallakati A, Mansour MC, Santangeli P, Gangireddy S, Swarup V, Chalhoub F, Atkins D, Bommana S, Verma A, Sanchez JE, Burkhardt JD, Barrett CD, Baheiry S, Ruskin J, Reddy V, Natale A. Feasibility and safety of uninterrupted rivaroxaban for periprocedural anticoagulation in patients undergoing radiofrequency ablation for atrial fibrillation: Results from a multicenter prospective registry. J Am Coll Cardiol. 2014;63(10):982–8.
46. Calkins H, Willems S, Gerstenfeld EP, Verma A, Schilling R, Hohnloser SH, Okumura K, Serota H, Nordaby M, Guiver K, Biss B, Brouwer MA, Grimaldi M. Uninterrupted Dabigatran versus Warfarin for Ablation in Atrial Fibrillation. N Engl J Med. 2017;376(17):1627–36.
47. Siegal D, Yudin J, Kaatz S, Douketis JD, Lim W, Spyropoulos a. C. Periprocedural Heparin Bridging in Patients Receiving Vitamin K Antagonists: Systematic Review and Meta-Analysis of Bleeding and Thromboembolic Rates. Circulation. 2012;126(13):1630–9.
48. Heidbuchel H, Verhamme P, Alings M, Antz M, Hacke W, Oldgren J, Sinnaeve P, Camm AJ, Kirchhof P. European Heart Rhythm Association Practical Guide on the use of new oral anticoagulants in patients with non-valvular atrial fibrillation. Europace. 2013 May;15(5):625–51.
49. Hoffmann BA, Kuck K-H, Andresen D, Spitzer SG, Hoffmann E, Schumacher B, Eckardt L, Brachmann J, Becker R, Steven D, Rostock T, Junger C, Senges J, Willems S. Impact of structural heart disease on the acute complication rate in atrial fibrillation ablation:

results from the German Ablation Registry. J Cardiovasc Electrophysiol. 2014;25(3):242–9.

50. Calkins H, Kuck KH, Cappato R, Brugada J, Camm a J, Chen S-A, Crijns HJG, Damiano RJ, Davies DW, DiMarco J, Edgerton J, Ellenbogen K, Ezekowitz MD, Haines DE, Haissaguerre M, Hindricks G, Iesaka Y, Jackman W, Jalife J et al. 2012 HRS/EHRA/ECAS expert consensus statement on catheter and surgical ablation of atrial fibrillation: recommendations for patient selection, procedural techniques, patient management and follow-up, definitions, endpoints, and research trial design. Heart Rhythm. 2012 Apr;9(4):632–96.

51. Kim J-S, Jongnarangsin K, Latchamsetty R, Chugh A, Ghanbari H, Crawford T, Yokokawa M, Good E, Bogun F, Pelosi F, Morady F, Oral H. The Optimal Range of International Normalized Ratio for Radiofrequency Catheter Ablation of Atrial Fibrillation During Therapeutic Anticoagulation With Warfarin. Circ Arrhythmia Electrophysiol. 2013;6(2):302–9.

52. Di Biase L, Burkhardt JD, Santangeli P, Mohanty P, Sanchez JE, Horton R, Gallinghouse GJ, Themistoclakis S, Rossillo A, Lakkireddy D, Reddy M, Hao S, Hongo R, Beheiry S, Zagrodzky J, Rong B, Mohanty S, Elayi CS, Forleo G et al. Periprocedural Stroke and Bleeding Complications in Patients Undergoing Catheter Ablation of Atrial Fibrillation With Different Anticoagulation Management: Results From the Role of Coumadin in Preventing Thromboembolism in Atrial Fibrillation (AF) Patient. Circulation. 2014;129(25):2638–44.

53. Ge Z, Faggioni M, Baber U, Sartori S, Sorrentino S, Farhan S, Chandrasekhar J, Vogel B, Qadeer A, Halperin J, Reddy V, Dukkipati S, Dangas G, Mehran R. Safety and efficacy of nonvitamin K antagonist oral anticoagulants during catheter ablation of atrial fibrillation: A systematic review and meta-analysis. Cardiovasc Ther. 2018 Oct;36(5):e12457.

54. Vugt SPG Van, Westra SW, Volleberg RHJA, Hannink G, Nakamura R, Asmundis C De, Chierchia G, Navarese EP, Brouwer MA. Meta-analysis of controlled studies on minimally interrupted vs . continuous use of non-vitamin K antagonist oral anticoagulants in catheter ablation for atrial fibrillation. Euopace. 2021;23:1961–9.

55. Sulkin M, Laughner J, Hilbert S, Kapa S, Kosiuk J, Younan P, Hindricks G, Bollmann A. A Novel Measure of Local Impedance Predicts Catheter-Tissue Contact and Lesion

Formation. Circ Arrhythm Electrophysiol. 2018;11(4):e005831.

56. Ikeda A, Nakagawa H, Lambert H, Shah DC, Fonck E, Yulzari A, Sharma T, Pitha J V., Lazzara R, Jackman WM. Relationship between catheter contact force and radiofrequency lesion size and incidence of steam pop in the beating canine heart: Electrogram amplitude, impedance, and electrode temperature are poor predictors of electrode-tissue contact force and lesion. Circ Arrhythmia Electrophysiol. 2014;7(6):1174–80.

57. Lyan E, Yalin K, Abdin A, Sawan N, Liosis S, Lange SA, Eitel I, Heeger CH, Meyer-Saraei R, Eitel C, Tilz RR. Mechanism, underlying substrate and predictors of atrial tachycardia following atrial fibrillation ablation using the second-generation cryoballoon. J Cardiol. 2019;73(6):497–506.

58. Hermida A, Kubala M, Traulle S, Buiciuc O, Quenum S, Hermida J-S. Prevalence and predictive factors of left atrial tachycardia occurring after second-generation cryoballoon ablation of atrial fibrillation. J Cardiovasc Electrophysiol. 2018;29:46–54.

59. Kawamura I, Neuzil P, Shrivamurthy P, Petru J, Funasako M, Minami K, Reddy VY. Does pulsed field ablation regress over time ? A quantitative temporal analysis of pulmonary vein isolation. Heart Rhythm. 2021;18(6):878–84.

60. Gunawardene MA, Schaeffer BN, Jularic M, Eickholt C, Maurer T, Akbulak RÖ, Flindt M, Anwar O, Hartmann J, Willems S. Coronary Spasm During Pulsed Field Ablation of the Mitral Isthmus Line. JACC Clin Electrophysiol. 2021;Sep 23;S2405-500X(21)00785-4.

61. Reddy VY. Coronary Arterial Spasm During Pulsed Field Ablation to Treat Atrial Fibrillation. Circulation. 2022;146:1808–19.

62. Koruth JS, Kawamura I, Buck E, Jerrell S, Brose R, Reddy VY. Coronary Arterial Spasm and Pulsed Field Ablation: Preclinical Insights. Vol. 8, JACC Clin Electrophysiol. 2022. p. 1579–80.

63. Marrouche NF, Brachmann J, Andresen D, Siebels J, Boersma L, Jordaens L, Merkely B, Pokushalov E, Sanders P, Proff J, Schunkert H, Christ H, Vogt J, Bänsch D. Catheter Ablation for Atrial Fibrillation with Heart Failure. N Engl J Med. 2018;(378):417–27.

64. Karasoy D, Gislason GH, Hansen J, Johannessen A, Torp-pedersen C, Køber L, Hvidtfeldt M, Cengiz O, Hansen ML. Oral anticoagulation therapy after radiofrequency ablation of atrial fibrillation and the risk of thromboembolism and serious bleeding : long- term follow-up in nationwide cohort of Denmark. Eur Heart J. 2015;36:307–14.

65. Duncker D, Sommer P, Busch S, Tilz RR, Althoff T, Iden L, Metzner A, Rillig A, Chun KRJ, Bourier F, Maurer T, Shin D-I. [Puncture techniques in invasive cardiac electrophysiology]. Herzschrittmacherther Elektrophysiol. 2021 Jun;32(2):274–84.
66. Kupó P, Pap R, Sághy L, Tényi D, Bálint A, Debreceni D, Basu-Ray I KA. Ultrasound guidance for femoral venous access in electrophysiology procedures-systematic review and meta-analysis. J Interv Card Electrophysiol. 2020;59(2):407–414.
67. Wiles BM, Child N, Roberts PR. How to achieve ultrasound-guided femoral venous access: the new standard of care in the electrophysiology laboratory. J Interv Card Electrophysiol. 2017 Jun;49(1):3–9.
68. Jackson N, McGee M, Ahmed W, Davies A, Leitch J, Mills M, Cambourn M, Ezad S, Boyle A, Attia J, Nanthakumar K, Barlow M. Groin Haemostasis With a Purse String Suture for Patients Following Catheter Ablation Procedures (GITAR Study). Heart Lung Circ. 2019 May;28(5):777–83.
69. Natale A, Mohanty S, Liu PY, Mittal S, Al-Ahmad A, De Lurgio DB, Horton R, Spear W, Bailey S, Bunch J, Musat D, O'Neill P, Compton S, Turakhia MP. Venous Vascular Closure System Versus Manual Compression Following Multiple Access Electrophysiology Procedures: The AMBULATE Trial. JACC Clin Electrophysiol. 2020 Jan;6(1):111–24.
70. Turagam MK, Musikantow D, Whang W, Koruth JS, Miller MA, Langan M-N, Sofi A, Choudry S, Dukkipati SR, Reddy VY. Assessment of Catheter Ablation or Antiarrhythmic Drugs for First-line Therapy of Atrial Fibrillation: A Meta-analysis of Randomized Clinical Trials. JAMA Cardiol. 2021 Jun;6(6):697–705.
71. Gunawardene MA, Frommeyer G, Ellermann C, Jularic M, Leitz P, Hartmann J, Lange PS, Anwar O, Rath B, Wahedi R, Eckardt L, Willems S. Left Atrial Posterior Wall Isolation with Pulsed Field Ablation in Persistent Atrial Fibrillation. J Clin Med. 2023 Sep;12(19):6304.
72. Kueffer T, Tanner H, Madaffari A, Seiler J, Haeberlin A, Maurhofer J, Noti F, Herrera C, Thalmann G, Kozhuharov NA, Reichlin T, Roten L. Posterior wall ablation by pulsed-field ablation: procedural safety, efficacy, and findings on redo procedures. Europace. 2023 Dec;26(1).
73. Driel VJ Van, Wessel H Van, Loh P, Doevendans PA, Goldschmeding R, Wittkampf FH, Vink A. Minimal coronary artery damage by myocardial electroporation ablation. 2013;144–9.

74. Neven K, Driel V Van, Wessel H Van, Es R Van. Epicardial linear electroporation ablation and lesion size. Heart Rhythm. 2014;11(8):1465–70.
75. Whitaker J, Rajani R, Chubb H, Gabrawi M, Varela M, Wright M, Niederer S, O'Neill MD. The role of myocardial wall thickness in atrial arrhythmogenesis. Europace. 2016 Dec;18(12):1758–72.
76. Ho SY. Anatomy and myoarchitecture of the left ventricular wall in normal and in disease. Eur J Echocardiogr. 2009 Dec;10(8):iii3-7.
77. Barkagan M, Leshem E, Shapira-Daniels A, Sroubek J, Buxton AE, Saffitz JE, Anter E. Histopathological Characterization of Radiofrequency Ablation in Ventricular Scar Tissue. JACC Clin Electrophysiol. 2019 Aug;5(8):920–31.
78. Chung F-P, Lin C-Y, Shirai Y, Futyma P, Santangeli P, Lin Y-J, Chang S-L, Lo L-W, Hu Y-F, Chang H-Y, Marchlinski FE, Chen S-A. Outcomes of catheter ablation of ventricular arrhythmia originating from the left ventricular summit: A multicenter study. Heart Rhythm. 2020 Jul;17(7):1077–83.
79. Younis A, Zilberman I, Krywanczyk A, Higuchi K, Yavin HD, Sroubek J, Anter E. Effect of Pulsed-Field and Radiofrequency Ablation on Heterogeneous Ventricular Scar in a Swine Model of Healed Myocardial Infarction. Circ Arrhythm Electrophysiol. 2022 Oct;15(10):e011209.
80. García-Bolao I, Ramos P, Luik A, S Sulkin M, R Gutbrod S, Oesterlein T, I Laughner J, Richards E, Meyer C, Yue A, Ullah W, Shepherd E, Das M. Local Impedance Drop Predicts Durable Conduction Block in Patients With Paroxysmal Atrial Fibrillation. JACC Clin Electrophysiol. 2022 May;8(5):595–604.
81. Münkler P, Gunawardene MA, Jungen C, Klatt N, Schwarzl JM, Akbulak RÖ, Dinshaw L, Hartmann J, Jularic M, Kahle A-K, Riedel R, Merbold L, Eickholt C, Willems S, Meyer C. Local impedance guides catheter ablation in patients with ventricular tachycardia. J Cardiovasc Electrophysiol. 2020 Jan;31(1):61–9.
82. Zheng X, Walcott GP, Hall JA, Rollins DL, Smith WM, Kay GN, Ideker RE. Electrode impedance: An indicator of electrode-tissue contact and lesion dimensions during linear ablation. J Interv Card Electrophysiol. 2000;4(4):645–54.
83. Garrott K, Laughner J, Gutbrod S, Sugrue A, Shuros A, Sulkin M, Yasin O, Bush J, Pottinger N, Meyers J, Kapa S. Combined local impedance and contact force for radiofrequency ablation assessment. Heart Rhythm. 2020 Aug;17(8):1371–80.

84. Alken F-A, Scherschel K, Kahle A-K, Masjedi M, Meyer C. Combined contact force and local impedance dynamics during repeat atrial fibrillation catheter ablation. Front Physiol. 2022;13:1001719.

85. Ciconte G, Velagić V, Mugnai G, Saitoh Y, Irfan G, Hunuk B, Ströker E, Conte G, Sieira J, Di Giovanni G, Baltogiannis G, Brugada P, De Asmundis C, Chierchia GB. Electrophysiological findings following pulmonary vein isolation using radiofrequency catheter guided by contact-force and second-generation cryoballoon: Lessons from repeat ablation procedures. Europace. 2015;18(1):71–7.

86. Aryana A, Singh SM, Mugnai G, Asmundis C De, Kowalski M, Pujara DK, Cohen AI, Singh SK, Fuenzalida CE, Prager N, Bowers MR, Neill PGO, Brugada P, Avila A, Chierchia G. Pulmonary vein reconnection following catheter ablation of atrial fibrillation using the second-generation cryoballoon versus open-irrigated radiofrequency : results of a multicenter analysis. J Interv Card Electrophysiol. 2016;(47):341–8.

87. Leshem E, Zilberman I, Tschabrunn CM, Barkagan M, Contreras-Valdes FM, Govari A, Anter E. High-Power and Short-Duration Ablation for Pulmonary Vein Isolation: Biophysical Characterization. JACC Clin Electrophysiol. 2018;4(4):467–79.

88. Ravi V, Poudyal A, Abid Q, Larsen T, Krishnan K, Sharma PS, Trohman RG, Huang HD. High-power short duration vs . conventional radiofrequency ablation of atrial fibrillation : a systematic review and meta-analysis. Europace. 2021;(0):1–12.

89. Hansom SP, Alqarawi W, Birnie DH, Golian M, Nery PB, Redpath CJ, Klein A, Green MS, Davis DR, Sheppard-Perkins E, Ramirez FD, Nair GM, Sadek MM. High-power, short-duration atrial fibrillation ablation compared with a conventional approach: Outcomes and reconnection patterns. J Cardiovasc Electrophysiol. 2021 May;32(5):1219–28.

90. Meissner A, Maagh P, Christoph A, Oernek A, Plehn G. Pulmonary vein potential mapping in atrial fibrillation with high density and standard spiral (lasso) catheters: A comparative study. J Arrhythmia. 2017;33(3):192–200.

91. Akerström F, Bastani H, Insulander P, Schwieler J, Arias M, Jensen-Urstad M. Comparison of regular atrial tachycardia incidence after circumferential radiofrequency versus cryoballoon pulmonary vein isolation in real-life practice. J Cardiovasc Electrophysiol. 2014;25(9):948–52.

92. Julia J, Chierchia G-B, de Asmundis C, Mugnai G, Sieira J, Ciconte G, Di Giovanni G, Conte G, Baltogiannis G, Saitoh Y, Wauters K, Irfan G, Brugada P. Regular atrial tachycardias

following pulmonary vein isolation for paroxysmal atrial fibrillation: a retrospective comparison between the cryoballoon and conventional focal tip radiofrequency techniques. J Interv Card Electrophysiol. 2015;42(2):161–9.

93. Wasmer K, Mönnig G, Bittner A, Dechering D, Zellerhoff S, Milberg P, Köbe J, Eckardt L. Incidence, characteristics, and outcome of left atrial tachycardias after circumferential antral ablation of atrial fibrillation. Heart Rhythm. 2012;9(10):1660–6.

94. Gunawardene MA, Schaeffer BN, Jularic M, Eickholt C, Akbulak RÖ, Hedenus K, Wahedi R, Anwar O, Gessler N, Hartmann J, Willems S. Pulsed field ablation in patients with complex consecutive atrial tachycardia in conjunction with ultra-high density mapping: Proof of concept. J Cardiovasc Electrophysiol Electrophysiol. 2022 Dec;33(12):2431–43.

95. Schaeffer B, Hoffmann B, Meyer C, Akbulak R, Moser J, Jularic M, Eickholt C, Nührich J, Kuklik P, Willems S. Characterization, Mapping and Ablation of Complex Atrial Tachycardia: Initial Experience with a Novel Method of Ultra High-Density 3D Mapping. J Cardiovasc Electrophysiol. 2016;27(10):1139–50.

96. Gerstenfeld EP, Callans DJ, Dixit S, Russo AM, Nayak H, Lin D, Pulliam W, Siddique S, Marchlinski FE. Mechanisms of Organized Left Atrial Tachycardias Occurring After Pulmonary Vein Isolation Edward. Circulation. 2004;110:1351–7.

97. Reddy VY, Peichl P, Anter E, Rackauskas G, Petru J, Funasako M, Minami K, Koruth JS, Natale A, Jais P, Marinskis G, Aidietis A, Kautzner J, Neuzil P. A Focal Ablation Catheter Toggling Between Radiofrequency and Pulsed Field Energy to Treat Atrial Fibrillation. JACC Clin Electrophysiol. 2023 Aug;9(8 Pt 3):1786–801.

98. Reddy VY, Gerstenfeld EP, Natale A, Whang W, Cuoco FA, Patel C, Mountantonakis SE, Gibson DN, Harding JD, Ellis CR, Ellenbogen KA, DeLurgio DB, Osorio J, Achyutha AB, Schneider CW, Mugglin AS, Albrecht EM, Stein KM, Lehmann JW et al. Pulsed Field or Conventional Thermal Ablation for Paroxysmal Atrial Fibrillation. N Engl J Med. 2023;389(18):1660–71.

99. Jungen C, Akbulak R, Kahle A-K, Eickholt C, Schaeffer B, Scherschel K, Dinshaw L, Muenkler P, Schleberger R, Nies M, Gunawardene MA, Klatt N, Hartmann J, Merbold L, Jularic M, Willems S, Meyer C. Outcome after tailored catheter ablation of atrial tachycardia using ultra-high-density mapping. J Cardiovasc Electrophysiol. 2020 Oct;31(10):2645–52.

100. Younis A, Buck E, Santangeli P, Tabaja C, Garrott K, Lehn L, Hussein AA, Nakhla S,

Nakagawa H, Yavin HD, Kanj M, Sroubek J, Saliba WI, Wazni OM. Efficacy of Pulsed Field vs Radiofrequency for the Reablation of Chronic Radiofrequency Ablation Substrate: Redo Pulsed Field Ablation. JACC Clin Electrophysiol. 2023 Oct;

101. Sanders P, Jaı P, Hsu L, Scave C, Rotter M, Takahashi Y, Pasquie J, Shah DC, Cle J. Electrophysiologic and clinical consequences of linear catheter ablation to transect the anterior left atrium in patients with atrial fibrillation. Heart Rhythm. 2004;1:176–84.
102. Chun K-RJ, Perotta L, Bordignon S, Khalil J, Dugo D, Konstantinous A, Fürnkranz AF, Schmidt B. Complications in Catheter Ablation of Atrial Fibrillation in 3,000 Consecutive Procedures. JACC Clin Electrophysiol. 2016;3(2):154–61.
103. Zanchi S, Chen S, Chun KRJ, Schmidt B. Ablation Index - guided high - power (50 W) short - duration for left atrial anterior and roofline ablation : Feasibility , procedural data , and lesion analysis (AI High - Power Linear Ablation). J Cardiovasc Electrophysiol. 2021;32(4):984–93.
104. Kueffer T, Seiler J, Madaffari A, Mühl A, Asatryan B, Stettler R, Haeberlin A, Noti F, Servatius H, Tanner H, Baldinger SH, Reichlin T, Roten L. Pulsed-field ablation for the treatment of left atrial reentry tachycardia. J Interv Card Electrophysiol. 2023 Sep;66(6):1431–40.
105. Phlips T, Verhaeghe L, Antole N, Koopman P, Vijgen J. Pulsed field ablation using a focal contact force catheter allowed successful ablation of a focal right atrial tachycardia in the proximity of the phrenic nerve. Hear Rhythm Case Reports. 2023;9(7):434–6.
106. Adelino R, Combes S, Bouazzaoui R El, Albenque J-P, Combes N, Boveda S. Pulsed-field ablation of recurrent right atrial tachycardia : expanding the use of electroporation beyond atrial fibrillation. Europace. 2022;25(4):1512.
107. Wieczorek M. Non-contact mapping in cardiac electrophysiology. Herzschrittmacherther Elektrophysiol. 2018 Sep;29(3):264–70.
108. Cuculich PS, Schill MR, Kashani R, Mutic S, Lang A, Cooper D, Faddis M, Gleva M, Noheria A, Smith TW, Hallahan D, Rudy Y, Robinson CG. Noninvasive Cardiac Radiation for Ablation of Ventricular Tachycardia. N Engl J Med. 2017 Dec;377(24):2325–36.

7. Schriftenverzeichnis des Verfassers

Originalarbeiten (Erst- oder Seniorautor, korrespondierender Autor)

1. Wahedi R, Willems S, Feldhege J, Jularic M, Hartmann J, Anwar O, Dickow J, Harloff T, Gessler N, **Gunawardene MA**. Pulsed-field versus cryoballoon ablation for atrial fibrillation-Impact of energy source on sedation and analgesia requirement. J Cardiovasc Electrophysiol. 2024 Jan;35(1):162-170. doi: 10.1111/jce.16141. Epub 2023 Nov 27. PMID: 38009545.

2.. **Gunawardene MA**, Frommeyer G, Ellermann C, Jularic M, Leitz P, Hartmann J, Lange PS, Anwar O, Rath B, Wahedi R, Eckardt L, Willems S. Left Atrial Posterior Wall Isolation with Pulsed Field Ablation in Persistent Atrial Fibrillation. J Clin Med. 2023 Sep 29;12(19):6304. doi: 10.3390/jcm12196304. PMID: 37834948; PMCID: PMC10573684.

3. **Gunawardene MA,** Schaeffer BN, Jularic M, Eickholt C, Akbulak RÖ, Hedenus K, Wahedi R, Anwar O, Gessler N, Hartmann J, Willems S. Pulsed field ablation in patients with complex consecutive atrial tachycardia in conjunction with ultra- high density mapping: Proof of concept. J Cardiovasc Electrophysiol. 2022 Dec;33(12):2431-2443. doi: 10.1111/jce.15713. Epub 2022 Nov 9. PMID: 36259717.

4. **Gunawardene MA,** Schaeffer BN, Jularic M, Eickholt C, Maurer T, Akbulak RÖ, Flindt M, Anwar O, Pape UF, Maasberg S, Gessler N, Hartmann J, Willems S. Pulsed-field ablation combined with ultrahigh-density mapping in patients undergoing catheter ablation for atrial fibrillation: Practical and electrophysiological considerations. J Cardiovasc Electrophysiol. 2022 Mar;33(3):345-356. doi: 10.1111/jce.15349. Epub 2022 Jan 9. PMID: 34978360.

5. **Gunawardene MA,** Gessler N, Wohlmuth P, Heitmann K, Anders P, Jaquet K, Herborn CU, Arnold D, Bein B, Bergmann MW, Herrlinger KR, Stang A, Schreiber R, Wesseler C, Willems S. Prognostic Impact of Acute Cardiovascular Events in COVID-19 Hospitalized Patients-Results from the CORONA Germany Study. J Clin Med. 2021 Sep 2;10(17):3982. doi: 10.3390/jcm10173982. PMID: 34501427; PMCID: PMC8432202.
Geteilte Erstautorenschaft: Gunawardene MA, Gessler N

6. **Gunawardene MA,** Eickholt C, Akbulak RÖ, Jularic M, Klatt N, Hartmann J, Schlüter M, Meyer C, Willems S, Schaeffer B. Ultra-high-density mapping of conduction gaps and atrial tachycardias: Distinctive patterns following pulmonary vein isolation with cryoballoon or contact-force-guided radiofrequency current. J Cardiovasc Electrophysiol. 2020 May;31(5):1051-1061. doi: 10.1111/jce.14413. Epub 2020 Mar 9. PMID: 32107811.

7. **Gunawardene M,** Münkler P, Eickholt C, Akbulak RÖ, Jularic M, Klatt N, Hartmann J, Dinshaw L, Jungen C, Moser JM, Merbold L, Willems S, Meyer C. A novel assessment of local impedance during catheter ablation: initial experience in humans comparing local and generator measurements. Europace. 2019 Jan 1;21:i34-i42. doi: 10.1093/europace/euy273. PMID: 30801126.

8. **Gunawardene MA,** Dickow J, Schaeffer BN, Akbulak RÖ, Lemoine MD, Nührich JM, Jularic M, Sinning C, Eickholt C, Meyer C, Moser JM, Hoffmann BA, Willems S. Risk stratification of patients with left atrial appendage thrombus prior to catheter ablation of atrial fibrillation: An approach towards an individualized use of transesophageal echocardiography. J Cardiovasc Electrophysiol. 2017 Oct;28(10):1127-1136. doi: 10.1111/jce.13279. Epub 2017 Jul 26. PMID: 28635023.

9. **Gunawardene MA,** Hoffmann BA, Schaeffer B, Chung DU, Moser J, Akbulak RO, Jularic M, Eickholt C, Nuehrich J, Meyer C, Willems S. Influence of energy source

on early atrial fibrillation recurrences: a comparison of cryoballoon vs. radiofrequency current energy ablation with the endpoint of unexcitability in pulmonary vein isolation. Europace. 2018 Jan 1;20(1):43-49. doi: 10.1093/europace/euw307. PMID: 27742775.
Geteilte Erstautorenschaft: Gunawardene MA, Hoffmann BA

10. **Gunawardene M**, Willems S, Schäffer B, Moser J, Akbulak RÖ, Jularic M, Eickholt C, Nührich J, Meyer C, Kuklik P, Sehner S, Czerner V, Hoffmann BA. Influence of periprocedural anticoagulation strategies on complication rate and hospital stay in patients undergoing catheter ablation for persistent atrial fibrillation. Clin Res Cardiol. 2017 Jan;106(1):38-48. doi: 10.1007/s00392-016-1021-x. Epub 2016 Jul 19. PMID: 27435077.

Originalarbeiten (Ko-Autor)

1. Turagam MK, Neuzil P, Schmidt B, Reichlin T, Neven K, Metzner A, Hansen J, Blaauw Y, Maury P, Arentz T, Sommer P, Anic A, Anselme F, Boveda S, Deneke T, Willems S, van der Voort P, Tilz R, Funasako M, Scherr D, Wakili R, Steven D, Kautzner J, Vijgen J, Jais P, Petru J, Chun J, Roten L, Füting A, Lemoine MD, Ruwald M, Mulder BA, Rollin A, Lehrmann H, Fink T, Jurisic Z, Chaumont C, Adelino R, Nentwich K, **Gunawardene M**, Ouss A, Heeger CH, Manninger M, Bohnen JE, Sultan A, Peichl P, Koopman P, Derval N, Kueffer T, Reddy VY. Clinical Outcomes by Sex After Pulsed Field Ablation of Atrial Fibrillation. JAMA Cardiol. 2023 Dec 1;8(12):1142-1151. doi: 10.1001/jamacardio.2023.3752. PMID: 37910101; PMCID: PMC10620676.

2. Dickow J, **Gunawardene MA**, Willems S, Feldhege J, Wohlmuth P, Bachmann M, Bergmann MW, Gesierich W, Nowak L, Pape UF, Schreiber R, Wirtz S, Twerenbold R, Sheikhzadeh S, Gessler N. Higher in-hospital mortality in SARS-CoV-2 omicron variant infection compared to influenza infection-Insights from

the CORONA Germany study. PLoS One. 2023 Sep 27;18(9):e0292017. doi: 10.1371/journal.pone.0292017. PMID: 37756299; PMCID: PMC10529565.

3. Turagam MK, Neuzil P, Schmidt B, Reichlin T, Neven K, Metzner A, Hansen J, Blaauw Y, Maury P, Arentz T, Sommer P, Anic A, Anselme F, Boveda S, Deneke T, Willems S, van der Voort P, Tilz R, Funasako M, Scherr D, Wakili R, Steven D, Kautzner J, Vijgen J, Jais P, Petru J, Chun J, Roten L, Füting A, Lemoine MD, Ruwald M, Mulder BA, Rollin A, Lehrmann H, Fink T, Jurisic Z, Chaumont C, Adeliño R, Nentwich K, **Gunawardene M**, Ouss A, Heeger CH, Manninger M, Bohnen JE, Sultan A, Peichl P, Koopman P, Derval N, Kueffer T, Rahe G, Reddy VY. Safety and Effectiveness of Pulsed Field Ablation to Treat Atrial Fibrillation: One-Year Outcomes From the MANIFEST-PF Registry. Circulation. 2023 Jul 4;148(1):35-46. doi: 10.1161/CIRCULATIONAHA.123.064959. Epub 2023 May 18. PMID: 37199171.

4. Tilz RR, Schmidt V, Pürerfellner H, Maury P, Chun KJ, Martinek M, Sohns C, Schmidt B, Mandel F, Gandjbakhch E, Laredo M, **Gunawardene MA**, Willems S, Beiert T, Borlich M, Iden L, Füting A, Spittler R, Gaspar T, Richter S, Schade A, Kuniss M, Neumann T, Francke A, Wunderlich C, Shin DI, Grosse Meininghaus D, Foresti M, Bonsels M, Reek D, Wiegand U, Bauer A, Metzner A, Eckardt L, Popescu SȘ, Krahnefeld O, Sticherling C, Kühne M, Nguyen DQ, Roten L, Saguner AM, Linz D, van der Voort P, Mulder BA, Vijgen J, Almorad A, Guenancia C, Fauchier L, Boveda S, De Greef Y, Da Costa A, Jais P, Derval N, Milhem A, Jesel L, Garcia R, Poty H, Khoueiry Z, Seitz J, Laborderie J, Mechulan A, Brigadeau F, Zhao A, Saludas Y, Piot O, Ahluwalia N, Martin C, Chen J, Antolic B, Leventopoulos G, Özcan EE, Yorgun H, Cay S, Yalin K, Botros MS, Mahmoud AT, Jędrzejczyk-Patej E, Inaba O, Okumura K, Ejima K, Khakpour H, Boyle N, Catanzaro JN, Reddy V, Mohanty S, Natale A, Blessberger H, Yang B, Stevens I, Sommer P, Veltmann C, Steven D, Vogler J, Kuck KH, Merino JL, Keelani A, Heeger CH. A worldwide survey on incidence, management and prognosis of

oesophageal fistula formation following atrial fibrillation catheter ablation: The POTTER-AF study. Eur Heart J. 2023 Apr 16:ehad250. doi: 10.1093/eurheartj/ehad250. Epub ahead of print. PMID: 37062040.

5. Konermann FM, Gessler N, Wohlmuth P, Behr J, Feldhege J, Glöckner C, **Gunawardene MA**, Herrlinger KR, Hölting T, Pape UF, Reinmuth N, Stang A, Sheikhzadeh S, Arnold D, Wesseler C. High in-hospital mortality in SARS-CoV-2 infected patients with active cancer disease during Omicron phase of the pandemic - Insights from the CORONA Germany Study. Oncol Res Treat. 2023 Feb 23. doi: 10.1159/000529788. Epub ahead of print. PMID: 36822167.

6. Anwar O, Chung DU, **Gunawardene MA**, Jungen C, Hartmann J, Meyer C, Gessler N, Willems S, Hakmi S, Eickholt C. A Simplified Approach to Pulmonary Vein Visualization during Cryoballoon Ablation of Atrial Fibrillation. Medicina (Kaunas). 2022 Nov 22;58(12):1700. doi: 10.3390/medicina58121700. PMID: 36556902; PMCID: PMC9781762.

7. Kostev K, Hagemann-Goebel M, Gessler N, Wohlmuth P, Feldhege J, Arnold D, Jacob L, **Gunawardene M**, Hölting T, Koyanagi A, Schreiber R, Smith L, Sheikhzadeh S, Wollmer MA. Is there an association between depression, anxiety disorders and COVID-19 severity and mortality? A multicenter retrospective cohort study conducted in 50 hospitals in Germany. J Psychiatr Res. 2022 Nov 29;157:192-196. doi: 10.1016/j.jpsychires.2022.11.031. Epub ahead of print. PMID: 36481563; PMCID: PMC9706218.

8. Sievering AW, Wohlmuth P, Geßler N, **Gunawardene MA**, Herrlinger K, Bein B, Arnold D, Bergmann M, Nowak L, Gloeckner C, Koch I, Bachmann M, Herborn CU, Stang A. Comparison of machine learning methods with logistic regression analysis in creating predictive models for risk of critical in-hospital events in COVID-19 patients on hospital admission. BMC Med Inform Decis Mak. 2022 Nov 28;22(1):309. doi: 10.1186/s12911-022-02057-4. PMID: 36437469; PMCID: PMC9702742.

9. Maurer T, Flindt M, Jularic M, Lemes C, Akbulak-Stegli RÖ, **Gunawardene MA,** Hartmann J, Eickholt C, Willems S, Schäffer B. A novel wide-band dielectric imaging system to guide radiofrequency ablation for pulmonary vein isolation. J Cardiovasc Electrophysiol. 2022 Dec;33(12):2467-2472. doi: 10.1111/jce.15705. Epub 2022 Oct 26. PMID: 36217995.

10. Gessler N, Wohlmuth P, Anwar O, Debus ES, Eickholt C, **Gunawardene MA**, Hakmi S, Heitmann K, Rybczynski M, Schueler H, Sheikhzadeh S, Tigges E, Wiest GH, Willems S, Adam E, von Kodolitsch Y. Sleep apnea predicts cardiovascular death in patients with Marfan syndrome: a cohort study. EPMA J. 2022 Jul 29;13(3):451-460. doi: 10.1007/s13167-022-00291-4. PMID: 36061830; PMCID: PMC9437159.

11. Ekanem E, Reddy VY, Schmidt B, Reichlin T, Neven K, Metzner A, Hansen J, Blaauw Y, Maury P, Arentz T, Sommer P, Anic A, Anselme F, Boveda S, Deneke T, Willems S, van der Voort P, Tilz R, Funasako M, Scherr D, Wakili R, Steven D, Kautzner J, Vijgen J, Jais P, Petru J, Chun J, Roten L, Füting A, Rillig A, Mulder BA, Johannessen A, Rollin A, Lehrmann H, Sohns C, Jurisic Z, Savoure A, Combes S, Nentwich K, **Gunawardene M**, Ouss A, Kirstein B, Manninger M, Bohnen JE, Sultan A, Peichl P, Koopman P, Derval N, Turagam MK, Neuzil P; MANIFEST-PF Cooperative. Multi-national survey on the methods, efficacy, and safety on the post-approval clinical use of pulsed field ablation (MANIFEST-PF). Europace. 2022 Sep 1;24(8):1256-1266. doi: 10.1093/europace/euac050. Erratum in: Europace. 2023 Jan 04;: PMID: 35647644; PMCID: PMC9435639.

12. Gessler N, **Gunawardene MA**, Wohlmuth P, Arnold D, Behr J, Gloeckner C, Herrlinger K, Hoelting T, Pape UF, Schreiber R, Stang A, Wesseler C, Willems S, Arms C, Herborn CU. Clinical outcome, risk assessment, and seasonal variation in hospitalized COVID-19 patients-Results from the CORONA Germany study. PLoS One. 2021 Jun 17;16(6):e0252867. doi: 10.1371/journal.pone.0252867. PMID: 34138888; PMCID: PMC8211271.
Geteilte Erstautorenschaft: Gunawardene MA, Gessler N

13. Gessler N, Willems S, Steven D, Aberle J, Akbulak RO, Gosau N, Hoffmann BA, Meyer C, Sultan A, Tilz R, Vogler J, Wohlmuth P, Scholz S, **Gunawardene MA**, Eickholt C, Lüker J. Supervised Obesity Reduction Trial for AF ablation patients: results from the SORT-AF trial. Europace. 2021 Oct 9;23(10):1548-1558. doi: 10.1093/europace/euab122. PMID: 33895833; PMCID: PMC8502497.

14. Jungen C, Akbulak R, Kahle AK, Eickholt C, Schaeffer B, Scherschel K, Dinshaw L, Muenkler P, Schleberger R, Nies M, **Gunawardene MA**, Klatt N, Hartmann J, Merbold L, Jularic M, Willems S, Meyer C. Outcome after tailored catheter ablation of atrial tachycardia using ultra-high-density mapping. J Cardiovasc Electrophysiol. 2020 Oct;31(10):2645-2652. doi: 10.1111/jce.14703. Epub 2020 Aug 11. PMID: 32748442.

15. Anwar O, **Gunawardene MA,** Dickow J, Scherschel K, Jungen C, Münkler P, Eickholt C, Willems S, Gessler N, Meyer C. Contemporary analysis of phrenic nerve injuries following cryoballoon-based pulmonary vein isolation: A single-centre experience with the systematic use of compound motor action potential monitoring. PLoS One. 2020 Jun 25;15(6):e0235132. doi: 10.1371/journal.pone.0235132. PMID: 32584880; PMCID: PMC7316283.

16. Alken FA, Klatt N, Muenkler P, Scherschel K, Jungen C, Akbulak RO, Kahle AK, **Gunawardene M**, Jularic M, Dinshaw L, Hartmann J, Eickholt C, Willems S, Stute F, Mueller G, Blankenberg S, Rickers C, Sinning C, Zengin-Sahm E, Meyer C. Advanced mapping strategies for ablation therapy in adults with congenital heart disease. Cardiovasc Diagn Ther. 2019 Oct;9(Suppl 2):S247-S263. doi: 10.21037/cdt.2019.10.02. PMID: 31737533; PMCID: PMC6837939.

17. Münkler P, **Gunawardene MA**, Jungen C, Klatt N, Schwarzl JM, Akbulak RÖ, Dinshaw L, Hartmann J, Jularic M, Kahle AK, Riedel R, Merbold L, Eickholt C, Willems S, Meyer C. Local impedance guides catheter ablation in patients with ventricular tachycardia. J Cardiovasc Electrophysiol. 2020 Jan;31(1):61-69. doi: 10.1111/jce.14269. Epub 2019 Nov 25. PMID: 31701589.

18. Dinshaw L, Schäffer B, Akbulak Ö, Jularic M, Hartmann J, Klatt N, Dickow J, **Gunawardene M,** Münkler P, Hakmi S, Pecha S, Sultan A, Lüker J, Pinnschmidt H, Hoffmann B, Gosau N, Eickholt C, Willems S, Steven D, Meyer C. Long-term efficacy and safety of radiofrequency catheter ablation of atrial fibrillation in patients with cardiac implantable electronic devices and transvenous leads. J Cardiovasc Electrophysiol. 2019 May;30(5):679-687. doi: 10.1111/jce.13890. Epub 2019 Mar 10. PMID: 30821012.

19. Schaeffer B, Willems S, Meyer C, Lüker J, Akbulak RÖ, Moser J, Jularic M, Eickholt C, Schwarzl JM, **Gunawardene M,** Kuklik P, Sultan A, Hoffmann BA, Steven D. Contact force facilitates the achievement of an unexcitable ablation line during pulmonary vein isolation. Clin Res Cardiol. 2018 Aug;107(8):632-641. doi: 10.1007/s00392-018-1228-0. Epub 2018 Mar 2. PMID: 29500567.

20. Fürnkranz A, Bordignon S, Dugo D, Perotta L, **Gunawardene M**, Schulte-Hahn B, Nowak B, Schmidt B, Chun JKR. Improved 1-year clinical success rate of pulmonary vein isolation with the second-generation cryoballoon in patients with paroxysmal atrial fibrillation. J Cardiovasc Electrophysiol. 2014

Aug;25(8):840-844. doi: 10.1111/jce.12417. Epub 2014 May 2. PMID: 24654794.

21. Bordignon S, Fürnkranz A, Dugo D, Perrotta L, **Gunawardene M**, Bode F, Klemt A, Nowak B, Schulte-Hahn B, Schmidt B, Chun KR. Improved lesion formation using the novel 28 mm cryoballoon in atrial fibrillation ablation: analysis of biomarker release. Europace. 2014 Jul;16(7):987-93. doi: 10.1093/europace/eut400. Epub 2014 Jan 19. PMID: 24446511.

22. Bordignon S, Chun KR, **Gunawardene M,** Fuernkranz A, Urban V, Schulte-Hahn B, Nowak B, Schmidt B. Comparison of balloon catheter ablation technologies for pulmonary vein isolation: the laser versus cryo study. J Cardiovasc Electrophysiol. 2013 Sep;24(9):987-94. doi: 10.1111/jce.12192. Epub 2013 Jun 25. PMID: 23800359.

23. Schmidt B, **Gunawardene M**, Krieg D, Bordignon S, Fürnkranz A, Kulikoglu M, Herrmann W, Chun KR. A prospective randomized single-center study on the risk of asymptomatic cerebral lesions comparing irrigated radiofrequency current ablation with the cryoballoon and the laser balloon. J Cardiovasc Electrophysiol. 2013 Aug;24(8):869-74. doi: 10.1111/jce.12151. Epub 2013 Apr 18. PMID: 23601001.

24. Fürnkranz A, Bordignon S, Schmidt B, **Gunawardene M**, Schulte-Hahn B, Urban V, Bode F, Nowak B, Chun JK. Improved procedural efficacy of pulmonary vein isolation using the novel second-generation cryoballoon. J Cardiovasc Electrophysiol. 2013 May;24(5):492-7. doi: 10.1111/jce.12082. Epub 2013 Feb 11. PMID: 23398599.

25. Bordignon S, Chun KR, **Gunawardene M**, Urban V, Kulikoglu M, Miehm K, Brzank B, Schulte-Hahn B, Nowak B, Schmidt B. Energy titration strategies with the endoscopic ablation system: lessons from the high-dose vs. low-dose laser

ablation study. Europace. 2013 May;15(5):685-9. doi: 10.1093/europace/eus352. Epub 2012 Nov 4. PMID: 23129544.

26. Chun KJ, Bordignon S, **Gunawardene M**, Urban V, Kulikoglu M, Schulte-Hahn B, Nowak B, Schmidt B. Single transseptal big Cryoballoon pulmonary vein isolation using an inner lumen mapping catheter. Pacing Clin Electrophysiol. 2012 Nov;35(11):1304-11. doi: 10.1111/j.1540-8159.2012.03475.x. Epub 2012 Aug 6. PMID: 22882344.

27. Schmidt B, **Gunawardene M**, Urban V, Kulikoglu M, Schulte-Hahn B, Nowak B, Bordignon S, Chun KJ. Visually guided sequential pulmonary vein isolation: insights into techniques and predictors of acute success. J Cardiovasc Electrophysiol. 2012 Jun;23(6):576-82. doi: 10.1111/j.1540-8167.2011.02247.x. Epub 2012 Jan 9. PMID: 22229948.

Übersichtsarbeiten / Reviews

(Erst- oder Seniorautor, korrespondierender Autor)

1. **Gunawardene M**, Hartmann J, Willems S. Asymptomatisches Vorhofflimmern : Screening und Therapie [Asymptomatic atrial fibrillation : Screening and therapy]. Herzschrittmacherther Elektrophysiol. 2023 Mar 13. German. doi: 10.1007/s00399-023-00933-8. Epub ahead of print. PMID: 36912974.

2. **Gunawardene MA,** Hartmann J, Kottmaier M, Bourier F, Busch S, Sommer P, Maurer T, Althoff T, Shin DI, Duncker D, Johnson V, Estner H, Rillig A, Iden L, Tilz R, Metzner A, Chun KRJ, Steven D, Jansen H, Jadidi A, Willems S. Fokale atriale Tachykardien: Diagnostik und Therapie [Focal atrial tachycardias: diagnostics and therapy]. Herzschrittmacherther Elektrophysiol. 2022 Dec;33(4):467-475. German. doi: 10.1007/s00399-022-00907-2. Epub 2022 Nov 7. PMID: 36342506.

3. **Gunawardene MA,** Willems S. Atrial fibrillation progression and the importance of early treatment for improving clinical outcomes. Europace. 2022 Jun 6;24(Suppl 2):ii22-ii28. doi: 10.1093/europace/euab257. PMID: 35661866.

4. **Gunawardene MA**, Hartmann J, Jularic M, Eickholt C, Gessler N, Willems S. Therapeutisches Management des nichtvalvulären Vorhofflimmerns [Therapeutic management of nonvalvular atrial fibrillation]. Herz. 2020 Sep;45(6):603-616. German. doi: 10.1007/s00059-020-04960-w. PMID: 32632547.

Übersichtsarbeiten / Reviews (Ko-Autor)

1. Willems S, **Gunawardene MA,** Eickholt C, Hartmann J, Schmoeckel M, Schäffer B. Medical, Interventional, and Surgical Treatment Strategies for Atrial Fibrillation. Dtsch Arztebl Int. 2022 Jan 10;(Forthcoming):arztebl.m2021.0303. doi: 10.3238/arztebl.m2021.0303. Epub ahead of print. PMID: 34789364.

2. Schäffer B, **Gunawardene MA,** Willems S. Update Vorhofflimmern – Was ist neu? [Update Atrial Fibrillation - Current Management strategies]. Dtsch Med Wochenschr. 2021 Aug;146(15):982-987. German. doi: 10.1055/a-1361-7362. Epub 2021 Aug 3. PMID: 34344034.
3. Bordignon S, Chun KR, **Gunawardene M**, Schulte-Hahn B, Nowak B, Fuernkranz A, Schmidt B. Endoscopic ablation systems. Expert Rev Med Devices. 2013 Mar;10(2):177-83. doi: 10.1586/erd.12.86. PMID: 23480087.

Fallberichte (Erst- oder Seniorautor, korrespondierender Autor)

1. **Gunawardene MA,** Schaeffer BN, Jularic M, Eickholt C, Maurer T, Akbulak RÖ, Flindt M, Anwar O, Hartmann J, Willems S. Coronary Spasm During Pulsed Field Ablation of the Mitral Isthmus Line. JACC Clin Electrophysiol. 2021 Dec;7(12):1618-1620. doi: 10.1016/j.jacep.2021.08.016. Epub 2021 Sep 29. PMID: 34600850.
2. **Gunawardene M,** Meyer C, Willems S, Hoffmann BA. Cryoablation of an atrioventricular nodal reentrant tachycardia in a patient with an implanted deep brain stimulator. HeartRhythm Case Rep. 2016 Mar 19;2(3):258-260. doi: 10.1016/j.hrcr.2016.02.003. PMID: 28491683; PMCID: PMC5419761.

Fallberichte (Ko-Autor)

1. Chun KR, Schulte-Hahn B, **Gunawardene M,** Schmidt B. Witnessed pulmonary vein arrest-endoscopically observed conversion of atrial fibrillation into sinus rhythm by laser balloon ablation. Herz. 2012 May;37(3):336-7. doi: 10.1007/s00059-011-3520-x. Epub 2011 Nov 11. PMID: 22071678.

8. Abbildungsverzeichnis

Visualisierung des PFA-Katheters in „Korb“-Konfiguration im Bereich der linken unteren Pulmonalvene (Aufsicht von hinten auf den linken Vorhof). B2+B3: Prä (B2)- und post (B3)- ultrahochauflösendes Voltagemap des linken Vorhofs mit Darstellung der linksatrialen Hinterwand mit Visualisierung des PFA-Katheters im Bereich der isolierten Hinterwand in der „Blumen“-Konfiguration (Aufsicht von hinten auf den linken Vorhof). Farbcodierung: Rot und Grau markieren die Narbenareale bzw. durch Ablation gesetzte Narben, lila gesundes Vorhofmyokard.

Abbildung 12: Linksatriale Verteilung der Fibrose bei den Patient:innen.

Abbildung 13: Linksatriale Tachykardie mit anteriorem Makroreentry. A: Fraktionierte Elektrogramme im Bereich des kritischen Isthmus des in B dargestellten ultrahochauflösenden Aktivierungsmaps einer linksatrialen anterioren Tachykardie (Ansicht B von vorne auf den linken Vorhof). C: Voltagemap des linken Vorhofes (Voltage ist farbkodiert: rot und grau zeigen die Narbe, lila gesundes Vorhofmyokard). D: Platzierung des PFA-Katheters im Bereich des kritischen Isthmus. E: Fluoroskopische Darstellung der „Blumen“-Konfiguration des PFA-Katheters im Bereich des kritischen Isthmus. G: Fraktionierte Elektrogramme des kritischen Isthmus auf den Elektroden des PFA-Katheters während der laufenden Tachykardie. H: Terminierung der atrialen Tachykardie mit dem 1. PFA Impuls in den Sinusrhythmus. F: *Groß dargestellt*: Ultrahochauflösendes Aktivierungsmap nach PFA-Ablation und erfolgreicher Blockierung der anterioren Linie; *klein dargestellt*: linksatriales Voltagemap post Ablation.

Abbildung 14: Linksatriale ultrahochauflösende Voltagemaps prä- und post-PFA-Ablation am Beispiel blockierter Linien. Linke Spalte prä-Ablation, rechte Spalte post-Ablation. Jede Zeile zeigt eine(n) Patient:in. Die Voltage ist farbkodiert: rot und grau zeigen die Narbe, lila gesundes Vorhofmyokard.

9. Tabellenverzeichnis

*Dysarthrie unmittelbar nach Prozedurende, ohne weitere Fokalneurologie und mit normalem kranialen CT (a. e. sedierungsbedingt).

Tabelle 6: Patientencharakteristika und prozedurale Daten. BMI, Body-Mass-Index; CHA2DS2-VASc Score (Score zur Evaluation des Schlaganfallrisikos); LA, linkes Atrium; min, Minuten; ml, Milliliter; PFA, Pulsed Field Ablation; UHDx ultra-hochauflösendes Mapping. Werte sind als Mittelwert ± Standardabweichung angegeben, [n] oder n (%).

Tabelle 7: Patientencharakteristika und prozedurale Daten. BMI, Body-Mass-Index; CHA2DS2-VASc Score (Score zur Evaluation des Schlaganfallrisikos); LA, linksatrial; min, Minuten; ml, Milliliter; PFA, Pulsed Field Ablation; UHDx ultra-hochauflösendes Mapping. Werte sind als Mittelwert ± Standardabweichung angegeben, [n] oder n (%).

10. Danksagung

Zunächst möchte ich mich an dieser Stelle allen Menschen meinen großen Dank aussprechen, die mich auf dem Weg zur Anfertigung dieser Habilitationsschrift unterstützt haben.

An dieser Stelle gilt mein besonderer Dank Herrn Prof. Dr. Christian Hamm und Herrn Prof. Dr. Samuel Sossalla für die enorme Unterstützung und Begleitung dieser Arbeit an der Medzinischen Klinik I, Abteilung für Kardiologie.

Besonders danken möchte ich meinem Mentor Herrn Prof. Dr. Stephan Willems für die hervorragende Zusammenarbeit der letzten Jahre, die kontinuierliche Unterstützung, die Aus- und Weiterbildung, das Vertrauen, die Motivation und endlose Wertschätzung für meine Person.

Besonders bedanken möchte ich mich bei Herrn Prof. Dr. Boris Schmidt und Herrn Prof. Dr. KR Julian Chun, die mir das Fundament meiner Begeisterung für die klinische Elektrophysiolgie gegeben und mich enorm auf meinem Weg unterstützt haben.

Außerdem möchte ich mich bei Herrn Prof. Dr. Boris A. Hoffmann bedanken, der mir den Einstieg in das universitäre Arbeiten und wissenschaftliche Denken nähergebracht hat und stets motiviert hat.

Mein weiterer Dank gilt Herrn Prof. Dr. Christian Meyer und Jens Hartmann, deren positive Energie und Rückendeckung mir stets die Möglichkeit zur Weiterentwicklung gegeben haben.

Ich danke den Kolleg:innen der Klinik für Kardiologie in Hamburg und Gießen, Herr Dr. Mario Jularic, Herr Dr. Benjamin Schäffer, Herr Prof. Oliver Dörr, Frau Dr. Victoria Johnson, Herr Dr. Jörn Schmitt, Herr PD Dr. Shibu Matthew und Herr PD Dr. Borislav Dinov für die Zusammenarbeit und die Unterstützung bei der Umsetzung dieser Arbeit sowie für die klinische Weiterbildung.

Nicht zuletzt bedanke ich mich bei Herrn Prof. Dr. Srinivas Dukkipati und Prof. Dr. Vivek Reddy, die trotz weiter Distanz meine Arbeit durch ihre Inspiration und Unterstützung geprägt haben.

Meinen Eltern, sowie meinen Geschwistern, meiner Nichte und Freunden danke ich für ihre Geduld, Ermutigungen zum Weitermachen und den Verzicht auf gemeinsame Zeit während der Arbeit an dieser Habilitation.

11. Erklärung der Habilitationsleistung

Hiermit erkläre ich, dass ich die vorliegende Arbeit bzw. die mir zuzuordnenden Teile im Rahmen einer kumulativen Habilitationsschrift, selbstständig und ohne unzulässige Hilfe oder Benutzung anderer als der angegebenen Hilfsmittel angefertigt habe. Alle Textstellen, die wörtlich oder sinngemäß aus veröffentlichten oder nichtveröffentlichten Schriften entnommen sind, und alle Angaben, die auf mündlichen Auskünften beruhen, sind als solche kenntlich gemacht. Ich versichere, dass ich für die nach §2 (3) der Habilitationsordnung angeführten bereits veröffentlichten Originalarbeiten als Erst-oder Seniorautor fungiere, da ich den größten Teil der Daten selbst erhoben habe, für das Design der Arbeiten verantwortlich bin und die Manuskripte maßgeblich gestaltet habe. Für alle von mir erwähnten Untersuchungen habe ich die in der „Satzung der Justus-Liebig-Universität zur Sicherung guter wissenschaftlicher Praxis“ niedergelegten Grundsätze befolgt. Ich versichere, dass alle an der Finanzierung der Arbeiten beteiligten Geldgeber in den jeweiligen Publikationen genannt worden sind. Ich versichere außerdem, dass die vorgelegte Arbeit weder im Inland noch im Ausland in gleicher oder ähnlicher Weise einer anderen Prüfungsbehörde vorgelegt wurde oder Gegenstand eines anderen Prüfungsverfahrens war. Mit der Überprüfung meiner Arbeit durch eine Plagiatserkennungssoftware bzw. ein internetbasiertes Softwareprogramm erkläre ich mich einverstanden.

Gießen, den 13.Februar 2024

Dr. med. Melanie Gunawardene
Erikastrasse 59
20251 Hamburg

12. Erklärung zu anderweitigen Habilitationen oder Habilitationsversuchen

Hiermit erkläre ich, dass ich an keiner Universität, weder im Inland noch im Ausland, bisher einen anderweitigen Habilitationsversuch oder eine anderweitige Habilitation unternommen habe. Ferner wird hiermit erklärt, dass ich mich nicht vor Abschluss des Habilitationsverfahrens an anderer Stelle zur Habilitation melden werde.

Gießen, den 13. Februar 2024

Dr. med. Melanie Gunawardene
Erikastrasse 59
20251 Hamburg

13. Zugrundeliegende Publikationen

Clin Res Cardiol
DOI 10.1007/s00392-016-1021-x

ORIGINAL PAPER

Influence of periprocedural anticoagulation strategies on complication rate and hospital stay in patients undergoing catheter ablation for persistent atrial fibrillation

Melanie Gunawardene[1] · S. Willems[1] · B. Schäffer[1] · J. Moser[1] · R. Ö. Akbulak[1] · M. Jularic[1] · C. Eickholt[1] · J. Nührich[1] · C. Meyer[1] · P. Kuklik[1] · S. Sehner[2] · V. Czerner[1] · B. A. Hoffmann[1]

Received: 26 May 2016 / Accepted: 8 July 2016

Abstract
Background The use of non-vitamin K antagonists (NOACs), uninterrupted (uVKA) and interrupted vitamin K antagonists (iVKA) are common periprocedural oral anticoagulation (OAC) strategies for atrial fibrillation (AF) ablation. Comparative data on complication rates resulting from OAC strategies for solely persistent AF (persAF) undergoing ablation are sparse. Thus, we sought to determine the impact of these OAC strategies on complication rates among patients with persAF undergoing catheter ablation.
Methods Consecutive patients undergoing persAF ablation were included. Depending on preprocedural OAC, three groups were defined: (1) NOACs (paused 48 h preablation), (2) uVKA, and (3) iVKA with heparin bridging. A combined complication endpoint (CCE) composed of bleeding and thromboembolic events was analyzed.
Results Between 2011 and 2014, 1440 persAF ablation procedures were performed in 1092 patients. NOACs were given in 441 procedures (31 %; rivaroxaban 57 %, dabigatran 33 %, and apixaban 10 %), uVKA in 488 (34 %), and iVKA in 511 (35 %). Adjusted CCE rates were 5.5 % [95 % confidence interval (CI) (3.1–7.8)] in group 1 (NOACs), 7.5 % [95 % CI (5.0–10.1)] in group 2 (uVKA), and 9.9 % [95 % CI (6.6–13.2)] in group 3. Compared to group 1, the combined complication risk was almost twice as high in group 3 [odd's ratio (OR) 1.9, 95 % CI (1.0–3.7), $p = 0.049$)]. The major complication rate was low (0.9 %). Bleeding complications, driven by minor groin complications, are more frequent than thromboembolic events ($n = 112$ vs. 1, $p < 0.0001$).
Conclusions Patients undergoing persAF ablation with iVKA anticoagulation have an increased risk of complications compared to NOACs. Major complications, such as thromboembolic events, are generally rare and are exceeded by minor bleedings.

Keywords Atrial fibrillation ablation · Periprocedural oral anticoagulation · Oral anticoagulation · Complication · Persistent atrial fibrillation · Catheter ablation · Vitamin K antagonists · Non-vitamin K antagonists

Introduction

Recently, oral anticoagulation (OAC) has been revolutionized by the introduction of non-vitamin K antagonists (NOACs) as an alternative option to vitamin K antagonists (VKA). For patients (pts) undergoing atrial fibrillation (AF) catheter ablation, it is, therefore, essential to establish safe periprocedural anticoagulation strategies, weighing out bleeding, and thromboembolic risks.

The first usage of periprocedural OAC was via the interruption of VKAs and bridging with low-molecular-weight heparin (LMWH). Subsequently, continuous periprocedural VKAs entered clinical practice [1, 2], followed by NOACs [3–10]. Despite their now routine usage, strategies regarding the continuation, discontinuation, and bridging of OACs before and after AF ablation are not uniform [3].

✉ Melanie Gunawardene
m.gunawardene@uke.de

[1] Department of Cardiology-Electrophysiology, University Heart Center Hamburg, University Hospital Hamburg Eppendorf, Martinistrasse 52, 20251 Hamburg, Germany

[2] Institute for Medical Biometry and Epidemiology, University Hospital Hamburg Eppendorf, Hamburg, Germany

Published online: 19 July 2016

Recently published, non-randomized prospective registry data indicate that the use of continuous NOACs as compared to uninterrupted VKAs (uVKA) is feasible and safe [4–6, 8, 9, 11]. In addition, the interruption of OAC during ablation seems feasible [12]. Regarding VKAs, interruption of VKAs and heparin bridging leads to an increased risk of overall and major bleeding rates [2, 13]. In uVKA therapy, an optimal international normalized ratio (INR) of 2.0–2.5 is recommended [14].

All the above-cited studies included pts with paroxysmal and persistent atrial fibrillation (persAF). However, comparative data on the influence of OAC strategies on complication rates of ablation procedures for solely persAF are rare. Pts with persAF are known to undergo longer and more complex ablation procedures compared to pts with paroxysmal AF [15, 16]. Consequently, the probability for periprocedural complications increases. Furthermore, pts with underlying cardiomyopathies appear more often with persAF, and comorbidities are more frequently present [17]. In addition, it is known that pts with paroxysmal AF with a moderate to high stroke risk are less likely prescribed to an appropriate OAC therapy compared to persAF pts [18].

Therefore, we sought to determine periprocedural complication rates among three OAC strategies [NOACs, uVKAs, and interrupted VKAs (iVKAs)] in pts undergoing solely persAF ablation.

Methods

Study population and anticoagulation strategy

We retrospectively analyzed consecutive persAF ablation procedures undertaken in our electrophysiology department. The study was approved by the institutional review board, and informed consent was obtained from all patients. We included all symptomatic pts with persAF, indication for catheter ablation and with a preprocedural anticoagulation in the form of NOACs or VKAs. Pts without OAC prior to ablation were excluded from the analysis. Depending on the preprocedural oral anticoagulation prescribed by prior physicians, three groups were defined: group 1) NOACs, group 2) uVKA (INR range 2.0–3.0), and group 3) iVKA [discontinuation of VKA and bridging with heparin (LMWH/unfractionated heparin)]. In group 1, we recommended the last intake of the NOAC to be 48 h before the ablation procedure according to the clinical practice and the guideline recommendation at that time [19]. This group is heterogeneous, including rivaroxaban, dabigatran, or apixaban. Discontinuation of the NOAC 48 h prior to ablation was recommended in all the types of NOACs. There was no heparin bridging in the NOAC group, and NOACs were restarted in the evening after the ablation procedure in all NOACs. In addition, patients in group 2 received their maintenance dose of VKA in the evening of the procedure day. In group 3, patients received weight-adapted LMWH doses in the evening of the procedure. Before hospital discharge, VKA was restarted in overlap with heparin.

Catheter ablation procedure

Before ablation, all pts underwent transesophageal echocardiography to rule out thrombus formation in the left atrial appendage. Ablation procedures were performed under deep sedation using continuous infusion of propofol (propofol, 1 mg/ml, B. Braun, Melsungen, Germany) as well as boluses of fentanyl (Fentanyl, 0.1 mg/ml, Rotexmedica, Trittau, Germany), [20].

Four diagnostic and ablation catheters were inserted through both Vv. femoralis. A double transseptal puncture using a modified Brockenbrough technique was performed (BRK Needle, St. Jude Medical Inc., St. Paul, MN, USA). To maintain an activated clotting time (ACT) of more than 300 s, intravenous unfractionated heparin (Heparin sodium, 25000 IU/5 ml, Rotexmedica) was administered immediately after the transseptal puncture.

After conduction of pulmonary vein (PV) angiograms, a three-dimensional electroanatomic mapping system [CARTO® (Biosense Webster, South Diamond Bar, CA, USA) or EnSite™ NavX™ (St. Jude Medical Inc.)] was used to define the left atrial anatomy. All ablation procedures were performed using radiofrequency current (RFC) energy with an irrigated-tip catheter [Thermocool®, Thermocool® Smarttouch® (Biosense Webster), TactiCath™ Quartz (St. Jude Medical)].

Ablation procedures followed the so-called "stepwise approach" aiming for AF termination [16, 21].

Definition of complications

We analyzed all complications occurring during periprocedural hospitalization. Periprocedural complications were categorized in major and minor bleedings, thromboembolic events (stroke and TIA), and further complications, such as pericardial effusion without hemodynamical relevance due to inflammatory response (no intervention required, <1 cm on echocardiography), myocardial infarction (MI), cardiac surgery, pacemaker implantation, cardiac or respiratory insufficiency, aortic mal-puncture, PV stenosis, and phrenic nerve palsy and death. Endpoints, such as MACE (major adverse cardiac event: death and MI) and MACCE (major adverse cardiac and cerebrovascular event: death, MI and stroke), were additionally recorded [17].

Major bleedings were defined according to current guidelines as: (1) hemodynamically relevant pericardial tamponades requiring pericardiocentesis, (2) groin complications [e.g., arteriovenous fistula (AVF), pseudoaneurysm, and hematoma] requiring blood transfusion or vascular surgery, and (3) resulting in a 20 % or greater fall in hematocrit [22]. Minor bleedings were defined as all bleeding complications not requiring invasive treatment, such as minor groin complications (AVF, pseudoaneurysm, and hematoma), hematuria, epistaxis, or hemoptysis. Furthermore, we defined a combined complication endpoint (CCE) as composed of any bleeding complications and thromboembolic events (stroke/TIA). The CCE was the primary basis of the statistical analysis in this study. This endpoint is based on several studies that focus on OAC-related complications during atrial fibrillation ablation. In these studies, solely bleeding and thromboembolic complications were analyzed [1, 2, 13, 14, 23].

Statistical analysis

All continuous values were expressed as mean ± standard deviation. Binary-coded and categorical data were described by the use of the median, interquartile range, and relative frequencies. For group comparisons, unpaired and paired *T* tests (for continuous data) as well as Fisher's exact test (for binary and categorical data) were used.

Models for the linear regression analysis with pairwise comparisons of adjusted predictions with consideration of repetitive measurements were constructed. Eight confounders (age, hypertension, coronary artery disease, BMI, gender, procedure duration, number of procedure, and year of procedure) were implemented in the regression model to make up for unequal patient characteristics due to non-randomization.

A p value <0.05 defined statistical significance. Statistics were calculated using a scientific graphic (GraphPad, Version 6, GraphPad Software Inc., La Jolla, CA, USA) and statistical software (Stata, Release 14, StataCorp LP, College Station, TX, USA).

Results

Baseline characteristics

A total of 1092 symptomatic patients with persAF treated between January 2011 and December 2014 were included in this analysis. The baseline characteristics are summarized in Table 1. Furthermore, mean duration of hospitalization (including the day of admission) was 4.0 ± 2.3 days.

Procedural data

We analyzed data from 1440 persAF ablation procedures, which were consecutively performed at our center. This resulted in 1.3 procedures per pt. Prior to the analysis, we ruled out 197 procedures due to the absence of OAC (Fig. 1). These 1440 procedures had the following distribution: $n = 441$ in group 1 (31 %; distribution of NOACs 57 % rivaroxaban, 33 % dabigatran, and 10 % apixaban), $n = 488$ (34 %) in group 2, and $n = 511$ (35 %) in group 3.

Procedural data are detailed in Table 2: initially, all pts included in this study suffered from persAF. This study also included re-procedures following prior persAF ablation, so that the specific indication of the current procedure varies and was primarily persAF ($n = 882$, 61.3 %) followed by consecutive atrial tachycardias ($n = 445$, 30.9 %). Complete PVI or Re-PVI were the major electrophysiological approaches performed during ablation (78 %) followed by ablation of CFAEs ($n = 742$, 52 %), ablation lines ($n = 381$, 26 %), focal ablation ($n = 303$, 21 %), and CTI ($n = 317$, 22 %). Preprocedural INR values were significantly different between all groups ($p < 0.0001$, Table 2).

Figure 2 demonstrates procedural complication rates in relation with preprocedural INR values in patients prescribed to VKA (including solely group 2 and 3). Lowest complication rates (6.59 and 6.79 %) were found within an INR range of 2.0–2.99. INR ranges lower than 2.0 demonstrate higher complications rates (11.1 and 11.1 %).

Conducting linear regression, adjusted intraprocedural ACT levels were significantly higher in group 2 [324.3 s, 95 % Confidence Interval (CI) (320.7–327.9)] as compared to group 1 [293.0 s; 95 % CI (289.5–296.5); $p < 0.0001$] and group 3 [291.5 s, 95 % CI (288.3–294.7); $p < 0.0001$]. There was no difference in ACT values between group 1 and group 3 ($p = 0.52$).

Adjusted intraprocedural heparin doses were significantly different among all groups (group 1 vs. 2 $p < 0.0001$, 2 vs. 3 $p < 0.0001$, 1 vs. 3 $p < 0.0001$) with highest doses in group 1 [11,364 IU; 95 % CI (10,959–11,783)] and lowest in group 2 [7749 IU; 95 % CI (7519–7988); group 3: 9212 IU; 95 % CI (8902–9533)].

Complication rates

The overall complication rate was 210 out of 1440 procedures (14.6 %) and is detailed in Table 3.

There were 13 major complications (0.90 %), including one stroke (group 2), four hemodynamically relevant pericardial tamponades requiring pericardiocentesis, one cardiac intervention (mitral clipping in a decompensated pt, group 3), and seven major groin complications requiring

Table 1 Baseline characteristics

Patients	All $n = 1092$	NOAC $n = 329$	Uninterrupted VKA $n = 333$	Interrupted VKA $n = 430$
Epidemiology				
Gender				
Male	736 (67.4 %)	233 (70.8 %)	214 (64.3 %)	289 (67.2 %)
Female	356 (32.6 %)	96 (29.2 %)	119 (35.7 %)	141 (32.8 %)
Age (years)	64.1 ± 9.93	64.1 ± 10.4	65.2 ± 9.06	63.1 ± 10.3
Initial AF type (*n*, %)				
Persistent	1008 (92.3 %)	312 (94.8 %)	296 (88.9 %)	400 (93.0 %)
Longstanding persistent	84 (7.69 %)	17 (5.2 %)	37 (11.1 %)	30 (7.0 %)
Arterial hypertension (*n*, %)	845 (77.4 %)	233 (70.8 %)	265 (79.6 %)	347 (80.7 %)
Hyperlipoproteinemia (*n*, %)	455 (41.7 %)	113 (34.4 %)	136 (40.8 %)	206 (47.9 %)
Coronary artery disease (*n*, %)	223 (20.4 %)	71 (21.6 %)	67 (20.1 %)	85 (19.8 %)
Valvular disease (*n*, %)	106 (9.71 %)	20 (6.07 %)	48 (14.4 %)	38 (8.84 %)
Tachycardiomyopathy due to AF (*n*, %)	70 (6.41 %)	24 (7.29 %)	24 (7.21 %)	22 (5.12 %)
Cardiomyopathy (*n*, %)	135 (12.4 %)	44 (13.4 %)	40 (12.0 %)	51 (11.9 %)
Diabetes (*n*, %)	103 (9.43 %)	26 (7.90 %)	31 (9.31 %)	46 (10.7 %)
Prior stroke/TIA (*n*, %)	120 (11.0 %)	28 (8.51 %)	44 (13.2 %)	48 (11.2 %)
Peripheral artery disease (*n*, %)	44 (4.03 %)	10 (3.04 %)	15 (4.50 %)	19 (4.42 %)
BMI (kg/m^2)	27.3 ± 4.05	26.9 ± 3.96	27.2 ± 3.86	27.7 ± 4.26
Longest AF episode (days)	148.3 ± 246.6	102.4 ± 134.4	168.1 ± 271.6	170.3 ± 289.3
Anti-arrhythmic drugs (median, *n*)	2 (2;3)	2 (1;3)	2 (2;3)	2 (2;3)
Left ventricular ejection fraction (%)	57.4 ± 8.4	56.8 ± 8.5	57.2 ± 8.6	58.1 ± 8.3
Laboratory findings				
TSH (μU/l)	1.76 ± 2.19	1.79 ± 2.08	1.74 ± 2.74	1.75 ± 1.76
Glomerular filtration rate (ml/min)	74.2 ± 20.8	78 ± 22.9	72 ± 20	73 ± 19.5
Creatinine (g/dl)	1.06 ± 0.41	1.02 ± 0.33	1.10 ± 0.56	1.07 ± 0.32
International normalized ratio	1.67 ± 0.6	1.06 ± 0.12	2.37 ± 0.36	1.52 ± 0.29
Scores: median (Q1;Q3)				
CHA_2DS_2-VASc	2 (1;3)	2 (1;3)	2 (2;3)	2 (1;3)
$CHADS_2$	1 (1;2)	1 (1;2)	1 (1;2)	1 (1;2)
HAS-BLED	2 (1;2)	1 (1;2)	2 (1;2)	2 (1;2)
EHRA	2 (2;3)	2 (2;3)	2 (2;3	2 (2;3)

AF atrial fibrillation, *BMI* body mass index, *$CHADS_2$ Score/CHA_2DS_2-VASc Score* is clinical estimations of the risk of stroke in patients with AF, *EHRA* European Heart Rhythm Association symptom score, *HAS-BLED* score is a clinical estimation of the bleeding risk in patients with AF, *NOAC* non-VKA, *No.* number, *TIA* transient ischemic attack, *TSH* thyroid-stimulating hormone, *VKA* vitamin K antagonist)

vascular surgery and/or blood transfusion. Furthermore, there was one major bleeding event caused by hemoptysis requiring interventional bronchoscopy and blood transfusion (group 3). There was no death. There were 113 (7.84 %) combined complication endpoints (CCE), mainly attributable to bleeding complications ($n = 112$, 7.78 %). A single stroke occurred (0.07 %).

Bleeding complications were the most frequent complication overall, led by minor groin complications (96/112; 85.7 %) not requiring any treatment. All bleeding complications combined, as well as major bleedings only, occurred significantly more often than thromboembolic events [all bleedings $n = 112$ (7.78 %) vs. 1 stroke (0.07 %), $p < 0.0001$; 13 major bleedings vs. one stroke, $p = 0.0018$). The highest overall bleeding rate was observed in group 3 at 10.8 %. The occurrence of complications led to a significantly longer in-hospital stay [4 days (q1-3: 3–7) with vs. 3 days (q1-3: 3–4) without complication, $p = 0.0002$].

Group comparison

Adjusted CCE rates were 5.5 % [95 % CI (3.1–7.8)] in group 1, 7.5 % [95 % CI (5.0–10.1)] in group 2, and 9.9 % [95 % CI (6.6–13.2)] in group 3. There was a significant

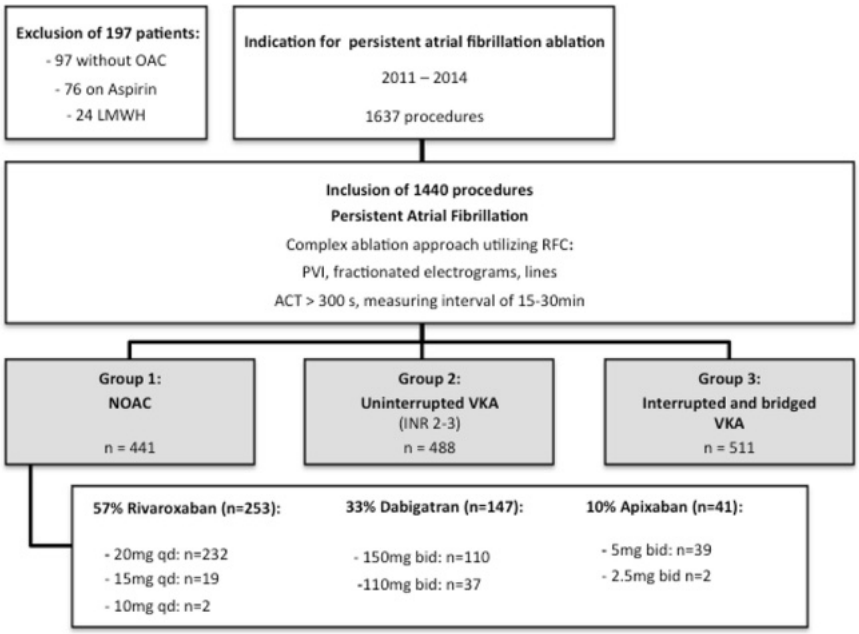

Fig. 1 Study flow chart. *ACT* activated clotting time, *bid* "bis in die" = twice daily, *LMWH* low-molecular weight heparin, *mins* minutes, *NOAC* non-VKA, *OAC* oral anticoagulation, *PVI* pulmonary vein isolation, *qd* "quaque die" = once daily, *RFC* radiofrequency current energy, *s* seconds, *VKA* vitamin K antagonist)

difference in CCE rates among the groups: compared to group 1, the combined complication risk was almost twice as high in group 3 [odd's ratio (OR) 1.9, 95 % CI (1.0–3.7), $p = 0.049$]. There was no difference between group 1 and group 2 [OR 1.4, 95 % CI (0.8–2.5), $p = 0.23$] or group 2 and group 3 [OR 1.4, 95 % CI (0.8–2.4), $p = 0.30$]. Of all confounders, only age showed an influence on CCE rates (Fig. 3).

The HAS-BLED score was predictive for bleedings (major and minor) in the whole study cohort [$n = 1440$; $p = 0.02$, OR = 1.16; 95 % CI (1.01–1.49)]. The same accounts for the CHA_2DS_2-VASC score [$p = 0.04$, OR = 1.23; 95 % CI (1.03–1.31)], respectively. In a subgroup analysis of group 3, the HAS-BLED score was not significantly predictive for bleeding [$p = 0.2$, OR = 1.19; 95 % CI (0.92–1.53)].

Absolute intravenous heparin doses and ACT values did not differ among procedures with and without complications (heparin 10,198 ± 3874 IU vs 9856 ± 3773 IU, $p = 0.2254$; ACT 303.9 ± 32.7 vs. 303.4 ± 39.7 s, $p = 0.54$).

NOACs

Rivaroxaban was the most frequent NOAC prescribed in this study population [253 pts, 57 %; of these 232 pts (92 %) were prescribed to the 20 mg dose, 19 pts (7.5 %) to 15 mg, and two pts (0.5 %) to 10 mg], followed by dabigatran [147 pts, 33 %; of these 110 pts (75 %) were prescribed to the 150 mg dose and 37 pts (25 %) to 110 mg twice daily] and apixaban [41 pts, 10 %; of these 39 pts (95 %) were prescribed to the 5 mg dose and two pts to 2.5 mg (5 %) twice daily]. Nine (15 %) patients subscribed to a low-dose NOAC have suffered from a bleeding event in the past. A reduced glomerular filtration rate was present in 13 (21 %) of the 61 pts that were subscribed to the lower dose regime of NOACs. There was no thromboembolic complication in the NOAC group with the lowest bleeding rates ($n = 23$, 5.22 %, Table 3).

Adjusted CCE rates were 12.0 % [95 % CI (6.9–17.2)] for dabigatran, 13.3 % [95 % CI (8.8–17.8)] for rivaroxaban, and 2.4 % [95 % CI (0.7–3.2)] for apixaban. There was no significant difference in adjusted complication rates among the different NOACs.

Table 2 Procedural parameters

Procedures	All $n = 1440$	NOAC $n = 441$	Uninterrupted VKA $n = 488$	Interrupted VKA $n = 511$
Indication current procedure				
PAF (*n*, %)	33 (2.29 %)	11 (2.49 %)	15 (3.07 %)	7 (1.37 %)
AF (*n*, %)	882 (61.3 %)	277 (62.8 %)	256 (52.5 %)	349 (68.3 %)
Longstanding persistent AF (*n*, %)	80 (5.56 %)	16 (3.63 %)	31 (6.35 %)	33 (6.46 %)
Atrial tachycardia (*n*, %)	445 (30.9 %)	137 (31.0 %)	186 (38.1 %)	122 (23.9 %)
Electrophysiological approaches (multiple possible)				
PVI (*n*, %)	666 (46.3 %)	215 (48.8 %)	199 (40.8 %)	252 (49.3 %)
Re-PVI (*n*, %)	461 (32.0 %)	128 (29.0 %)	169 (34.6 %)	164 (32.1 %)
Defragmentation (*n*, %)	742 (51.5 %)	215 (48.8 %)	254 (52.1 %)	273 (53.4 %)
Lines (*n*, %)	381 (26.5 %)	109 (24.7 %)	153 (31.4 %)	119 (23.3 %)
Cavotricuspid Isthmus (*n*, %)	317 (22.0 %)	100 (22.7 %)	107 (21.9 %)	110 (21.5 %)
Focal ablation (*n*, %)	303 (21.0 %)	82 (18.6 %)	116 (23.8 %)	105 (20.6 %)
Ablation procedure				
Duration (min)	174.2 ± 63.5	171.6 ± 62.6	176.4 ± 62.9	174.3 ± 64.8
Flouro time (min)	37.9 ± 19.6	34.9 ± 18.9	37.8 ± 19.3	40.5 ± 20.0
Dose area product (cGycm^2)	5567.4 ± 20071.7	4715.6 ± 6148.4	4629.4 ± 5292.1	7203.9 ± 32794.9
Cumulative energy (J)	102874.9 ± 70801	98799.8 ± 60418.9	104307.3 ± 80168.3	105035.6 ± 69600.4
RFC duration (s)	3927.5 ± 3033.7	3771.3 ± 2318.7	3924.1 ± 2511.8	4065.6 ± 3905.2
RFC count (*n*)	40.1 ± 26.2	39.5 ± 26.4	39.3 ± 25.7	41.3 ± 26.5
Energy mean (W)	26.9 ± 10.9	26.9 ± 9.6	26.8 ± 11.0	27.2 ± 11.9
Intraprocedural ACT levels				
ACT > 300 s (%)	48.7 ± 31.3	40.6 ± 28.2	64.4 ± 27.9	39.9 ± 31.3
Mean ACT (s)	303.5 ± 38.7	293.0 ± 34.9	324.3 ± 38.9	291.5 ± 32.5
Standard deviation ACT (s)	40.0 ± 30.8	42.2 ± 30.7	43 ± 36.5	34.7 ± 22.4
Heparin (IU)	9909 ± 3789.5	11975.6 ± 4166.1	8142.0 ± 2702.4	9753.6 ± 3381.5

AF atrial fibrillation, *ACT* activated clotting time, *IU* international units, *PAF* paroxysmal AF, *PVI* pulmonary vein isolation, *RFC* radiofrequency current energy

The last intake of the NOAC was recommended to be 48 h before the procedure. However, the real timeframe was spread between 2 and 168 h with a median of 48 h (q1–q3 48–72). The timeframe was not different in procedures with and without complications (median 48 h (q1–3: 48–72) in both the groups, $p = 0.445$; Fig. 4).

Discussion

Major findings

In our study, we found that the iVKA strategy was associated with an increased risk of periprocedural complications (CCE) when compared to NOACs in pts with persAF undergoing catheter ablation. Another major finding was that thromboembolic events are rare and were exceeded by minor bleeding complications. Furthermore, these complications led to a prolonged hospital stay.

There were no thromboembolic events when NOACs were paused 48 h preablation in this persAF cohort. Despite significantly different intraprocedural administered heparin doses among the groups, no effect of heparin dose was found between procedures with and without periprocedural complications.

Combined complication endpoint

Our data show an increased CCE rate in the iVKA as compared to the NOAC group. This rate is primarily determined by minor bleeding complications, as there was only one stroke reported in group 2. Higher bleeding rates in iVKAs are a well described issue, as previously reported by other authors [2, 13, 23]. An explanation for this could be the difficulty in reliably quantifying a patients' coagulation status, especially when restarting the VKA and simultaneously administering LMWH. It is, therefore, understandable that the periprocedural strategy of iVKAs

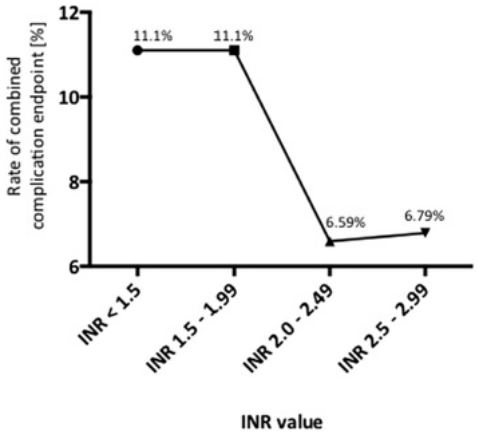

Fig. 2 Combined complication endpoint rates depending on INR value in patients subscribed to vitamin K antagonists. *INR* international normalized ratio

has nowadays been abandoned by many electrophysiology centers.

However, the above-mentioned studies have only compared uVKAs to iVKAs. Another study has compared iVKAs to rivaroxaban and dabigatran [12]. They found fewer groin complications in pts treated with dabigatran compared to iVKAs and no differences between iVKAs and rivaroxaban. Our data extend on these findings by revealing an increased complication rate in iVKAs compared to NOACs (including apixaban). Regarding INR values, in pts taking VKAs, our data show lower complication rates when INR values range between 2.0 and 2.99. Kim et al. reported similar results with an optimal INR range of 2.1–2.5 [14].

In this study, the major complication rate was low (0.9 %) and comparable to similar studies [12, 23]. Bleeding complications accounted for a major part of the total complication rate and were caused mainly by minor groin complications that did not require treatment. Yet, periprocedural complications did lead to prolonged hospital stays.

An increase in age was associated with a higher CCE rate in our study. Data regarding age are discrepant across current literature, ranging from a non-increased to an increased risk of complication in aged pts undergoing catheter ablation [24–26]. Yet, the cause of this discrepancy remains unknown. It might be explained by a multifactorial genesis, e.g., different patient populations, previous anticoagulation, comorbidities, and experience of ablation center.

The CHA_2DS_2-VASc and HAS-BLED scores are predictive for bleeding complications in our study cohort. In our study, there was only one thromboembolic event. Therefore, the influence of the CHA_2DS_2-VASc score on stroke rates cannot be determined in our study. Other studies reported more frequent postablation thromboembolic event rates in high-risk pts with increased CHA_2DS_2-VASc scores [27, 28]. The follow-up time in these studies was much longer (up to 489 days after ablation) as compared to our study. We only analyzed in-hospital, postablation thromboembolic events.

The HAS-BLED Score was not predictive for increased bleeding risks in group 3. A reason why the HAS-BLED score is predictive in the whole study cohort but not in the subgroup analysis (only group 3) could be the fact that the sample size is smaller in the subgroup analysis and statistical significance cannot be reached.

NOACs

This study included the NOACs dabigatran, rivaroxaban, and apixaban. Despite pausing NOACs 48 h preablation in pts with persAF, not a single thromboembolic event occurred in 441 pts. Rillig et al. reported similar findings with no occurrence of any cerebrovascular event in 444 pts on NOACs with any type of AF (paroxysmal, persistent, and longstanding persistent), [29]. The median CHA_2DS_2-VASc score in this group was 2. This result is consistent with our findings.

In addition, we verified the recommended 48-h NOAC withholding period by directly questioning all pts about their last medication intake. When comparing procedures with and without periprocedural complications, there were no differences in timeframes of the last NOAC intake. Based on the results of our study, as well as those of Rillig et al. pausing NOACs 48 h before ablation, according to 2013's practical guidelines, seem feasible and safe [19].

The latest anticoagulation studies for ablation urge the continuous use of periprocedural OAC [8, 9, 11]. Furthermore, the current updated guidelines recommend withholding NOACs 18–24 h before ablation; NOACs should then be restarted 6 h post ablation [30]. It remains unknown whether continuous NOAC administration leads to higher bleeding complications, as bleedings are already the most common complication found in our study. Bleedings under continuous NOACs could be more difficult to manage as antidotes either do not exist or are not routinely implemented. Furthermore, it is unknown if uninterrupted NOAC therapy during ablation will lead to a decrease in periprocedural stroke rates. Due to the low incidence of periprocedural strokes, larger patient populations are needed to resolve this question.

Table 3 Periprocedural complication rates

	All $n = 1440$	NOAC $n = 441$	Uninterrupted VKA $n = 488$	Interrupted VKA $n = 511$
Combined complication endpoint	113 (7.85 %)	23 (5.22 %)	35 (7.17 %)	55 (10.8 %)
Bleedings	112 (7.78 %)	23 (5.22 %)	34 (6.97 %)	55 (10.8 %)
Major bleedings	12 (0.83 %)	2 (0.45 %)	3 (0.61 %)	7 (1.37 %)
Pericardial tamponade	4 (0.28 %)	1 (0.23 %)	2 (0.41 %)	1 (0.2 %)
Major Groin bleeding	7 (0.49 %)	1 (0.23 %)	1 (0.20 %)	5 (0.98 %)
Hemoptysis (incl. transfusion)	1 (0.07 %)	0	0	1 (0.2 %)
Minor bleedings	101 (7.01 %)	21 (4.76 %)	29 (6.35 %)	48 (9.39 %)
Groin	96 (6.67 %)	20 (4.54 %)	29 (5.94 %)	49 (9.00 %)
Other[a]	5 (0.35 %)	1 (0.23 %)	2 (0.41 %)	2 (0.39 %)
Stroke/TIA [MACCE]	1 (0.07 %)	0	1 [stroke] (0.20 %)	0
Other complications	97 (6.73 %)	32 (7.25 %)	31 (6.35 %)	34 (6.65 %)
Pericardial Effusion without hemodynamical relevance	67 (4.65 %)	24 (5.44 %)	19 (3.89 %)	24 (4.7 %)
MACE	0	0	0	0
Cardiac surgery/intervention	1 (0.07 %)	0	0	1 [Mitralvalve Clip] (0.2 %)
Further complications[b]	29 (2.01 %)	8 (1.81 %)	12 (2.46 %)	9 (1.76 %)
Overall complication rate	210 (14.6 %)	55 (12.5 %)	66 (13.5 %)	89 (17.4 %)
Overall complication rate per procedure (at least one complication)	200 (13.9 %)	53 (12.0 %)	66 (13.5 %)	81 (15.9 %)

MACE major adverse cardiac event, *MACCE* major adverse cardiac and cardiovascular event, *NOAC* non VKA, *TIA* transient ischemic attack, *VKA* vitamin K antagonist

[a] Hematuria, epistaxis, hemoptysis not requiring intervention, or blood transfusion

[b] Pacemaker-Implantation, cardiac or respiratory insufficiency, aortic mal-puncture

We found non-significantly lower complication rates in pts taking the pre-OAC apixaban as compared to rivaroxaban and dabigatran. Only 10 % of pts in group 1 were subscribed to apixaban in our study. Hence, case numbers are low and a definitive conclusion cannot be drawn. Di Biase et al. investigated pts on continuous apixaban versus on uVKA [11]. There were no statistical differences with regard to complications between apixaban and VKA. However, there was no comparison with other NOACs. Rillig et al. observed no difference in major complications between pts prescribed to dabigatran, rivaroxaban, or apixaban [29]. Further data are required to follow up on our findings.

Intraprocedural heparin administration

In our study, the lowest ACT levels were observed in the NOAC group, despite having the highest intraprocedural heparin doses. In the uVKA group, however, low heparin doses led to higher ACT levels. These findings have been reported previously by other authors [4, 31, 32]. The reason for higher heparin requirements in NOACs remains uncertain. A multifactorial genesis seems to be the underlying cause, and the above-mentioned authors have generated various hypotheses, such as: when pausing the NOAC, the intensity of therapeutic OAC at the time of ablation could be lower than under uVKA therapy. Furthermore, NOACs bind to antithrombin or factor-Xa, both of which are heparin targets. This could lead to competition at the binding site and to increased heparin administration.

Unfractionated heparin doses were higher in OAC with NOACs compared to uVKAs and iVKAs, without an increase in complication rate. We therefore hypothesize that periprocedural complications, especially bleeding complications, are not dependent on the amount of heparin administered. Possible explanations could be the short acting time of unfractionated heparin or the fact that intraprocedural coagulation status is controlled by ACT levels. Complications seem therefore influenced by the periprocedural OAC strategy and not by the dose of intraprocedural heparin. In clinical practice, this could reduce the fear of administering higher heparin doses when low ACT levels are measured.

At latest, our data represent a real-world cohort from a high-volume center and give valuable insight into daily clinical practice.

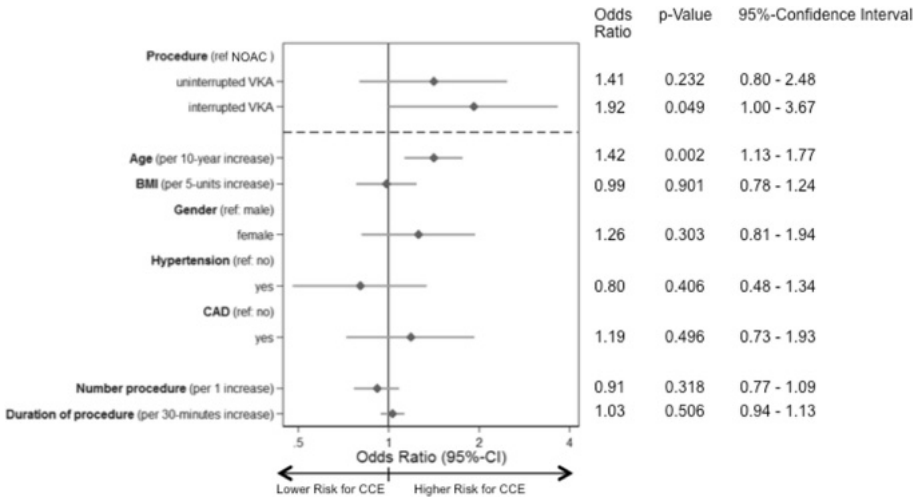

Fig. 3 Forest plot of the linear regression model: difference of combined complication rates among the three periprocedural oral anticoagulation groups and influence of the confounders. Age, *BMI* body mass index, gender, hypertension, *CAD* coronary artery disease, *CCE* combined complication endpoint, *NOAC* non VKA, *VKA* Vitamin K antagonist

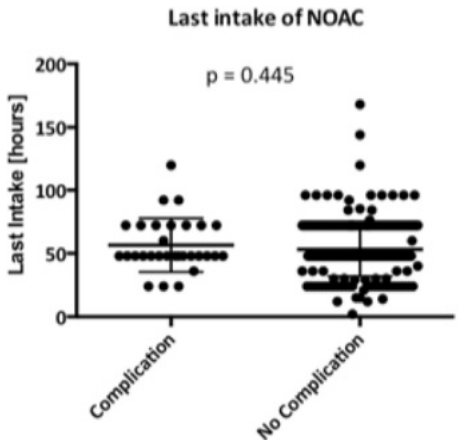

	Complication	No Complication
Q1	48 hrs	48 hrs
Median	48 hrs	48 hrs
Q3	72 hrs	72 hrs
Min.	24 hrs	2 hrs
Max.	120 hrs	168 hrs

Fig. 4 Last intake (in hours) of non-vitamin K antagonists (NOAC) in procedures with and without complications. *hrs* hours, *Max*. maximal, *Min*. minimal, *Q1* quartile 1, *Q3* quartile 3

Study limitations

The two primary limitations of this study were that the data come from only one center and that the analysis of the persAF cohort was done in a retrospective fashion over the years 2011–2014. As a result, there was a bias caused by historical changes in OAC strategies. However, we accounted for this bias by including the survey year in the linear regression model. Furthermore, we included numerous confounders in the model to account for differences in patient characteristics due to non-randomization. In addition, no pts in this study cohort were prescribed edoxaban, as this medication had not received market approval at the time the study was conducted. Moreover,

our trial focused on persAF; pts suffering from PAF were not included in this study.

Conclusion

Patients undergoing persistent atrial fibrillation ablation with interrupted vitamin K antagonists are exposed to an increased risk of complications compared to NOACs. Thromboembolic events are in general rare and are exceeded by minor bleeding complications. Complications lead to a prolonged hospital stay. Despite pausing NOACs 48 h before ablation in patients with persistent atrial fibrillation, not a single thromboembolic event occurred in this cohort.

Compliance with ethical standards

Conflict of interest On behalf of all authors, the corresponding author states that there is no conflict of interest.

References

1. Santangeli P, Di Biase L, Horton R, Burkhardt JD, Sanchez J, Al-Ahmad A et al (2012) Ablation of atrial fibrillation under therapeutic warfarin reduces periprocedural complications evidence from a meta-analysis. Circ Arrhythmia Electrophysiol 5(2):302–311
2. Nairooz R, Sardar P, Payne J, Aronow WS, Paydak H (2015) Meta-analysis of major bleeding with uninterrupted warfarin compared to interrupted warfarin and heparin bridging in ablation of atrial fibrillation. Int J Cardiol 187:426–429
3. Weitz JI, Healey JS, Skanes AC, Verma A (2014) Periprocedural management of new oral anticoagulants in patients undergoing atrial fibrillation ablation. Circulation 129(16):1688–1694
4. Bassiouny M, Saliba W, Rickard J, Shao M, Sey A, Diab M et al (2013) Use of dabigatran for periprocedural anticoagulation in patients undergoing catheter ablation for atrial fibrillation. Circ Arrhythmia Electrophysiol 6(3):460–464
5. Kim J-S, She F, Jongnarangsin K, Chugh A, Latchamsetty R, Ghanbari H et al (2013) Dabigatran vs warfarin for radiofrequency catheter ablation of atrial fibrillation. Heart Rhythm 10(4):483–489
6. Kaess B, Ammar S, Reents T, Dillier R, Lennerz C, Semmler V et al (2015) Comparison of safety of left atrial catheter ablation procedures for atrial arrhythmias under continuous anticoagulation with apixaban versus phenprocoumon. Am J Cardiol 115(1):47–51
7. Garg J, Chaudhary R, Krishnamoorthy P, Shah N, Natale A, Bozorgnia B (2016) Safety and efficacy of uninterrupted periprocedural rivaroxaban in patients undergoing atrial fibrillation catheter ablation: a metaanalysis of 1362 patients. Int J Cardiol 203:906–908
8. Nagao T, Inden Y, Shimano M, Fujita M, Yanagisawa S, Kato H et al (2015) Feasibility and safety of uninterrupted dabigatran therapy in patients undergoing ablation for atrial fibrillation. Intern Med 54(10):1167–1173
9. Lakkireddy D, Reddy YM, Di Biase L, Vallakati A, Mansour MC, Santangeli P et al (2014) Feasibility and safety of uninterrupted rivaroxaban for periprocedural anticoagulation in patients undergoing radiofrequency ablation for atrial fibrillation: results from a multicenter prospective registry. J Am Coll Cardiol 63(10):982–988
10. Ewen S, Rettig-Ewen V, Mahfoud F, Böhm M, Laufs U (2014) Drug adherence in patients taking oral anticoagulation therapy. Clin Res Cardiol 103(3):173–182
11. Di Biase L, Lakkireddy D, Trivedi C, Denke T, Martinek M, Mohanty S (2015) Feasibility and safety of uninterrupted periprocedural apixaban administration in patients undergoing radiofrequency catheter ablation for atrial fibrillation: results from a multicenter study. Hear Rhythm 12:1162–1168
12. Winkle RA, Mead RH, Engel G, Kong MH, Patrawala RA (2014) Peri-procedural interrupted oral anticoagulation for atrial fibrillation ablation: comparison of aspirin, warfarin, dabigatran, and rivaroxaban. Europace 16(10):1443–1449
13. Siegal D, Yudin J, Kaatz S, Douketis JD, Lim W, Spyropoulos AC (2012) Periprocedural heparin bridging in patients receiving Vitamin K antagonists: systematic review and meta-analysis of bleeding and thromboembolic rates. Circulation 126(13):1630–1639
14. Kim J-S, Jongnarangsin K, Latchamsetty R, Chugh A, Ghanbari H, Crawford T et al (2013) The optimal range of international normalized ratio for radiofrequency catheter ablation of atrial fibrillation during therapeutic anticoagulation with warfarin. Circ Arrhythmia Electrophysiol 6(2):302–309
15. Vogler J, Willems S, Sultan A, Schreiber D, Lüker J, Servatius H et al (2015) Pulmonary vein isolation versus defragmentation. J Am Coll Cardiol 66(24):2743–2752
16. Schreiber D, Rostock T, Frohlich M, Sultan A, Servatius H, Hoffmann BA et al (2015) Five-year follow-up after catheter ablation of persistent atrial fibrillation using the stepwise approach and prognostic factors for success. Circ Arrhythm Electrophysiol 8(2):308–317
17. Hoffmann BA, Kuck K-H, Andresen D, Spitzer SG, Hoffmann E, Schumacher B et al (2014) Impact of structural heart disease on the acute complication rate in atrial fibrillation ablation: results from the German Ablation Registry. J Cardiovasc Electrophysiol 25(3):242–249
18. Hsu JC, Chan PS, Tang F, Maddox TM, Marcus GM (2015) Differences in anticoagulant therapy prescription in patients with paroxysmal versus persistent atrial fibrillation. Am J Med 128(6):654.e1–654.e10
19. Heidbuchel H, Verhamme P, Alings M, Antz M, Hacke W, Oldgren J et al (2013) European heart rhythm association practical guide on the use of new oral anticoagulants in patients with non-valvular atrial fibrillation. Europace 15(5):625–651
20. Salukhe TV, Willems S, Drewitz I, Steven D, Hoffmann BA, Heitmann K et al (2012) Propofol sedation administered by cardiologists without assisted ventilation for long cardiac interventions: an assessment of 1000 consecutive patients undergoing atrial fibrillation ablation. Europace 14(3):325–330
21. Lankveld T, Zeemering S, Scherr D, Kuklik P, Hoffmann BA, Willems S et al (2016) Atrial fibrillation complexity parameters derived from surface ECGs predict procedural outcome and long-term follow-up of stepwise catheter ablation for atrial fibrillation. Circ Arrhythm Electrophysiol 9(2):e003354
22. Calkins H, Kuck KH, Cappato R, Brugada J, Camm AJ, Chen S-A et al (2012) 2012 HRS/EHRA/ECAS expert consensus statement on catheter and surgical ablation of atrial fibrillation: recommendations for patient selection, procedural techniques, patient management and follow-up, definitions, endpoints, and research trial design. Heart Rhythm 9(4):632–696
23. Di Biase L, Burkhardt JD, Santangeli P, Mohanty P, Sanchez JE, Horton R et al (2014) Periprocedural stroke and bleeding complications in patients undergoing catheter ablation of atrial fibrillation with different anticoagulation management: results from

the role of Coumadin in preventing thromboembolism in atrial fibrillation (AF) patient. Circulation 129(25):2638–2644
24. Bunch TJ, Weiss JP, Crandall BG, May HT, Bair TL, Osborn JS et al (2010) Long-term clinical efficacy and risk of catheter ablation for atrial fibrillation in octogenarians. Pacing Clin Electrophysiol 33:146–152
25. Nademanee K, Amnueypol M, Lee F, Drew CM, Suwannasri W, Schwab MC et al (2015) Benefits and risks of catheter ablation in elderly patients with atrial fibrillation. Heart Rhythm 12(1):44–51
26. Spragg DD, Dalal D, Cheema A, Scherr D, Chilukuri K, Cheng A et al (2008) Complications of catheter ablation for atrial fibrillation: incidence and predictors. J Cardiovasc Electrophysiol 19(6):627–631
27. Nührich JM, Kuck KH, Andresen D, Steven D, Spitzer SG, Hoffmann E et al (2015) Oral anticoagulation is frequently discontinued after ablation of paroxysmal atrial fibrillation despite previous stroke: data from the German Ablation Registry. Clin Res Cardiol 104(6):463–470
28. Kornej J, Kosiuk J, Hindricks G, Arya A, Sommer P, Rolf S et al (2015) Sex-related predictors for thromboembolic events after catheter ablation of atrial fibrillation: the Leipzig Heart Center AF Ablation Registry. Clin Res Cardiol 104(7):603–610
29. Rillig A, Lin T, Plesman J, Heeger C-H, Lemes C, Metzner A et al (2016) Apixaban, rivaroxaban and dabigatran in patients undergoing atrial fibrillation ablation. J Cardiovasc Electrophysiol 27(2):147–153
30. Heidbuchel H, Verhamme P, Alings M, Antz M, Diener HC, Hacke W et al (2015) Updated European Heart Rhythm Association Practical Guide on the use of non-vitamin K antagonist anticoagulants in patients with non-valvular atrial fibrillation. Europace 17(10):1467–1507
31. Nagao T, Inden Y, Yanagisawa S, Kato H, Ishikawa S, Okumura S et al (2015) Differences in the activated clotting time among uninterrupted anticoagulants during the periprocedural period of atrial fibrillation ablation. Heart Rhythm 12(9):1972–1978
32. Bin Abdulhak A, Kennedy K, Gupta S, Giocondo M, Ramza B, Wimmer A (2015) Effect of pre-procedural interrupted apixaban on heparin anticoagulation during catheter ablation for atrial fibrillation: a prospective observational study. J Cardiovasc Electrophysiol 44(2):91–96

ESC European Society of Cardiology

Europace (2019) **21**, i34–i42
doi:10.1093/europace/euy273

CLINICAL RESEARCH

A novel assessment of local impedance during catheter ablation: initial experience in humans comparing local and generator measurements

Melanie Gunawardene[1]*, Paula Münkler[1,2], Christian Eickholt[1], Ruken Ö. Akbulak[1], Mario Jularic[1], Niklas Klatt[1], Jens Hartmann[1], Leon Dinshaw[1], Christiane Jungen[1,2], Julia M. Moser[1], Lydia Merbold[3], Stephan Willems[1,2], and Christian Meyer[1,2]*

[1]Department of Cardiac Electrophysiology, University Heart Center, University Hospital Hamburg Eppendorf, Martinistrasse 52, 20246 Hamburg, Germany; [2]DZHK (German Center for Cardiovascular Research), Partner Site Hamburg/Kiel/Luebeck, Berlin, Germany; and [3]Boston Scientific, Marlborough, MA, USA

Received 19 April 2018; editorial decision 18 October 2018; accepted 10 November 2018

Aims A novel measure of local impedance (LI) has been found to predict lesion formation during radiofrequency current (RFC) catheter ablation. The aim of this study was to investigate the utility of this novel approach, while comparing LI to the well-established generator impedance (GI).

Methods and results In 25 consecutive patients with a history of atrial fibrillation, catheter ablation was guided by a 3D-mapping system measuring LI in addition to GI via an ablation catheter tip with three incorporated mini-electrodes. Local impedance and GI before and during RFC applications were studied. In total, 381 RFC applications were analysed. The baseline LI was higher in high-voltage areas (>0.5 mV; LI: 110.5 ± 13.7 Ω) when compared with intermediate-voltage sites (0.1–0.5 mV; 90.9 ± 10.1 Ω, $P < 0.001$), low-voltage areas (<0.1 mV; 91.9 ± 16.4 Ω, $P < 0.001$), and blood pool LI (91.9 ± 9.9 Ω, $P < 0.001$). During ablation, mean LI drop (△LI; 13.1 ± 9.1 Ω) was 2.15 times higher as mean GI drop (△GI) (6.1 ± 4.2 Ω, $P < 0.001$). Baseline LI correlated with △LI: a mean LI of 99.9 Ω predicted a △LI of 12.9 Ω [95% confidence interval (12.1–13.6), R^2 0.41; $P < 0.001$]. This relationship was weak for baseline GI predicting △GI (R^2 0.06, $P < 0.001$). Catheter movements were represented by rapid LI changes. The duration of an RFC application was not predictive for catheter–tissue coupling with no further change of △LI ($P = 0.247$) nor △GI ($P = 0.376$) during prolonged ablation.

Conclusion Local impedance can be monitored during ablation. Compared with the sole use of GI, baseline LI is a better predictor of impedance drops during ablation and may provide useful insights regarding lesion formation. However, further studies are needed to investigate if this novel approach is useful to guide catheter ablation.

Keywords Atrial fibrillation • Catheter ablation • Radiofrequency current • Impedance • Ultra high-density mapping

Introduction

Radiofrequency current (RFC) is the most widely used energy form to perform catheter ablation of cardiac arrhythmias.[1] Radiofrequency current energy creates myocardial lesions by resistive heating of the myocardial tissue, followed by heat conduction to the adjacent tissue.[1] To date, impedance places an important role in lesion formation during RFC ablation[2–4]: first of all, better contact with the tissue causes higher impedances.[5] Secondly, to create adequate, deep lesions by resistive heating, a sufficient resistive load (which is equivalent to a high impedance) is well known to be required at the catheter–tissue interface.[5,6] Thirdly, a drop of impedance during energy delivery is predictive for lesion formation as it implicates damage to the underlying tissue.[6,7] Therefore, changes of resistivity directly reveal information about electrical coupling between the catheter tip and underlying tissue.[6,7]

Several technologies have attempted to measure the resistive load at the catheter–tissue interface via impedance. Radiofrequency

* Corresponding author. Tel: +49 40 7410 54120; fax: +49 40 7410 54125. *E-mail address:* c.mey@web.de; m.gunawardene@uke.de

What's new?

- The drop in local impedance (LI) measured from an ablation catheter tip with three incorporated mini-electrodes during radiofrequency current (RFC) application is about twice as high as the generator impedance (GI) drop.
- Higher LI at the start of an application predicts larger impedance drops during ablation, rather than the RFC GI.
- Baseline LI in high-voltage areas is higher when compared with intermediate- and low-voltage ablation sites as well as compared with blood pool LI.
- Local impedance can be monitored during ablation and may provide useful insights regarding catheter stability, tissue characteristics, and lesion formation compared with the sole use of GI.

current generators measuring transthoracic impedance of the energy delivery pathway from an ablation catheter tip electrode to an indifferent electrode on the skin are well established.[6] While RFC generators measure a modest impedance difference between blood and tissue, significant variation in the bulk of transthoracic impedance (including muscle, lung, and bone impedance) limits the utility of transthoracic/generator impedance (GI) as a precise measure of the actual local catheter–tissue coupling.[6]

Piorkowski *et al.*[8] presented an approach to estimate local impedance (LI) from the ablation catheter tip with a three-terminal model and two body-surface electrodes and were able to distinguish between contact and non-contact to the tissue with this method. However, this approach was reported to be confounded by remote structures and drift.[8–10]

Recently, a novel measure of LI recorded from miniature-electrodes integrated in an ablation catheter tip has shown to be a sufficient measure of LI predicting catheter–tissue contact and lesion formation during RFC catheter ablation in an experimental setting.[6] Yet, how this measure of LI can guide catheter ablation in humans is not known. The aim of this study was to investigate the clinical utility of this approach using LI recorded from miniature-electrodes during catheter ablation in patients with a history of symptomatic, recurrent atrial fibrillation (AF).

Objective

To investigate the utility of a novel measure of LI from an ablation catheter tip with three incorporated mini-electrodes during catheter ablation procedures and how LI is related to the well-established GI.

Methods

Study design

This study was a single-centre, pilot study with an explorative design. To investigate how LI is related to GI and low-voltage areas, consecutive patients with recurrent AF or atrial tachycardia (AT), after prior ablation for paroxysmal or persistent AF from 11/2017 until 01/2018 were enrolled. Written informed consent was obtained from all patients. The study was conducted in accordance with the provisions of the Declaration of Helsinki and its amendments. The institutional review board of the University Heart Center Hamburg approved the study.

Catheter ablation procedure

Catheter ablation was performed under deep sedation using a continuous infusion of propofol (1 mg/mL, B. Braun, Melsungen, Germany) combined with boluses of fentanyl (0.1 mg/mL, Rotexmedica, Trittau, Germany), as previously described.[11]

Intravenous heparin (heparin sodium, 25 000 IU/5 mL, Rotexmedica) was administered during the procedure aiming at an activated clotting time of 300–350 s.

Via both femoral veins, one long (SL0™, 8 Fr, St Jude), one steerable sheath (ZURPAZ™ 8.5 Fr, Boston Scientific, Marlborough, MA, USA), and two short haemostatic sheaths (Fast-Cath™, 6 Fr and 8 Fr, Daig Inc., Minnetonka, MN, USA) were inserted, followed by positioning of a reference catheter into the coronary sinus.

To access the left atrium (LA), one transseptal puncture using a modified Brockenbrough technique was performed and both, the long sheath and the steerable sheath were navigated into the LA. A 64-pole mini-basket mapping catheter (Orion™, Boston Scientific) was introduced to the LA via the steerable sheath. After LA angiography was completed, the mini basket catheter was used in combination with an ultra high-density mapping system (Rhythmia™, Boston Scientific) to reconstruct the LA geometry and to create activation- and/or voltage maps. An open-irrigated ablation catheter with three miniature-electrodes incorporated within the distal tip electrode (IntellaNav MiFi™ OI, Boston Scientific) was used for additional mapping and ablation.

The ablation strategy depended on the underlying rhythm at the beginning of the procedure: in case of recurrent paroxysmal AF, sole re-pulmonary vein isolation (Re-PVI) was performed. In patients with persistent AF, we performed the previously described stepwise approach[12] consisting of Re-PVI and substrate modification, if necessary. If a patient presented in AT, the underlying mechanism was identified, followed by specific ablation, as previously described.[13] During ablation, RFC was applied in a temperature-controlled fashion with a flush rate of 20 mL/min, a maximum of 30 W and temperature limit of 45°C. In voltage maps, high-voltage areas were defined by a voltage of more than 0.5 mV[14,15] when compared with intermediate voltage of 0.1–0.5 mV and low-voltage areas of <0.1 mV.

Local impedance measurement

Local impedance was measured by an open-irrigated single-tip mapping and ablation catheter (IntellaNav MiFi™ OI, Boston Scientific, *Figure 1*). The features of this novel ablation catheter have been described before[6]: from the tip of the catheter, the centre of each miniature-electrode is 2.0 mm away. Each electrode has a diameter of 0.80 mm. Local impedance is measured by a four-electrode method with separate circuits for field creation and field measurements.[6] Between the tip electrode and the proximal ring of the ablation catheter a non-stimulatory alternating current (5.0 μA at 14.5 kHz) is operated. Simultaneously, voltage is assessed passively between the miniature-electrodes and distal ring of the catheter.[6] To convert into impedance, these measured voltage values are divided by the stimulatory current. The maximum LI from the three miniature-electrodes was then displayed on the graphical user interface-screen of the ultra high-density mapping system and used for all analysis. The user interface displays the maximum LI value of all of the three miniature-electrode LI measurements. These maximum values were used for analysis in this study.

In each patient, after the electro-anatomical map of the LA was completed, blood pool impedance (as a non-contact reference) was

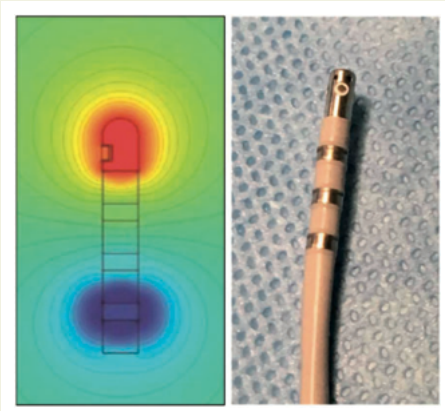

Figure 1 Field creation and ablation catheter for local impedance measurement. (Left panel) Simulation of the potential field created by injecting non-stimulatory current between the distal electrode and the proximal ring. A single miniature-electrode is shown in the distal tip. (Right panel) Photography of the open-irrigated ablation catheter with three miniature-electrodes (one is shown in the figure) at the distal tip electrode (IntellaNav MiFi^{TM} OI, Boston Scientific). Adapted with permission from Sulkin/Laughner *et al.*[6]

measured via the ablation catheter in the LA chamber, as indicated by the absence of electrograms on the conventional and mini-electrodes.

At the start of the RFC application the LI of the ablation site was recorded (so called 'baseline LI' in the following). In case of a dragged ablation lesion, LI measurements were only analysed until the first movement of the catheter. For each stable location of the catheter, which was verified by the electro-anatomical map, fluoroscopy, tactile feedback from the catheter and local electrograms,[8] the maximum LI drop (△LI) was analysed additionally.

The videos of the ablation procedures were exported from the mapping system (Rhythmia^{TM}, Boston Scientific) and displayed the procedure in real-time. Radiofrequency current applications were then retrospectively analysed. We excluded all lesions with instability of the catheter (not meeting the abovementioned criteria), interference with the mini-basket-catheter and applications with a duration of less than 10 s.

Generator impedance

Correspondingly to LI measurements, a RFC generator (EP Shuttle^{TM}, Stockert, Biosense Webster Inc., Diamond Bar, CA, USA) was used to record GI. The generator measured the system impedance by using a two-electrode method that included the same circuit for both field creation and field measurements.[6] Alternating current (500 kHz) was driven by the generator between the tip electrode of the ablation catheter to an indifferent electrode on the patient's skin.

Analogously to LI, GI was measured at the start of each ablation application (baseline GI) and the maximum GI drop (△GI) was additionally analysed for each lesion. Applications without GI information were excluded from analysis.

Table 1 Patients characteristics

	Patients (n = 25)
Male gender, *n* (%)	15 (60)
Age (years)	66.3 ± 12.8
Arterial hypertension, *n* (%)	15 (60)
Cardiomyopathy, *n* (%)	3 (12)
Coronary artery disease, *n* (%)	3 (12)
Diabetes, *n* (%)	1 (4)
Prior stroke/TIA, *n* (%)	5 (20)
BMI (kg/m^2)	27.0 ± 4.1
CHA_2DS_2-VASc score	2.6 ± 1.6
Indication for re-ablation, *n* (%)	
Recurrence of paroxysmal AF	4 (16)
Recurrence of persistent AF	11 (44)
Left/right atrial tachycardia	10 (40)
Number of prior ablations, *n*	2.4 ± 1.6

AF, atrial fibrillation; BMI, body mass index; CHA_2DS_2-VASc score is a clinical estimation of the risk of stroke in patients with atrial fibrillation; scores range from 0 to 9, with higher scores indicating a greater risk of stroke, Congestive heart failure, Hypertension, Age >75 years, Diabetes, previous Stroke, transient ischaemic attack, or thromboembolism, Vascular disease, Age 65–75 years, and Sex category; TIA, transient ischaemic attack.

Statistical analysis

Binary-coded and categorical data were described as counts and relative frequencies. Continuous data were expressed as mean ± standard deviation or by median and interquartile range. For group comparisons, Wilcoxon matched-pairs signed rank tests for paired values as well as a Mann–Whitney *U*-tests for unpaired values were performed. Additionally, a one-way analysis of variance (ANOVA) test was performed for analysis of the different anatomical locations. Further, linear regression analysis was calculated to determine relationships between LI and GI as well as △LI and △GI. A statistical significance was defined as a *P*-value <0.05. Statistics were calculated using 'R' [R Core Team (2017), A Language and Environment for Statistical Computing, R Core Team, R Foundation for Statistical Computing. Vienna, Austria, 2017] and GraphPad Prism 6.0 (GraphPad Software Inc., San Diego, CA, USA).

Results

Patients characteristics and procedural parameters

In 25 consecutive patients with a history of AF, catheter ablation, and analysis of LI were performed. An initial series of five patients (n = 5/30) was not included for analysis to avoid a learning-curve bias. Baseline characteristics are shown in *Table 1*. These 25 patients underwent 2.4 ± 1.6 prior catheter ablation procedures and returned for re-ablation due to recurrence of paroxysmal AF in four patients (16%, n = 4/25), persistent AF in 11 patients (44%, n = 11/25), and AT in 10 patients (40%, n = 10/25).

Procedural data are summarized in *Table 2*. The mean procedure duration and fluoroscopy times were 156.6 ± 53.1 min and 18.1 ± 10.3 min, respectively. A mean of 24.6 ± 16.5 RFC applications

Table 2 Procedural parameters

	Patients (n = 25)
Procedure duration (min)	156.6 ± 53.1
Fluoroscopy time (min)	18.1 ± 10.3
RFC applications (n)	24.6 ± 16.5
RFC duration (s)	1637.8 ± 1190.0
Cumulative energy (J)	44 605 ± 34 869
LA volume (mL)	96.6 ± 51.4
LA mapping time (min)	13.2 ± 10.3
LA mapping points (n)	9958.1 ± 8064.1
Ablation strategies, n (%)	
All PVs isolated	7 (28)
Re-PVI	18 (72)
Defragmentation	4 (16)
Ablation of LAT	9 (36)
Ablation of RAT	3 (12)
Re-CTI	8 (32)
Complications, n (%)	
Access site related	1 (4) minor groin haematoma
Pericardial tamponade	1 (4)
TIA/stroke	–
PV stenosis	–
Phrenic nerve palsy	–
Atrio-oesophageal fistula	–
Death	–

CTI, cavotricuspid isthmus ablation; LA, left atrium; LAT, left atrial tachycardia; PV, pulmonary vein; PVI, PV isolation; RAT, right atrial tachycardia; RFC, radiofrequency current; TIA, transient ischaemic attack.

were deployed per ablation procedure with a total count of 616 RFC applications without any steam popping.

Local and generator impedances

Of all 616 RFC applications counted by the generator, 381 (61.8%, n = 381/616) had a complete high quality data set with a RFC application >10 s and were included in the study analysis.

Overall, blood pool impedance levels tended to be lower when compared with baseline LI of myocardial tissue [99.9 ± 14.9 Ω, (n = 447)] vs. blood pool (91.9 ± 9.9 Ω, P = 0.052).

Baseline LI was lower when compared with baseline GI [LI: 99.9 ± 14.9 Ω (n = 447) vs. GI: 115.1 ± 11.7 Ω GI, P < 0.001], (*Figure 2A*). The mean impedance drop during RFC application was more than two times higher for △LI when compared with △GI [△LI: 13.1 ± 9.1 Ω (n = 389) vs. △GI: 6.1 ± 4.2 Ω (n = 362), P < 0.001], (*Figure 2B*).

The linear regression analysis revealed that a higher baseline LI in the LA predicted higher △LI during ablation [adjusted R^2 = 0.41, P < 0.001, slope = 0.39, 95% confidence interval (CI) (0.34–0.44), *Figure 2D*]. This means that a mean baseline LI of 99.9 Ω predicted a △LI of 12.9 Ω (95% CI (12.1–13.6)]. For the 1st quartile (q1), (90.0 Ω) and the 3rd quartile (q3), (109 Ω) of baseline LI, the predicted △LI was 8.9 Ω; [95% CI (8.0–9.9)] and 16.4 Ω [95% CI (15.5–17.2)], respectively.

The baseline GI was only a poor predictor of △GI [adjusted R^2 = 0.06; P < 0.001, slope = 0.09; 95% CI (0.05–0.14), *Figure 2C*]. A mean baseline GI (116.7 Ω) predicted a △GI of 6.0 Ω [95% CI (5.5–6.4)]. For the 1st quartile (109 Ω) and the 3rd quartile (175 Ω) of baseline GI, the predicted △GI was 5.1 Ω; [95% CI (4.6–5.8)] and 6.7 Ω [95% CI (6.2–7.3)], respectively.

The duration of an RFC application was not predictive for catheter–tissue coupling: once the maximum △LI or the maximum △GI were observed, prolongation of the RFC application did not further lower the LI nor GI, respectively (△LI: P = 0.247; △GI: P = 0.376).

Of 13 patients with right and/or left AT, specific termination into sinus rhythm was achieved in ten patients (n = 10/13, 76.9%) during ablation. The termination of AT was observed within a median of 7s (q1–q3: 5–13) of RFC delivery, with a mean △LI of 8.5 ± 4.6 Ω and a mean △GI of 4.2 ± 1.8 Ω at the time of termination. After a further median of 25 s (q1–q3: 15–32) of ablation, these RFC applications reached a maximum △LI of 14.8 ± 8.3 Ω and a maximum △GI of 8.8 ± 3.7 Ω. A power of 27.2 ± 2.4 W was applied in these termination lesions.

In a subset of 67 lesions (17.6%, n = 67/381, nine patients), the voltage values of different ablation sites were analysed: the mean baseline LI was higher in high-voltage areas of >0.5 mV (LI: 110.5 ± 13.7 Ω) when compared with ablations sites with intermediate voltage of 0.1–0.5 mV (LI: 90.9 ± 10.1 Ω, P < 0.001), low-voltage areas of <0.1 mV (LI 91.9 ± 16.4 Ω, P < 0.001) and compared with blood pool LI (LI: 91.9 ± 9.9 Ω, P < 0.001), (*Figure 3A*). The baseline LI at low- and intermediate voltage ablation sites was observed to be 4 Ω (q1–q3: 0, 25–9 Ω) higher (equals a 5% increase) than the individual patient's blood pool LI (n = 8 patients, n = 46 lesions). In 35 out of 46 lesions a numerical increase of baseline LI was found in low-voltage areas compared with the patients' blood pool impedance. Voltage maps were performed in sinus rhythm (n = 4/9 patients, 44.4%) or during AT (n = 5/9, 55.6%).

Baseline LI and baseline GI differed in areas of low (P < 0.001), intermediate (P < 0.001), and high voltage (P = 0.001) with wider ranges of LI standard deviations, (*Figure 3B*). A presentative example showing the LI in a LA low-voltage area in a patient with an AT is shown in the Supplementary material online, *Figure*.

Measurement of baseline LI among different anatomical localizations revealed a higher LI in the coronary sinus with 133.8 ± 21.7 Ω (n = 5), compared with left atrial LI: 99.6 ± 14.5 Ω (n = 355, P = 0.001), right atrial LI: 99.0 ± 14.3 Ω (n = 73, P = 0.002), and LI of the cavotricuspid isthmus region: 96.7 ± 10.3 Ω (n = 43, P < 0.001) as well as the blood pool LI: 91.9 ± 9.9 (n = 5; P = 0.003), (*Figure 4*).

Within the 90-days blanking period following the procedure, eight patients (n = 7/25, 28%) developed an AF/AT recurrence (n = 5 AF, n = 2 AT). During a median follow-up of 160 (q1–q3: 117–174) days, four patients (n = 4/25, 16%) developed an AF/AT recurrence after the blanking period (n = 2 AF, n = 2 AT; two of these patients already had an early AF recurrence within the blanking period).

Technical considerations and safety

Local impedance was successfully used during Re-PVI in 18 patients (18/25; 72%), substrate modification in four patients (4/25; 16%), cavotricuspid isthmus ablation in eight patients (8/25; 32%), and ablation of AT in 11 patients (11/25; 44%, *Table 2*) without the presence of any documented charring. *Figure 5* shows an example of real-time LI

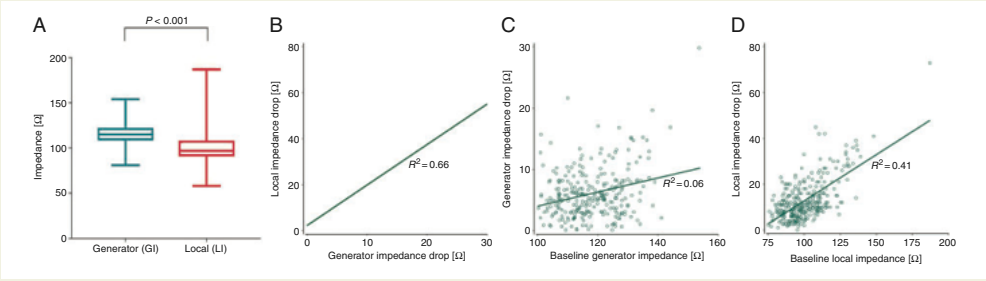

Figure 2 Relationship between LI and GI. (*A*) Discrimination between GI and LI.(*B*) Relationship between impedance drop of local impedance (△LI) compared with generator impedance (△GI): the local drop measured via the ablation catheter is more than two times higher when compared with the impedance drop of the generator.(*C*) Correlation between start impedances and generator impedance drops: the start impedance of the generator correlates poorly with the subsequent drop of impedance. (*D*) Correlation between local start impedances and local impedance drops: a higher local start impedances predicts higher △LI values. GI, generator impedance; LI, local impedance.

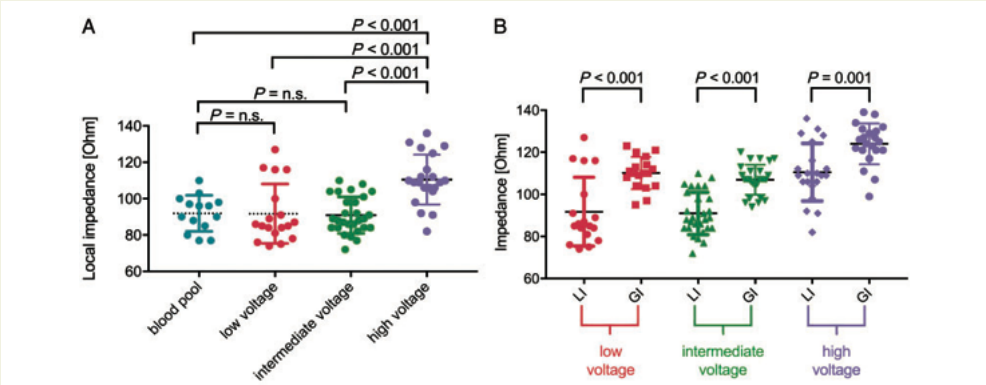

Figure 3 Relationship between impedance and voltage.(*A*) Local impedance values in low, intermediate and high-voltage areas of ablation, as well as the comparison towards blood pool impedance is shown. (*B*) The difference in local and generator impedance in low-, intermediate-, and high-voltage areas of ablation is shown. GI, generator impedance; LI, local impedance.

measurement during re-isolation of a left inferior pulmonary vein (PV). Here, an anterior gap of PV reconnection was detected by high-resolution activation mapping and confirmed by local mini-electrode signals (MIFI M3-M1) before RFC delivery. Acute pulmonary vein isolation occurred then within 4 s of ablation.

Twenty-three ablation procedures were performed successfully without any complications. In one patient a minor groin haematoma was documented and successfully treated conservatively. In another patient a pericardial tamponade manifested shortly after a RFC application with a rapid △LI of 45 Ω during an ongoing AT with a critical isthmus along the left atrial roof. Immediate, successful pericardiocentesis was performed, the AT was terminated by rapid atrial pacing and the patient was discharged 4 days later in a good medical condition.

In consequence, during the following ablation procedures ($n = 8$), RFC applications were stopped when a maximum cut-off △LI of <40 Ω was observed. After completion of this study, 97 additional atrial ablation procedures were performed in our department using this 40 Ω cut-off value without occurrence of a single pericardial tamponade. In this whole series, exceeding the here presented study population including 122 patients there was one transient dysarthria and two groin arteriovenous fistula with subsequent thrombin injection. No further complications occurred.

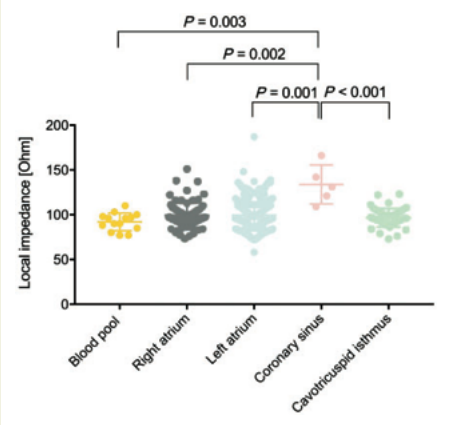

Figure 4 Local impedance among different anatomical localizations.

Further, during the ablation procedures, we observed different scenarios of how the real-time LI curves can present during RFC application, shown in *Figure 6*: (1) In this example, a very rapid and steep LI drop of 33 Ω within a few seconds was observed and energy delivery stopped. (2) Contact of the ablation catheter with the electrodes of the mini-basket catheter led to artefacts resulting in non-physiologic LI measurements of 316 Ω, in this example (△LI was 230 Ω during this interference). Therefore, LI cannot be determined during ablation when RF delivery is performed on the mini-basket catheter. (3) Instable catheter position resulted in systolic and diastolic movements of the catheter with rapid changes of the LI standard deviation. Image (4) shows an example of ablation in a low-voltage area: the baseline impedance (LI: 73 Ω) as well as △LI (−2.8 Ω) were comparably low. (5) When the ablation catheter was dragged during ablation, after an initial LI drop, LI raised again whenever the catheter was moved to a new position. (6) Lastly, respiration movements were reflected by fluctuating LI curves which could be observed in the changes of the real-time recordings during ablation.

Discussion

Major findings

The major findings of this study are as follows:

(1) Local impedance measurements from an ablation catheter tip with three incorporated mini-electrodes are related to the local tissue voltage. Baseline LI in high-voltage areas is higher when compared with intermediate- and low-voltage ablation sites as well as compared with blood pool LI.
(2) The drop in LI during RFC application was about twice as high as the GI drop.
(3) Higher LI at the start of an application predicted larger LI drops during ablation, while GI at baseline was not a good predictor for the GI drop during ablation.

Local and generator impedance measurements

Local impedance is a direct measure of the resistive load on the ablation catheter and provides a surrogate for the distal electrode surface area covered by myocardium.[6] It can distinguish between catheter–tissue contact from non-contact, as has been demonstrated by initial experimental findings and is supported by the here presented study.[6] Noteworthy and not surprisingly, observed LI was lower than GI measurements. In contrast, during ablation the △LI was greater than the △GI. This observation of larger LI drops were also in accordance with findings from prior experimental studies.[6] Therefore, the data of the present study indicate that LI makes it more likely the operator will achieve a target LI drop, as the baseline LI is more predictive than GI. It seems that △LI could be a more sensitive parameter for electrical coupling between catheter tip and tissue, when compared with the well-established △GI. The quality of LI data is not expected to be influenced by the generator. In experimental studies, △LI was a better predictor of lesion dimensions than △GI.[6]

So far, the optimal decrease of LI for lesion formation as well as the optimal modality over time during ablation cannot be defined. However, a surrogate parameter for acute efficacy in this study was provided by addressing the time course of LI and its decrease during RF delivery before AT termination into sinus rhythm. Additionally, when discussing the optimal decrease of LI, safety aspects need to be considered. In this study, a rapid decrease of the LI was seen in the patient with the cardiac tamponade. Nguyen *et al.*[16] support this finding and showed an association between the occurrence of steam pops and more rapid initial GI reduction during catheter ablation (1.40 Ω/s with vs. 0.38 Ω/s without steam pops). However, additional studies are warranted and underway to evaluate the safety of the here presented approach. No general safety recommendation can be made at this time.

Furthermore, our finding that higher start LI values were associated with larger △LI, is in line with the fact that higher initial impedance values are associated with better contact to the tissue.[5] RFC energy appears to be better transferred to the underlying tissue if high LI is measured due to better contact.[5,6] However, our study does not provide any information on the quality of the tissue contact, since so far, no contact force measurements are available for the presented approach. As information on the quality of tissue contact is missing, LI might not be able to detect excessive contact, a very important element to avoid complications. This needs further studies in the future.

Potential benefit of local impedance measurement

More than two decades ago, Josephson *et al.*[17] impressively demonstrated by some elegant studies in an experimental model of myocardial infarction, the potential value of LI to distinguish between healthy and diseased tissue. In our present study, LI in high-voltage areas was higher than in low-voltage areas. This supports the concept that LI is useful to distinguish between healthy and scarred myocardium, also

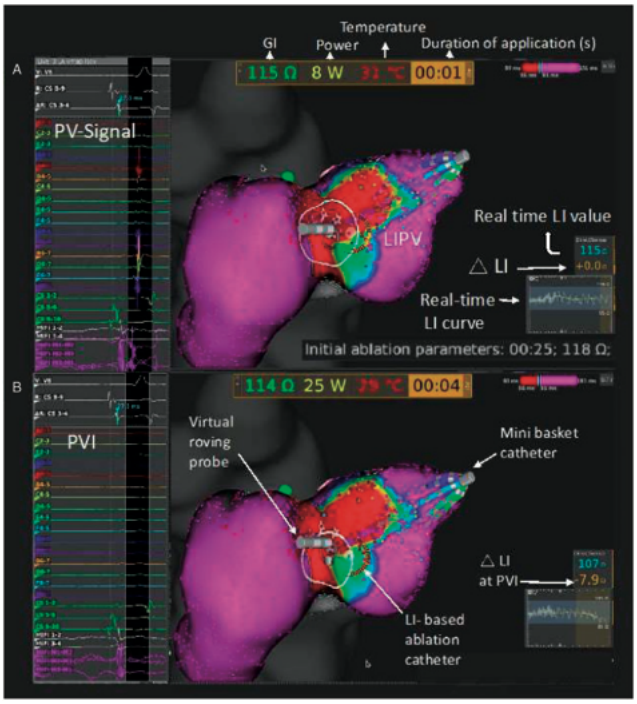

Figure 5 Local impedance measurement during ablation of a reconnected pulmonary vein. The Rhythmia™ activation map of a reconnected LIPV with an anterior gap is shown. On the top of each image, the information provided by the radiofrequency current generator is displayed; on the left, PV electrograms can be found and on the right, the LI information is provided. Image (*A*) shows the reconnected LIPV with a LI of 115 Ω and a GI of 118 Ω at the start of the RF application. The △LI is visualized right below the real-time LI value on the Rhythmia™ map in yellow. The lower image (*B*) demonstrates PVI occurring within 4 s with a 7.9 Ω-local impedance drop, which is shown in the real-time LI-curve in yellow. The drop in the generator was 4 Ω only. GI, generator impedance; LI, local impedance; LIPV, left inferior pulmonary vein; △LI = drop of local impedance; PVI, pulmonary vein isolation; RF, radiofrequency.

on the atrial level in humans. In addition, LI measurements by the ablation catheter were useful to distinguish healthy myocardium from blood pool, reflecting contact vs. non-contact. Noteworthy, mean baseline LI could only be used to reliably distinguish being in the blood pool vs. high voltage tissue, but not in intermediate or low voltage tissue. This finding could be explained by enrolment of patients undergoing re-do ablation procedures. Lang *et al.*[18] not only showed a difference in impedance between the LA and the PVs, but did also find lower impedances of the LA and PVs in patients undergoing repeat catheter ablation. Noteworthy, we found a slightly higher LI in low-/intermediate-voltage areas compared with the patients' individual blood pool. Therefore, LI might be an adjunct parameter in addition to the fluoroscopy, local electrograms and the 3D map to assess tissue contact in low-voltage areas. It remains unclear whether and how these findings might be influenced by different causes of myocardial scarring such as atrial fibrosis or low voltage due to prior ablation; different areas within the heart need to be explored in more detail.[17]

Regarding voltage measurements, further studies to determine LI cut-offs in different chambers and voltage areas are needed.

Up to now, real-time mechanical coupling during ablation is facilitated by the use of contact force (CF) sensing catheters.[19,20] A modest linear relationship between contact force over time (so called force-time-integral) and lesion depth has been shown.[21] However, in specific situations, such as ablation in the coronary sinus, CF can be misleading. While CF of the ablation catheter is low in the coronary sinus, the resistive load is high as more surface area of the electrode becomes enveloped by tissue rather than by blood.[5] Therefore, a large amount of RF energy could be delivered to the myocardium. In these kind of specific situations, LI alone or in combination with other parameters could be more informative about lesion formation than the sole use of CF, as CF is only of limited value to predict impedance drops during RFC delivery. LI could be a real-time measure for electrical coupling allowing an estimation of lesion size during ablation, as is supported by experimental evidence.

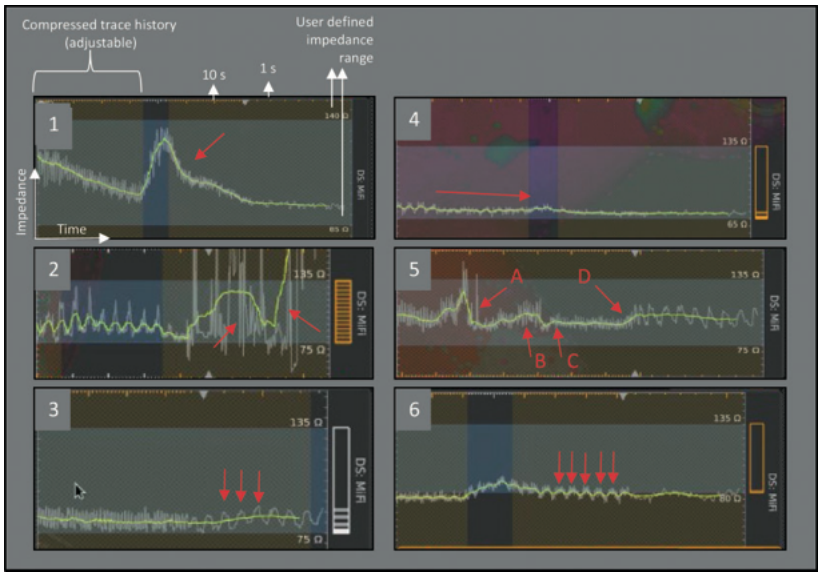

Figure 6 Different real-time local impedance curves during RF ablation. Different real-time curves of local impedances (LI) during RF ablation are shown. These LI-curves are exported from the Rhythmia™ map and show the mean LI as a yellow curve and the LI-standard deviation as a white curve. (1) A rapid and immense impedance drop of minus 33 Ω leading to premature stop of the ablation application for patients' safety (the LI at the start of the application was 128 Ω) is shown. (2) Placement of the ablation catheter next to the mini-basket catheter led to interference of the impedance measurement with implausible LI values (LI was 316 Ω and △ LI was 230 Ω during interference). (3) Instable catheter position led to systolic and diastolic movements of the catheter with rapid changes of the LI standard deviation shown by the white curves, around the yellow mean-LI curve. (4) Example of ablation in a low-voltage area: the start impedance (LI: 73 Ω) as well as △ LI (△ LI −2.8 Ω) were comparably low. (5) Example of a dragged ablation lesion: (*A*) shows the drop of the LI at the first ablation site, (*B*) then the catheter was moved and LI raised again due to movement of the catheter to an unablated tissue location, (*C*) followed by a second LI drop after the catheter was positioned at the second ablation site. (*D*) When the catheter was moved for the third time, LI raised again. (6) Example of local impedance fluctuations due to respiration. Notice the variability of the mean LI-curve (yellow).

Limitations

The present study has several limitations. First, the design of our study was explorative and we retrospectively analysed the real-time videos, exported from the electroanatomical mapping system. Next, we excluded RFC applications from the analysis to reliably include only solid and reproducibly quantifiable lesions. In consequence, only a limited sample size of 67 lesions was available to investigate the relationship of LI and voltage. Therefore, statistical power needs to be critically judged. Next, we only investigated LI in recurrent AF/AT ablation procedures. However, we present an early experience of LI-measurement and delivered specific details on >350 ablation lesions. Additional studies are warranted and underway to evaluate the safety of the here presented approach. Clinical implementation of this approach in other ablation procedures including catheter ablation of ventricular arrhythmias, in healthy and diseased myocardium needs to be studied in detail in the future. So far, the clinical results of this study show only a preliminary outcome. Noteworthy, we did not investigate effectiveness of RFC ablation guided by LI measurement. This is currently investigated in the LOCALIZE study (ELectrical COupling Information From The Rhythmia™ HDx Mapping System And DireCtSense™ Technology In The Treatment Of Paroxysmal AtriaL FibrIllation-A Non-RandomiZed, ProspEctive Study). In addition, no precise estimation of lesion size in humans is possible yet.

Finally, a limitation of the used catheter might be that there is currently no simultaneous combination of LI and contact force measurements available. Therefore, further studies are warranted to answer the question how precisely LI can indicate catheter–tissue contact in scared myocardium and to which extend it is able to guide catheter ablation in these situations.

Conclusion

Local impedance measurements are related to the voltage of the underlying tissue. Compared with the GI, baseline LI is a better predictor of impedance drops during ablation. Therefore, LI can be

monitored during ablation and may provide useful insights regarding catheter–tissue contact, catheter stability and lesion formation compared with the sole use of GI. Further studies are warranted to follow-up on our initial findings.

Supplementary material

Supplementary material is available at *Europace* online.

Acknowledgements

The authors thank Jake Laughner, PhD and Matt Sulkin, PhD (Boston Scientific Corp., St. Paul, MN, USA, 55112, Electrophysiology) for disclosing their previous findings on local impedance measurement to us, as well as for advise on data acquisition and engaging discussions/comments that greatly improved this article.

Funding

This work is supported by the DZHK (German Centre for Cardiovascular Research) [FKZ 81Z4710141 and 81X2710149].

Conflict of interest: L.M.: employee at Boston Scientific, Field Clinical Specialist Rhythmia™. C.E.: compensation for participation on speaker's bureau for Boston Scientific. C.M.: compensation for participation as consultant for Biotronik (also research grant), Biosense Webster, Boston Scientific, Medtronic, Philips Research Europe and on speaker's bureau for Abbott, Boston Scientific, Medtronic. S.W.: compensation for participation on speaker's bureau and consultant or on advisory board for: Boehringer Ingelheim, Bayer, Daiichi-Sankyo, BMS, Abbott. All other authors declared no conflict of interest.

References

1. Calkins H, Hindricks G, Cappato R, Kim Y, Saad EB, Aguinaga L *et al.* 2017 HRS/EHRA/ECAS/APHRS/SOLAECE expert consensus statement on catheter and surgical ablation of atrial fibrillation. *Europace* 2018;**20**:157–208.
2. Harvey M, Kim YN, Sousa J, El-Atassi R, Morady F, Calkins H *et al.* Impedance monitoring during radiofrequency catheter ablation in humans. *Pacing Clin Electrophysiol* 1992;**15**:22–7.
3. Reichlin T, Knecht S, Lane C, Kühne M, Nof E, Chopra N *et al.* Initial impedance decrease as an indicator of good catheter contact: insights from radiofrequency ablation with force sensing catheters. *Heart Rhythm* 2014;**11**:194–201.
4. Inaba O, Nagata Y, Sekigawa M, Miwa N, Yamaguchi J, Miyamoto T *et al.* Impact of impedance decrease during radiofrequency current application for atrial fibrillation ablation on myocardial lesion and gap formation. *J Arrhythm* 2018;**34**:247–53.
5. Zheng X, Walcott GP, Hall JA, Rollins DL, Smith WM, Kay GN *et al.* Electrode impedance: an indicator of electrode-tissue contact and lesion dimensions during linear ablation. *J Interv Card Electrophysiol* 2000;**4**:645–54.
6. Sulkin M, Laughner J, Hilbert S, Kapa S, Kosiuk J, Younan P *et al.* A novel measure of local impedance predicts catheter-tissue contact and lesion formation. *Circ Arrhythm Electrophysiol* 2018;**4**:e005831.
7. Ikeda A, Nakagawa H, Lambert H, Shah DC, Fonck E, Yulzari A *et al.* Relationship between catheter contact force and radiofrequency lesion size and incidence of steam pop in the beating canine heart: electrogram amplitude, impedance, and electrode temperature are poor predictors of electrode-tissue contact force and lesion. *Circ Arrhythm Electrophysiol* 2014;**7**:1174–80.
8. Piorkowski C, Sih H, Sommer P, Miller SP, Gaspar T, Teplitsky L *et al.* First in human validation of impedance-based catheter tip-to-tissue contact assessment in the left atrium. *J Cardiovasc Electrophysiol* 2009;**20**:1366–73.
9. van Es R, Hauck J, van Driel VJHM, Neven K, van Wessel H, Doevendans PA *et al.* Novelmethod for electrode-tissue contact measurementwithmulti-electrode catheters Rene. *Europace* 2018;**20**:149–56.
10. Gaspar T, Sih H, Hindricks G, Eitel C, Sommer P, Kircher S *et al.* Use of electrical coupling information in AF catheter ablation: a prospective randomized pilot study. *Heart Rhythm* 2013;**10**:176–81.
11. Gunawardene MA, Hoffmann BA, Schaeffer B, Chung D-U, Moser J, Akbulak RO *et al.* Influence of energy source on early atrial fibrillation recurrences: a comparison of cryoballoon vs. radiofrequency current energy ablation with the endpoint of unexcitability in pulmonary vein isolation. *Europace* 2018;**20**:43–9.
12. Vogler J, Willems S, Sultan A, Schreiber D, Lüker J, Servatius H *et al.* Pulmonary vein isolation versus defragmentation. *J Am Coll Cardiol* 2015;**66**:2743–52.
13. Schaeffer B, Hoffmann BA, Meyer C, Akbulak RÖ, Moser J, Jularic M *et al.* Characterization, mapping and ablation of complex atrial tachycardia: initial experience with a novel method of ultra high-density 3D mapping. *J Cardiovasc Electrophysiol* 2016;**27**:1139–50.
14. Frontera A, Takigawa M, Martin R, Thompson N, Cheniti G, Massoullié G *et al.* Electrogram signature of specific activation patterns: analysis of atrial tachycardias at high-density endocardial mapping. *Heart Rhythm* 2018;**15**:28–37.
15. Garcia-Bolao I, Ballesteros G, Ramos P, Menendez D, Erkiaga A, Neglia R *et al.* Identification of pulmonary vein reconnection gaps with high-density mapping in redo atrial fibrillation ablation procedures. *Europace* 2018;**20**:f351–8.
16. Nguyen DT, Zipse M, Borne RT, Zheng L, Tzou WS, Sauer WH. Use of tissue electric and ultrasound characteristics to predict and prevent steam-generated cavitation during high-power radiofrequency ablation. *J Am Coll Cardiol* 2018;**4**:491–500.
17. Fallert MA, Mirotznik MS, Downing SW, Savage EB, Foster KR, Josephson ME *et al.* Myocardial electrical impedance mapping of ischemic sheep hearts and healing aneurysms. *Circulation* 1993;**87**:199–207.
18. Lang CCE, Gugliotta F, Santinelli V, Mesas C, Tomita T, Vicedomini G *et al.* Endocardial impedance mapping during circumferential pulmonary vein ablation of atrial fibrillation differentiates between atrial and venous tissue. *Heart Rhythm* 2006;**3**:171–8.
19. Reddy VY, Shah D, Kautzner J, Schmidt B, Saoudi N, Herrera C *et al.* The relationship between contact force and clinical outcome during radiofrequency catheter ablation of atrial fibrillation in the TOCCATA study. *Heart Rhythm* 2012;**9**:1789–95.
20. Neuzil P, Reddy VY, Kautzner J, Petru J, Wichterle D, Shah D *et al.* Electrical reconnection after pulmonary vein isolation is contingent on contact force during initial treatment: results from the EFFICAS I study. *Circ Arrhythm Electrophysiol* 2013;**6**:327–33.
21. Shah DC, Lambert H, Nakagawa H, Langenkamp A, Aeby N, Leo G. Area under the real-time contact force curve (force-time integral) predicts radiofrequency lesion size in an in vitro contractile model. *J Cardiovasc Electrophysiol* 2010;**21**:1038–43.

Received: 6 November 2019 | Revised: 29 January 2020 | Accepted: 17 February 2020

DOI: 10.1111/jce.14413

ORIGINAL ARTICLE

WILEY

Ultra–high-density mapping of conduction gaps and atrial tachycardias: Distinctive patterns following pulmonary vein isolation with cryoballoon or contact–force-guided radiofrequency current

Melanie A. Gunawardene[1,2] | Christian Eickholt[1,2] | Ruken Ö. Akbulak[1] | Mario Jularic[1,2] | Niklas Klatt[1] | Jens Hartmann[1,2] | Michael Schlüter[3] | Christian Meyer[1,4] | Stephan Willems[1,2] | Benjamin Schaeffer[1]

[1]Department of Cardiac Electrophysiology, University Heart Center, University Hospital Hamburg Eppendorf, Hamburg, Germany

[2]Department of Cardiology, Asklepios Hospital St Georg, Hamburg, Germany

[3]Asklepios proresearch, Hamburg, Germany

[4]DZHK (German Center for Cardiovascular Research), partner site Hamburg/Kiel/Lübeck, Berlin, Germany

Correspondence
Melanie A. Gunawardene, MD, Department of Cardiology, Asklepios Klinik St Georg, Lohmühlenstr 5, 20099 Hamburg, Germany.
Email: melanie.gunawardene@gmail.com

Disclosures: None.

Funding information
Deutsches Zentrum für Herz-Kreislaufforschung, Grant/Award Numbers: FKZ 81Z4710141, 81X2710149

Abstract

Introduction: The aim of this study was to investigate electrophysiological findings in patients with arrhythmia recurrence undergoing a repeat ablation procedure using ultra–high-density (UHDx) mapping following an index procedure using either contact–force (CF)-guided radiofrequency current (RFC) pulmonary vein isolation (PVI) or second-generation cryoballoon (CB) PVI for treatment of atrial fibrillation (AF).

Methods and Results: Fifty consecutive patients with recurrence of AF and/or atrial tachycardia (AT) following index CF-RFC PVI (n = 21) or CB PVI (n = 29) were included. A 64-pole mini-basket mapping catheter in combination with an UHDx-mapping system-guided ablation was used. RFC was applied using a catheter tip with three incorporated mini-electrodes. PV reconnection rates were higher after CF-RFC PVI (CF-RFC: 2.5 ± 1.3 PVs vs CB: 1.4 ± 0.9 PVs; $P = .0025$) and left PVs were more frequently reconnected (CF-RFC: 64% PVs vs CB: 35% PVs; $P = .0077$). Fractionated signals along the antral index ablation line (FS) were found in 30% of CB-PVI patients (CF-RFC: 9.5% vs CB:30%; $P = .098$) targeted for ablation. In five cases, FS were a critical part of maintaining consecutive AT. The main AT mechanism found during reablation (n = 45 ATs) was macroreentry (80% [36/45], CF-RFC: 78.9% vs CB: 80.8%; $P = 1.0$) with a variety of circuits throughout both atria.

Conclusion: UHDx mapping is sensitive in detecting conduction gaps along the index ablation line. Left PVs are more frequently reconnected after initial CF-RFC PVI. FS are a common finding after CB PVI and can maintain certain forms of ATs. ATs after index PVI are mostly macroreentries with a broad spectrum of entities.

KEYWORDS

atrial fibrillation, contact-force radiofrequency catheter ablation, cryoballoon ablation, pulmonary vein isolation, ultra–high-density mapping

1 | INTRODUCTION

Success rates of catheter ablation for atrial fibrillation (AF) have improved with current technologies: radiofrequency current (RFC) and cryoballoon (CB) ablation are associated with similar clinical outcomes.[1] However, recurrences after an index pulmonary vein isolation (PVI) frequently occur due to PV reconnection and according to conduction gaps along the ablation lines.[2] Different gap patterns have been described after index PVI with RFC versus CB.[3,4] A less-common but clinically relevant finding is the occurrence of atrial tachycardia (AT) after stand-alone PVI without prior substrate modification.[5,6]

Compared to conventional three-dimensional mapping, ultra–high-density (UHDx) mapping provides detailed insights due to the higher resolution of local electrograms.[7]

Data on UHDx mapping of PV reconnections and, in particular, AT following stand-alone PVI are limited.[4,5] Therefore, repeat procedures with UHDx mapping and subsequent local impedance-based ablation after an index PVI with contact–force (CF)-guided RFC or with the second-generation cryoballoon (CB) were compared in this study. The aims of the study were (a) the evaluation of gap patterns in reconnected PVs and (b) the characterization of AT mechanisms.

2 | METHODS

2.1 | Study design

This study was a single-center, prospective, nonrandomized study. Consecutive patients with recurrent AF and/or AT after an index stand-alone PVI for paroxysmal or persistent AF performed between November 2017 and December 2018 were enrolled; all patients underwent their first reablation with UHDx mapping. Two groups were defined according to whether the index PVI was performed by CF-guided RFC or the CB. Written informed consent was obtained from all patients. The study was conducted in accordance with the provisions of the Declaration of Helsinki and its amendments. The institutional review board approved the study.

2.2 | Index PVI with contact–force-guided radiofrequency current

Catheter ablation and periprocedural management of patients at our institution have been reported before.[8] After the transseptal puncture, a sequential left atrial reconstruction was performed using a circumferential mapping catheter in combination with a three-dimensional (3D) mapping system (CARTO 3, Biosense Webster or EnSite Precision, Abbott). Wide-area circumferential PVI of the ipsilateral PVs was performed by the use of an irrigated CF-sensing RFC ablation catheter (Thermocool SmartTouch, Biosense Webster or Tacticath, Abbott), (max. 30 Watts for 30-60 seconds, target minimal CF of 10*g*,[9] under Visitag control when using CARTO 3). In all CARTO-guided index CF-RFC PVI procedures performed after 2017, the use of the ablation index has been implemented into the workflow. A maximum of 25 Watts was applied while ablating at the posterior LA wall. Luminal esophageal temperature was monitored by a multipolar temperature-sensing catheter (CIRCA-S-CATH; Circa Scientific, Englewood, CO).

2.3 | Index PVI with the cryoballoon

PVI with the second-generation CB has been reported before.[8] After a single transseptal puncture (BRK-1; St Jude, Medical, St Paul, MN), the 28 mm CB (Arctic Front Advance; Medtronic Inc, Minneapolis, MN) was introduced into the LA via a 12 F steerable sheath (FlexCath; Medtronic). PV mapping to record electrograms was performed before, during, and after freezing, with an endoluminal spiral mapping catheter (Achieve; Medtronic). Target application time and protocols varied over the course of the study. Initially, 240 seconds and a bonus freeze were applied (protocol #1). With protocol #2, bonus freezes were abolished. In 2018, a time-to-effect protocol (#3) was established: if real-time PVI occurred within 60 s of a freeze, the total freezing time was reduced to 180 s, without additional bonus freezes.

During the ablation of right-sided PVs, the phrenic nerve was paced while recording the diaphragmatic compound motor action potential, as described previously.[10] Luminal esophageal temperature was monitored by a multipolar temperature-sensing catheter (CIRCA-S-CATH; Circa Scientific, Englewood, CO).

2.4 | Reablation procedure using UHDx mapping

All patients underwent a reablation procedure using UHDx mapping. UHDx mapping was performed, as previously described.[11,12] After transseptal puncture using a modified Brockenbrough technique to access the left atrium (LA), a long sheath (SL0, 8 F; St Jude) as well as a steerable sheath (ZURPAZ, 8.5 F; Boston Scientific, Marlborough, MA) were navigated into the LA. A steerable 6-F decapolar diagnostic catheter (Inquiry, 2-5-2 mm spacing; St Jude) was placed in the coronary sinus as a reference. A 64-pole mini-basket mapping catheter (Orion; Boston Scientific) was introduced to the LA via the steerable sheath. Following LA angiography, the mini-basket catheter was used in combination with an UHDx mapping system (Rhythmia, Boston Scientific) to reconstruct LA geometry and to create activation and/or voltage maps. In all patients, activation and voltage maps of the LA were created to assess PV reconnection. In general, the first map was always performed under the rhythm that was present at baseline.

PV reconnection was defined as the presence of a PV spike. Pacing maneuvers were used to differentiate possible far-field signals, if necessary. An activation, as well as a voltage map of the PV ostium, was created. The earliest activation in conjunction with a possible gap in the voltage map was used to further narrow down the location of the conduction gap. Additionally, UHDx mapping of the index ablation line was performed to screen for fractionation and

amplitude of local electrograms. Finally, the ablation catheter was placed at the assumed gap and local electrograms were used to identify a local gap signal. In the case of PV reconnection, repeat PVI (Re-PVI) was performed targeting the specific gaps along the initial ablation line. Gaps were categorized into 16 segments, as reported before.[4] If a common PV ostium was present, middle segments were not included. Additionally, the gaps were confirmed by (a) either complete PV isolation during RFC delivery and disappearance of a prior local activity (PV spike) or (b) by observation of a change in the activation sequence of the PV spike during RFC ablation.[4] A waiting period of at least 20 minutes was mandated after reisolation.

Depending on the underlying rhythm during the procedure and the documented type of arrhythmia in prior electrocardiogram (ECG) recordings, different procedural strategies were pursued:

1. If sinus rhythm was present at the beginning of the procedure, localization of PV gaps and according ablation was performed. In the case of paroxysmal AF, no further ablation was performed.
2. In patients with persistent AF, the previously described stepwise approach was performed consisting of Re-PVI after identification of reconnection sites and subsequent substrate modification, if necessary.[13] If only re-PVI was performed, electrical cardioversion was performed prior to gap mapping of the PVs as per the discretion to the investigator.
3. If a patient presented in AT, the underlying AT mechanism was identified by analysis of wave front propagation, activation patterns, areas of slow conduction, anatomical and functional barriers and lines of block within the 3D map, followed by specific ablation, as previously described.[12] If AT was documented prior to the procedure but the patient presented in sinus rhythm, atrial pacing (programmed stimulation or burst pacing) was performed for induction of the AT after Re-PVI. The mechanism of AT was defined as either macroreentry or nonmacroreentry.[12] A centrifugal activation pattern indicated a nonmacroreentry AT. In this case, the mechanism was further evaluated as either focal ATs (showing radial activation from a distinct focal source) or localized reentry ATs (showing continuous, fractionated activation covering the entire cycle length in an area of less than 2 cm in diameter or the presence of a dominant small and stable rotational activation pattern, as defined before[12]).

2.5 | Ablation using local impedance monitoring

Local impedance (LI) was measured by an open-irrigated single-tip mapping and ablation catheter (IntellaNav MiFi OI; Boston Scientific). The technical aspects of this approach have been described before.[11] At the beginning of RFC delivery, baseline LI and baseline generator impedance (GI) using an RFC generator (EP Shuttle; Stockert, Biosense Webster Inc, Diamond Bar, CA) were analyzed, as well as LI and GI drops and the time until the impedance drop during RFC ablation.

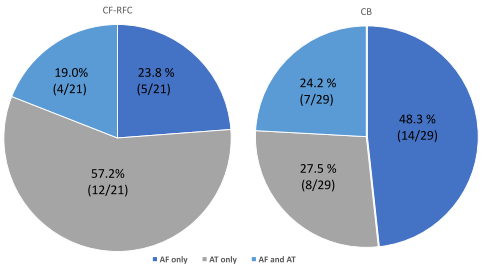

FIGURE 1 Indication for reablation. AF, atrial fibrillation; AT, atrial tachycardia; CB, cryoballoon; CF-RFC, contact–force-guided radiofrequency current

2.6 | Statistical analysis

Continuous data are expressed as mean ± standard deviation or as median and interquartile range. For group comparisons, the Student *t* test or the Mann-Whitney *U* test for unpaired variables were utilized. Categorical data are described as absolute and relative frequencies; they were compared using the χ^2 or Fisher's exact test. Statistical significance was assumed at a $P < .05$. Statistical analyses utilized the GraphPad Prism 7.0 software (GraphPad Software Inc, San Diego, CA).

3 | RESULTS

3.1 | Baseline and procedural characteristics

Between 11/2017 and 12/2018, 50 consecutive patients with recurrence of AF/AT undergoing UHDx mapping after an index PVI with either CF-RFC (n = 21) or the CB (n = 29) were included in the study. Three patients (n = 2 CF-RFC, n = 1 CB) also received a cavotricuspid isthmus (CTI) ablation additional to PVI in the index procedure. Ablation within the left atrium was restricted to PVI with no further substrate modification.

A repeat ablation was performed due to recurrence of AF in 19 patients (38.0%; CF-RFC: 23.8%; CB: 48.3%), AT in 20 patients (40.0%; CF-RFC: 57.2%; CB: 27.5%), and both AF and AT in 11 patients (22.0%; CF-RFC: 19.0%; CB: 24.2%; Figure 1); the difference in distribution between the 2 groups was statistically not significant ($P = .094$). Baseline patient characteristics are shown in Table 1. The time between Index PVI and the UHDx reablation procedure was 335 days (median; interquartile range [IQR] 232-622 days; CF-RFC: 359 [244-489] days; CB: 330 [207-867] days; $P = .106$).

Procedural parameters and complications are provided in Table 2. There was a single pericardial tamponade in the CF-RFC group, requiring immediate pericardiocentesis. The patient was discharged from the hospital, 3 days later, in good medical condition. The ablation strategy subsequent to UHDx mapping were repeat PVI due to PV reconnection (45 patients, 90%), substrate modification

TABLE 1 Baseline patient characteristics

	All	CF-RFC	CB	
	n = 50	n = 21	n = 29	*P* value
Age, y	69.4 ± 9.1	67.5 ± 9.4	70.8 ± 8.7	.215
Male gender	23 (46.0)	12 (57.1)	11 (37.9)	.252
Hypertension	33 (66.0)	13 (61.9)	20 (69.0)	>.999
Prior stroke/TIA	5 (10)	2 (9.5)	3 (10.3)	>.999
BMI, kg/m^2	25.5 ± 3.3	26.6 ± 3.7	25.5 ± 3.3	.334
CHA_2DS_2-VASc score	3 (2-4)	3 (2-4.5)	3 (2-4)	.441
Initial type of AF				
PAF	22 (44.0)	8 (38.1)	14 (48.3)	.569
Persistent AF	28 (56.0)	13 (61.9)	15 (51.7)	
Time between Index PVI and first reablation, d	335 (232-622)	359 (244-489)	330 (207-868)	.106

Note: Values are mean ± standard deviation, median (first-third quartile) or n (%). CHA2DS2-VASc score is a clinical estimation of the risk of stroke in patients with atrial fibrillation; scores range from 0 to 9, with higher scores indicating a greater risk of stroke.
Abbreviations: AF, atrial fibrillation; BMI, body mass index; CB, cryoballoon PVI; CF-RFC, contact–force-guided radiofrequency current PVI; CHA_2DS_2-VASc, Congestive heart failure, Hypertension, Age above 75 years, Diabetes, previous Stroke, transient ischemic attack, or thromboembolism, Vascular disease, Age 65 to 75 years, and Sex category; PAF, paroxysmal atrial fibrillation; PVI, pulmonary vein isolation; TIA, transient ischemic attack.

(11 patients, 22%) for persistent AF, targeting of ATs (31 patients, 62%) and ablation of fractionated signals along the antral index ablation line (11 patients, 22%; Table 2) in the two groups. These findings are described in detail below.

3.2 | Pulmonary vein reconnection and conduction gaps

PV reconnection rates identified by UHDx mapping were higher after index CF-RFC PVI (2.5 ± 1.3 PVs per patient) than after index PVI using the CB (1.4 ± 0.9 PVs; *P* = .003). In total, 52 of 85 PVs (61.2%) were reconnected after index CF-RFC PVI vs 41/114 PVs (36.0%) after index CB PVI (*P* = .005; Figure 2A). In the CF-RFC group, seven patients (7/21, 33.3%) showed a reconnection of all PVs, whereas no patient in the CB-PVI group had reconnection of all PVs (*P* = .0012). Isolation of all four PVs was found in 1 of 21 (4.8%) CF-RFC patients and in 4 of 29 (13.8%) CB patients.

Additionally, left-sided PVs were more frequently reconnected after index CF-RFC PVI (27/42, 64.3%) than after index CB PVI (20/56, 35.7%; *P* = .0077; Figure 2B,C). The reconnection rate of right-sided PVs was similar in both groups (25/43 [58.1%] vs 24/58 [41.4%], *P* = .110).

In total, 58 (CF-RFC: 58/52PVs, 1.12 gaps per reconnected PV) and 49 conduction gaps (CB: 49/41 PVs, 1.20 gaps per reconnected PV) were identified in the two groups (Figure 3). After index CF-RFC

TABLE 2 Procedural parameters of UHDx reprocedure

Procedural parameters	All	CF-RFC	CB	
	n = 50	n = 21	n = 29	*P* value
Initial rhythm at reprocedure				.127
• Sinus rhythm	28 (56.0)	9 (42.9)	19 (65.5)	
• Atrial fibrillation	10 (20.0)	4 (19.0)	6 (20.7)	
• Atrial tachycardia	12 (24.0)	8 (38.1)	4 (13.8)	
Procedure time, min	153.2 ± 54.9	161.5 ± 57.8	147.6 ± 53.0	.387
Fluoroscopy time, min	18.3 ± 9.2	19.0 ± 10.8	17.8 ± 8.2	.649
UHDx-LA mapping points	10,438 ± 6,639	11,951 ± 6,181	9,390 ± 6859	.212
Mapped LA volume, ml	126.2 ± 57.2	112.9 ± 39.1	135.2 ± 66.0	.219
Electrophysiological findings				
• PV reconnection	45 (90.0)	20 (95.2)	25 (86.2)	.383
• Substrate modification	11 (22.0)	2 (9.5)	9 (31.0)	.098
• Ablation of ATs	31 (62.0)	16 (76.2)	15 (51.7)	.139
• Ablation of fractionated signals along the antral index ablation line	11 (22.0)	2 (9.5)	9 (31.0)	.098
All complications	4 (8)	1 (4.8)	3 (10.3)	.630
• Pericardial tamponade	1 (2)	1 (4.8)	0 (0)	
• Intermittent dysarthria[a]	1 (2)	0 (0)	1 (3.4)	
• Minor groin complication	2 (4)	0 (0)	2 (6.9)	

Note: Values are mean ± standard deviation, [n] or n (%).
Abbreviations: AF, atrial fibrillation; AT, atrial tachycardia; CF-RFC, contact–force-guided radiofrequency current PVI; CB, cryoballoon PVI; CT, computed tomograpgy; LA, left atrium; PV, pulmonary vein; PVI, pulmonary vein isolation; SR, sinus rhythm; UHDx, ultra-high density.
[a]Dysarthria occurred immediately after awakening, without a clear focal neurological deficit (also normal CT scan) and was, therefore, rather associated with the anesthesia itself.

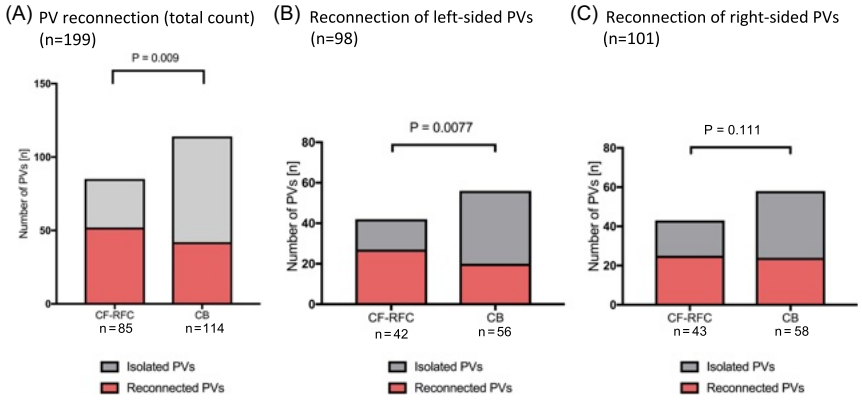

FIGURE 2 Reconnection of pulmonary veins in the two study groups. CB, cryoballoon; CF-RFC, contact–force-guided radiofrequency current; PV, pulmonary vein

PVI, the majority of the conduction gaps were found anterior to the left inferior PV (n = 9), at the carina region of the upper and lower left PVs (n = 7 and 4, respectively) and anterior to the right inferior PV (n = 6). In contrast, after CB PVI, the majority of the conduction gaps were found along the inferior segments of the right inferior PV (n = 16), followed by gaps anterior to the left upper PV (n = 6) (Figure 3). The most frequently reconnected PVs were the left inferior PV in the CF-RFC group and the right inferior PV in the CB group. There was no relevant difference in conduction gaps along the posterior wall between the two groups ($P = 1.0$).

3.3 | Fractionated signals along the antral index ablation line

With UHDx mapping, fractionated signals along the antral index ablation line were identified in two patients (9.5%) after index CF-RFC PVI and nine patients (31.0%) after index CB PVI ($P = .092$) (Figure 4). In one (1/2, 50%) patient of the CF-RFC group and in four (4/9; 44.4%) patients of the CB-PVI group, these fractionated signals along the index ablation line were identified as the critical isthmus of the underlying AT (all being macroreentries). In the CF-RFC group,

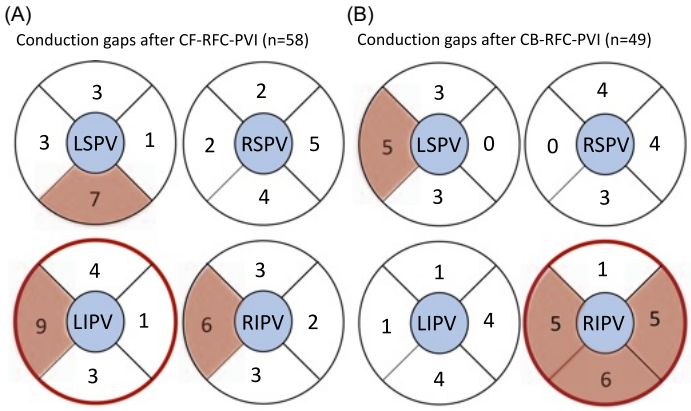

FIGURE 3 Localization of conduction gaps in reconnected pulmonary veins. Numbers in quadrants represent numbers of conduction gaps. Regions, where conduction gaps were found at least five times, are shaded in red. CB, cryoballoon; CF-RFC, contact–force-guided radiofrequency current; LIPV, left inferior pulmonary vein; LSPV, left superior pulmonary vein; PVI, pulmonary vein isolation; RIPV, right inferior pulmonary vein; RSPV, right superior pulmonary vein

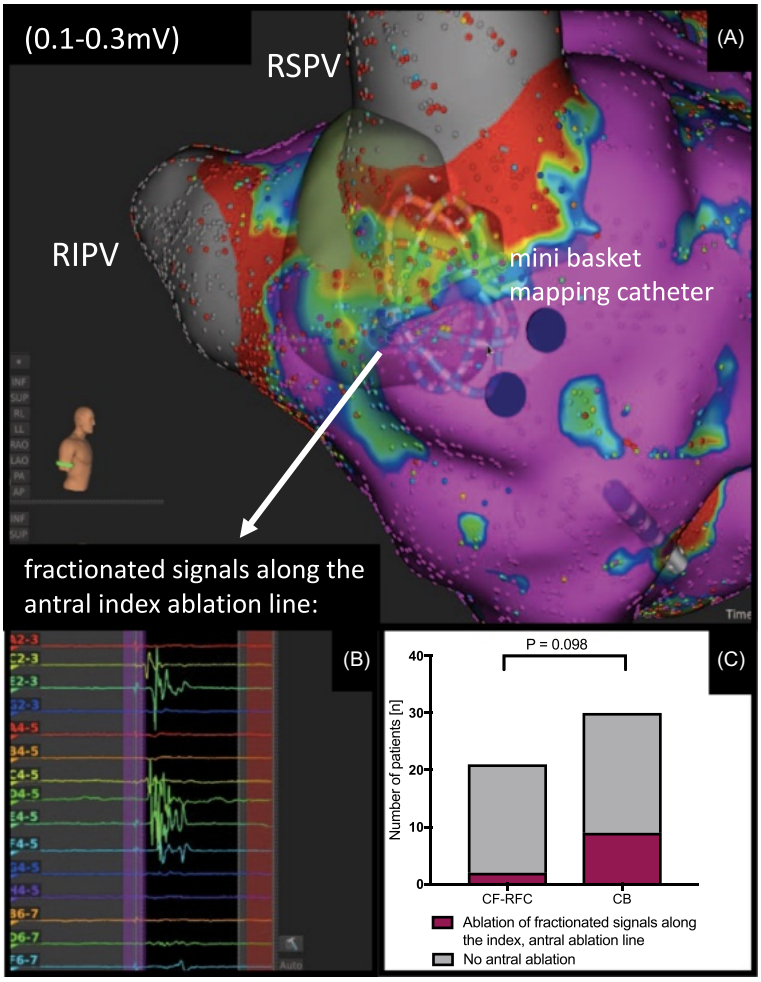

FIGURE 4 Example of signals along the antral index ablation line in an ultra–high-density (UHDx) map of the left atrium. A, Voltage UHDx map of the LA showing the mini-basket catheter at the antral index ablation line of the right upper and lower pulmonary vein. B, Electrograms from the mini-basket catheter positioned at the index ablation line, displaying fractionated antral signals. C, Number of patients with fractionated signals along the antral index ablation line in both groups. CB, cryoballoon; CF-RFC, contact–force-guided radiofrequency current; LA, left atrium; RSPV, right upper pulmonary vein; RIPV, right lower pulmonary vein

the AT was associated with the index ablation line anterior to the left inferior PV (LIPV, PV isolated), in the CB group, all four ATs were associated with fractionated signals anterior to the right superior PV (RSPV; 3/4 PVs isolated). Thus, in 5 of 11 patients (45.5%) detected fractionated signals along the antral index ablation line indicated a critical site for AT maintenance in the activation map. Ablation at these sites terminated AT promptly in all cases (n = 4 into sinus rhythm, n = 1 into another AT during ablation).

3.4 | Atrial tachycardia

ATs were found in 16 patients (16/21, 76.2%) after index CF-RFC PVI and in 15 patients (15/29, 51.7%) after CB PVI ($P = .139$), Figure 1. In total, 45 ATs were subsequently ablated (CF-RFC n = 19 vs CB: n = 26). Of these 45 ATs, 14 (31.1%) were present at baseline, 10 (22.2%) were induced in patients presenting in sinus rhythm and matched the clinical documentation of the AT, five

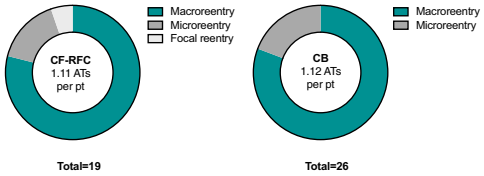

FIGURE 5 Distribution of atrial tachycardia mechanisms. AT, atrial tachycardia; CB, cryoballoon; CF-RFC, contact–force-guided radiofrequency current; pt, patient

(11.1%) occurred secondary to AF ablation and substrate modification, nine (20.0%) ATs terminated into a secondary AT during ablation, seven (15.6%) patients had an ECG recording of typical atrial flutter prior to the procedure. Of all patients with AT ablation, a majority of 67.8% (21/31) presented with persistent AF at index PVI and 32.2% (10/31) of AT patients with paroxysmal AF at the index PVI.

In general, the main AT mechanism identified with UHDx was macroreentry (n = 36; CF-RFC: 15/19 [78.9%] vs CB: 21/26 [80.8%]; $P = 1.0$) of which 14 (39%) were CTI-dependent, constituting the most frequent AT (14/45, 31.1%) with no difference between groups (CF-RFC: 6/19 [31.6%] vs CB: 8/26 [30.8%], $P = .753$), followed by microreentry (n = 8; CF-RFC: 3/19 [15.7%] vs CB: 5/26 [19.2%], $P = 1.0$) and focal AT (n = 1; CF-RFC: 1/19 [5.4%] vs CB: 0%, P = 0.422) (Figure 5).

Beside CTI-dependent macoreentries, the critical isthmus of ATs could be located at the anterior left atrium (7/45, 15.6%) and along the index ablation lines (5/45, 11.1%) (Figure 6). Of the anterior ATs, five (5/7, 71.4%) were macroreentries and two (2/7, 28.6%) were microreentries. All five ATs originating from the index ablation line were macroreentries.

Of the eight microreentries, three (37.5%) were found in the left atrial appendage (LAA)/ridge region, two (25.0%) in the anterior LA, another two (25.0%) in the right atrium, and one (12.5%) had a septal origin (Figure 6). The one focal AT was a PV-dependent AT (associated with the left superior PV, LSPV). More than one AT per patient was present in three patients (14.3%) of the CF-RFC group and seven patients (24.1%) of the CB group ($P = .488$).

There was no difference in the incidence of ATs associated with the index PVI procedure (including ATs originating from the antral index ablation line, LAA/ridge ATs, PV-dependent ATs) in either group (CF-RFC: 7/19 [36.8%] vs CB: 5/26 [19.2%]; $P = .306$). In detail, in the CF-RFC group, there were seven ATs (36.8%) associated with the index CF-RFC ablation procedure: five ATs (71.4%) originating from the LAA/ridge region (two microreentries, three macroreentries), one (14.3%) from the index ablation line (anterior of LIPV; macroreentry), and one was a focal PV tachycardia from the LSPV (14.3%). Moreover, there were three macroreentries with a critical isthmus in the anterior LA (Figure 6) not associated with the index PVI.

In the CB group, five ATs (5/26, 19.2%) were associated with the index PVI procedure: four macroreentries (80.0%) originated from the index ablation line (all anterior of the RSPV) and one macroreentry (20.0%) from the LAA/ridge region. In addition, there were four ATs with a critical isthmus at the anterior LA (two macroreentries, two microreentries). There were two roof-dependent and

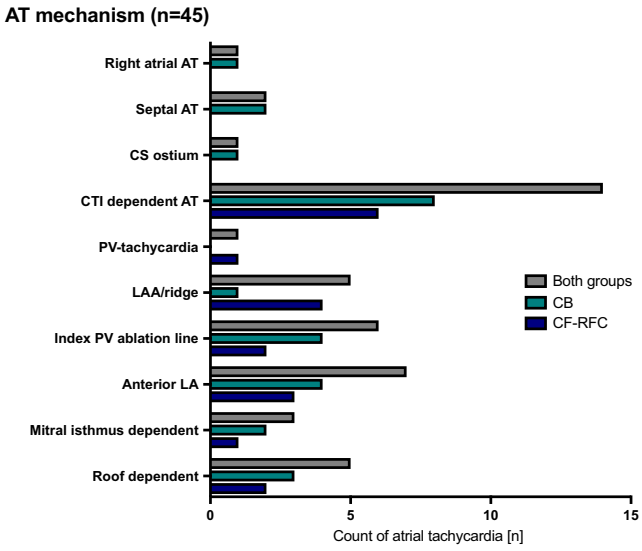

FIGURE 6 Critical sites of atrial tachycardias. AT, atrial tachycardia; CB, cryoballoon; CF-RFC, contact–force-guided radiofrequency current; CTI, cavotricuspid isthmus; CS, coronary sinus; LAA, left atrial appendage; PV, pulmonary vein; pt, patient

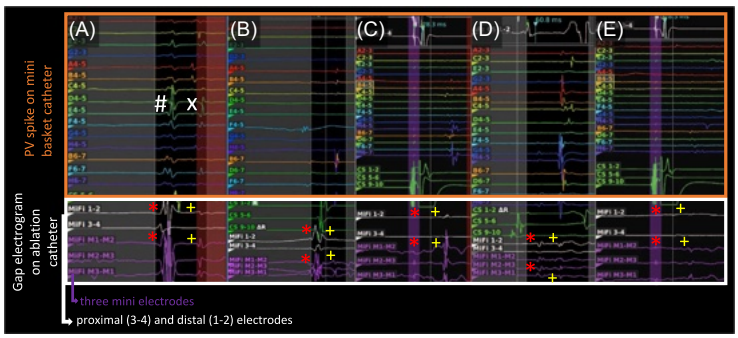

FIGURE 7 Common electrograms (gap signals) with the use of mini-electrodes during pulmonary vein reisolation. In all panels, variants of the mini-basket catheter inside the pulmonary veins are shown. The mini-basket catheter displays a far-field atrial electrogram (#) as well as the PV spike (gap signal [X]). After mapping, the ablation catheter was placed on the conduction gap and local electrograms of these gaps on the single-tip catheter electrodes are shown in all panels (*Far-field atrial signal on ablation catheter, +gap signal on ablation catheter). These were all sites of successful ablation. A, The gap signal is sharp and clear on the mini-electrodes (+) and vague on the distal/proximal electrodes (+). B, The gap signal is only visible on the mini-electrodes but not on the proximal and distal electrodes (+). C, There is no far-field (*); the gap signal is small and blurred on the distal/proximal electrodes but large and sharp on the mini-electrodes. D, The gap signal is of low voltage in all electrodes. E, Distal/proximal electrodes show no electrograms at all, but the gap signal is found as a low-voltage signal on the mini-electrodes

two mitral isthmus gauche (MIG)-dependent macroreentries in the CB group (Figure 6).

3.5 | Local impedance-guided ablation with the use of mini-electrodes

Monitoring of local impedance (LI) during repeat RFC ablation was successful in all patients. Real-time PVI with proof of entrance block using the mini-basket-catheter was observed in 63.6% (68/107) of all conduction gaps. In 39 cases (36.4%), no real-time PVI was present. In these cases, the mini-basket catheter was either positioned distally/closed within the PV or positioned in another PV to avoid catheter interference during ablation.

For twelve conduction gaps (12/107, 11.2%), the electrogram for the gap was only seen on the mini-electrodes of the ablation catheter and was not visible on the distal and proximal electrodes of the ablation catheter. Figure 7 shows examples of common electrograms (gap signals) during Re-PVI with the use of mini-electrodes.

Baseline impedances at the ablation site of the conduction gaps along the index ablation line, regarding GI (CF-RFC 117.4 ± 9.1 vs CB 116.8 ± 8.0 Ω; $P = .734$) and LI (CF-RFC 100.7 ± 14.6 vs CB 100.5 ± 12.36 Ω; $P = .942$), did not differ between the two groups. Also, drop of GI (CF-RFC: median 6 [3-11] vs CB: median 6 [4-8] Ω; $P = .395$) and drop of LI (CF-RFC: median 9.9 [8-18] vs CB: median 12 [7-18] Ω; $P = .981$) during ablation of the conduction gaps did not differ. The time until PVI, when closing the gaps, was equal in both groups (CF-RFC: median 9 [IQR 5-24] seconds vs CB: median 9 [5-12] seconds; $P = .292$). Termination of ATs was achieved at an LI drop of 6.7 ± 4.3 Ω in CF-RFC patients and at an LI drop of 12.8 ± 9.4 Ω in CB patients ($P = .087$).

4 | DISCUSSION

The major findings of this study are as follows:

1. UHDx mapping is sensitive in detecting and characterizing conduction gaps along the ablation lines after index PVI with CB or CF-RFC.
2. Pulmonary vein reconnection was present in a large number of patients, and left-sided PVs were more frequently reconnected after index CF-RFC PVI than after index CB PVI.
3. The use of mini-electrodes on the ablation catheter enables higher resolution of local electrograms and facilitates an effective and precise ablation of the conduction gaps.
4. Atrial tachycardias after stand-alone PVI occur with a broad spectrum of entities and show most often a macroreentry mechanism. ATs directly associated with the index ablation line for PV isolation are found frequently but there is no difference between CF-RCF and CB PVI.
5. Fractionated signals along the antral index ablation line are a common finding after stand-alone PVI and can maintain certain forms of atrial tachycardias.

4.1 | Pulmonary vein reconnection

New ablation technologies have been developed to increase lesion durability and expectantly procedural outcomes. RFC and CB are both routine techniques to perform an index PVI in clinical practice.[1] However, although utilizing the newest technologies such as contact–force-guided RFC ablation and the use of uniform cooling

of the second-generation CB, AF and/or AT may recur.[8] AF recurrence is frequently associated with PV reconnection, as shown previously and in the present study.[3,4,14-16] The PV reconnection rate in this study was higher in the CF-RFC group than in the CB group, confirming prior findings.[3] The localization of conduction gaps varies in the current literature, ranging from higher reconnection rates of the right-sided PVs after RFC as compared to CB,[3,4] to the LSPV being less frequently reconnected after CB than after RFC ablation.[3] In contrast, in this study, left-sided PVs were more frequently reconnected after index CF-RFC PVI than after index CB PVI. Our findings, however, are in line with a multicenter study by Aryana et al.[2] This discrepancy may be explained by different ablation strategies and the use of different catheters (first- vs second-generation CB; non-CF and CF catheters; different mapping systems) throughout the studies.

During reablation, precise detection and closure of the remaining gaps along the index ablation lines is crucial to establish continuous linear lesions around the PV ostia and to optimize the quality of AF ablation. UHDx mapping delivers an abundance of local electrograms with very high local resolution and enables more precise detection of these conduction gaps than the conventional approach using circumferential mapping catheters,[7,17] explaining the reconnection rate in our study. All patients in this study had arrhythmia recurrence, most likely caused by conduction gaps along the ablation line. Yet, five patients showed no PV reconnection.

Additionally, Ruiz-Granell et al[4] reported that gaps after RFC ablation are better detected with activation maps, and gaps after CB PVI with voltage maps, when using UHDx mapping. Taking this into account, it is well known that wavefront direction and cycle length affect left atrial electrogram amplitude.[18] However, our study does not provide any information on the electrogram's amplitudes along the conduction gaps in different underlying rhythms, such as sinus rhythm, AF or constant atrial pacing.

Local impedance may indicate the local voltage and scarring.[11] Interestingly, in our study, the localization of the conduction gaps after index CF-RFC or CB PVI showed no difference in baseline local impedance values. Therefore, no difference in local scar quality (regarding the conduction gaps) appears to be present between the two groups in this study. Another interesting aspect is the question whether RF or CB leads to more antral lesions after index PVI and, therefore, larger scars in the left atrium: Ruiz-Granell et al[4] found no statistically significant differences in the distance between ablation lesions in the posterior wall between the CB vs RF.

Additionally, we found that mini-electrodes on the ablation catheter could further augment identification of the conduction gaps due to a higher resolution of electrograms, which cannot be found on the conventional proximal and distal tip electrodes (Figure 7). This could lead to a better determination of the underlying ablation target and may, therefore, enable a more precise ablation and effective lesion creation, while avoiding unnecessary ablation.

4.2 | Atrial tachycardia after stand-alone PVI

The occurrence of atrial tachycardias after stand-alone PVI without substrate modification is a known but less frequent finding during reablation, with incidences between 2.8% and 11.3%.[5,6,19-21] Several small studies comparing ATs after stand-alone RFC or CB PVI have been conducted, and the results are very heterogeneous.[5,6,19-23] Interestingly, the findings are divergent, varying from studies that describe only PV-dependent, focal AT[22,23] to a study from Lyan et al[5] that reports only left atrial macroreentries after CB PVI without any PV association in the AT mechanism. The authors report mainly mitral isthmus gauche (MIG) and roof-dependent macroreentries.[5] In the present study, macroreentries were the most common form of AT mechanism as well.[5] However, in our study, we found an association with the prior (index) ablation in 27% of cases. For the first time, we report macroreentries with a critical isthmus in the index ablation line after stand-alone CF-RFC or CB PVI. Furthermore, classic macroreentries associated with the anterior wall, MIG, and roof were found in our study, as well as other entities.

We report for the first time UHDx mapping of these complex redo procedures, including ATs, after index PVI with CF-RFC or the CB. Due to its higher resolution and an improved algorithm of activation mapping, this may provide more detailed insights into different AT mechanisms. Additionally, we analyzed induced and consecutive ATs during redo procedures and found patients with more than one AT. All these findings may also explain the broad spectrum of AT entities in this small study cohort, ranging from PV to non-PV-dependent ATs, macroreentries, and microreentries as well as left- and right-sided ATs. Non-PV-dependent ATs may be due to substrate modification during the reprocedure, due to atrial scarring and progressive disease[24] or due to collateral damage during the index ablation, such as a much greater antral ablation than intended. PV-dependent ATs could be prevented by a better index PVI with establishment of continuous and transmural lesions. Therefore, it is interesting to see whether the incidence of ATs that are either PV-dependent or originate from the antral index ablation line can be prevented by optimizing the index procedure. To improve on these shortcomings, additional tools such as the ablation index for RFC ablation (which was only partially included in this study) or the release of the fourth-generation CB are now implemented in clinical practice.[25,26] It has already been reported that a minimum ablation index is associated with PV reconnection.[27] It remains to be seen whether the incidence and mechanisms of ablation-associated ATs will change with these newer tools. So far, there are no data regarding this issue.

4.3 | Fractionated signals along the antral index ablation line

To our knowledge, this is the first approach to systematically describe fractionated signals along the antral index ablation line during UHDx mapping. In our study, these signals were a common finding after stand-alone PVI and were found tendentially more often after CB than CF-RFC PVI. The occurrence of such signals may imply a substrate for further pathologies, as they may constitute the substrate for

consecutive arrhythmias. In this study alone, these signals were directly linked to a significant number of ATs. In the past, it has been discussed whether CB ablation may lead to more homogenous lesion than RFC ablation.[28] Our findings, however, suggest that fractionated signals may be found more often after index CB PVI than after index CF-RFC PVI, thereby questioning that notion. Fractionated antral signals may be of low voltage and their detection may be facilitated with UHDx mapping.

4.4 | Limitations

The present study has some limitations. First, the design of our single-center study was explorative and, therefore, the sample size in the current study is small. We aimed to include patients with ATs after stand-alone PVI, which is a rare finding. Considering that, compared to the current literature,[4,5] our study provides a representative cohort and delivers new insight into this topic. Finally, the design was prospective but nonrandomized.

5 | CONCLUSION

UHDx mapping is sensitive in characterizing conduction gaps along the ablation lines after index PVI with CB or CF-RFC. The additional use of mini-electrodes during ablation enables higher resolution of local electrograms and can be helpful in the detection and closure of these gaps. Atrial tachycardias after stand-alone CF-RFC or CB PVI reveal a broad spectrum of mechanisms; they are most often sustained (in either group) by macroreentries. Fractionated signals along the antral index ablation lines are a common finding after stand-alone PVI and can maintain certain forms of atrial tachycardias.

ACKNOWLEDGMENTS

The authors thank Lydia Merbold (Boston Scientific Corp, Marlborough, MA), Dr Paula Muenkler, Dr Leon Dinshaw, and Dr Christiane Jungen (all from the University Heart Center Hamburg) for their clinical support as well as for advice on data acquisition and engaging discussions/comments that greatly improved this article. This work is supported by the DZHK (German Centre for Cardiovascular Research) (FKZ 81Z4710141 and 81X2710149).

ORCID

Melanie A. Gunawardene http://orcid.org/0000-0001-7561-7185
Christian Eickholt http://orcid.org/0000-0002-5458-9688
Christian Meyer http://orcid.org/0000-0003-0217-3960
Benjamin Schaeffer http://orcid.org/0000-0002-8044-8408

REFERENCES

1. Kuck K-H, Brugada J, Fürnkranz A, et al. Cryoballoon or radiofrequency ablation for paroxysmal atrial fibrillation. *N Engl J Med*. 2016;9(374(23)):2235-2245.
2. Aryana A, Singh SM, Mugnai G, et al. Pulmonary vein reconnection following catheter ablation of atrial fibrillation using the second-generation cryoballoon versus open-irrigated radiofrequency: results of a multicenter analysis. *J Interv Card Electrophysiol*. 2016;47(47):341-348.
3. Ciconte G, Velagić V, Mugnai G, et al. Electrophysiological findings following pulmonary vein isolation using radiofrequency catheter guided by contact-force and second-generation cryoballoon: lessons from repeat ablation procedures. *Europace*. 2015;18(1):71-77.
4. Ruiz-Granell R, Ballesteros G, Andreu D, et al. Differences in scar lesion formation between radiofrequency and cryoballoon in atrial fibrillation ablation: a comparison study using ultra-high-density mapping. *Europace*. 2019;21(2):250-258.
5. Lyan E, Yalin K, Abdin A, et al. Mechanism, underlying substrate and predictors of atrial tachycardia following atrial fibrillation ablation using the second-generation cryoballoon. *J Cardiol*. 2019;73(6):497-506.
6. Hermida A, Kubala M, Traulle S, Buiciuc O, Quenum S, Hermida J-S. Prevalence and predictive factors of left atrial tachycardia occurring after second-generation cryoballoon ablation of atrial fibrillation. *J Cardiovasc Electrophysiol*. 2018;29:46-54.
7. García-Bolao I, Ballesteros G, Ramos P, et al. Identification of pulmonary vein reconnection gaps with high-density mapping in redo atrial fibrillation ablation procedures. *EP Eur*. 2017;0:1-8.
8. Gunawardene MA, Hoffmann BA, Schaeffer B, et al. Influence of energy source on early atrial fibrillation recurrences: a comparison of cryoballoon vs. radiofrequency current energy ablation with the endpoint of unexcitability in pulmonary vein isolation. *Europace*. 2018;20(1):43-49.
9. Makimoto H, Heeger CH, Lin T, et al. Comparison of contact force-guided procedure with non-contact force-guided procedure during left atrial mapping and pulmonary vein isolation: impact of contact force on recurrence of atrial fibrillation. *Clin Res Cardiol*. 2015;104(10):861-870.
10. Franceschi F, Dubuc M, Guerra PG, et al. Diaphragmatic electromyography during cryoballoon ablation: A novel concept in the prevention of phrenic nerve palsy. *Heart Rhythm*. 2011;8(6):885-891.
11. Gunawardene M, Münkler P, Eickholt C, et al. A novel assessment of local impedance during catheter ablation: Initial experience in humans comparing local and generator measurements. *Europace*. 2019;21:I34-I42.
12. Schaeffer B, Hoffmann BA, Meyer C, et al. Characterization, mapping, and ablation of complex atrial tachycardia: initial experience with a novel method of ultra high-density 3D mapping. *J Cardiovasc Electrophysiol*. 2016;27(10):1139-1150.
13. Vogler J, Willems S, Sultan A, et al. Pulmonary vein isolation versus defragmentation. *J Am Coll Cardiol*. 2015;66(24):2743-2752.
14. Galand V, Pavin D, Behar N, et al. Localization of gaps during redo ablations of paroxysmal atrial fibrillation: Preferential patterns depending on the choice of cryoballoon ablation or radiofrequency ablation for the initial procedure. *Arch Cardiovasc Dis*. 2016;109(11):591-598.
15. Schmidt B, Chun KRJ, Metzner A, Fuernkranz A, Ouyang F, Kuck K-H. Pulmonary vein isolation with high-intensity focused ultrasound: results from the HIFU 12F study. *Europace*. 2009 Oct;11(10):1281-1288.
16. Ouyang F, Antz M, Ernst S, et al. Recovered pulmonary vein conduction as a dominant factor for recurrent atrial tachyarrhythmias after complete circular isolation of the pulmonary veins: lessons from double lasso technique. *Circulation*. 2005;111:127-135.
17. Meissner A, Maagh P, Christoph A, Oernek A, Plehn G. Pulmonary vein potential mapping in atrial fibrillation with high density and standard spiral (lasso) catheters: a comparative study. *J Arrhythmia*. 2017;33(3):192-200.
18. Iso K, Watanabe I, Kogawa R, et al. Wavefront direction and cycle length affect left atrial electrogram amplitude. *J Arrhythmia*. 2017;33(4):269-274.
19. Akerström F, Bastani H, Insulander P, Schwieler J, Arias M, Jensen-Urstad M. Comparison of regular atrial tachycardia incidence after

circumferential radiofrequency versus cryoballoon pulmonary vein isolation in real-life practice. *J Cardiovasc Electrophysiol*. 2014;25(9):948-952.
20. Juliá J, Chierchia G-B, de Asmundis C, et al. Regular atrial tachycardias following pulmonary vein isolation for paroxysmal atrial fibrillation: a retrospective comparison between the cryoballoon and conventional focal tip radiofrequency techniques. *J Interv Card Electrophysiol*. 2015;42(2):161-169.
21. Wasmer K, Mönnig G, Bittner A, et al. Incidence, characteristics, and outcome of left atrial tachycardias after circumferential antral ablation of atrial fibrillation. *Heart Rhythm*. 2012;9(10):1660-1666.
22. Mikhaylov EN, Bhagwandien R, Janse PA, Theuns DA, Szili-torok T. Regular atrial tachycardias developing after cryoballoon pulmonary vein isolation: incidence, characteristics, and predictors. *Europace*. 2013;15:1710-1717.
23. Gerstenfeld EP, Callans DJ, Dixit S, et al. Mechanisms of organized left atrial tachycardias occurring after pulmonary vein isolation. *Circulation*. 2004;110:1351-1357.
24. Schaeffer B, Akbulak RÖ, Jularic M, et al. High-density mapping and ablation of primary nonfocal left atrial tachycardia. *JACC Clin Electrophysiol*. 2019;5(4):417-426.
25. Hussein A, Das M, Chaturvedi V, et al. Prospective use of ablation index targets improves clinical outcomes following ablation for atrial fibrillation. *J Cardiovasc Electrophysiol*. 2017;28(9):1037-1047.
26. Straube F, Dorwarth U, Pongratz J, et al. The fourth cryoballoon generation with a shorter tip to facilitate real-time pulmonary vein potential recording: feasibility and safety results. *J Cardiovasc Electrophysiol*. 2019;30(6):918-925.
27. Das M, Loveday JJ, Wynn GJ, et al. Ablation index, a novel marker of ablation lesion quality: prediction of pulmonary vein reconnection at repeat electrophysiology study and regional differences in target values. *Europace*. 2017;19(5):775-783.
28. Avitall B, Urboniene D, Rozmus G, Lafontaine D, Helms R, Urbonas A. New cryotechnology for electrical isolation of the pulmonary veins. *J Cardiovasc Electrophysiol*. 2003;14(3):281-286.

How to cite this article: Gunawardene MA, Eickholt C, Akbulak RÖ, et al. Ultra–high-density mapping of conduction gaps and atrial tachycardias: Distinctive patterns following pulmonary vein isolation with cryoballoon or contact–force-guided radiofrequency current. *J Cardiovasc Electrophysiol*. 2020;31:1051–1061. https://doi.org/10.1111/jce.14413

Received: 25 August 2021 | Revised: 14 October 2021 | Accepted: 8 November 2021

DOI: 10.1111/jce.15349

ORIGINAL ARTICLES

WILEY

Pulsed-field ablation combined with ultrahigh-density mapping in patients undergoing catheter ablation for atrial fibrillation: Practical and electrophysiological considerations

Melanie A. Gunawardene MD[1,2] | Benjamin N. Schaeffer MD[1,2] | Mario Jularic MD[1,2] | Christian Eickholt MD[1,2] | Tilman Maurer MD[1,2] | Ruken Ö. Akbulak MD[1,2] | Max Flindt MD[1,2] | Omar Anwar MD[1,2] | Ulrich F. Pape MD[2,3] | Sebastian Maasberg MD[2,3] | Nele Gessler MD[1,2,4,5] | Jens Hartmann MD[1,2] | Stephan Willems MD[1,2,4]

[1]Department of Cardiology and Intensive Care Medicine, Asklepios Hospital St. Georg, Hamburg, Germany

[2]Faculty of Medicine, Semmelweis University, Budapest, Hungary

[3]Department of Internal Medicine, Asklepios Hospital St. Georg, Hamburg, Germany

[4]DZHK (German Center for Cardiovascular Research), Partner Site Hamburg/Kiel/Lübeck, Berlin, Germany

[5]Asklepios Proresearch, Hamburg, Germany

Correspondence
Melanie A. Gunawardene, Department of Cardiology, Asklepios Klinik St. Georg, Lohmühlenstr. 5, 20099 Hamburg, Germany.
Email: melanie.gunawardene@gmail.com

Disclosures: None.

Abstract

Background: Pulsed-field ablation (PFA) yields a novel ablation technology for atrial fibrillation (AF). PFA lesions promise to be highly durable, however clinical data on lesion characteristics are still limited.

Objective: This study sought to investigate PFA lesion creation with ultrahigh-density (UHDx) mapping.

Methods: Consecutive AF patients underwent PFA-based pulmonary vein isolation (PVI) using a multispline catheter (Farwave, Farapulse Inc.). Additional ablation, including left atrial posterior wall isolation (LAPWI) and mitral isthmus ablation (MI) were performed in a subset of persistent AF patients. The extent of PFA-lesions and decrease of LA-voltage were assessed with pre- and post PFA UHDx-mapping (Orion™ catheter and Rhythmia™ 3D-mapping system, Boston Scientific).

Results: In 20 patients, acute PVI was achieved in 80/80 PVs, LAPW isolation in 9/9 patients, MI ablation in 2/2 (procedure time: 123 ± 21.6 min, fluoroscopy time: 19.2 ± 5.5 min). UHDx-mapping subsequent to PVI revealed early PV-reconnection in five case (5/80, 6.25%). Gaps were located at the anterior-superior PV ostia and were successfully targeted with additional PFA. Repeat UHDx mapping after PFA revealed a significant decrease of voltage along the PV ostia (1.67 ± 1.36 mV vs. 0.053 ± 0.038 mV, $p < .0001$) with almost no complex electrogram-fractionation at the lesion border zones. PFA-catheter visualization within the mapping system was feasible in 17/19 (84.9%) patients and adequate in 92.9% of ablation sites.

Conclusion: For the first time illustrated by UHDx mapping, PFA creates wide antral circumferential lesions and homogenous LAPW isolation with depression of tissue voltage to a minimum. Although with a low incidence, early PV reconnection can still occur also in the setting of PFA.

KEYWORDS

atrial fibrillation, left posterior wall isolation, pulmonary vein isolation, pulsed-field ablation, ultrahigh-density mapping

1 | INTRODUCTION

Recently, pulsed-field ablation (PFA) has been introduced as a novel non-thermal energy source for catheter ablation of atrial fibrillation (AF).[1] First experiences show high acute and chronic pulmonary vein isolation (PVI) rates with a beneficial safety profile due to the myocardial sensitivity of this novel ablation approach.[2] Collateral damage to adjacent tissue such as the esophagus has not been documented so far.[2] Yet, clinical experience is limited and especially data regarding lesion characterization is sparse but highly relevant.[1,2] One study using high-density mapping demonstrated that the level of antral pulmonary vein (PV) lesion does not regress over time.[3] Visualization of the current multielectrode PFA catheter within a three-dimensional (3D) mapping system potentially facilitates catheter handling and enhances ablation while decreasing the need for fluoroscopy. In this study, we assessed acute PFA lesion formation (by the Farwave catheter, Farapulse Inc.) and level of PV isolation using ultrahigh-density mapping (UHDx; with the multi-electrode Orion™ mapping catheter and the Rhythmia™ 3D mapping system, Boston Scientific) combined with PFA catheter visualization in symptomatic AF patients undergoing PVI by PFA, including persistent AF patients receiving additional PFA lesions. This is the first description of a series of patients performed outside of the initial first-in-human work that has been published.[4]

2 | METHODS

2.1 | Study design

This study is a single-center, observational, prospective study. Consecutive patients eligible for catheter ablation of atrial fibrillation, including paroxysmal and persistent atrial fibrillation (AF), were enrolled in May 2021. The study was investigator-initiated without external funding; the authors are responsible for design, execution, and conduct of the study. The statistical analyses and interpretation of the data were approved by all authors, who attest to the accuracy of the data and of all analyses. Written informed consent was obtained from all patients. The study was conducted in accordance with the provisions of the Declaration of Helsinki and its amendments. The institutional review board and ethics committee approved the study.

2.2 | Catheter ablation

All patients underwent PFA-guided pulmonary vein isolation (PVI). In patients with persistent AF, additional ablation lesions were performed at the discretion of the treating electrophysiologist. This included left atrial posterior wall (LAPW) isolation and mitral isthmus (MI) ablation. Three-dimensional UHDx mapping of the left atrium (LA) was performed before and directly after PFA to assess the extent and formation of the ablation lesions and to correlate the visualized ablation catheter to the extent of the resulting lesions. In cases with LAPW ablation, esophagogastroduodenoscopy was performed post procedurally.

Before ablation, intracardiac thrombus formation was ruled out by transesophageal echocardiography. Oral anticoagulation was minimally interrupted on the morning of the procedure and restarted 6 h after sheath removal.

Procedures were performed under deep sedation using a continuous infusion of propofol (1 mg/ml) and boluses of midazolam (1 mg/ml) and sufentanyl (0.1 mg/ml). Intravenous heparin (25 000 IU/5 ml) was applied to reach an activated clotting time of at least 300 s. To minimize vagal responses, 1 mg of intravenous atropine (0.5 mg/ml) was administered to all patients before ablation.

2.3 | Pulsed-field ablation system

The PFA system has been described in detail before.[1] It consists of three components: a custom generator that delivers a high-voltage pulsed-field waveform over multiple channels, a multispline PFA catheter (Farwave, Farapulse Inc.), and a 13-French (F) steerable sheath (Faradrive, Farapulse Inc.). The PFA catheter is a 12-F over-the-wire device with five splines that each contain four electrodes, available in two sizes representative of its maximal diameter: 31 and 35 mm. The catheter can be configured into different shapes (a *basket* or a *flower configuration)* for energy delivery. The therapeutic waveform was structured as a hierarchical set of biphasic, microsecond-scale pulses released in a bipolar fashion between the electrodes. The generator output ranged from 1.8 to 2.0 kV) per application,[3] with 1.9 kV selected for PVI in our study protocol.

2.4 | Workflow of PFA and ultrahigh-density mapping

After femoral venous access, a decapolar diagnostic catheter (Inquiry™, 2-5-2 mm spacing; St. Jude Medical) was placed into a superior lateral, ventricular branch of the coronary sinus to secure ventricular pacing in case of a vagal response during PFA and as a reference catheter for the mapping system. After transseptal puncture and left atrial (LA) angiography, the 64-pole mini-basket mapping catheter (Orion™, Boston Scientific) was used in combination with an UHDx electroanatomical mapping system (Rhythmia™, Boston Scientific) to reconstruct LA and PV geometry and to create voltage maps via a long sheath. After LA-mapping, the catheter was placed in the inferior vena cava to obtain the field tracking for PFA-catheter visualization. The left atrial sheath was exchanged by a 13-French deflectable sheath (Faradrive, Farapulse Inc) and the PFA-catheter (Farawave, Farapulse Inc) was introduced to the LA. PVI was performed in all patients using at least 8 applications at an output of 1.9 kV (4 *basket*, 4 *flower* configuration). The catheter was slightly rotated between a pair of applications to ensure circumferential PV ostial and antral coverage. If required – for example, for anatomical

constraints to catheter positioning – all eight applications were performed in only one configuration (either *basket* or *flower*). After eight applications, all PV ostia were checked for isolation using an appropriately-sized *basket* configuration of the catheter. If applicable, LAPW isolation and MI ablation using the *flower* pose – with the guidewire retracted – followed in persistent AF patients. During the procedure, the PFA catheter was visualized within the 3D map. After PVI and possible additional lesions, the PFA catheter was extracted and the 64-pole mini-basket mapping catheter was introduced again for repeat mapping. Detailed UHDx mapping of the ablation line was performed to confirm PV and LAPW/MI isolation, as described before.[5] There was no specified waiting time before remapping. If conduction gaps/PV reconnections were found, the mapping catheter was again replaced by the PFA catheter, additional ablation of the PV was performed with up to 2.0 kV. Another final UHDx-remap followed re-isolation.

2.5 | PFA catheter visualization

To improve catheter handling and positioning in alignment to the PV ostium, the PFA catheter was visualized in the UHDx electroanatomical mapping system. Five equatorial electrodes (A3–E3) were connected to the mapping system amplifier. An impedance tracked six-electrode catheter with 17 mm interelectrode center to center spacing was defined in the mapping system. To achieve a closed circular shape for visualization, both the first and last electrodes were assigned within the mapping system software to the physical pin associated with electrode A3. The catheter shape was defined as flexible and tracking limits were adapted to allow catheter size to vary from undeployed via *basket* shape up to *flower* pose. Initial procedures indicated long-term tracking quality would improve when the 64-pole mini-basket mapping catheter remained in the inferior vena cava or right atrium during PFA catheter manipulation in the LA, and the protocol was adapted accordingly. To avoid possible damage to or interference with the recording system amplifier, both body surface ECG and intracardiac EGM channels from the CS catheter were routed through the Recording System Module (RSM, Farapulse). For PFA applications, the mapping system's electromagnetic (EM) sensor was temporarily disconnected.

After the procedure, the location of the visualized catheter in the three-dimensional UHDx map was retrospectively correlated to the level of PV isolation, posterior wall ablation, and mitral isthmus line.

2.6 | Analysis of ultrahigh-density maps

Mapping was preferred during sinus rhythm with prior cardioversion of AF if required (Table 2: rhythm during mapping was sinus rhythm in 18 (90%) and AF in 2 (10%) patients). In the pre-ablation UHDx-map, baseline voltage was assessed (scar cutoff: <0.3 mV). In the Postablation map, activation- and voltage maps were performed to confirm PV isolation, as described before.[5]

Pre and postablation measurements: To analyze degree, homogeneity, and continuity of PFA ablation lesion, voltage at six representative and evenly distributed locations around each pair of PV were assessed (Figure 1E). Additionally, peri- and postprocedurally, the included signal processing software (Lumipoint™, Boston Scientific) was used to analyze fractionation and complex components of activation (peak cutoff: 5–7) along the ablation sites and border zone of ablation lesions.[6]

In patients who received only PVI: The following spatial measurements were made consistent with a previously-published method[3]: (1) the surface areas of the posterior left- and right-sided PV antral isolation, (2) the LAPW surface area with voltage pre- and post-PFA, and (3) the distance between the ipsilateral, antral levels of isolation at superior, middle and inferior latitudes of the LAPW,[3] (Figures 1A,B and 1D). The surface area of each PV ostium and the area of the circular antral ablation lesion was measured around each ipsilateral PV pair (Figure 1C).

In patients receiving additional ablation lesions: LAPW and/or mitral isthmus (MI) isolation was assessed and confirmed by activation- and voltage map as well as by Lumipoint™ (Boston Scientific). The total ablated area including antral PV lesions, pre- and post-PFA LAPW surface area and possible further lesions were measured.

2.7 | Statistics

Continuous data are expressed as mean ± standard deviation or as median and interquartile range. For group comparisons, Student's *t*-test (paired or unpaired) or the Mann–Whitney *U* test for unpaired variables were utilized. Categorical data are described as absolute and relative frequencies; they were compared using the χ^2 or Fisher's exact test. Statistical significance was assumed at a p-value < .05. Statistical analyses utilized the GraphPad Prism 7.0 software (GraphPad Software Inc.).

3 | RESULTS

3.1 | Baseline and procedural characteristics

We enrolled twenty consecutive patients in this study cohort. Eleven patients of the cohort received PVI only. Additional ablation was performed in the other nine patients (Table 1). Baseline characteristics of the patients are shown in Table 1. In *PVI only* patients, 63.6% (7/11) of patients had paroxysmal AF. In patients receiving additional ablation, 100% (9/9) of patients suffered from persistent AF and four of nine had underlying tachycardiomyopathy.

Procedural parameters are shown in Table 2: total procedure time in all patients was 123 ± 21.6 min (including UHDx mapping and PFA ablation) with a mean fluoroscopy time of 19.2 ± 5.5 min.

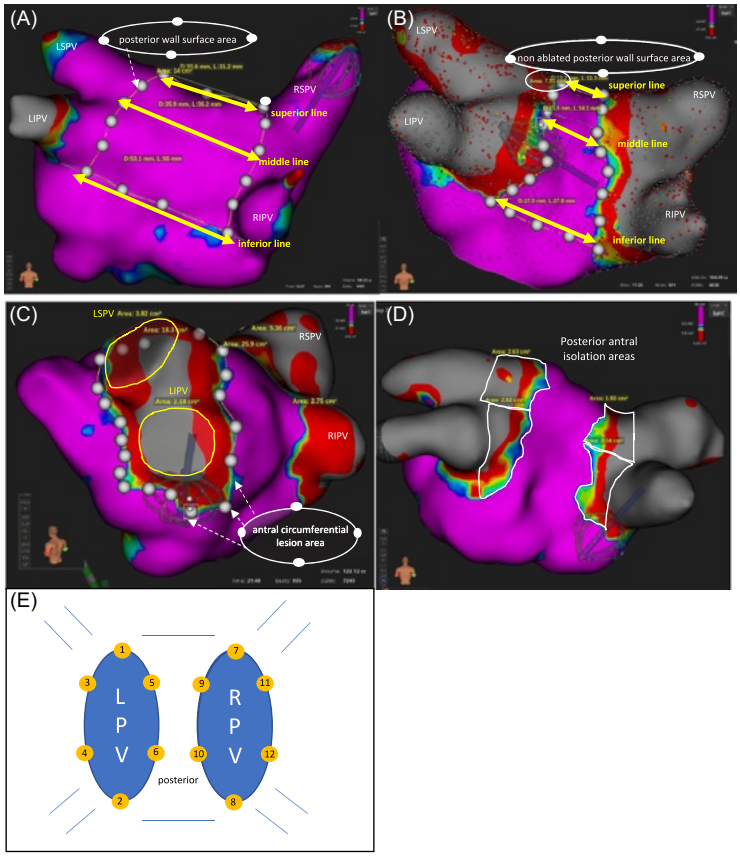

FIGURE 1 Methods for measurements of surface areas and distances in pre- and postablation ultrahigh-density maps in the study cohort. (A) Pre-ablation UHDx voltage map and measurement of LAPW surface area (indicated by the white dots) and pre-ablation superior, middle and inferior line. (B) Postablation UHDx voltage map and measurement of the non-ablated LAPW surface area (indicated by the white dots) and postablation superior, middle, and inferior line. (C) Measurement of the PV ostia sizes of the LSPV and LIPV and the area of the circumferential antral ablation along the ipsilateral lateral PV pair (indicated by the whit dots). (D) Measurements of the posterior surface areas of the left- and right-sided pulmonary vein antral isolation areas. (E) Voltage was measured at six sites per PV pair prior and postablation. LAPW, left atrial posterior wall; LIPV, left inferior pulmonary vein; LPV, left pulmonary veins; LSPV, left superior pulmonary vein; PV, pulmonary vein; UHDx, ultrahigh density; RIPV, right inferior pulmonary vein; RPV, right pulmonary veins; RSPV, right superior pulmonary vein

3.2 | Pulsed-field ablation

Left atrial PFA catheter time was 49.0 ± 13.7 min with longer LA-PFA times in patients receiving additional ablation with 58.3 ± 14.5 versus 41.5 ± 7.0 min in PVI only patients ($p = .0015$), Table 2. LA-PFA fluoroscopy time was 15.0 ± 3.8 min ($p = .9910$ among groups). A median of 32 (Q1:32–Q3:36) PFA applications in total (median of 8 per PV) were utilized to isolate all 80 PVs in 20 patients (including 2 left common PV ostia [LCPV], 2 right middle PVs). After the initial eight applications, four left superior PVs (including 1 LCPV) were not isolated (demonstrated with PFA catheter) and either isolated after ablation of the ipsilateral inferior PV ($n = 3$) or with additional 4 PFA applications ($n = 1$). In 10 PVs (5 RSPVs and 5 RIPVs) only one PFA catheter configuration (either *flower* [$n = 8$] or *basket* only [$n = 2$]) was applied due to limitation of catheter movement/placement.

After this initial ablation, all 80 PVs were checked with the smallest *basket* shape of the PFA-catheter to confirm isolation.

LAPW ablation was performed in nine patients with a median of 10 (Q1:8–Q3:12) PFA applications in *flower* configuration. All nine LAPW isolations (9/9, 100%) were successfully isolated. Two patients received additional mitral isthmus ablation with 8 and 12 PFA applications (*flower* configuration), respectively, Table 2 and Figure 2.

TABLE 1 Baseline patient characteristics

	All $n = 20$	PVI only patients $n = 11$	Additional ablation patients $n = 9$
Age (years)	70.3 ± 9.7	75.2 ± 6.2	64.4 ± 10.2
Male gender	12 (60.0)	6 (54.5)	6 (66.7)
Hypertension	16 (8.0)	9 (81.8)	7 (77.8)
BMI (kg/m^2)	26.0 ± 4.8	25.9 ± 5.3	26.1 ± 4.5
CHA_2DS_2-VASc score	2.5 [2–4]	3 [2–3.5]	2 [1–4]
Type of AF			
PAF	7 (35.0)	7 (77.8)	0 (0.0)
Persistent AF	13 (65.0)	4 (22.0)	9 (100.0)
Left atrial diameter (mm)	43.8 ± 4.9	45.2 ± 4.1	42.1 ± 5.8
Left ventricular function			
Normal (ejection fraction 50%–70%)	15 (75.0)	10 (90.9)	5 (55.6)
Mild dysfunction (40%–49%)	1 (5.0)	0 (0)	1 (11.1)
Moderate dysfunction (30%–39%)	2 (10.0)	1 (9.1)	1 (11.1)
Sever dysfunction (<30%)	2 (10.0)	0 (0)	2 (22.2)

Note: Values are mean ± standard deviation, median [first–third quartile] or *n* (%).

Abbreviations: AF, atrial fibrillation; BMI, body mass index; **CHA_2DS_2-VASc score** is a clinical estimation of the risk of stroke in patients with atrial fibrillation; scores range from 0 to 9, with higher scores indicating a greater risk of stroke = **C**ongestive heart failure, **H**ypertension, **A**ge > 75 years, **D**iabetes, previous **S**troke, transient ischemic attack, or thromboembolism, **V**ascular disease, **A**ge 65–75 years, and **S**ex **c**ategory; PAF, paroxysmal atrial fibrillation.

3.3 | Pulmonary vein reconnection

Postablation UHDx mapping revealed five early PV reconnections (5/80, 6.25% reconnection rate) ($n = 2$ LSPV, $n = 3$ RSPV, example shown in Figure 3). All gaps were located at the anterior-superior aspect of the PV ostium. A median of 4 (Q1:4–Q3:8) additional PFA applications with 2.0 kV were delivered to isolate reconnected PVs. At the end of the procedures, all PVs were isolated, confirmed by UHDx mapping.

3.4 | Ultrahigh-density mapping

Pre- and post UHDx mapping was performed in 19/20 patients (one patient did not receive postablation mapping due to a safety issue, see the section below). Findings of UHDx mapping are shown in Tables 2 and 3. Mapped LA volume (incl. PVs) was 148 ± 24.7 ml with 7261 ± 3517 acquired mapping points. Voltage along the PV ostia decreased significantly prior and post PFA ablation (1.67 ± 1.36 mV vs. 0.053 ± 0.038 mV, $p < .0001$). In cases with PVI only, antral ablations lesions around the PVs led to a significant decrease of the non-ablated LAPW area (16.9 ± 3.6 cm^2 vs. 9.4 ± 2.6 cm^2, $p < .001$) with a significant decrease of all measured distances between the ipsilateral level of isolation (superior, middle, and inferior; Table 3 and Figure 1). The total circumferential antral lesion areas of the lateral and right sides were 20.5 ± 3.8 and 25.5 ± 5.7 cm^2, respectively. Size of the PV ostia and posterior pulmonary vein antral isolation areas are shown in Table 3.

LAPW isolation was successful in all mapped patients (Figure 2), covering the total LAPW area (18.8 ± 1.7 cm^2 pre-ablation vs. 19.2 ± 1.7 cm^2 postablation, $p = .6174$; Table 3). The mitral isthmus was shown to be successfully blocked in both patients (Figure 2).

Lumipoint™ analysis showed no complex fractionated electrograms along the PV ostia in 16/19 (84.2%) and none on the posterior wall in 5/8 (62.5%) patients. Along 3/19 (15.8%) patients' PV ostia and in 3/8 (37.5%) LAPW isolations, exceptionally small areas of fractionation with a mean of 0.5 ± 0.22 cm^2 were detected.

3.5 | PFA catheter visualization

PFA catheter visualization was feasible in 17/19 (89.5%) patients. After initial visualization in two patients failed, the workflow was adjusted (see *Methods*) and visualization was thereafter present in all patients. Location of catheter visualization was matched well with the level of isolation in all left PVs (17/17 patients, 100%) and in 15/17 (88.2%) patients for the right PVs (Figure 4). For LAPW ablation, visualization was adequate in 7/8 (87.5%) patients (in total 39/42 ablations sites, 92.3%) (Figure 4). There was only one map shift (1/19, 5.3%).

TABLE 2 Procedural parameters

Procedural parameters	All *n* = 20	PVI only patients *n* = 11	Additional ablation patients *n* = 9
Procedural data			
• Sinus rhythm	9 (45.0)	7 (63.6)	2 (22.2)
• Atrial fibrillation	11 (55.0)	4 (36.4)	7 (77.8)
Total procedure time (min)	123 ± 21.6	121.1 ± 20.6	125.4 ± 23.8
Total fluoroscopy time (min)	19.2 ± 5.5	20.3 ± 5.5	17.9 ± 5.5
Pulsed-field ablation			
Time of PFA catheter in the left atrium (min)	49.1 ± 13.8	41.5 ± 7.0	58.3 ± 14.5
Fluoroscopy time during PFA (min)	15.0 ± 2.9	15.0 ± 2.9	15.0 ± 4.8
Total PFA applications per patient for PVI	32 [32–36]	32 [32–33]	36 [32–36]
LSPV	8 [8–8]	8 [8–8]	8 [8–8]
LIPV	8 [8–8]	8 [8–8]	8 [8–8]
RSPV	8 [8–10.5]	8 [8–9]	8 [8–12]
RIPV	8 [8–8]	8 [8–8]	8 [8–8]
Left atrial posterior wall	10 [8–12]	N/A	10 [8–12]
Mitral isthmus line	10 [9–11]	N/A	10 [9–11]
PFA catheter size			
31 mm	15	10	5
35 mm	5	1	4
Ultrahigh-density mapping			
Rhythm during mapping			
Sinus rhythm	18 (90.0)	10 (90.9)	8 (88.9)
Atrial fibrillation	2[a] (10.0)	1 (9.1)	1 (11.1)
UHDx- LA mapping points	7261 ± 3517	7740 ± 3016	6677 ± 4162
Mapped LA volume (ml)	148 ± 24.7	134 ± 19.5	164 ± 20.4
LA mapping time (total), (min)	35.7 ± 10.2	36.5 ± 10.5	34.6 ± 10.3
Prior ablation, (min)	17.2 ± 3.0	17.9 ± 3.1	16.5 ± 2.9
Post ablation (including all remaps), (min)	19.3 ± 7.4	20.2 ± 6.2	18.1 ± 8.9
Patients with visualization of PFA catheter in mapping system	18 (90)	9 (91.8)	9 (100.00)
Map shift (number of patients)	1 (5.0)	1 (9.1)	0.0
All complications	1 (5.0)	0 (0.0)	1 (11.1)
• Pericardial tamponade	0 (0.0)	0 (0.0)	0 (0.0)
• Phrenic nerve palsy	0 (0.0)	0 (0.0)	0 (0.0)
• Access complications (groin)	0 (0.0)	0 (0.0)	0 (0.0)
• Esophageal lesion	0 (0.0)	N/A	0 (0.0)
• Coronary spasm	1 (5.0)	0 (0.0)	1 (11.1)

Note: Values are mean ± standard deviation, [*n*] or *n* (%), median [first–third quartile].

Abbreviations: LAPW, left atrial posterior wall; LIPV, left inferior pulmonary vein; LSPV, left superior pulmonary vein; RSPV, right superior pulmonary vein; RIPV, right inferior pulmonary vein; PFA indicates pulsed-field ablation, PVI, pulmonary vein isolation; UHDx, ultra high density.

[a]In both patients, cardioversion was not successful at the beginning of the procedure. Successful cardioversion to sinus rhythm was then performed in both patients at the end of the procedure, after ablation and remapping.

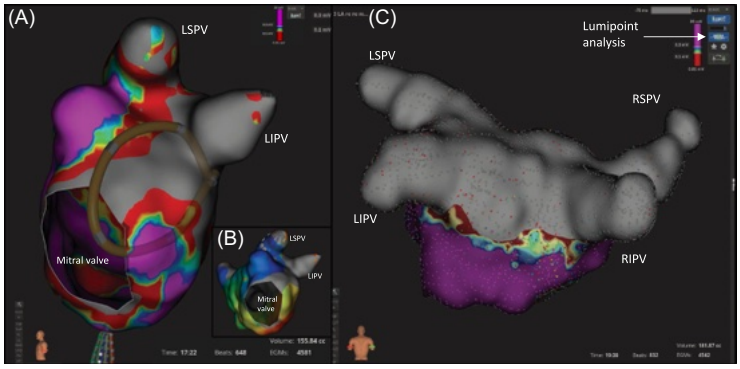

FIGURE 2 Mitral isthmus line and left atrial posterior wall ablation. (A) UHDx voltage map of blocked mitral isthmus line with PFA catheter visualized in *flower* pose for ablation (orange ring), (B) activation map of the blocked mitral isthmus line). (C) Example of lesion quality after LAPW ablation in UHDx mapping. No complex electrogram activation can be found along the ablation sites during the Lumipoint™ analysis. LAPW, left atrial posterior wall; LIPV, left inferior pulmonary vein; LSPV, left superior pulmonary vein; PFA, pulsed-field ablation; PV, pulmonary vein; UHDx, ultrahigh density; RIPV, right inferior pulmonary vein; RPV, right pulmonary veins; RSPV, right superior pulmonary vein

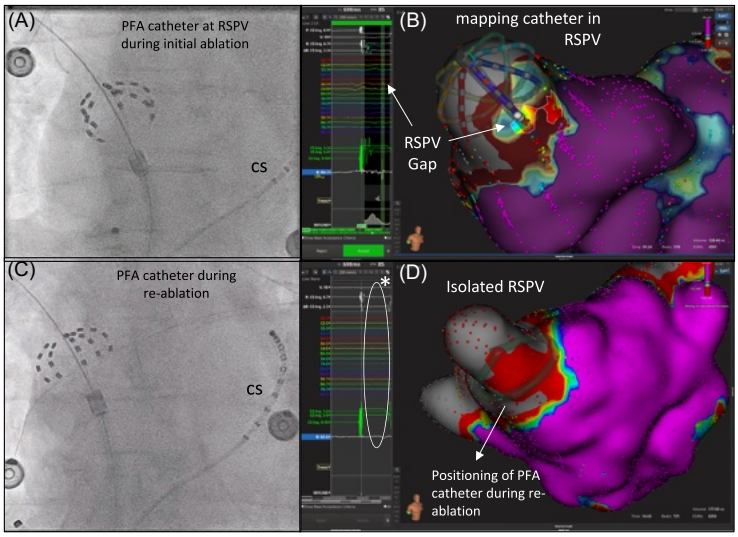

FIGURE 3 Pulmonary vein reconnection. (A) PFA catheter initially positioned at the RSPV with deployment of eight applications in total (starting with 4 *baskets* followed by 4 *flowers*). Notice the imperfectly aligned angle of the sheath towards the pulmonary vein ostium. (B) Repeat mapping using the 64-pole mini basket mapping catheter revealed a gap at the anterior-superior aspect of the RSPV (arrows highlight the recorded delayed PV signal and the corresponding location of the gap identified by Lumipoint™). (C) Re-ablation of the RSPV gap with clocking of the sheath to cover the anterior aspect of the PV, additionally leading to a better alignment of the sheath and the catheter along the PV ostium. (D) Successful PV isolation of the RSPV with the PFA catheter in *basket*-configuration (green ring) shown in the UHDx map. PFA, pulsed-field ablation; PV, pulmonary vein; RSPV, right superior pulmonary vein; UHDx, ultrahigh density

TABLE 3 Ultrahigh-density map measurements

Measurements	Preablation map *n* = 20	Postablation map *n* = 19	*p*-value
Voltage along PV ostia (all 12 sites, *n* = 468) (mV)	1.67 ± 1.36	0.053 ± 0.038	<.0001
Left atrial posterior wall surface area[a] (cm^2)			
Non ablated LAPW area: *PVI only* patients	16.9 ± 3.6	9.4 ± 2.6	<.0001
Ablated LAPW area: *additional ablation* patients	18.8 ± 1.7	19.2 ± 1.7	.6174
Superior line (mm)	41.2 ± 7.7	19.4 ± 10.9	.0001
Middle line (mm)[b]	42.5 ± 6.0	16.7 ± 6.5	<.0001
Inferior line (mm)[b]	47.6 ± 7.9	25.2 ± 7.7	<.0001
LPV ostia total (cm^2)		5.2 ± 1.1	
LSPV ostia (cm^2)		2.9 ± 0.9	
LIPV ostia (cm^2)		2.3 ± 0.8	
RPV ostia total (cm^2)		6.7 ± 1.5	
RPSV ostia (cm^2)		3.9 ± 1.1	
RIPV ostia (cm^2)		2.8 ± 0.8	
Lateral circumferential antral lesion area (cm2)[b]		20.5 ± 3.8	
Septal circumferential antral lesion area (cm2)[b]		25.5 ± 5.7	
Posterior pulmonary vein antral isolation areas[b]:			
LSPV (cm^2)		2.2 ± 0.9	
LIPV (cm^2)		2.8 ± 0.8	
RSPV (cm^2)		2.5 ± 1.1	
RIPV (cm^2)		2.3 ± 0.8	
Total ablation area (cm^2) (in additional ablation patients only)		59.3 ± 8.3	

Abbreviations: LAPW, left atrial posterior wall; LIPV, left inferior pulmonary vein; LSPV, left superior pulmonary vein; RSPV, right superior pulmonary vein; RIPV, right inferior pulmonary vein; PFA, pulsed-field ablation, PVI, pulmonary vein isolation; UHDx, ultra high density.

[a]The area of left atrial posterior wall (LAPW) was assessed prior to ablation in the UHDx map. After ablation in PVI only patients the remaining non-ablated area of the LAPW was measured and in patients with LAPW isolation the total ablated area of the LAPW was assessed.

[b]PVI only.

3.6 | Safety and complications

Phrenic nerve capture but no phrenic nerve palsy was found in all 20 patients during PFA ablation. There were no pericardial tamponades and no access complications. A vagal response resulting in 34 s of asystole was seen in one patient. This was the only patient who did not receive atropine before ablation. No further vagal responses were seen in atropine-treated patients. All nine patients with LAPW isolation received postprocedural esophagogastroduodenoscopy 1.4 ± 0.8 days after ablation, revealing no esophageal lesions.

In one patient receiving additional ablation at the mitral isthmus, ST elevations in the inferior (II, III, aVF) and lateral leads (V5–6) occurred on the patients' ECG, a few seconds after the last of eight PFA applications. Immediate coronary angiogram showed a coronary spasm of the circumflex artery, corresponding to the location of the endocardial ablation site. After intracoronary application of nitroglycerin, the coronary spasm and ECG changes resolved completely (details on the case have been published separately[7]). There was no postablation UHDx map performed in this patient.

4 | DISCUSSION

Major findings of this study are:

1. PFA creates wide antral circumferential lesions for PVI with depression of tissue voltage to a minimum using UHDx mapping for the first time in this setting. Additionally, all LAPWs were isolated and lesions were shown to be exceptionally homogenous with negligible small areas of complex fractionation along the border of ablation sites.

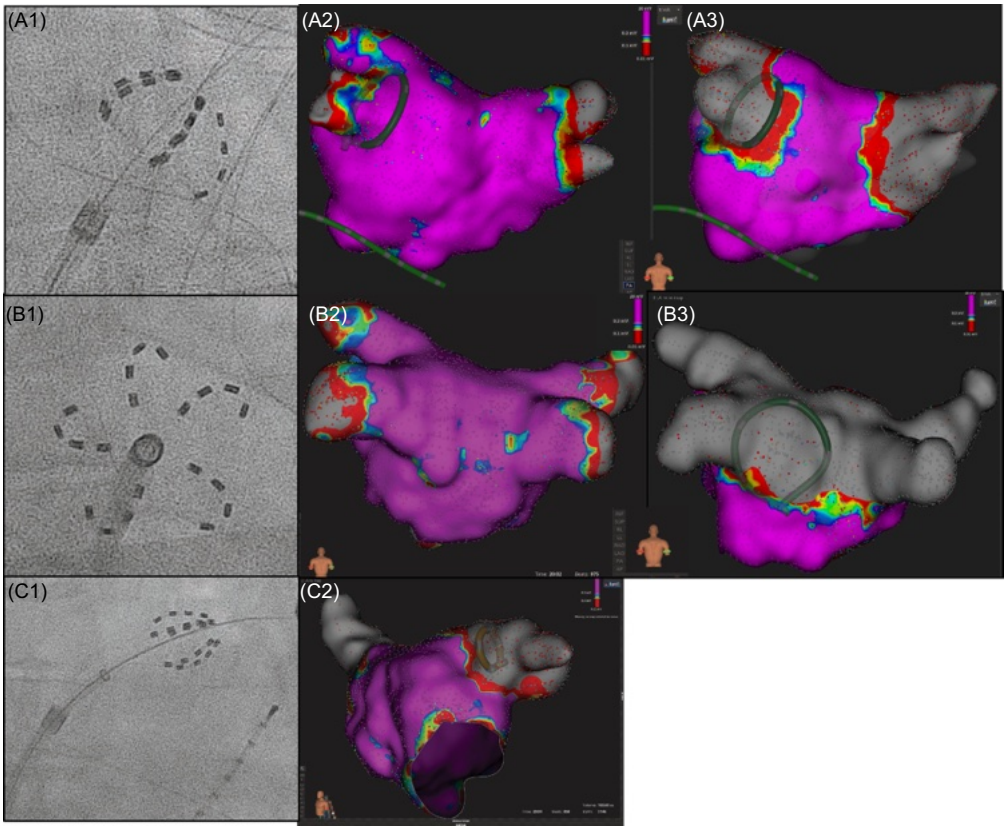

FIGURE 4 Visualization of the PFA catheter: (A) *Basket*-configuration (A1: fluoroscopy, A2: UHDx map with positioning of the basket at the LIPV ostium pre-ablation (green ring), A3: prior positioning of the *basket* (green ring) is matching the level of isolation in the postablation map). (B) *Flower*-configuration (B1: fluoroscopy, B2: UHDx map of the LAPW pre-ablation, B3: prior positioning of the *flower* is matching the level of LAPW isolation in the post-ablation map (green ring). (C) *Appropriately-sized basket* configuration of PFA catheter (yellow ring) to check pulmonary isolation after 8 PFA applications (C1 fluoroscopy) is shown in a UHDx map positioned in the LSPV. LAPW, left atrial posterior wall; LIPV, left inferior pulmonary vein; LSPV, left superior pulmonary vein; PFA, pulsed-field ablation; PV, pulmonary vein; UHDx, ultrahigh density

2. Visualization of the PFA catheter within the UHDx mapping system via an impedance-based approach is feasible and was optimized during the study resulting in accurate guiding and prediction of the level of PV isolation.
3. Despite high efficacy in acute PVI, early PV reconnection was found in 6.25% of pulmonary veins using UHDx mapping.

4.1 | Ultrahigh-density mapping and area of isolation after PFA

UHDx mapping is known to deliver very precise electroanatomical information due to high resolution of the local electrograms (smaller electrodes with closer spacing) as compared with conventional mapping tools.[8,9] Wide antral circumferential lesions after PVI are associated with better rhythm control and the preferred ablation strategy.[10]

In our study, PFA created wide antral circumferential lesions with area measurements being in line with a recently published quantitative PFA lesion analysis by Kawamura et al.[3] Comparable with their findings the nonablated LAPW in our study was $9.4 \pm 2.6\,cm^2$. Differences between the two studies, however, were a different low voltage cutoff, defined as <0.5 mV as compared with <0.3 mV in our study. Additionally, with UHDx-mapping, more than seven thousand electrograms points were collected in the present study as compared with only a median of 653 by Kawamura et al.[3] Yet, measurements of PV ostia and LAPW were similar.

In a further retrospective analysis of post-PVI remapping procedures, Kawamura et al. compared PFA-based PV isolation areas

and nonablated posterior wall areas to thermal ablation cohorts (including RF and balloon technologies) and no difference was found.[11] Notably, in the balloon-cohort, sparing of the posterior aspect of the carina with notch-like normal voltage areas were reported but were not seen in the PFA or RF cohort.[11]

Preclinical data assessing histopathological PFA lesions showed that PFA lesions were composed of organized, homogeneous fibrosis replacing the myocardium with well-demarcated border zones that were consistent with their gross appearance.[12] Compared with that, RF lesions appeared disorganized and heterogeneous with greater inflammatory response.[12] In our study, we saw depression of tissue voltage to a minimum during acute post-PFA UHDx mapping. All LAPWs were isolated and lesions were shown to be exceptionally homogenous with almost no complex fractionation along the ablation sites and especially the ablation border zones. The absence of these fractionations, as seen in acute PFA lesions, could minimize proarrhythmic effects and subsequent atrial arrhythmias.[5]

PFA catheter visualization was feasible in all patients after adapting the workflow (placing the mapping catheter in the inferior vena cava for field tracking). This is the first report of PFA-catheter visualization into UHDx electroanatomical mapping system in a patient series. The circular catheter rendering was already used in previous research with other standard electroanatomical mapping systems to mitigate the absence of a dedicated PFA catheter model.[2] Also in our study, the PFA catheter was only visualized in a circular form via the equatorial electrodes. Therefore, exact visualization of a *basket* or *flower* pose in the mapping system was not possible. Yet, the position of the circular form of the PFA catheter matched the level of lesion scars in most patients and was therefore adequate in predicting the level of isolation. In the future, this could help to reduce the need for fluoroscopy. For now, PFA remains a fluoroscopy-dependent ablation strategy, particularly in the absence of intracardiac echocardiography. Additionally, information regarding tissue contact is missing with the current PFA device.

4.2 | Pulmonary vein reconnection and practical considerations

Our study revealed early acute PV reconnections after initially-confirmed PVI in a small number of patients during post-PFA UHDx mapping. This is a novel finding, as the previously published studies of Reddy et al. show a first-pass PFA PVI rate of 100%,[2] even when testing for dormant conductions with adenosine during the waiting period.[4] Also, Kawamura et al. found no acute PV reconnections during post-PFA mapping with a multispline diagnostic catheter.[3] However, repeat-mapping procedures 2–3 months after initial PFA ablation, reported PV reconnection.[4] PV reconnections rates were small, ranging from 4% of PVs[2,4] to 16% of patients[3] in previous studies. Pooled data of the IMPULSE, PEFCAT, and PEFCAT II trials showed that PV reconnections were only observed in superior PVs.[4] This is in line with our findings where acute PV reconnections only occurred in superior PVs and in the superior-anterior aspect of the PV ostium, as revealed by UHDx-mapping.

Possible explanations for acute PV reconnection are given in the following: *first*, when looking at the mechanical features of the over-the-wire PFA catheter, the catheter tends to turn posteriorly and to the roof when advanced to the PV ostium, away from the anterior aspect of the PV antrum. In all previously published studies regarding this topic, intracardiac echocardiography (ICE) was used to assess adequate catheter positioning at the PV.[2,4] In our study, no ICE was used.

Second, the variability of the PFA catheter's *basket* configuration may correlate with acute isolation success. Standard *basket* configurations have a convex distal end that can self-center the device when the guidewire is biased to one – that is, superior – aspect of the PV. However, if a larger *basket* shape is chosen, the distal end of the catheter is flat, which does not facilitate a self-centering effect and may lead to a compromise in circumferential lesion creation. In the majority of this initial experience, the larger *basket* was selected with guidance shifting to standard deployments in later patients.

Third, after confirmation of initial PVI with the electrodes of the PFA catheter in various positions, we mapped all patients with UHDx which is known to be more precise in detecting conduction gaps as compared with conventional mapping catheters as Garcia-Bolao et al.[8] *Fourth*, PFA energy delivery failing to reach durable, transmural ablation lesions could also be an issue explaining the occurrence of conduction gaps after PVI. Transmurality with biphasic PFA was reported to be as high as 90.8% in histological assessment in swine atrial tissue.[12]

Fifth, recently, the effects of epicardial connections involving PVs in catheter ablation of AF have been revealed during high-density mapping after radiofrequency-guided PVI.[13] Epicardial connections were most frequently found at the carina region but were also located at the roof of the right pulmonary veins.[13] Ablation of such epicardial connections could also challenge PFA-guided ablation. However, at this point, the discussion remains purely speculative, and more data are needed.

All conduction gaps were found in the anterior superior aspect of the PV ostia. Therefore, to achieve optimal lesion creation, it seems advisable to rotate the sheath anteriorly for at least two of the applications in each pair and to limit the applied pressure of the catheter against the PV ostium. Movement of the splines and electrodes should be monitored closely to ensure optimal contact while maintaining an even shape of the catheter resulting in an optimal electrical field; (Figure 3C). Additionally, a waiting period after initial PVI should be considered as the detection and treatment of early PV reconnections leads to further reduction of “late” PV reconnections. Also, we confirmed that visualization of the PFA catheter in the map is feasible and could be helpful when positioning the catheter at the PV ostium.

In general, PV reconnection is a common finding in thermal ablation technologies such as radiofrequency (RF) or cryoballoon[5] and is the major finding in patients with arrhythmia recurrence.[14] Durable

PV isolation of all PVs may be difficult to achieve with thermal ablation but can be optimized when using certain protocols, e.g. the "CLOSE"-protocol integrating the so-called ablation index and inter-lesion distance-measurements leading to 62% PVI durability of all PVs.[15] Also, the development of new generation cryoballoons increased PVI durability of all PVs to 79% of patients.[16] And exactly here, PFA shows promising results of durable PVI being as high as of 84%–100% of patients.[1,2,4]

Location of conduction gaps after thermal ablation varies in the literature most likely due to variation of indifferent ablation strategies and the use of different catheters (first- vs. second-generation cryoballoon; noncontact-force and contact-force RF catheters; different mapping systems).[5,17,18] However, the inferior aspect of the right inferior PV seems a *sweet spot* for reconnection after cryoballoon PVI[5] and left-sided PVs were more frequently reconnected after contact-force RF during UHDx mapping.[5] Up to now, the current findings suggest that rare conduction gaps after PFA have only been reported on superior PVs.

4.3 | Safety and complications

Collateral damage of adjacent tissue is a limitation of thermal energy sources for catheter ablation of arrhythmias, leading to rare (<0.05%) life-threatening complications such as atrioesophageal fistula.[19] New ablation strategies, such as high-power short-duration (HPSD) RF ablation cause more local resistive heating and local atrial tissue destruction without conductive heating of more distant tissue that might cause less distant collateral damage.[20] Studies show markedly low esophageal injury after HPSD ablation.[21–23]

Compared with cryo or RF ablation, PFA is strictly sensitive to myocardium, successfully sparing the esophagus in preclinical (histopathology) and clinical data (magnet resonance imaging).[24,25] In the PersAFOne trial by Reddy et al, no esophageal lesion was detected after LAPW isolation during post-procedural esophagogastroduodenoscopy.[2] This is in alignment with our findings where LAPW isolation was successful in all patients without any detection of esophageal lesions.

However, in the present study, a reversible coronary artery spasm caused by PFA occurred concurrently with mitral isthmus ablation. A full case report of this finding has been published elsewhere.[7] Although the esophagus was spared from any injury in our study, PFA may still cause collateral damage if it is delivered directly next to adjacent organs/structures or at significantly higher doses[2] as PFA can lead to reversible stunning of adjacent tissue cells.[26] Therefore, it seems advisable to apply PFA with caution close to coronary arteries.[7]

Interestingly, vagal responses are commonly observed during PFA.[4] However, our study showed that applying atropine before the first PFA application seemed to overcome the issue of vagal responses as no pacing was required in any of the atropine-treated patients.

4.4 | Limitations

The present study yields some limitations. First, the design of our single-center study was explorative and observational and therefore the sample size in the current study is small limiting the impact of the results.

Only intraprocedural parameters are shown in this manuscript (anonymized data input) and the study is a nonrandomized investigation of consecutive patients during the clinical routine. As compared to prior published studies, we present only acute remapping data. There is no chronic remapping information and therefore no statement regarding chronic PFA lesion patterns in UHDx mapping can be made. Further studies investigating atropine administration or ventricular pacing for vagal responses after PFA applications are needed as data regarding this topic are yet limited.

5 | CONCLUSION

As illustrated by UHDx mapping, PFA creates wide antral circumferential PVI lesions and homogenous LAPW isolation with depression of tissue voltage to a minimum. PFA, therefore, seems to be a promising new technology for catheter ablation of atrial fibrillation. However, early PV reconnection can still occur with a low rate after PFA.

ACKNOWLEDGMENTS

The authors thank Charles Eggert (FARAPULSE, Inc.), Lydia Merbold (Boston Scientific Corp.), Daniel Schlarmann (Boston Scientific Corp.), and Tobias Oesterlein (Boston Scientific Corp.) for their clinical and technical support as well as for engaging discussions/comments that helped to improve this article.

ORCID

Melanie A. Gunawardene http://orcid.org/0000-0001-7561-7185
Omar Anwar http://orcid.org/0000-0001-9738-4685

REFERENCES

1. Reddy VY, Neuzil P, Koruth JS, et al. Pulsed field ablation for pulmonary vein isolation in atrial fibrillation. *J Am Coll Cardiol*. 2019; 74(3):315-326.
2. Reddy VY, Anic A, Koruth J, et al. Pulsed field ablation in patients with persistent atrial fibrillation. *J Am Coll Cardiol*. 2020;76(9): 1068-1080.
3. Kawamura I, Neuzil P, Shivamurthy P, et al. Does pulsed field ablation regress over time? A quantitative temporal analysis of pulmonary vein isolation. *Heart Rhythm*. Published online February 27, 2021. doi:10.1016/j.hrthm.2021.02.020
4. Reddy VY, Dukkipati SR, Neuzil P, et al. Pulsed field ablation of paroxysmal atrial fibrillation. *JACC Clin Electrophysiol*. 2021;7(5): 614-627.
5. Gunawardene MA, Eickholt C, Akbulak RÖ, et al. Ultra-high-density mapping of conduction gaps and atrial tachycardias: Distinctive patterns following pulmonary vein isolation with cryoballoon or contact-force-guided radiofrequency current. *J Cardiovasc Electrophysiol*. 2020; 31(5):1051-1061.

6. Alken FA, Klatt N, Muenkler P, et al. Advanced mapping strategies for ablation therapy in adults with congenital heart disease. *Cardiovasc Diagn Ther*. 2019;9(Suppl 2):247-S263.
7. Gunawardene MA, Schaeffer BN, Jularic M, et al. Coronary spasm during pulsed field ablation of the mitral isthmus line. *JACC Clin Electrophysiol*. Published online September 23, 2021.
8. García-Bolao I, Ballesteros G, Ramos P, et al. Identification of pulmonary vein reconnection gaps with high-density mapping in redo atrial fibrillation ablation procedures. *EP Eur*. 2017;0:1-8.
9. Anter E, Tschabrunn CM, Josephson ME. High-resolution mapping of scar-related atrial arrhythmias using smaller electrodes with closer interelectrode spacing. *Circ Arrhythm Electrophysiol*. 2015;8(3):537-545.
10. Kiuchi K, Kircher S, Watanabe N, et al. Quantitative analysis of isolation area and rhythm outcome in patients with paroxysmal atrial fibrillation after circumferential pulmonary vein antrum isolation using the pace-and-ablate technique. *Circ Arrhythm Electrophysiol*. 2012;5(4):667-675.
11. Kawamura I, Neuzil P, Shivamurthy P, et al. How does the level of pulmonary venous isolation compare between pulsed field ablation and thermal energy ablation (radiofrequency, cryo, or laser)? *Europace*. 2021;0:1-10.
12. Koruth J, Kuroki K, Iwasawa J, et al. Preclinical evaluation of pulsed field ablation. *Circ Arrhythm Electrophysiol*. 2019;12:e007781.
13. Sun X, Niu G, Lin J, Suo N. The incidence and location of epicardial connections in the era of contact force guided ablation for pulmonary vein isolation. *J Cardiovasc Electrophysiol*. 2021;32(9):2381-2390.
14. Ouyang F, Antz M, Ernst S, et al. Recovered pulmonary vein conduction as a dominant factor for recurrent atrial tachyarrhythmias after complete circular isolation of the pulmonary veins: lessons from double lasso technique. *Circulation*. 2005;111:127-135.
15. De Pooter J, Strisciuglio T, El Haddad M, et al. Pulmonary vein reconnection no longer occurs in the majority of patients after a single pulmonary vein isolation procedure. *JACC Clin Electrophysiol*. 2019;5(3):295-305.
16. Reddy VY, Sediva L, Petru J, et al. Durability of pulmonary vein isolation with cryoballoon ablation: results from the Sustained PV Isolation with Arctic Front Advance (SUPIR) Study. *J Cardiovasc Electrophysiol*. 2015;26(5):493-500.
17. Ciconte G, Velagić V, Mugnai G, et al. Electrophysiological findings following pulmonary vein isolation using radiofrequency catheter guided by contact-force and second-generation cryoballoon: Lessons from repeat ablation procedures. *Europace*. 2015;18(1):71-77.
18. Ruiz-Granell R, Ballesteros G, Andreu D, et al. Differences in scar lesion formation between radiofrequency and cryoballoon in atrial fibrillation ablation: a comparison study using ultra-high-density mapping. *Europace*. 2019;21(2):250-258.
19. Hindricks G, Potpara T, Serbia C, et al. ESC Guidelines for the diagnosis and management of atrial fibrillation developed in collaboration with the EuropeanAssociation of Cardio-Thoracic Surgery (EACTS). *Eur Heart J*. 2020;2020(0):1-126.
20. Winkle RA. High - power short - duration ablation: turn up the heat to cool down the esophagus. *J Cardiovasc Electrophysiol*. 2019;30:1884-1885.
21. Chen S, Schmidt B, Seeger A, et al. Catheter ablation of atrial fibrillation using ablation index-guided high power (50 W) for pulmonary vein isolation with or without esophageal temperature probe (the AI-HP ESO II). *Heart Rhythm*. 2020; 17(11):1833-1840.
22. Chen S, Chun KRJ, Tohoku S, et al. Esophageal endoscopy after catheter ablation of atrial fibrillation using Ablation-Index Guided High-Power: Frankfurt AI-HP ESO-I. *JACC Clin Electrophysiol*. 2020;6(10):1253-1261.
23. Winkle RA, Mohanty S, Patrawala RA, et al. Low complication rates using high power (45–50 W) for short duration for atrial fibrillation ablations. *Heart Rhythm*. 2019;16(2):165-169. doi:10.1016/j.hrthm.2018.11.031
24. Koruth JS, Kuroki K, Kawamura I, et al. Pulsed field ablation versus radiofrequency ablation. *Circ: Arrythym Electrophysiol*. 2020;13(3):e008303.
25. Cochet H, Nakatani Y, Sridi-cheniti S, et al. Pulsed field ablation selectively spares the oesophagus during pulmonary vein isolation for atrial fibrillation. *Europace*. 2021;0:1-9.
26. Kotnik T, Rems L, Tarek M, Miklavčič D. Membrane electroporation and electropermeabilization: mechanisms and models. *Annu Rev Biophys*. 2019;48:63-91.

How to cite this article: Gunawardene MA, Schaeffer BN, Jularic M, et al. Pulsed-field ablation combined with ultrahigh-density mapping in patients undergoing catheter ablation for atrial fibrillation: Practical and electrophysiological considerations. *J Cardiovasc Electrophysiol*. 2022;33:345-356. doi:10.1111/jce.15349

Received: 27 June 2022 | Revised: 19 August 2022 | Accepted: 17 September 2022

DOI: 10.1111/jce.15713

FEATURED ARTICLES

WILEY

Pulsed field ablation in patients with complex consecutive atrial tachycardia in conjunction with ultra-high density mapping: Proof of concept

Melanie A. Gunawardene MD[1,2] | Benjamin N. Schaeffer MD[1,2] | Mario Jularic MD[1,2] | Christian Eickholt MD[1,2] | Ruken Ö. Akbulak MD[1,2] | Katja Hedenus MD[1,2] | Rahin Wahedi MD[1,2] | Omar Anwar MD[1,2] | Nele Gessler MD[1,2,3,4] | Jens Hartmann MD[1,2] | Stephan Willems MD[1,2,3]

[1]Asklepios Hospital St. Georg, Department of Cardiology and Intensive Care Medicine, Hamburg, Germany

[2]Semmelweis University, Budapest, Hungary

[3]DZHK (German Center for Cardiovascular Research), partner site Hamburg/Kiel/Lübeck, Berlin, Germany

[4]Asklepios Proresearch, Hamburg, Germany

Correspondence

Melanie A. Gunawardene, MD, Department of Cardiology, Asklepios Klinik St. Georg, Lohmühlenstr. 5, 20099 Hamburg, Germany.
Email: melanie.gunawardene@gmail.com

Disclosures: Speaker's fee MAG, SW: Farapulse Inc.

Abstract

Introduction: Catheter-ablation (CA) of consecutive left atrial tachycardias (LAT) can be challenging. Pulsed field ablation (PFA) yields a novel nonthermal CA technology for treatment of atrial fibrillation (AF). There is no data regarding PFA of LAT. This study sought to investigate PFA of consecutive LAT following prior CA of AF.

Methods: Consecutive patients with LAT underwent ultrahigh-density (UHDx) mapping. Subsequent to identification of the AT mechanism, PFA was performed at the assumed critical sites for LAT maintenance. Continuous ablation lines were performed if required and evaluated with pre- and post-PFA HDx-mapping.

Results: Fifteen patients (age 70 ± 10, male 73%) who underwent 3.6 ± 2 prior AF-CA procedures were included. The total mean procedure and fluoroscopy times were 141 ± 43 and 18 ± 10 min, respectively. All 19 of 19 (100%) LAT were successfully ablated with PFA. Two AT located at the right atria required RF-ablation. LAT were identified as localized reentry (n = 1) and macro-reentry LAT (n = 18) and targeted with PFA. All LAT terminated with PFA either to sinus rhythm (9/15) or a secondary AT (6/15 and subsequently to SR); 63% (12/19) terminated with the first PFA-application. All lines (13 roof, 11 anterior, 1 mitral) were blocked. LA-posterior-wall isolation (LAPWI) was successfully achieved when performed (10/10). AF/AT free survival was 80% (12/15) after 153 [88–207] days of follow-up. No procedure-related complications occurred.

Conclusion: PFA of consecutive LAT is feasible and safe. Successful creation of ablation lines and LAPWI can be achieved in a short time. PFA may offer the opportunity for effective ablation of atrial arrhythmias beyond AF.

KEYWORDS

atrial fibrillation; atrial tachycardia, high-density mapping; left posterior wall isolation; pulsed field ablation

Abbreviations: AF, atrial fibrillation; AT, atrial tachycardia; CA, catheter ablation; LAPW, left atrial posterior wall; LAPWI, left atrial posterior wall isolation; LAT, left atrial tachycardia; SR, sinus rhythm; PFA, pulsed field ablation; PVI, pulmonary vein isolation; RF, radiofrequency; UHDx, ultra-high-density.

1 | INTRODUCTION

Catheter ablation (CA) is effective in establishing long-term rhythm control in atrial fibrillation (AF) patients.[1] However, arrhythmia recurrences can occur.[1]

Consecutive left atrial tachycardias (LAT) are not uncommon following AF ablation, especially after prior substrate modification or in patients with left atrial scarring.[2,3] LAT are usually structurally defined by scars or fibrosis and consist of macroreentry circuits characterized by propagation pathways between nonconducting areas or may circuit around large anatomical obstacles.[4] Furthermore, localized reentry or focal mechanism can be discriminated when a centrifugal activation pattern is present.[2]

As conservative therapeutic options for LAT are limited, patients with consecutive LAT often require repeat CA.[5] However, mapping, characterization, and ablation of these LAT can be challenging due to a complex underlying substrate and a great variability of AT mechanism and localization throughout the atria.[6] Ultra–high-density (UHDx) mapping of LAT provides detailed insights due to the higher resolution of local electrograms and is therefore a valuable resource in understanding complex AT mechanisms and guidance for ablation.[7,8]

However, even if the AT's mechanism and ablation target is well understood, effective ablation and durable block of created ablation lines can limit success of AT ablation. Recently, pulsed field ablation (PFA) has been introduced as a novel nonthermal energy source for CA of AF.[9] First experiences show high lesion durability and chronic pulmonary vein isolation (PVI). Voltage maps delineate wide, homogenous ablation lesions with a beneficial safety profile due to the myocardial sensitivity of electroporation, sparing adjacent tissue.[10,11] Thus, PFA may allow for safe substrate modification and ablation of LAT including the left atrial posterior wall (LAPW).[10] Successful integration of PFA catheters into a UHDx mapping system has been reported lately[11] and may offer additional benefits, especially in the setting of LAT mapping and ablation.

Therefore, the objective of this study was to investigate PFA-based ablation of consecutive AT following prior catheter ablation of AF in conjunction with UHDx mapping.

2 | METHODS

2.1 | Study design

This study is a single-center, observational, prospective study. Consecutive patients eligible for CA of consecutive AT following prior CA for AF, including paroxysmal and persistent AF, were enrolled from September 2021 until April 2022. The study was investigator-initiated without external funding; the authors are responsible for design, execution, and conduct of the study. The statistical analyses and interpretation of the data was approved by all authors, who attest to the accuracy of the data and of all analyses. Written informed consent was obtained from all patients. The institutional review board and ethics committee approved the study. The study was conducted in accordance with the provisions of the Declaration of Helsinki and its amendments.

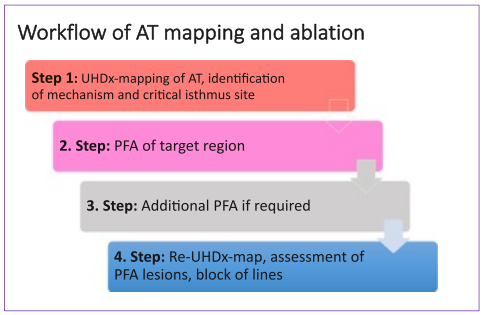

FIGURE 1 Flow chart of the AT mapping and ablation workflow. AF, atrial fibrillation; AT, atrial tachycardia; PFA, pulsed field ablation; UHDx, ultra-high-density.

2.2 | Catheter ablation

All patients underwent three-dimensional UHDx (Orion™ catheter and Rhythmia™ Mapping system; Boston Scientific) and PFA of LAT (Figure 1). Subsequent to identification of the AT mechanism, the assumed critical isthmus and optimal PFA target site was determined. Ablation was performed using a multispline catheter (Farwave; Farapulse Inc.). Focal ablation was performed in case of localized-reentry. This means that linear lesions were not necessarily performed by PFA in cases of localized reentries, in which sole ablation of local area of the critical isthmus was sufficient.

Continuous ablation lines were created in case of macro-reentry LAT aiming to connect two anchor points such as mitral valve annulus and PV-isolation lines. Additional ablation, including repeat pulmonary vein isolation (PVI) and left atrial posterior wall isolation (LAPWI) was performed by PFA if required or rational. If the AT was present at the beginning of the procedure, then activation and parallel voltage mapping was performed. In case of sinus rhythm, AT was induced by rapid atrial stimulation. Patients with initial AF were only included in this study, if consecutive AT emerged during PFA.

In case of right-sided ATs (e.g., typical atrial flutter or ATs close to the AV-node) ablation was preferably performed by conventional radiofrequency (RF) ablation.

Extent of PFA-lesions and block of lines were assessed with pre- and post-PFA UHDx-mapping.

In cases with LAPWI, esophagogastroduodenoscopy was performed after ablation procedure.

Before ablation, transesophageal echocardiography was performed to rule out intracardiac thrombus formation. New oral anticoagulants were minimally interrupted at the morning of the

procedure and restarted 6 h after sheath removal. In patients on VKA, ablation was performed in the therapeutic INR range of 2–3.

Using a continuous infusion of propofol (1 mg/ml) and boluses of midazolam (1 mg/ml) and sufentanyl (0.1 mg/ml), catheter ablation was performed under deep sedation. To reach an activated clotting time of at least 300 s, intravenous heparin (25 000 IU/5 ml) was applied. To minimize vagal responses, 1 mg of intravenous atropine (0.5 mg/ml) was administered to all patients before PFA, except for patients with implantable devices.

2.3 | Work flow of UHDx mapping and PFA

2.3.1 | Step 1

The use of UHDx mapping in combination with PFA has been reported in detail before.[11] After gaining left atrial access via transseptal puncture and left atrial (LA) angiography, the 64-pole mini-basket mapping catheter (Orion™; Boston Scientific) was used in combination with an UHDx electroanatomical mapping system (Rhythmia™; Boston Scientific) to reconstruct LA and PV geometry and to map the activation sequence of the AT. Electrogram annotation was performed automatically by the mapping system using previously reported prespecified criteria.[6]

After LA-mapping, the underlying AT mechanism was identified by analysis of wave front propagation, activation patterns, areas of slow conduction, anatomical and functional barriers and lines of block within the UHDx map, as reported before.[6] To identify the critical isthmus and optimal ablation site voltage maps were analyzed. Further, a signal processing software (Lumipoint™; Boston Scientific) was used for analysis of left atrial activation timing, fractionation and complex components of activation.[12]

The mechanism of AT was defined as either macroreentry or nonmacroreentry.[6] A centrifugal activation pattern indicated a nonmacroreentry AT. In this case, the mechanism was further evaluated as either focal ATs (showing radial activation from a distinct focal source) or localized reentry ATs (showing continuous, fractionated activation covering the entire cycle length in an area of less than 2 cm in diameter or the presence of a dominant small and stable rotational activation pattern, as defined before).[6] If possible, entrainment mapping was avoided.

After finalizing the LAT map and determination of the PFA target site, the mapping catheter was then placed in the inferior vena cava to obtain field tracking for PFA-catheter visualization. The left atrial sheath was exchanged by a 13 French (inner diameter) deflectable sheath (Faradrive; Farapulse Inc.) and the PFA-catheter (Farawave; Farapulse Inc.) was introduced to the LA for ablation of the AT.

2.3.2 | Steps 2 and 3

The PFA system has been described in detail before.[9,11] The multispline PFA catheter can be configured into different shapes (a *basket* or a *flower configuration)* for energy delivery. The therapeutic waveform was structured as a hierarchical set of biphasic, microsecond-scale pulses released in a bipolar fashion between the electrodes[13] and 2.0 kV were selected for ablation in our study protocol.

In case of a macroreentry LAT, ablations lines were created by PFA. Depending on the mechanism of the identified localized reentry, local PFA ablation and/or creation of lines was possible.

To create ablation lines, the PFA catheter was positioned at the ablation target site either in a *basket* or a *flower* configuration, whichever was better to achieve a stabile catheter position at the preferred site. The PFA catheter was visualized in the electroanatomical mapping system in a circular shape.[11] After ablation of the AT's critical isthmus, the ablation line was completed. Following ablation sites were chosen in close proximity to the prior sites to achieve continuous lines. At least two applications were deployed at each site. The endpoint was anatomical completion of the lines with connection of two nonconducting structures in the LA (e.g., PVI antral ablation lines, mitral valve annulus). Further, we aimed for abolishment of all signals along the lines. Anterior, roof and mitral isthmus lines were created. Any line, including the mitral isthmus line, was conducted at the site of the critical isthmus depending on the location in the UHDx map.

LAPWI was conducted with the *flower* configuration and two PFA applications per site.

In case of a reconnected PV, all PVs of the patient were targeted for reablation with PFA to homogenize antral scarring. Eight PFA impulses were applied per PV (4 *baskets*, 4 *flowers*).

2.3.3 | Step 4

Subsequent to ablation, the PFA catheter was extracted and the 64-pole mini-basket mapping catheter was introduced to the LA again for repeat mapping. Detailed UHDx mapping of the ablation lines was performed to confirm block of lines, PVI and LAPWI, as described before using a scar cut off value of <0.3 mV.[7,11] Block of lines was assessed by repeat UHDx-mapping. In sinus rhythm or paced rhythm indicated by a block of conduction along the line or collision of wave fronts. If maps were unclear appropriate pacing maneuvers were performed. Patients underwent a structured follow-up including telephone-calls, routine visits at the referring cardiologist and 24-h Holter-ECG and/or rhythm monitoring via implanted cardiac devices such as pacemakers and ICDs.

2.4 | Statistics

Continuous data are shown as mean ± standard deviation or as median and interquartile range. For group comparisons, Student's *t* test (paired or unpaired) or the Mann–Whitney *U* test for unpaired variables were utilized. Categorical data are demonstrated as absolute and relative frequencies; they were compared using the chi-square or Fisher's exact test. Statistical significance was assumed

at a $p < .05$. Statistical analyses utilized the GraphPad Prism 9.0 software (GraphPad Software Inc.).

3 | RESULTS

3.1 | Baseline and procedural characteristics

Fifteen patients with AT (mean age 70 ± 10 year, 73% male) who underwent 3.6 ± 2 prior CA procedures for AF/AT were included in the study. Baseline characteristics of the patients are shown in Table 1. Three patients (3/15, 20%) were currently on antiarrhythmic drugs before the procedure (2 flecainide, 1 amiodarone).

All 15 patients underwent prior pulmonary vein isolation with a mean of 2.5 ± 1 PVI and re-PVI.

TABLE 1 Baseline patient characteristics

	All (*n* = 15)
Age (years)	70.2 ± 9.7
Male gender, *n* (%)	11 (73.0)
Hypertension, *n* (%)	13 (86.7)
BMI (kg/m^2)	26.9 ± 8.5
CHA_2DS_2-VASc score	2 [3–4]
Current ablation procedure (*n*)	4 [3–6]
History of AF/AT (years)	7.5 ± 3
Initial type of AF	
– PAF, *n* (%)	1 (7.0)
– Persistent AF, *n* (%)	14 (93.0)
Prior AAD therapy (*n*)	
• None	5 (33.3)
• Class Ic	4 (26.7)
• Class III	6 (40.0)
Left atrial diameter (mm)	45.7 ± 15.1
Left ventricular function	
– Normal (ejection fraction 50%–70%), *n* (%)	12 (80.0)
– Mild dysfunction (40%–49%), *n* (%)	2 (13.3)
– Moderate dysfunction (30%–39%), *n* (%)	1 (6.7)
– Sever dysfunction (<30%), *n* (%)	0 (0)

Note: Values are mean ± standard deviation, median [first-third quartile], or *n* (%).

Abbreviations: AAD, antiarrhythmic drug; AF, atrial fibrillation; BMI, body mass index; **CHA_2DS_2-VASc score** is a clinical estimation of the risk of stroke in patients with atrial fibrillation; scores range from 0 to 9, with higher scores indicating a greater risk of stroke = **C**ongestive heart failure, **H**ypertension, **A**ge > 75 years, **D**iabetes, previous **S**troke, transient ischemic attack, or thromboembolism, **V**ascular disease, **A**ge 65–75 years, and **S**ex **c**ategory; PAF, paroxysmal atrial fibrillation.

Five patients (5/15; 33%) received a prior anterior line, four (4/15; 27%) underwent prior roof line ablation, prior mitral isthmus line was conducted in four patients (4/15; 27%), one (1/15; 7%) underwent a RF guided posterior box lesion and 11 patients (11/15;73%) underwent right atrial isthmus ablation during prior catheter ablation procedures for AF/AT.

All 15 patients underwent PFA-guided ablation of LAT. Procedural parameters are given in Table 2: total mean procedure and LA PFA times were 141 ± 43 and 50 ± 19 min with a minimum LA-PFA time of 18 min in one patient, respectively. Mean total fluoroscopy and LA PFA fluoroscopy times were 18 ± 10 and 9 ± 4 min, respectively. Of all 15 patients, AT was present in 13 patients at the beginning of the procedure. One patient was in sinus rhythm with induction of AT by atrial burst pacing and another patient presented initially in AF that terminated to AT during PFA-guided LAPW ablation and repeat PVI.

3.2 | Characterization of atrial tachycardia

Twenty-one ATs with a mean cycle length of 312 ± 94 ms were mapped and targeted. This included two consecutive right-sided AT, one focal AT located at the CS-ostium and one common type atrial flutter. Right-sided AT occurred in patient #1 consecutively after successful termination of LA microreentry and was found at the CS ostium. In patient #4, typical atrial flutter occurred during burst atrial pacing after termination of left anterior macroreentry tachycardia.

Of the 19 LAT, one localized reentry at the patients' LA ridge (between the left PVs and left atrial appendage, Figure 2) and 18 macro-reentries were targeted with PFA. Of the 18 macroreentries, 7 were located to the anterior LA, 5 were perimitral flutter, 4 roof-dependent, 1 LAA-associated, and 1 reentry was detected on the LAPW. In perimitral AT, the critical isthmus was found mostly at the anterior wall (4/5 patients, 80%) and at the mitral isthmus in 1 patient (1/5; 20%). Examples of different AT mechanisms and PFA are shown in Figures 3 and 4.

All patients had considerable left atrial scarring shown in the pre-ablation UHDx voltage map (15/15 patients, 100%) (Figure 5). These significant scar areas were located at the anterior LA in 13/15 patients, at the LA roof in 11/15, at the LAPW in 10/15, at the lateral LA in 8/15 and at the LA septum in 7/15 patients (Figure 6). The mapped LA volume (including PVs) was 165 ± 53 ml (Table 2).

The assumed critical isthmus/PFA ablation site of LAT was at the anterior LA in 11 cases, LA-ridge in 1, LAA base in 1, roof in 4, LAPWI in 1 and mitral isthmus in 1 case.

In total, 11 ATs showed a critical isthmus in the anterior LA. Of these 11 "anterior" cases, 4 (4/11; 36%) were perimitral ATs with left anterior scarring leading to creation of an anterior ablation line. Of these four patients, only one patient (1/4, 25%) received a prior anterior ablation line (during prior catheter ablation) revealing a gap. Seven (7/11; 64%) "anterior" ATs showed anterior macroreentry without perimitral involvement; three of these patients received a prior anterior ablation line and showed gaps

TABLE 2 Procedural parameters

	All *n* = 15
Procedural data	
Initial rhythm	
• Atrial tachycardia, *n* (%)	13 (86.6)
• Sinus rhythm, *n* (%)	1 (6.7)
• Atrial fibrillation, *n* (%)	1 (6.7)
Total procedure time (min)	140.6 ± 43.4
Total fluoroscopy time (min)	18.1 ± 10.2
Pulsed field ablation	
Time of PFA catheter in the left atrium (min)	40 [47.5-56]
Fluoroscopy time during PFA (min)	9.4 ± 3.6
PFA applications	34 [28–44]
LAPW (*n* = 10)	16 [11–20]
Mitral isthmus line (*n* = 1)	4 [4-4]
Anterior line (*n* = 11)	20 [12–29]
Roof line (*n* = 13)	7 [6–11]
Ridge (*n* = 1)	20 [20]
LAA (*n* = 1)	4 [4-4]
Total PFA applications per patient for Re-PVI (*n* = 8 patients)	
LSPV	8 [8-8]
LIPV	8 [8-8]
RSPV	8 [8-8]
RIPV	8 [8-8]
PFA catheter size	
31 mm	13 (86.7)
35 mm	2 (13.3)
Ultra high-density mapping	
Rhythm during mapping	
• Atrial tachycardia, *n* (%)	15 (100.0)
UHDx- LA mapping points (LAT map)	10535 ± 4894
Mapped LA Volume (ml)	165 ± 53
LA mapping time (total), (min)	15.2 ± 6.2
Patients with visualization of PFA catheter in mapping system, *n* (%)	15 (100)
***All complications, n* (%)**	0 (0.0)
• Pericardial tamponade, *n* (%)	0 (0.0)
• Stroke/TIA	0 (0.0)
• Phrenic nerve palsy, *n* (%)	0 (0.0)
• Access complications (groin), *n* (%)	0 (0.0)
• Esophageal lesion, *n* (%)	0 (0.0)
• Coronary spasm, *n* (%)	0 (0.0)

Note: Values are mean ± standard deviation, [*n*] or *n* (%), median [first-third quartile].

Abbreviations: LAPW, left atrial posterior wall; LIPV, left inferior pulmonary vein; LSPV, left superior pulmonary vein; PFA indicates pulsed field ablation, PVI, pulmonary vein isolation; RSPV, right superior pulmonary vein; RIPV, right inferior pulmonary vein; TIA, transient ischemic attack; UHDx, ultra-high-density.

within this ablation line. All seven patients received a PFA-created anterior ablation line.

Summarized, a total of four (4/11, 36%) patients showed at least one gap in a prior anterior ablation line from previous catheter ablation procedures.

Another patient suffered from perimitral AT in whom the critical isthmus was not at the anterior LA wall. This patient received a prior mitral isthmus line that was found to not be blocked. Therefore, PFA-guided mitral isthmus ablation was performed in this one patient.

3.3 | PFA of atrial tachycardia

All 19 LAT were successfully ablated with PFA (90%, 19/21). All LAT terminated with PFA either to sinus rhythm (9/15 cases) or a secondary AT (6/15 and subsequently to SR). Twelve LATs (12/19, 63%) terminated with the 1st PFA-impulse (example Figure 3). Of the two right-sided AT, both were ablated with conventional RF technology.

A total of 38 ± 17 PFA applications per patient (including *basket* and *flower* configuration) were required for creation of ablation lines (Table 2). Using the PFA catheter, anterior line ablation was performed in 11/15 cases, LAPWI in 10/15, roofline ablation in 13/15 (10 cases including LAPWI), mitral isthmus ablation in one case, ridge ablation in one case, LAA ablation (at the base of the LAA). In one case LAA isolation occurred. Here, an anterior macroreentry AT due to two gaps within a previously attempted anterior line was present. A roof line and mitral isthmus line had already been blocked by previous ablation. PFA of the gaps in the anterior line made a consecutive LAA isolation unavoidable.

PV-reconnection was found in seven patients with 2 ± 0.9 reconnected PVs per patient. Yet, repeat PVI of at least one PV was performed in 8/15 cases to anchor lines, complete LAPWI, extend antral PVI area or target ostial potentials along the initial ablation line, requiring 20 ± 10 PFA applications.

Repeat UHDx mapping in sinus rhythm revealed isolated LAPW in 9/10 cases, with additional ablation required in one patient to

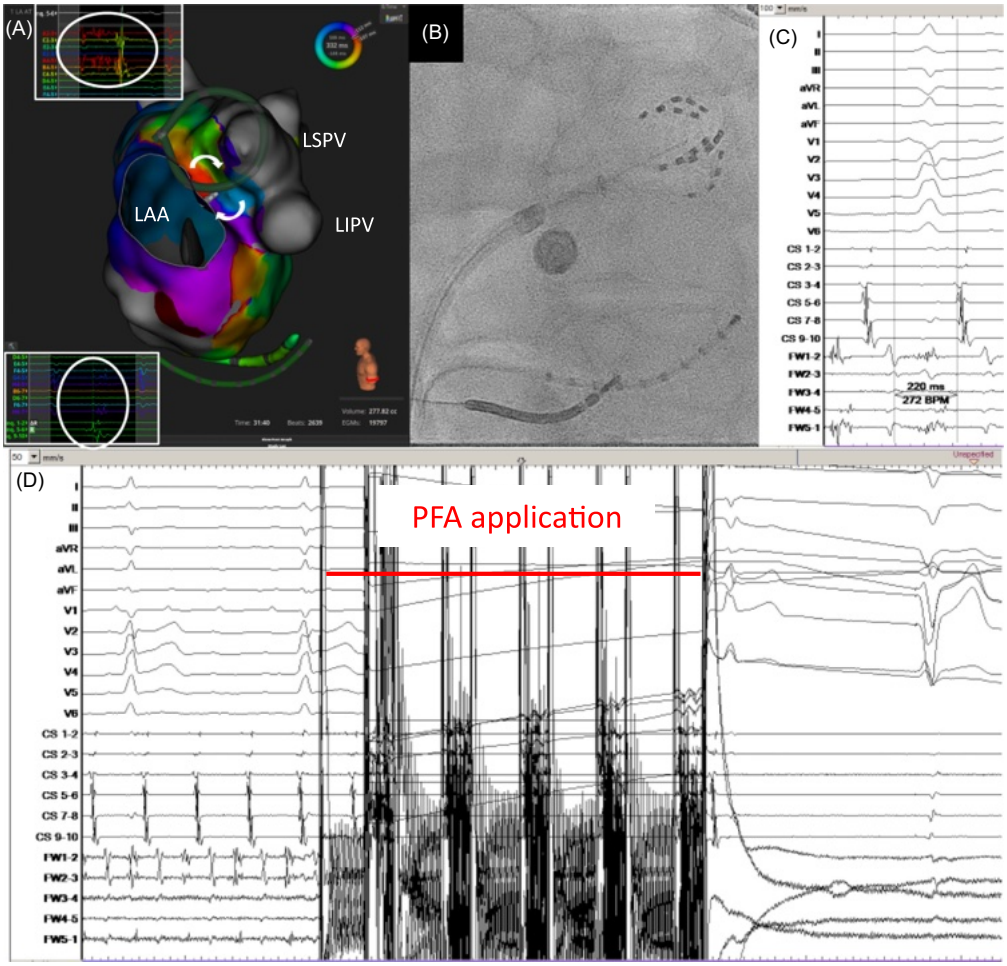

FIGURE 2 Left atrial localized reentry. (A) Localized reentry at the ridge between the LAA and left pulmonary veins shown by UHDx map with the electrograms covering the entire cycle length. The PFA catheter is visualized at the ablation site in the 3D map. (B) Fluoroscopic image of the PFA catheter positioned at the ablation site at the ridge. (C) Intracardiac tracings of the PFA catheter positioned at the ablation site; 220 ms of the 340 ms tachycardias cycle length can be demonstrated on the electrodes of the PFA splines. (D) Specific termination of the AT during PFA. AT, atrial tachycardia; LAA, left atrial appendage; PFA, pulsed field ablation; UHDx, ultra-high density mapping.

complete LAPWI. After reablation, all 10 LAPW were isolated. Anterior lines, mitral isthmus and roof lines were completed in all cases demonstrated by UHDx-3D-mapping.

In regard to intra-atrial conduction delay, timing from onset of the P-wave on the surface ECG to the LAA was 180.8 ± 39.2 ms after creating linear anterior lesions.

In detail, the surface area of the complete left anterior wall was 22.4 ± 5.9 mm^2 and the mean anterior LA scar area before ablation was 12.9 ± 4.6 mm^2. After PFA, mean ablation area of anterior lines was 16.7 ± 4.1 mm^2, which was related to an ablation area of 75.9 ± 14.8% of the complete LA anterior wall. Examples of voltage maps after LA anterior linear ablation are shown in Figure 8. Mean LAPWI ablation area was 14.3 ± 4.7 mm^2 and was related to a mean of 100% of the LAPW. Mean ablation area of roof lines was 5.07 ± 1.5 mm^2 with a mean line width of 15.8 ± 3.8 mm.

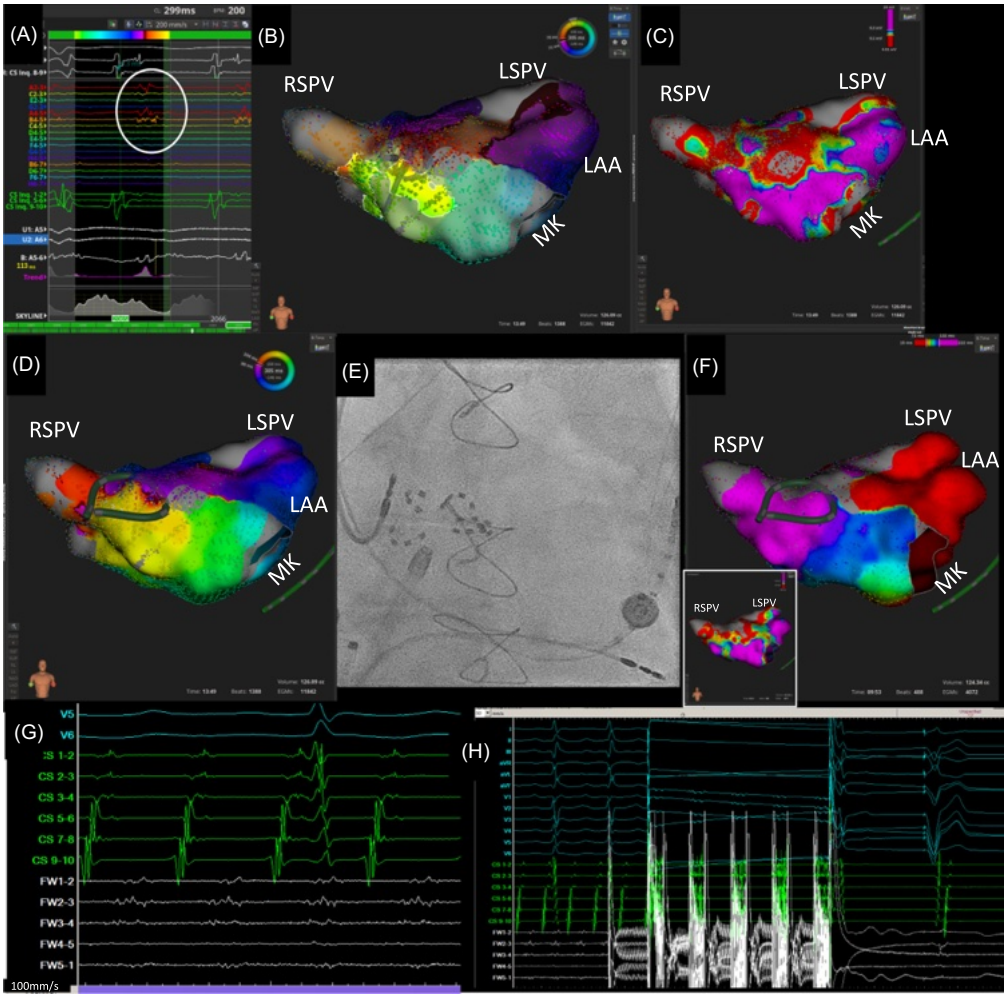

FIGURE 3 Left anterior macroreentry. (A, B) Fractionated electrograms shown by the Orion™ mapping catheter at the critical isthmus of a left anterior macroreentry and signal analysis of the UHDx map with the Lumipoint™ software. (C) Voltage UHDx map of the LA showing a large anterior scar. The patient already presented with an anterior scar in the prior CA procedure and creation of an anterior line with RF was attempted during the prior CA procedure. (D) Activation map of the anterior macroreentry. The white arrows indicate the propagation of the activation. (E) Fluoroscopic image of the PFA catheter positioned at the ablation site at the anterior superior LA close to the RSPV. (F) Block of the anterior line by PFA (indicated by black arrows) after termination of the AT and completion of the anterior line shown in the postablation UHDx map. In small: postablation voltage map of the anterior LA. (G) Intracardiac tracings of the PFA catheter positioned at the ablation site; the fractionated electrograms at the critical isthmus can be demonstrated on the electrodes of the PFA splines. (H) Specific termination of the AT during PFA. AT, atrial tachycardia; LAA, left atrial appendage; LSPV, left superior pulmonary vein; MK, mitral valve; PFA, pulsed field ablation; RSPV, right superior pulmonary vein; UHDx, ultra-high density mapping.

3.4 | Safety and complications

There were no complications in the study cohort (no access complication, no stroke, no pericardial tamponade).

Nine of ten patients with LAPW isolation received postprocedural esophagogastroduodenoscopy 1.7 ± 0.7 days after ablation, revealing no esophageal lesions. There were no further PFA-specific complications such as phrenic nerve paralysis, PV stenosis or coronary spasms.

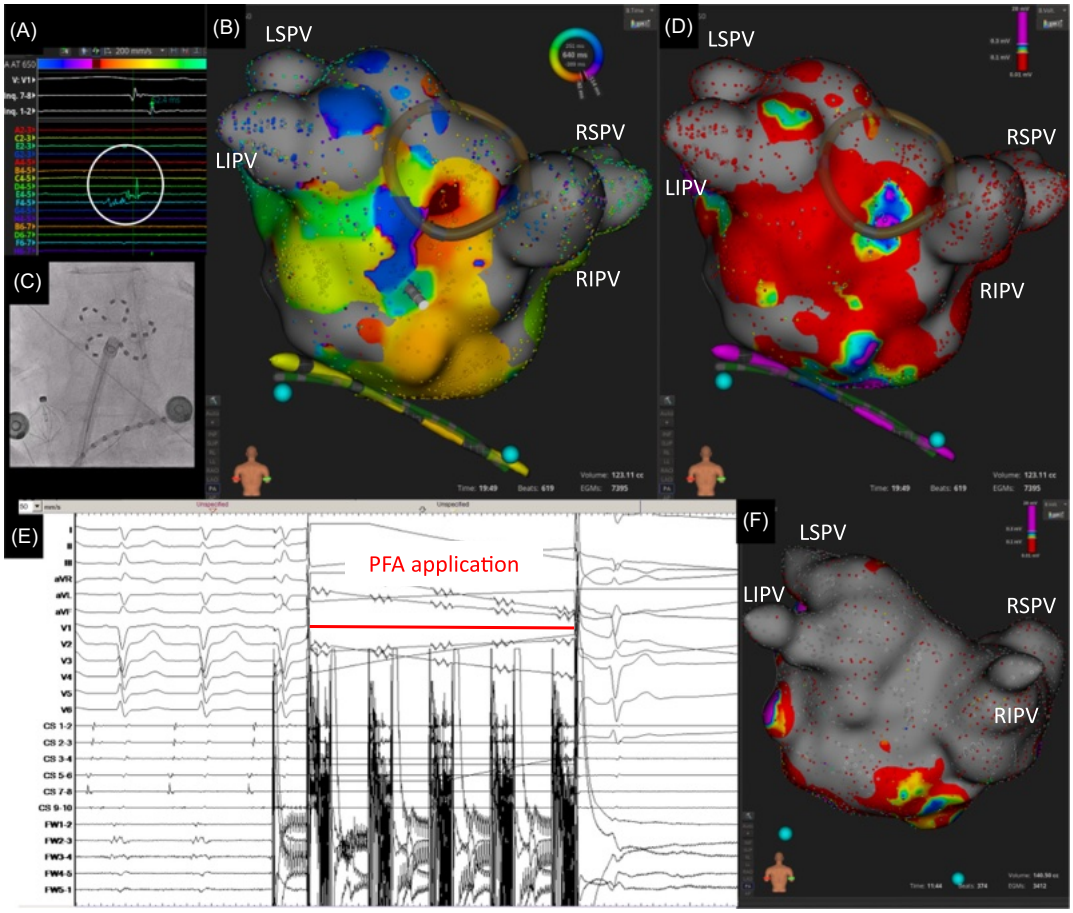

FIGURE 4 Posterior left atrial tachycardia. (A) Electrograms at the critical isthmus of the AT at the LAPW depicted by the UHDx mapping catheter. (B) UHDx activation map of the macroreentry at the LAPW. The PFA catheter is positioned at the ablation site and visualized in the mapping system. (C) Fluoroscopy of the PFA catheter positioned at the ablation site of the LAPW. (D) UHDx voltage map before ablation. The PFA catheter is positioned at the ablation site and visualized in the mapping system. (E) Specific termination of the AT during PFA. (F) UHDx voltage map after PFA ablation and LAPW isolation. AT, atrial tachycardia; LAPW, left atrial posterior wall isolation; PFA, pulsed field ablation; UHDx, ultra-high density mapping.

3.5 | Follow up

A median follow-up of 230 [148–285] days showed three early AF/AT recurrences (20%, 3/15) within the 90 days blanking period and one patient with a true AT recurrence 224 days after ablation (6.7%, 1/15). The follow-up (including a 90 days blanking period) is shown in Figure 7.

The three early AF/AT recurrences occurred 14 [9–22] days after PFA. Two of the three early AF/AT recurrences were treated by electrical cardioversion, one with medical cardioversion. The three patients with early arrhythmia recurrence showed no recurrence after the first month postPFA and 269 ± 35 days of follow up and were off antiarrhythmic drugs.

One patient suffered from AT recurrence 224 days after ablation. The patient was prescribed with sotalol by his outpatient cardiologist and received an electrical cardioversion. The patient refused to undergo another ablation at that point in time. Of the whole study cohort, two patients were still on antiarrhythmic drugs during the follow up, one patient received flecainide and the other one was the patient with AT recurrence and sotalol-prescription.

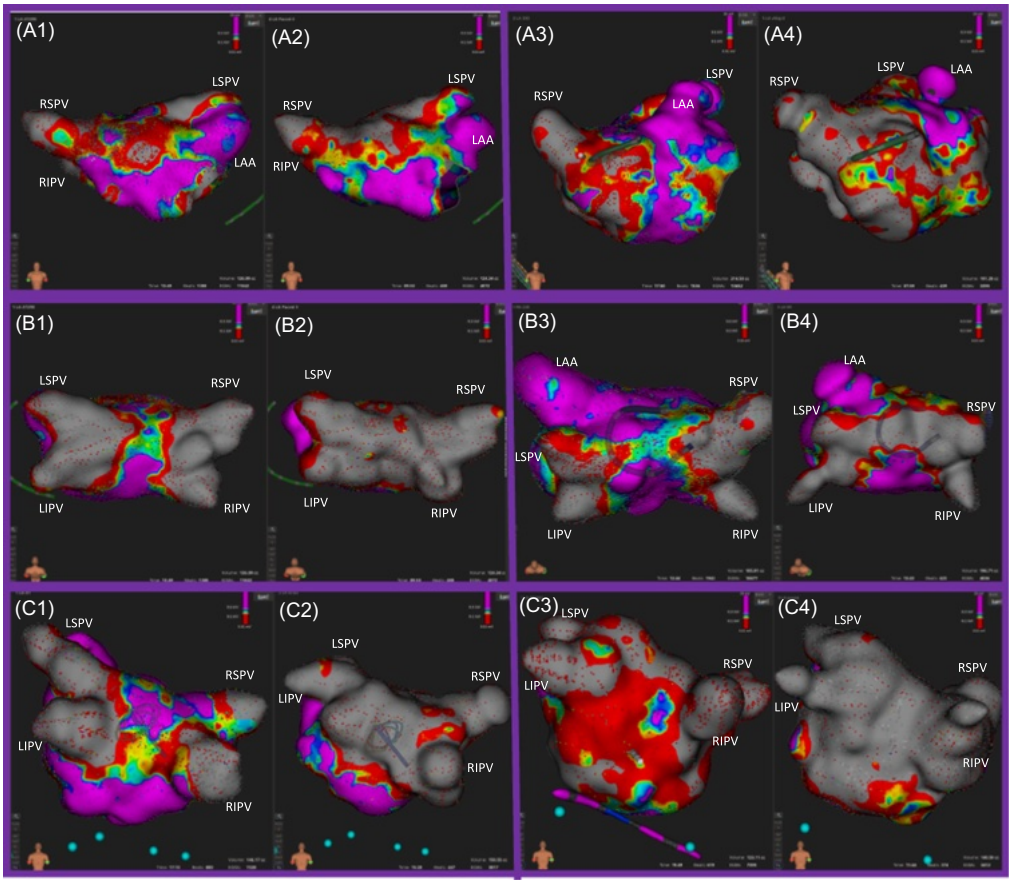

FIGURE 5 Pre- and post-PFA-ablation UHDx voltage maps. A1+3, preablation UHDx voltage map of the anterior LA; A2+4, postablation UHDx voltage map with blocked anterior line (A1-2 and A3-4 show one patient each). B1+3, preablation UHDx voltage map of the LA roof; B2+4, postablation UHDx voltage map with blocked roof line (B1-2 and B3-4 show one patient each). C1+3, preablation UHDx voltage map of the posterior LA; C2+4, postablation UHDx voltage map with LAPWI (C1-2 and C3-4 show one patient each). UHDx indicates ultra-high density mapping.

4 | DISCUSSION

Major findings of this study are:

(1) PFA of consecutive left atrial tachycardia in conjunction with UHDx mapping is feasible and safe.
(2) The majority of LATs were terminated by the first PFA impulse and PFA showed favorable outcomes regarding freedom from arrhythmia during intermediate-term follow up.
(3) Successful creation of ablation lines and LAPWI can be achieved in a short time.

To the best of our knowledge, our study appears the first to evaluate PFA-based ablation of consecutive AT following prior catheter ablation of AF in conjunction with UHDx mapping.

In this study, we present a cohort of 15 patients with consecutive AT undergoing their 4.6 ± 1.7 catheter ablation procedure. All patients suffered from considerably left atrial scarring comprising large areas of the LA in all patients. PV reconnection was still found in 7/15 patients during the current reprocedure but was not identified as crucial for the current arrhythmia. This again underscores that effective ablation and durable block of created ablation lines, including PVI, are needed but not easily achieved. Our presented

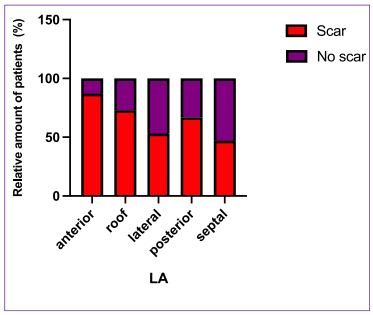

FIGURE 6 Relative distribution of LA scar localization. LA, left atrium.

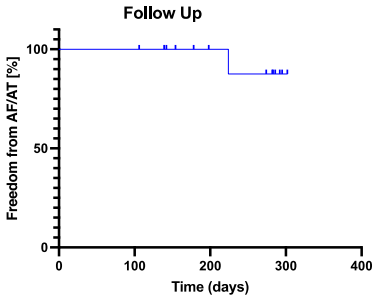

FIGURE 7 Follow up. Patients follow up with a 90-day blanking period

intermediate follow-up showed favorable outcomes regarding freedom from atrial arrhythmia.

4.1 | UHDx mapping

In conjunction with UHDx mapping, identification of the AT mechanism and critical isthmus site was possible in all patients of this study leading to successful termination of all ATs. High-density mapping has been shown to be a useful tool in identifying AT mechanisms by improving accuracy in delineating ultra-low-voltage areas that are critical for maintenance of the AT circuit.[14] In consecutive AT patients following prior AF/AT ablation, analysis of the high-density activation map alone, without entrainment, identified 83.6% of the AT diagnosis, reported by Vlachos et al.[14] Combining activation and entrainment mapping, AT mechanisms were identified in all patients.[14] Further, use of UDHx mapping led to fewer atrial arrhythmia recurrences as compared to conventional ablation methods in a single-center study including 100 patients undergoing reablation for AF.[15]

In our study, the majority of LAT (58%) were terminated by the first PFA impulse. Yet, not all were terminated by the first PFA impulse. This finding indicates that if terminations occurred, it was rather specific than caused by a "local" electrical cardioversion due to the ultra-rapid electrical field created by the PFA generator. In some cases of a macroreentry, completion of the ablation line may be necessary to terminate AT. However, AT termination by PFA does not always imply the correctness of the diagnosis of the AT mechanisms. Therefore, detailed UHDx mapping and analysis was performed prior ablation to identify the critical isthmus.

The current study is lacking a RF control group. However, we reported outcome data after tailored catheter ablation of atrial tachycardia using UHDx mapping and RF-guided ablation in 250 consecutive AT patients before[16]: patients underwent ablation of consecutive AT after a mean number of 2.2 ± 0.1 previous catheter ablation procedures. Following tailored ablation of reentry ATs, freedom from any arrhythmia after a median follow up of 535 days was obtained in 53% after a single procedure and in 73% after 1.4 ± 0.4 ablation procedures (range: 1–4). A total of 228 patients (91%) were free from any arrhythmia recurrence after 210 days (interquartile range: 152–494) when including optimal usual care.

In comparison, we reported three early AF/AT recurrences within and one AT recurrence after the 90-day blanking period in our limited initial PFA experience of 15 patients during a median follow up of 230 days. PFA for AT ablation, therefore, shows favorable intermediate-term outcomes.

4.2 | Ablation lines and lesion durability

Prior studies showed that despite repeated ablation, complete block of anterior line with conventional radiofrequency (RF) ablation was a low as 58% and that incomplete or recovered ablation lines can cause AT recurrences.[17,18] Achievement of complete block of all ablation lines significantly prolongs procedure times.[6,17] Additionally, extensive RF ablation beyond PVI is associated with an increased complication risk for cardiac tamponades.[17,19]

In this regard, PFA provides a novel option after failed RF ablation. With PFA, all ablation lines were completely blocked at the end of the procedure in this study.

Reddy et al. demonstrated a 100% chronic PV isolation rate in the initially published PFA patient cohort that was invasively remapped 3 months after PVI suggesting high durability of PFA lesions.[9]

Up to now, no intracardiac repeat-mapping or long-term follow-up of PFA for mitral isthmus and LA anterior wall ablation have been published. Whether, long-term linear PFA for AT is equally effective remains unclear, although acute success and intermediate-term outcome in this study was high. The PFA catheter design is favorable for PVI, as we demonstrate here, it is also effective in ablation beyond PVI.

Although at least two PFA applications were targeted per ablation site, patients required a large number (up to 38 ± 17 PFA applications per patient) to block all ablation lines. Therefore, more

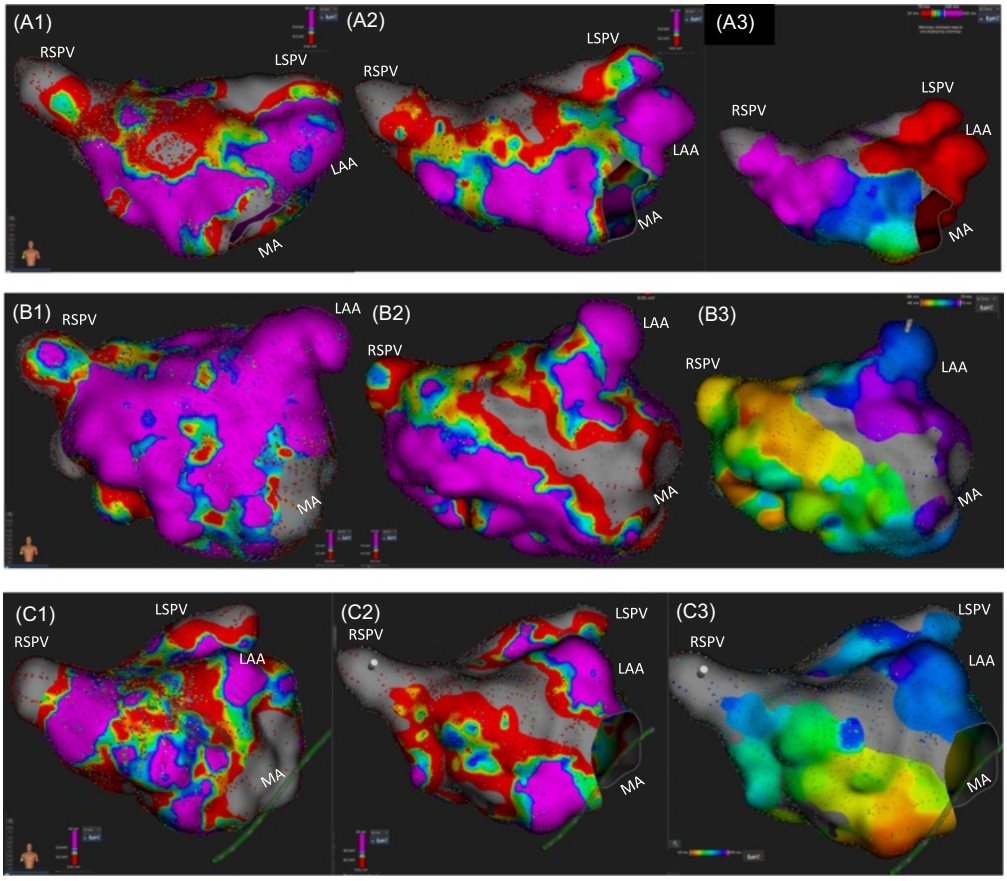

FIGURE 8 Three examples of anterior ablation lines created by pulsed-field-ablation. (A–C) One patient each: A1–C1: UHDx LA voltage map of the anterior wall prior ablation (A1: patient with immense prior LA scarring and prior anterior ablation line performed with radiofrequency ablation, B1: patient with only small areas of anterior scarring and no prior anterior ablation line, C1: patient with immense anterior scarring without prior anterior ablation line. A2-C2: UHDx LA voltage map of the anterior wall after PFA. A3-C3: UHDx activation maps of the anterior wall revealing complete block of anterior line. LA, left atrial; LAA, left atrial appendage; LSPV, left superior pulmonary vein; MA, mitral annulus, PFA, pulsed field ablation; RSPV, right superior pulmonary vein; UHDx, ultra-high-density-mapping.

than two PFA applications per site can be warranted and an adequate overlap is necessary to achieve block of line.

Yet, further developments of conventional energy sources and ablation strategies also need to be taken into account when discussing improvements in creation of ablation lines. Recently, the so called "high-power short-duration" (HPSD) RF approach has gained more attention in performing CA of AF. HPSD is associated with higher freedom from atrial arrhythmia, higher first-pass isolation and lower acute PV reconnection rates compared to conventional RF ablation.[20] With the HPSD approach, complete block of anterior and roof line was as high as 97% and 100% in a single center study, respectively.[21]

Although PFA could terminate all LAT in our study cohort, in two cases right atrial tachycardias were detected and ablation was performed with RF energy. Due to the PFA catheter design, ablation can only be performed in the basket or flower configuration leading to rather large ablation lesions that may be difficult to apply to structures close to the AV node. Therefore, we decided to ablate right-sided AT with conventional RF energy. In the future, a development of a focal PFA—tip catheter would therefore be desirable.

In our study, we were able to create and block all anterior, roof and mitral isthmus lines with PFA. In the recently published Manifest PF survey of 24 European centers, roof lines and mitral isthmus lines were frequently deployed in 12.5% and 4.2% and sometimes in 25% and

33.2% of the participating centers, respectively.[22] Anterior lines were not frequently performed in any center but sometimes in 25%.[22] This survey supports our data for feasibility of this PFA-guided ablation strategy. However, detailed analysis of indication and verification of completion of ablation lines is missing in the reported multicenter experience. Of note, caution must be taken when applying PFA at the mitral isthmus line as occurrence of coronary spasm has been reported.[23] In this cohort, no coronary spasm occurred.

In the case of the consecutive LAA isolation, we conducted a complete anterior line. One could discuss that closing of only one of the two gaps within the anterior line might have been enough to avoid LAA isolation and terminate AT. However, if closing of a single distinct gap in an incomplete line may be possible with the current PFA catheter design (large lesion size, yet not fully integrated into 3D mapping systems) is also open for discussion.

4.3 | Left atrial posterior wall isolation

Reddy et al. proposed PFA-guided LAPWI as an additional ablation strategy for patients with persistent AF, in whom a "PVI only" approach might not be promising to achieve long term rhythm control.[10] Therefore, LAPWI may be beneficial for substrate modification in persistent AF patients.

LAPWI was successfully performed in 10 patients in our study. Yet, one LAPW reconnected during remapping and required Re-PFA impulses to successfully isolate the LAPW of this patient. This could indicate that a certain degree of contact may also be necessary in PFA to create durable lesions. Information about contact however is missing in the current PFA system. Nevertheless, the limited published data on LAPWI so far demonstrate high acute and chronic LAPW isolation rates.[10,11] In our cohort, no esophageal lesion was detected. Also, in the Manifest-PF survey no esophageal lesion was found in a large patient cohort of 1758 patients undergoing PFA including LAPWI in a minor portion of patients.[22]

4.4 | Extend ablation with PFA

An advantage of PFA is that ablation can be performed in a considerably short time with a PFA impulse taking only a few seconds. Total ablation time is therefore low. Combined with the beneficial safety profile of PFA, large substrate modification and fast block of lines can be performed straightforward. This could be especially helpful in patients with large atria and extensive areas of scar and/or fibrosis in the setting of prior chronic AF and frequent prior ablation procedures. Although PFA targets large parts of the atrium and ablation lines appear to be wider as the thinner point-by-point created RF lesions, this study cohort existed only of patients with already significant atrial myopathy and scarring. One may argue that ablation lesions created by PFA are too wide for linear ablation affecting large portions of the LA. A "Stiff LA syndrome" can be a problem after extensive catheter ablation of the left atrium[24] by potentially compromising atrial mechanical performance. Yet, in a study by Takahashi et al., the stepwise ablation approach in persistent AF patients was able to achieve sinus rhythm and had a significant impact on LA electrical activity but was also associated with recovery of LA function.[25] The study even reported a decrease in LA diameter and an improvement of left ventricular function in patients with an initially reduced LV ejection fraction ≤45%.[25]

The patients of this study cohort presented with already immense atrial scarring, most likely caused due to both: atrial myopathy with recurrent AF/AT and prior catheter ablations with proarrhythmic substrate. Hence, the rationale of our approach was to target this proarrhythmic substrate and homogenize atrial scars.

Studies such as DECAAF-II failed to show that targeting of MRI-guided atrial fibrosis with extensive RF energy is beneficial in treating patients with persistent AF.[26] One of many explanations could be creation of inhomogeneous and disorganized scaring, reported by analysis of histopathological RF lesions before.[27] Contrary, histopathological PFA lesions were composed of organized, homogeneous fibrosis replacing the myocardium with well-demarcated border zones that were consistent with their gross appearance.[27]

Also in a clinical setting, PFA was able to demonstrate that acute PFA lesions were exceptionally homogenous with negligible small areas of complex fractionation along the border of ablation sites and depression of tissue voltage to a minimum, using UHDx mapping.[11] Whether these acute findings can be translated to long term outcomes, needs to be awaited.

4.5 | Limitations

The present study yields some limitations. The design of our single-center study was explorative and therefore the sample size in the current study is small limiting the impact of the results. The follow up presented in this study is short.

As compared to prior published studies about LAPWI, we present only acute remapping data. There is no chronic remapping information and therefore no statement regarding chronic PFA lesion patterns in UHDx mapping can be made.

Another limitation is that right-sided AT were not ablated by PFA but by RF energy due to the possible proximity to the AV node. Further, if feasible, entrainment mapping was avoided in our study to not alter the AT mechanism or terminate it. However, entrainment maneuvers might be necessary to differentiate between active and passive circuits in complex atrial tachycardia. There is no radiofrequency control group in this study.

5 | CONCLUSION

PFA of consecutive LAT is feasible and safe. Successful creation of ablation lines and left atrial posterior wall isolation with PFA can be achieved in a short time and shows favorable intermediate-term outcomes. PFA in conjunction with 3D UHDx-mapping may offer the opportunity for effective ablation of atrial arrhythmias beyond AF.

ACKNOWLEDGMENTS

The authors thank the medical staff including all nurses and technicians from the St. Georg's EP Lab.

DATA AVAILABILITY STATEMENT

All relevant data are within the manuscript. No data has been shared.

ORCID

Melanie A. Gunawardene http://orcid.org/0000-0001-7561-7185
Omar Anwar http://orcid.org/0000-0001-9738-4685

REFERENCES

1. Hindricks G, Potpara T, Serbia C, et al. 2020 ESC Guidelines for the diagnosis and management of atrial fibrillation developed in collaboration with the European Association of Cardio-Thoracic Surgery (EACTS). *Eur Heart J*. 2020;42(5):373-498.
2. Schaeffer B, Akbulak RÖ, Jularic M, et al. High-density mapping and ablation of primary nonfocal left atrial tachycardia. *JACC Clin Electrophysiol*. 2019;5(4):417-426.
3. Rostock T, Drewitz I, Steven D, et al. Characterization, mapping, and catheter ablation of recurrent atrial tachycardias after stepwise ablation of long-lasting persistent atrial fibrillation. *Circ Arrhythm Electrophysiol*. 2010;3(2):160-169.
4. Saoudi N, Cosío F, Waldo A, et al. A classification of atrial flutter and regular atrial tachycardia according to electrophysiological mechanisms and anatomical bases. A statement from a Joint Expert Group from the working group of arrhythmias of the European Society of Cardiology and the North American Society of Pacing and Electrophysiology. *Eur Heart J*. 2001;22(14):1162-1182.
5. Brugada J, Katritsis DG, Arbelo E, et al. 2019 ESC guidelines for themanagement of patients with supraventricular tachycardia. *Eur Heart J*. 2020;41(5):655-720.
6. Schaeffer B, Hoffmann BA, Meyer C, et al. Characterization, mapping, and ablation of complex atrial tachycardia: initial experience with a novel method of ultra high-density 3D mapping. *J Cardiovasc Electrophysiol*. 2016;27(10):1139-1150.
7. Gunawardene MA, Eickholt C, Akbulak RÖ, et al. Ultra-high-density mapping of conduction gaps and atrial tachycardias: distinctive patterns following pulmonary vein isolation with cryoballoon or contact-force-guided radiofrequency current. *J Cardiovasc Electrophysiol*. 2020;31(5):1051-1061.
8. García-Bolao I, Ballesteros G, Ramos P, et al. Identification of pulmonary vein reconnection gaps with high-density mapping in redo atrial fibrillation ablation procedures. *EP Eur*. 2018;20(FI_3):f351-f358.
9. Reddy VY, Neuzil P, Koruth JS, et al. Pulsed field ablation for pulmonary vein isolation in atrial fibrillation. *J Am Coll Cardiol*. 2019;74(3):315-326.
10. Reddy VY, Anic A, Koruth J, et al. Pulsed field ablation in patients with persistent atrial fibrillation. *JACC*. 2020;76(9):1068-1080.
11. Gunawardene MA, Schaeffer BN, Jularic M, et al. Pulsed-field ablation combined with ultrahigh-density mapping in patients undergoing catheter ablation for atrial fibrillation: practical and electrophysiological considerations. *J Cardiovasc Electrophysiol*. 2022;33(3):345-356.
12. Alken FA, Klatt N, Muenkler P, et al. Advanced mapping strategies for ablation therapy in adults with congenital heart disease. *Cardiovasc Diagn Ther*. 2019;9(Suppl 2):247-S263.
13. Kawamura I, Neuzil P, Shivamurthy P, et al. Does pulsed field ablation regress over time? A quantitative temporal analysis of pulmonary vein isolation. *Heart Rhythm*. 2021;18:878-884.
14. Vlachos K, Efremidis M, Derval N, et al. Use of high-density activation and voltage mapping in combination with entrainment to delineate gap-related atrial tachycardias post atrial fibrillation ablation. *Europace*. 2021;23(7):1052-1062.
15. Ikeda Y, Kato R, Mori H, et al. Impact of high-density mapping on outcome of the second ablation for atrial fibrillation. *J Interv Card Electrophysiol*. 2021;60(1):135-146.
16. Jungen C, Akbulak R, Kahle A-K, et al. Outcome after tailored catheter ablation of atrial tachycardia using ultra-high-density mapping. *J Cardiovasc Electrophysiol*. 2020;31(10):2645-2652.
17. Sanders P, Jaïs P, Hocini M, et al. Electrophysiologic and clinical consequences of linear catheter ablation to transect the anterior left atrium in patients with atrial fibrillation. *Heart Rhythm*. 2004;1:176-184.
18. Calkins H, Hindricks G, Cappato R, et al. 2017 HRS/EHRA/ECAS/APHRS/SOLAECE expert consensus statement on catheter and surgical ablation of atrial fibrillation. *Heart Rhythm*. 2017;14(10):e275-e444.
19. Chun K, Perrotta L, Bordignon S, et al. Complications in catheter ablation of atrial fibrillation in 3,000 consecutive procedures. *JACC Clin Electrophysiol*. 2016;3(2):154-161.
20. Donlon NE, Nugent TS, Power R, et al. High-power short duration vs. conventional radiofrequency ablation of atrial fibrillation: a systematic review and meta-analysis. *Europace*. 2021;23(5):710-721.
21. Zanchi S, Chen S, Chun KRJ, Schmidt B. Ablation index—guided high—power (50 W) short-duration for left atrial anterior and roofline ablation: feasibility, procedural data, and lesion analysis (AI high-power linear ablation). *J Cardiovasc Electrophysiol*. 2021;32(4):984-993.
22. Ekanem E, Reddy VY, Schmidt B, et al. Multi-national survey on the methods, efficacy, and safety on the post-approval clinical use of pulsed field ablation (MANIFEST-PF). *Europace*. 2022;24(8):1256-1266.
23. Gunawardene MA, Schaeffer BN, Jularic M, et al. Coronary spasm during pulsed field ablation of the mitral isthmus line—research letter. *JACC Clin Electrophysiol*. 2021;7(12):1618-1620.
24. Packer M. Effect of catheter ablation on pre-existing abnormalities of left atrial systolic, diastolic, and neurohormonal functions in patients with chronic heart failure and atrial fibrillation. *Eur Heart J*. 2019;40:1873-1879.
25. Takahashi Y, O'neill MD, Hocini M, et al. Effects of stepwise ablation of chronic atrial fibrillation on atrial electrical and mechanical properties. *JACC*. 2007;49:1306-1314.
26. Marrouche NF, Greene T, Dean JM, et al. Efficacy of LGE-MRI-guided fibrosis ablation versus conventional catheter ablation of atrial fibrillation: the DECAAF II trial: study design. *J Cardiovasc Electrophysiol*. 2021;32(4):916-924.
27. Koruth J, Kuroki K, Iwasawa J, et al. Preclinical evaluation of pulsed field ablation. *Circ Arrhythm Electrophysiol*. 2019;12:e007781.

How to cite this article: Gunawardene MA, Schaeffer BN, Jularic M, et al. Pulsed field ablation in patients with complex consecutive atrial tachycardia in conjunction with ultra-high density mapping: Proof of concept. *J Cardiovasc Electrophysiol*. 2022;33:2431-2443. doi:10.1111/jce.15713